Requirement Analysis Framework of Naval Military System for Expeditionary Warfare

A Thesis
Presented to
The Academic Faculty

By

Hyun Seop Lee

In Partial Fulfillment
of the Requirements for the Degree
Doctor of Philosophy in the
School of Aerospace Engineering

Georgia Institute of Technology
December 2013

Requirement Analysis Framework of Naval Military System for Expeditionary Warfare

Approved by:

Professor Dimitri N. Mavris,
Committee Chair
School of Aerospace Engineering
Georgia Institute of Technology

Professor Daniel P. Schrage
School of Aerospace Engineering
Georgia Institute of Technology

Assistant Professor Vitali Volovoi
School of Aerospace Engineering
Georgia Institute of Technology

Dr. Santiago Balestrini-Robinson
Georgia Tech Research Institute
Georgia Institute of Technology

Dr. Jean Charles Domercant
School of Aerospace Engineering
Georgia Institute of Technology

Date Approved: Nov. 15, 2013

TABLE OF CONTENTS

LIST OF TABLES

LIST OF FIGURES

SUMMARY

Military systems are getting more complex due to the demands of various types of missions, rapidly evolving technologies, and budgetary constraints. In order to support complex military systems, there is a need to develop a new naval logistic asset that can respond to global missions effectively. This development is based on the requirement which must be satisfice-able within the budgetary constraints, address pressing real world needs, and allow designers to innovate. This research is conducted to produce feasible and viable requirements for naval logistic assets in complex military systems. The process to find these requirements has diverse uncertainties about logistics, environment and missions. To understand and address these uncertainties, this research includes instability analysis, operational analysis, sea state analysis and disembarkation analysis. By the adaptive Monte-Carlo simulation with maximum entropy, uncertainties are considered with corresponding probabilistic distribution. From Monte-Carlo simulation, the concept of Probabilistic Logistic Utility (PLU) was created as a measure of logistic ability. To demonstrate the usability of this research, this procedure is applied to a Medium Exploratory Connector (MEC) which is an Office of Naval Research (ONR) innovative naval prototype. Finally, the preliminary design and multi-criteria decision-making method become capable of including requirements considering uncertainties.

CHAPTER I

INTRODUCTION

Due to the demands of various types of missions, rapidly evolving technologies, and budgetary constraints, military systems has been becoming more complex. In order to support complex military systems, there is a need to develop a new naval logistic asset that can effectively respond to global missions. This development is based on requirements which must be satisfice-able within the budgetary constraints, address pressing real world needs, and allow designers to innovate. The following research is conducted to produce feasible and viable requirements for naval logistic assets in complex military systems. The process of requirement development includes diverse uncertainties about logistics, environment and missions. To understand and address these uncertainties, this analysis process includes instability analysis, operational analysis, sea state analysis and disembarkation analysis. By applying an adaptive Monte-Carlo simulation with maximum entropy, uncertainties can be considered with a corresponding probabilistic distribution. From the Monte-Carlo simulation, the concept of Probabilistic Logistic Utility (PLU) was created as a measure of logistic ability. Demonstrated with the usability of this research, this procedure is applicability to Medium Exploratory Connector (MEC), which is an Office of Naval Research (ONR) innovative naval prototype. Through the application of the previously mentioned methods, the preliminary design and multi-criteria decision making method become capable of including requirements considering uncertainties.

1.1 Paradigm Shift in Naval Operational Concept

The Navy's operational vision for the 21st century, Sea Power 21, identifies three fundamental concepts for continued operational effectiveness: Sea Strike, Sea Shield, and Sea Base. Sea Strike is the ability to project precise and persistent offensive power from the sea; Sea Shield extends defensive assurance throughout the world; and Sea Base enhances operational independence and support for the joint force [16]. The purpose of the Sea Base is to develop a maneuverable, scalable collection of platforms that enable power projection from the sea [23]. The DoD Dictionary defined Sea-basing as “the deployment, assembly, command projection, reconstitution, and reemployment of joint power from the sea without reliance on land bases within the operational area” [22].

Due to difficulties the United States has experienced in securing bases on foreign territory, military concepts have moved away from land based operations, requiring the U.S. Navy to be capable of projecting power ashore. In addition, developing political and diplomatic factors can continue to decrease the availability of land bases, causing even more of a drive towards sea-based projection [100]. For example, an increase political pressures against using bases on foreign soil prohibited the United States from obtaining permission to establish land bases in Saudi Arabia and Turkey leading up to the invasion of Iraq [7]. Admiral Moore and General Hanlon stated "Sea Basing exploits the operational shift in warfare from mass to precision and information, employing the 70 percent of the earth's surface that is covered with water as a vast maneuver area in support of the joint force" [105].

The Sea Base concept has been developed from this aforementioned demand. The Sea Base construct provides potential abilities to project power ashore, which will result in minimizing the magnitude of forces ashore and the need to build up logistical

stockpiles on foreign territory. This includes the capability to assemble, equip, project, support, and sustain these forces without reliance on land bases within the Joint Operations Area [23].

The concept for Sea-basing is described in Figure 1.1. Immediate employment becomes enabled by eliminating the need for diplomatic arrangements for the purpose of forward basing coupled with forward positioning [8]. The expected benefits of Sea-basing include secured access worldwide for military operations, improvement in immediate response capability, enhanced forward-defense posture, rapid initiation of joint command and control, significantly swift transition from crisis to joint forcible entry, and a higher degree of force tailorability and scalability [74].

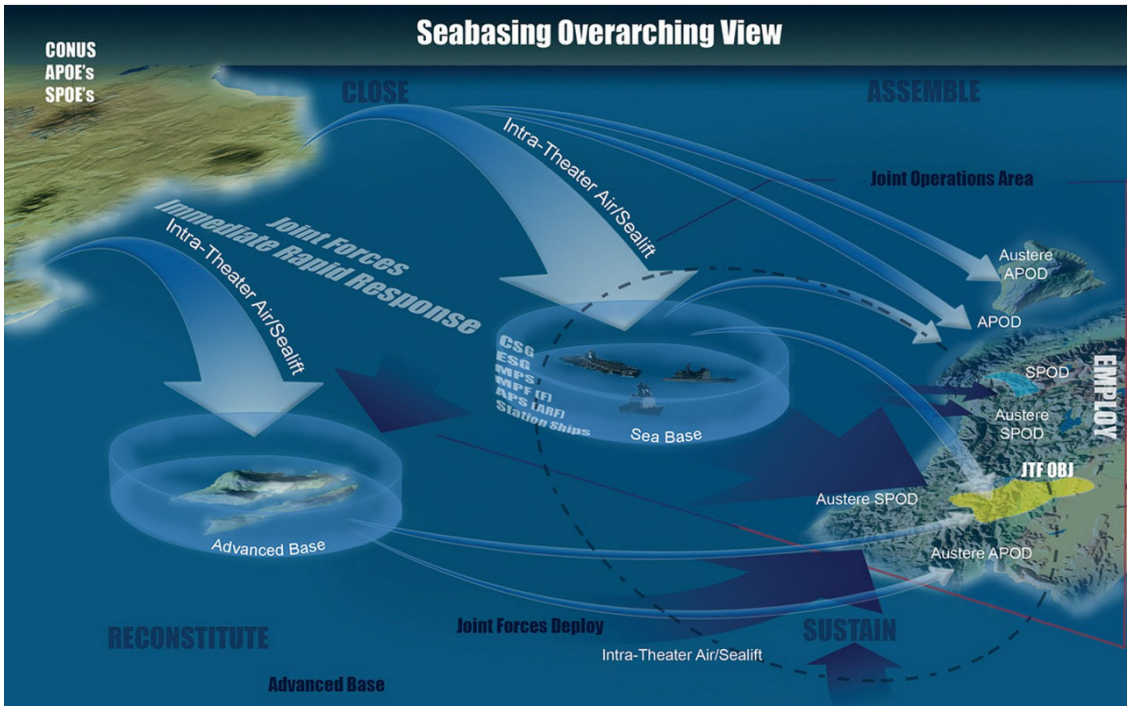

Figure 1.1 Sea Base overarching view [117]

The composition of the Sea Base is not completely established and is intended to be tailorable to each operation, but it will comprise distributed forces including carrier strike groups (CSGs) , expeditionary strike groups (ESGs), maritime pre-positioning groups (MPG), combat logistics force ships (CLF), connectors, and coalition force and sister services ships [7]. Those components are shown in Figure 1.2. The Sea Base's contributing elements do not operate in isolation but are instead part of a logistical chain from production in the continental United States (CONUS) to use by the war fighter in theater. The Sea Base connectors are contributing elements to the logistical function and need to be analyzed as part of a larger throughput process [32]. This has led to the recommendation by the National Research Council that a comprehensive systems analysis of Sea-basing ships and connectors needs to be undertaken at a macro level to validate the requirements, such as range, speed, and capacity for cargo and personnel [74].

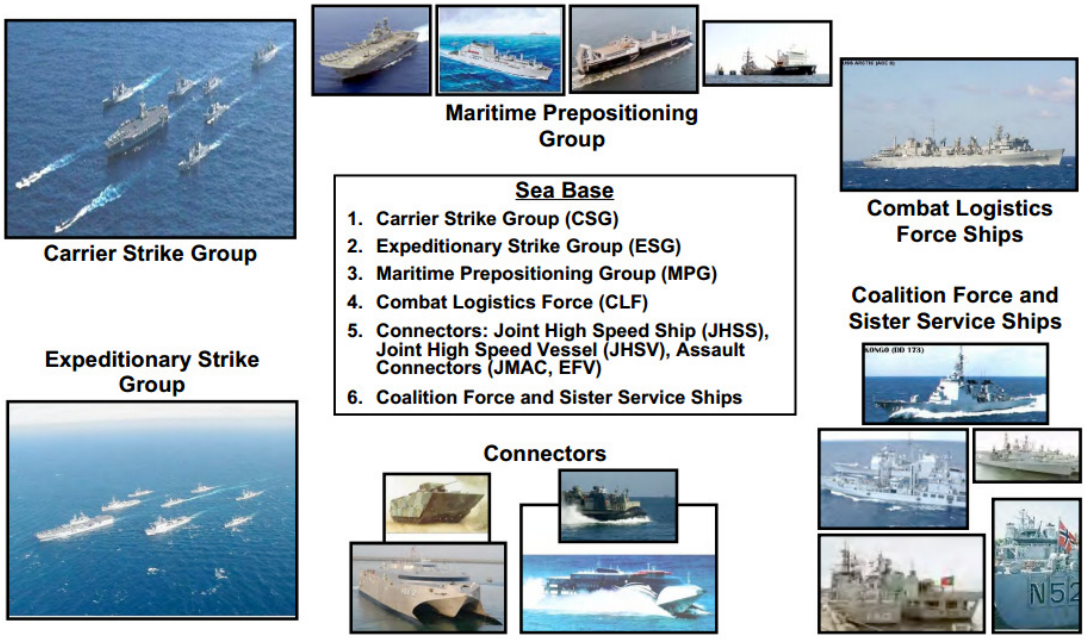

Figure 1.2 Joint Sea-basing Components [118]

1.2 Needs for New Vessels and Challenges

One of the greatest challenges to the Sea-basing concept is the capability to transfer cargo, troops, and equipment from the Sea Base to the coastline [82]. The current alternative craft cannot meet the all requirement for the objectives of the Sea Base, considering the traditional iron triangle of speed, range and payload. The major capability in meeting the objectives of the Sea Base are the required stand-off distances, high sea state transfer capabilities, desire for insertion during one period of darkness, and the need for over-the-beach delivery [32]. Therefore, A new long range, medium lift connector needs to be developed to address breaking the iron triangle and be designed to meet the requirements in order to capitalize on the promised Sea-basing capabilities. To meet the needs of the Sea-basing concept, it has been suggested that future surface connectors must be able to operate in three modes [80]: fuel efficient and good sea-keeping mode, high-speed shallow water mode, and amphibious mode to traverse sand bars and mud flats.

These three modes cannot be achieved by any existing vessel and formed the starting requirements outlined in the Office of Naval Research's (ONR) Broad Agency Announcement (BAA) soliciting proposals for a prototype demonstrator of a medium exploratory connector (MEC). The basic requirements highlight an important gap in existing connectors. A new type of connector is required based on the need for a self deployed asset that can deliver intact units with options for interface and transfer of cargo. This thesis will explore the modeling needs and requirements definition for this MEC.

The MEC is a vessel which can operate in multiple modes. It can self deploy from an intermediate support base to the sea base and then be used as a high speed connector from the sea base to the shore, transporting wheeled and tracked vehicles and other heavy equipment and cargo through the surf zone and onto the beach, where it can discharge its cargo without the need for a port. The research about MEC is investigating and developing multiple technologies that will allow a single vessel to transform operational modes and accomplish the MEC mission. The MEC will deliver game changing capability in the way material and personnel are transported from the sea base and onto the shore. It will be capable of long range open ocean transit of 2500 nm at 20 kts, cargo transfer at the sea base in high sea states, high speed transit between the sea base and the shore of 500 nm range at 40 kts, and transformation to a fully amphibious vehicle - delivering material and personnel “feet dry” on the beach [81]. Figure 1.3 illustrates concept models of MEC performing different missions.

Figure 1.3 Concept Models of Medium Exploratory Connector [44]

In order to conduct a research about the capabilities of a new vessel like MEC, the concept should be verified as a component of the Sea Base. The Sea Base is identified as a complex system-of-systems (SoS) by the Defense Science Board [82]. The definition of SoS by the Defense Acquisition Guidebook is a set or arrangement of systems that results from independent systems integrated into a larger system that delivers unique capabilities [119]. Also, the Systems Engineering Guide for Systems of Systems recognizes the importance of incorporating system interdependencies in systems acquisition [83].

The difficulty in assessing the impact of a new vessel's capabilities in the Sea Base at the SoS level is that the effects of all subsystems are significantly complex. First, the operational research must cover a large number of interdependent systems. Furthermore, these interactions are nonlinear and unpredictable so that conducting research about each subsystem individually is insufficient. These variety of scenarios at the SoS level depend depend not only on the composition of fleets, but also on the operations and the area where the operation is performed. These components make the complexity of SoS higher and these technical obstacles bring the need of flexible modeling to consider varius types of operations and environmental conditions. In addition, all aforementioned components, such as the composition of the Sea Base, required cargo and troops, mission type, difficulty of operation, etc., have significant degrees of uncertainties. Therefore, the design process of new vessels should include flexible modeling which can cover the uncertainties in worldwide operational situations. In particular, expeditionary vessels can take part in an operation in any part of the world and their design process must be able to consider more complicated requirements than other vessel types.

Another challenge of ship design is the consideration of lifespan. Naval assets like ships are supposed to service for more than two decades. Figure 1.4 shows the average service lifes of recently decommissioned ships of four classes: Tarawa, Ticonderoga, Oliver hazard perry and Austin class. Those ships were launched from 1960's to 1980's and decommissioned from late 1990's to 2000's. Average service lifes are 35, 21, 22, and 40 years. Likewise, Figure 1.5 describes the service lifes of LSV, LCU-2000 and LCM-8. The service lifes are extended to longer than 35 years by the Service Life Extension Program (SLEP) [103]. These long term service life means that new vessel design should be developed in order to satisfy the requirements in four decades future. [18][19]

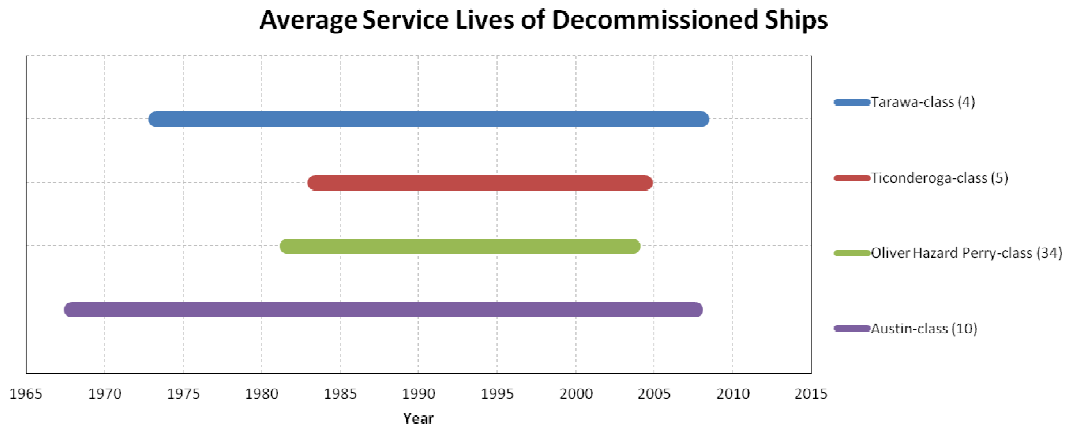

Figure 1.4 Average Service Lives of Decommissioned Ships [94][47][48][49]

Figure 1.5 Extended Service Life by SLEP [103]

This complex system needs the approach of system Engineering. The first step of DoD 5000 phases, the system development process by the Department of Defense, start with the mission need determination [25]. Then, the concept exploration process and concept and technology development process are following at the same time. Overall procedures of system engineering is shown in the Table 1.1. These processes are included in the concept development stages of system engineering. The initial step of the concept development phase is the needs analysis. Based on the operational deficiency and technological opportunities, the needs analysis makes outputs of system operational requirements and system studies for concept exploration. The methodology of the needs analysis in systems engineering is applied to estimate the requirements to develop the complex system of naval connector in the future.

Table 1.1 Status of system materialization [58]

Phase / Level	Needs analysis	Concept exploration	Concept definition	Advanced development	Engineering design	Integration & Evaluation
System	***Define operational objectives***	***Explore concepts***	***Define selected concepts***	Validate concepts		Test & evaluation
Subsystem	Visualization	Define Functions	Define configuration	Validate selected subsystem		Integrate & test
Component		Visualization	Select & Define Functions	Validate & specify construction	Design & test	Integrate
Subcomponent			Visualization	Define Functions	Design	
Part				Visualization	Select or adapt	

1.3 Observations

A traditional instability analysis conducted by O'Brien includes political, social, and economical factors [75][76]. Recently, humanitarian operations have become important considering the tsunami in the Indian Ocean in 2004 and the earthquake in Haiti in 2010. Therefore, a natural disaster factors need to be included. To support the decision making, this decision support method integrates forecasting relative factors, performing statistical simulation, and preliminary design.

Recently, Beisecker conducted research on the effectiveness of the MEC [2]. Part of her research focused on identifying the factors that had the highest contribution to the variability in the MEC's effectiveness. She employed a discrete event simulation (DES) on a large-scale amphibious logistic operation. Her approach provided insight into which factors are more critical to the design of a large amphibious connector under various operational conditions, ranging from major combat operations to humanitarian assistance and disaster relief missions. As well as the discrete event simulation, the approach based on the statistical analysis and forecasting can support the decision making for the design of all navy ships including MEC.

The research proved that a large portion of the MEC's effectiveness is dependent on factors that are beyond the designer's control, furthermore, the impact that different design requirements have on the MEC's effectiveness. These factors include: the distance from the supply point to the disembarkation point, the number of simultaneous disembarkation points, and the sea state encountered through transit. These factors depend on the location of the operation, the ability of the craft to climb a beach, and the

location of the supply depots such as Sea Based assets, Intermediary Staging Bases (ISB), and Continental United States (CONUS). Therefore, the following analyses are critical to analyzing the effectiveness of the MEC: forecasting the likelihood of operating in different areas of the world, quantifying their local conditions, estimating the environmental conditions, analyzing the impact of establishing new ISBs, or closing down existing ones [2].

Therefore, motivation for the proposed theoretical formulation and methodologies has emerged from the following observations.

- Decision makers need to understand information efficiently and intuitively at the high level. The real-time interactive decision support tool can provide the data they need quickly and in a visual format.
- The previous instability analysis by O'Brien includes political, social, and economical factors. The addition of a natural disaster factor can improve the accuracy of the prediction.
- The discrete event simulation in Beisecker's research can be improved by inputting actual values of substantial factors. In addition, instability analysis can provide importance to each scenario.
- A discrete event simulation based on a small number of scenarios cannot guarantee a valid representation of the overall global scenario. Accordingly, because more experiments are required, there is a need for an efficient sampling technique

- The landing condition in the current DES model is not analyzed from real scenario data. Landing condition needs to be estimated from geographical database efficiently.

1.4 Research Goals

Complex military systems are becoming more challenging due to the requirements of various types of missions, rapidly evolving technologies, budgetary constraints, and operational uncertainties. Furthermore, the design of future naval assets must take into account the role of Sea Bases that have very complicated subsystems. This problem requires a system of systems approach and a discrete event simulation of the operational research is an excellent solution for this problem. However, the method based on only a few scenarios is insufficient to reflect the overall global situation. The objective of this research is to develop a framework that can quantitatively assess the impacts of new capabilities and vessels at the systems-of-systems level with reasonable representation of the actual worldwide operational environment. This methodology must at the systems of systems level be able to capture the effectiveness of a new vessel in cooperating in a Sea Base mission. It must also be capable of capturing the complicated requirements for statistically predictable threats and must be able to provide fair comparison of new systems such as the MEC. For this new quantitative assessment, this study includes the analyses of instability, shipping lane, disembarkation, and operational research. The results of these analyses become representative through a Monte-Carlo simulation with maximum entropy. In addition, the research enables two types of applications, preliminary design and multi-criteria decision making.

The general layout is as follows. Chapter 2 provides background information on instability analysis, a new paradigm for U.S. Navy's operational analysis, and sampling algorithm using the maximum entropy concept. In addition, it explains the concept of a medium exploratory connector that is used for this research. Chapter 3 presents the overall procedures for the estimation of global effectiveness and a multi-criteria decision making method based on the instability analysis, shipping lane estimation, sea state analysis, disembarkation analysis and operational analysis. Chapter 4 presents a series of research questions developed through observations found in a literature search and a study of the technical challenges. This chapter outlines the hypothesis to be tested and presents the reason of these hypotheses and roles in this research. From chapter 5 to 8, each chapter explains the detailed work of the corresponding analysis: instability analysis, shipping lane estimation and sea state analysis, disembarkation analysis, and operational analysis. Chapter 9 describes the method to estimate the global effectiveness of new assets and proposes the concept of probabilistic logistic usability, a measure of effectiveness. Chapter 10 shows the application of this procedure which is the process of preliminary design of the medium exploratory connector. Chapter 11 presents another application of this research, a multi-criteria decision making (MCDM) method. In this research, a software tool is developed to support decision makers. Chapter 12 describes the procedure to estimate the usuability of a new vessel with scenarios. Chapter 13 introduces this software, DESTINA, and explains how to use this decision supporting tool. Finally, chapter 14 presents conclusion and future works to improve this research project's methodology.

CHAPTER II

BACKGROUND

2.1 Instability Analysis based on the Socio-Economic and Political Factors [75][76]

Since the end of the cold war, ethnic and religious animosities, economic dislocations, civil war, famine, and natural disasters have contributed to conflict and political instability in the states extending from Haiti to the vast archipelago of Indonesia. These conflicts and instabilities frequently challenge national security interests; at other times, the human rights atrocities that often accompany these dislocations offend the moral imperatives of individual states as well as the international community.

Increasingly, Western powers, acting alone or in concert with international organizations, have responded to these post–cold war crises in myriad ways, including peacekeeping operations in the Balkans, Sierra Leone, and East Timor; enforcing sanctions in the Persian Gulf and no-fly zones over Iraq; conducting humanitarian operations and evacuating civilian noncombatants in Africa; and conducting maritime interdictions in the Caribbean. The uncertainty surrounding where and when these crises might erupt around the globe has frustrated crisis response planners and humanitarian relief officials who often must plan, prepare, and budget for these contingencies months, even years, in advance.

To deal with this uncertainty in an environment where humanitarian disasters have increasingly come to compete for scarce resources with threats to more vital national interests, policy analysts, planners, diplomats, and legislators need tools and

models to help them anticipate when and where these crises are likely to emerge. Gurr and Moore have noted that those who make foreign and international policy seek more than explanation: they want better early warnings of impending conflicts so that preventative diplomacy and other conflict management tools can be brought into play [39].

Recognizing this need, many scholars have conducted research based on the concept of "crisis early warning" [87][120][51]. Although each of these studies provided a unique contribution to the development of early warning insights and capabilities, it is the research conducted by the State Failure Task Force (SFTF), a commission of prominent scholars and contractors set up by former Vice President Al Gore's office in 1994, that has received the most recent attention in academic and policy circles.

The U.S. government tasked and funded the SFTF to identify and examine key factors associated with serious state crises and to develop a methodology that could identify "critical thresholds" in these factors so that the task force might provide early warning of state failures up to 2 years in advance. State failures include four types of events: genocides and politicides, ethnic wars, revolutionary wars, and adverse or disruptive regime transitions. First, the genocides and politicides mean sustained policies by states or their agents, by contending authorities that result in the deaths of a substantial portion of members of communal or political groups. Second, the ethnic wars include secessionist civil wars, rebellions, protracted communal warfare, and sustained episodes of mass protest by politically organized communal groups. Third, the revolutionary wars are defined as sustained military conflicts between insurgents and central governments, aimed at displacing the regime. Last, the adverse or disruptive regime transitions are

major, abrupt shifts in patterns of governance, including state collapse, periods of severe instability, and shifts toward authoritarian rule.

The SFTF used logistic regression, neural networks, and genetic algorithms to identify patterns in the relationships between hundreds of explanatory factors and different types of state failures. The best global model included only three independent variables—measurements of a country's level of democracy, trade openness, and infant mortality rate. Using only these factors in a logistic regression, the SFTF was able to discriminate historical state failures from stable countries about two-thirds of the time. King and Zeng have pointed out that the research conducted by the task force used a limited number of methodological grounds [55]. The authors provided a state failure forecasting model that outperforms those published by the SFTF to date by using neural network models, a corrected version of the state failure project's baseline model with two additional variables (legislative effectiveness and fraction of population in the military).

O'Brien has extended this line of work in several ways: First, the author forecasted the likelihood of country instability, i.e., the conditions conducive to instability for every major country of the world from 2001 to 2015 [75][76]. To do this, the author identified and evaluated macro-structural factors at the nation-state level that, when combined with triggers such as assassinations or natural disasters, have historically been associated with different kinds and levels of intensity of conflict over the period from 1975 to 1999. For this historical data, a data set of state conflicts from the KOSIMO database is used to validate macro-structural factors as relevant contributors to country instability. The KOSIMO data project identified 74 mostly nonviolent crises, 121 violent crises, and 61 wars over the period from 1975 to 1999 [121]. Figure 2.1 summarizes

instability levels of these conflict types and provides corresponding examples. Despite the existence of a large amount of operationalized data on violent interstate conflict as one subset of political conflict, there are shortcomings in data on domestic and nonviolent conflict and growing inadequacies between the reality of political conflict and its conceptualization in quantitative conflict research. This is mainly due to fundamental changes in conflict patterns over the past few decades and an understandable fixation by researchers on violence as a central explanandum in conflict research. In response to these shortcomings, the authors propose an integrated and dynamic databank that contains nonviolent and violent as well as domestic and international political conflicts on a global scale between 1945 and 1998. The main hypothesis of the KOSIMO project states that the analysis of an integrated and dynamic databank of political conflict will lead to more accurate propositions about current and future trends of political conflict than conclusions drawn on the basis of databanks that contain exclusively violent conflicts. Then O'Brien forecasted the conditions conducive to conflict (i.e., country instability) over the long term. The model developed by O'Brien did not provide forecasting of the occurrence of conflict because no specific observation was available to identify the specific events that might trigger particular conflicts in the future. However, the author concluded that his model could forecast the possibility of the conflicts 5 years in advance with about 80% accuracy [75][76].

Figure 2.1. Index of Instability [75][76]

Second, O'Brien forecasted the likelihood not only that an instability in some binary sense would occur in any given country in any given year but also that the instability would occur within a certain range or level of intensity, e.g., low, moderate, or high level of violence [75][76]. To achieve this, the author included violent and nonviolent conflict events in the data set to construct an approximate index of country instability for use in validation analyses. The index of instability placed stringent demands on the algorithm used for classification and forecasting. The increased fidelity would be more useful to policy makers as a means for conducting threat assessments and allocating scarce resources to prevent or deter conflict. O'Brien used a pattern classification algorithm developed by Chen called Fuzzy Analysis of Statistical Evidence (FASE) to examine the patterns in the relationship between different configurations of macro-structural variables of a country and the likelihood that country will experience a given intensity level of instability [11]. FASE is a hybrid method that incorporates theoretical elements from statistics, possibility theory, and fuzzy logic which is a branch of fuzzy set theory that is used most often in the field of engineering to discriminate between vague concepts or when quantitative precision is lacking. FASE is based on the

principle of inverse inference and possesses properties not unlike many Bayesian classifiers. This nonparametric technique is particularly well suited for pattern classification problems and was developed specifically for the study on which O'Brien was based.

Third, O'Brien validated a model that could forecast country instability out 15 years by using a split-sample validation design. One portion of the historical database (the training set) is used to train or fit a model of country instability. To determine how well the patterns in these relationships can be discerned by the algorithm and ultimately forecast, O'Brien used the macro-structural values only in the other portion of the data set (the test set) to estimate the likelihood that countries with a given configuration of macro-structural values would experience a certain level of intensity of instability. The author then compared the model's projections with actual occurrences in each country over the period covered in the test set and computed some performance metrics. The results of these out-of-sample validation analyses provided insight into how accurate the "true" forecasts (e.g., projections into the future) would be likely to be [75][76].

Finally, elsewhere O'Brien generated annual forecasts of the likelihood of country instabilities over the period from 2001 to 2015. To achieve this O'Brien used the entire historical data set of 171 countries as a training set. Then using the historical data as a baseline, the author applied a simple forecasting algorithm to project out the trend exhibited by each macro-structural factor for each of the 171 countries to the year 2015, On the basis of the patterns exhibited in the training set over the period from 1975 to 1999 and the forecast values of the macro-structural factors, O'Brien computed the likelihood that each country will experience a certain level of instability over each of the

15 years from 2001 to 2015. Figure 2.2 shows the ACTOR (analyzing complex threats for operations and readiness) forecast result for 2001 provided by O'Brien [75][76].

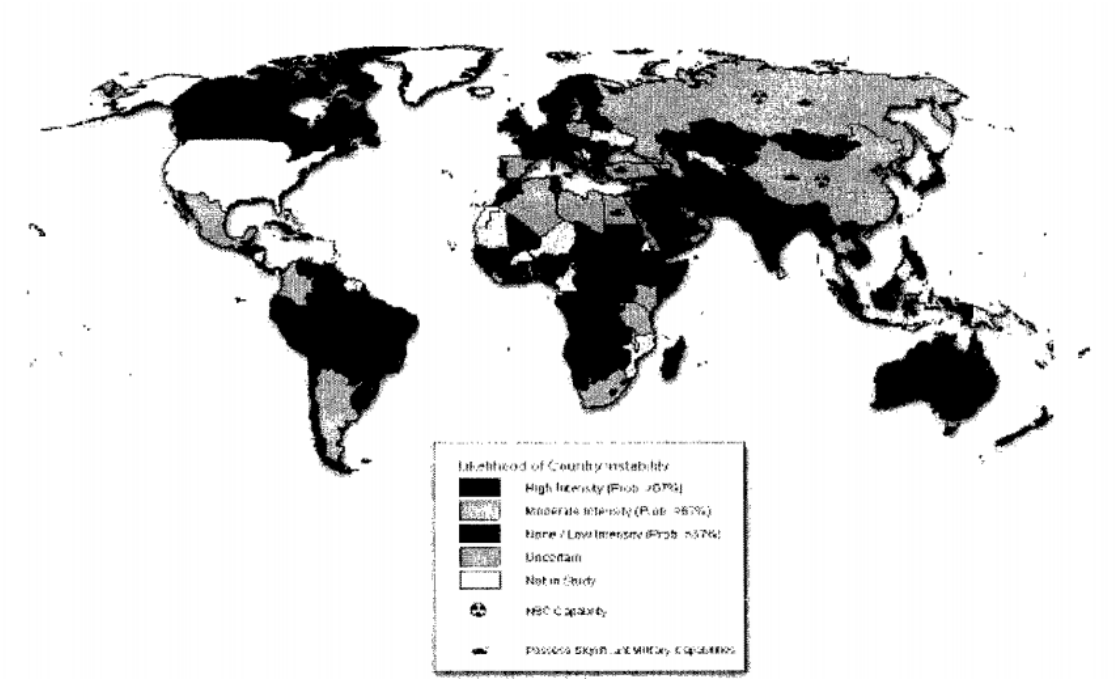

Figure 2.2. Instability Analysis Results For 2001 by O'Brien [75]

One of the limitations of the forecasting model developed by O'Brian was that availability of certain data is limited, such as environmental degradation. The data on ethnic and religious groups are somewhat more plentiful; however, discrepancies often exist between different sources in estimates of the size and characteristics of ethnic and religious groups. Second, the approach taken by O'Brien was of limited utility to the short-term operator who needed to know what kind of conflict might occur (e.g., civil war, interstate war), when it would occur (e.g., within a 3-month window), and the type of event that might trigger it (e.g., a leadership assassination, mass protest and mobilization, or cancellation of popular elections). The approach by O'Brien relied on macro-structural attributes to the neglect of more dynamic causal factors because only a

country's macro-structural attributes could be statistically forecast into the future with a reasonable degree of expected accuracy. Consequently, the model could anticipate the oiliness of the rags but not the spark that will set them ablaze. This limitation could be addressed to some extent by incorporating into the historical training set more dynamic factors, such as indicators of antigovernment protest and government repression. This would allow one to conduct "what-if" drills, develop alternative scenarios, and examine how changes in protest and government repression (or any other modeled factor) might interact with macro-structural factors to alter a country's prospects for stability [75][76].

2.2 Kosimo Database [121]

The Heidelberg Institute for International Conflict Research (HIIK) is an independent and interdisciplinary registered association located at the Department of Political Science at the University of Heidelberg. Since 1991 the HIIK has been committed to the distribution of knowledge about the emergence, course and settlement of interstate and intrastate political conflicts. The Conflict Barometer is published annually and contains the current research result. Furthermore, the HIIK is updating and maintaining the conflict database CONIS (Conflict Information System).

The first edition of the database CONIS had been developed in 2003 especially for the reasons of conflict early warning. It contains the data for the dynamics of development of more than 800 political intrastate and interstate conflicts all over the world since 1945, among them the conflicts presented in the Conflict Barometer. It is updated to Conflict Barometer 2008.

The common of CONIS and the HIIK considers political conflicts a special type of social systems. Because of this methodology conflicts can be gathered empirically and displayed in their whole possible dynamic, starting from a non-violent conflict to a war and to possible de-escalation. Therefore the structure of the CONIS database with its several ten thousand information points allows for a detailed view on conflicts, which also makes transparent the course of violent conflicts of a low intensity. CONIS contains course data for the following variables: intensity, directly involved conflict actors, constellation of the actors, conflict item, and affected country. Since 2003 the CONIS research group has been implementing several research projects basing on the gathered data. The first version of the database, COSIMO 1, comprises data on national and international conflicts from 1945 to 1998 as version 1.3. It was developed in a research project led by Prof. Dr. Frank R. Pfetsch at the University of Heidelberg in 1991.

2.3 A Global Risk Analysis based on the Natural Disaster [21]

Earthquakes, floods, drought, and other natural hazards continue to cause tens of thousands of deaths, hundreds of thousands of injuries, and billions of dollars in economic losses each year around the world. The Emergency Events Database (EM-DAT), a global disaster database maintained by the Centre for Research on the Epidemiology of Disasters (CRED) in Brussels, records upwards of 600 disasters globally each year [122]. Disaster frequency appears to be increasing. Disasters represent a major source of risk for the poor and wipe out development gains and accumulated wealth in developing countries.

As the recognition grows that natural disaster risk must be addressed as a development issue rather than one strictly of humanitarian assistance, so must our efforts to develop the tools to effectively mainstream disaster risk management into development activities. This project has attempted to develop a global, synoptic view of the major natural hazards, assessing risks of multiple disaster-related outcomes and focusing in particular on the degree of overlap between areas exposed to multiple hazards. The overall goal is to identify geographic areas of highest disaster risk potential in order to better inform development efforts.

In this research they assess the risks of two disaster-related outcomes: mortality and economic losses. They estimate risk levels by combining hazard exposure with historical vulnerability for two indicators of elements at risk— gridded population and gross domestic product (GDP) per unit area—for six major natural hazards: earthquakes, volcanoes, landslides, floods, drought, and cyclones. By calculating relative risks for grid cells rather than for countries as a whole, they are able to estimate risk levels at subnational scales.

The global analysis is limited by issues of scale as well as by the availability and quality of data. For a number of hazards, they had only 15- to 25-year records of events for the entire globe and relatively crude spatial information for locating these events. Data on historical disaster losses, and particularly on economic losses, are also limited.

While the data are inadequate for understanding the absolute levels of risk posed by any specific hazard or combination of hazards, they are adequate for identifying areas that are at relatively higher single or multiple hazard risk. In other words, they do not feel

that the data are sufficiently reliable to estimate, for example, the total mortality risk from flooding, earthquakes, and drought over a specified period. Nevertheless, they can identify those areas that are at higher risk of flood losses than others and at higher risk of earthquake damage than others, or at higher risk of both. They can also address in general terms the exposure and potential magnitude of losses to people and their assets in these areas. Such information can inform a range of disaster prevention and preparedness measures, including prioritization of resources, targeting of more localized and detailed risk assessments, implementation of risk-based disaster management and emergency response strategies, and development of long-term land use plans and multiple hazard risk management strategies.

A set of case studies explores risks from particular hazards or for localized areas in more detail, using the same theoretical framework as the global analysis. They hope that in addition to providing interesting and useful results, the global analysis and case studies will stimulate additional research, particularly at national and local levels, which will be increasingly linked to policy making and practice in disaster risk reduction. Within the constraints summarized above, they developed three indexes of disaster risk: First, mortality risks, assessed for global gridded population, second, risks of total economic losses, assessed for global gridded GDP per unit area, and last, risks of economic losses expressed as a proportion of the GDP per unit area for each grid cell

Risks of both mortality and economic losses are calculated as a function of the expected hazard frequency and expected losses per hazard event. They obtained global hazard data on cyclones, drought, earthquakes, floods, landslides, and volcanoes from a variety of sources. The global hazard data sets were improved upon or, in the case of

droughts and landslides, created specifically for the analysis. Vulnerability was estimated by obtaining hazard-specific mortality and economic loss rates for World Bank regions and country wealth classes within them based on 20 years of historical loss data from the EM-DAT database.

They masked out low-population and nonagricultural areas where risks of losses are negligible. After calculating the expected losses for each remaining grid cell, they ranked the grid cells and classified them into deciles (10 classes composed of roughly equal numbers of cells). Cells falling into the highest three deciles for either mortality or economic losses are considered disaster risk hotspots.

Among the findings are that on the order of 25 million square kilometers, about 19 percent of the Earth's land area and 3.4 billion people are relatively highly exposed to at least one hazard. Some 3.8 million square kilometers and 790 million people are relatively highly exposed to at least two hazards. About 0.5 million square kilometers and 105 million people are relatively highly exposed to three or more hazards shown in Figure 2.3.

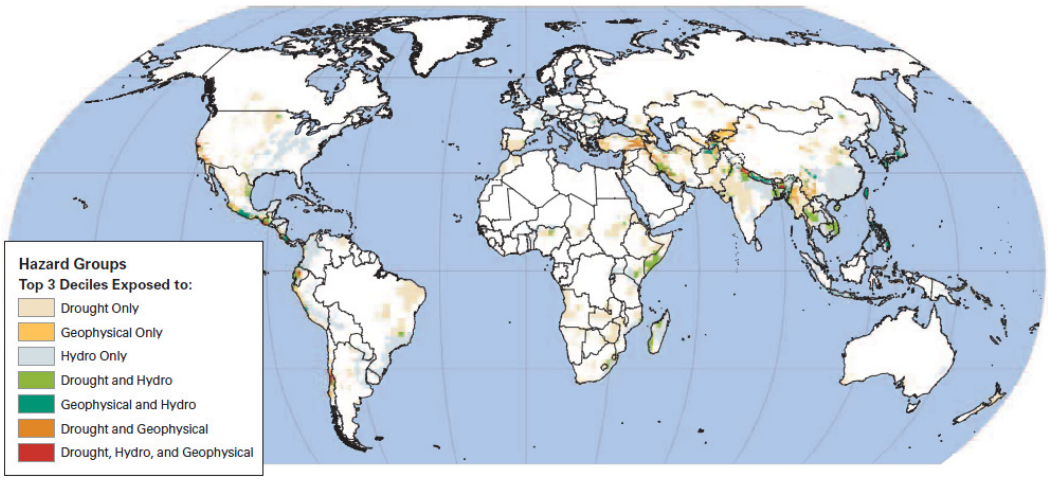

Figure 2.3. Global Distribution of Areas Highly Exposed to Hazards, by Hazard Type [21]

The fact that some areas of the world are subject to multiple hazards will not surprise many residents of those areas, but what this analysis reveals is the extent to which, at global and regional scales, there is substantial overlap between different types of hazards and population concentrations. The world's geophysical hazards—earthquakes and volcanoes—tend to cluster along fault boundaries characterized by mountainous terrain. Hazards driven mainly by hydro-meteorological processes—floods, cyclones, and landslides—strongly affect the eastern coastal regions of the major continents as well as some interior regions of North and South America, Europe, and Asia. Drought is more widely dispersed across the semiarid tropics. The areas subject to both geophysically- and hydro-meteorologically-driven hazards fall primarily in East and South Asia and in Central America and western South America. Many of these areas are also more densely populated and developed than average, leading to high potential for casualties and economic losses. Of particular concern in these areas are possible interactions between different hazards, for example, landslides triggered by cyclones and flooding, or earthquakes that damage dams and reservoirs needed for drought and flood protection.

The global analysis supports the view that disaster risk management is a core issue of development. The degree to which exposure to hazards in developed countries has not led to relatively high mortality in the past two decades in these areas. Areas of Europe and North America that are highly exposed to natural hazards as shown in Figure 2.4, for example, have not experienced correspondingly high mortality from these hazards over the past two decades. The United States is noteworthy in that more than one-third of its population lives in hazard-prone areas but only 1 percent of its land area ranks high in mortality risk.

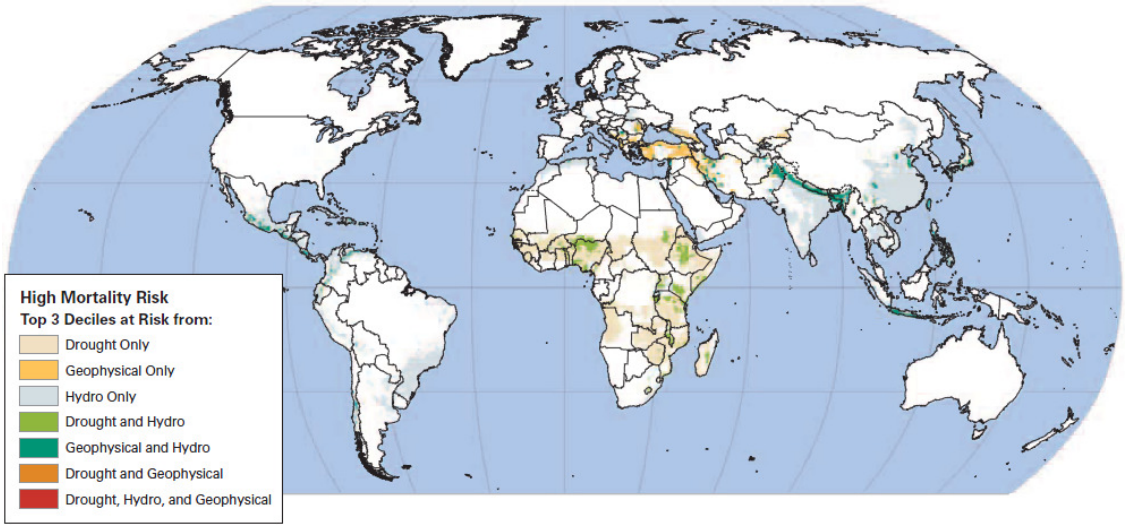

Figure 2.4 Global Distribution of Highest Risk Disaster by Mortality Risks[21]

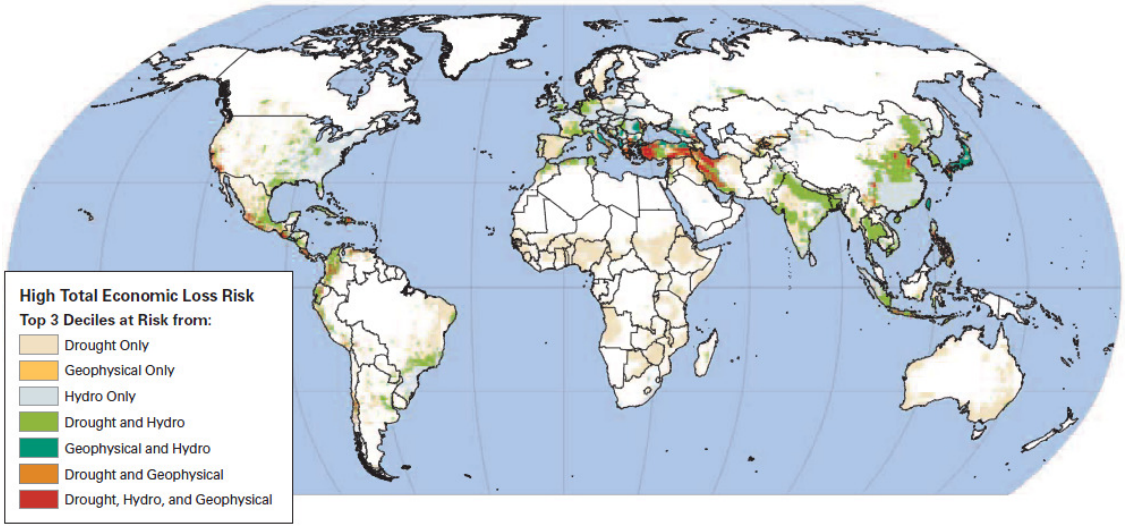

Figure 2.5 Global Distribution of Highest Risk Disaster by Total Economic Loss Risks [21]

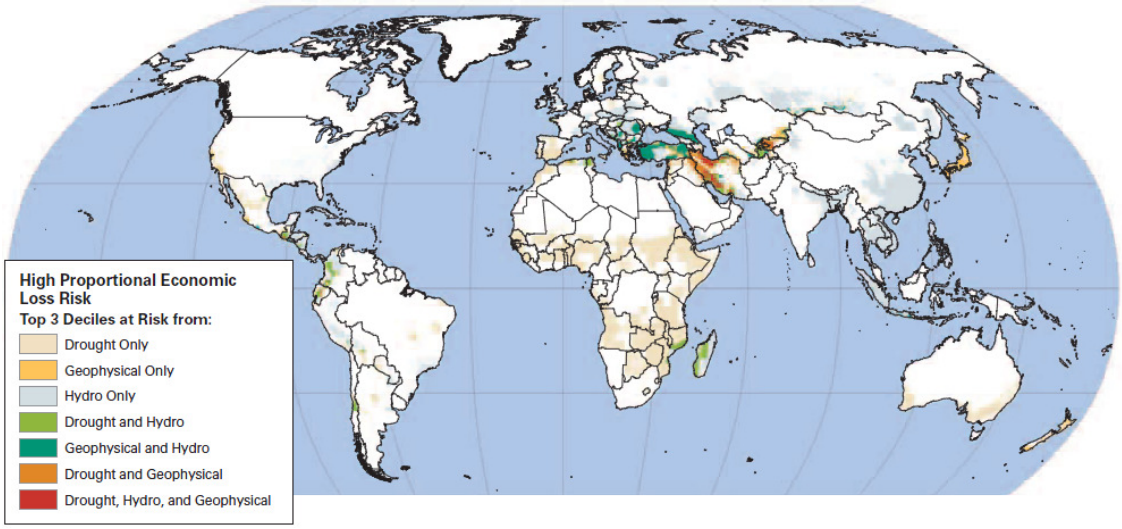

Figure 2.6 Global Distribution of Highest Risk Disaster by a Proportion of GDP Per Unit Area [21]

Figure 2.5 shows the types of hazards for which each grid cell appeared in the top three deciles of the global risk distribution for mortality and economic losses. Figure 2.5 shows that areas at high risk of economic losses are more widely distributed in industrial and lower-middle-income countries than areas of high mortality risk. In addition to portions of Central America and East and South Asia, large areas of the eastern Mediterranean and Middle East appear at high risk of loss from multiple hazards. These regions still rank high when the risk is recalculated by dividing the losses per grid cell by each grid cell's GDP estimate in Figure 2.6. In contrast, much of Europe and the United States no longer rank among the highest risk areas when grid cells are ranked according to losses as a proportion of GDP.

The statistics also suggest that future disasters will continue to impose high costs on human and economic development. In 35 countries, more than 1 in 20 residents lives in an area identified as relatively high in mortality risk from three or more hazards. More

than 90 countries have more than 10 percent of their total population in areas at relatively high mortality risk from two or more hazards in Figure 2.7. And 160 countries have more than one fourth of their total population in areas at relatively high mortality risk from one or more hazards in Figure 2.8,2.9, and 2.10 Similarly, many of the areas at higher risk of loss from multiple hazards are associated with higher-than-average densities of GDP, leading to a relatively high degree of exposure of economically productive areas.

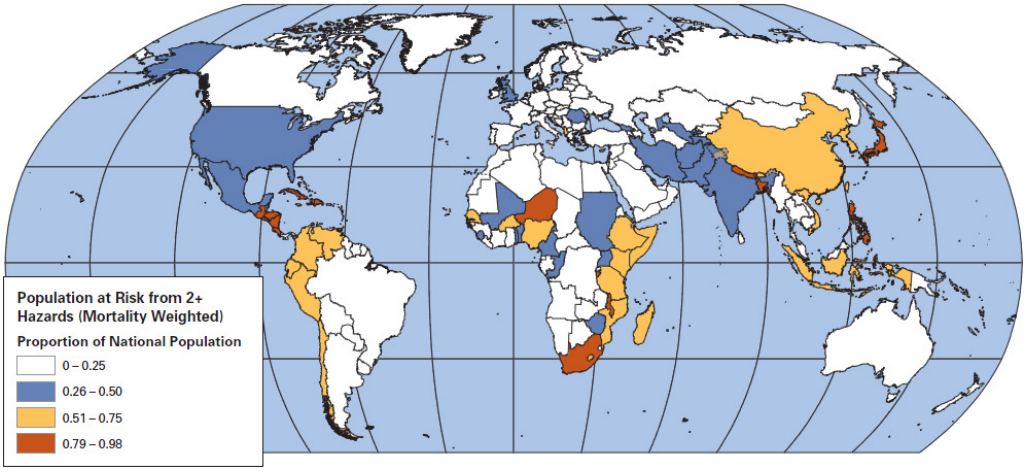

Figure 2.7 Highest Risk Areas from Two or More Hazards (Mortality) [21]

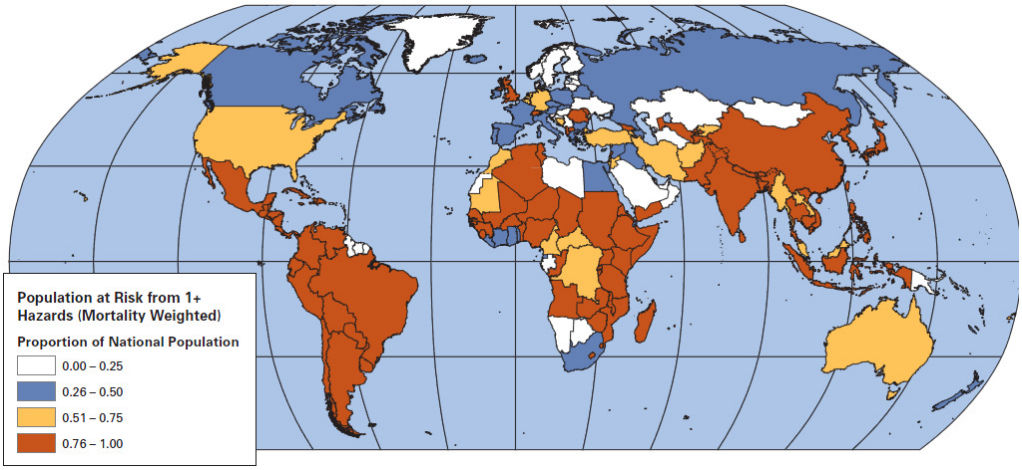

Figure 2.8 Highest Risk Areas from One or More Hazards (Mortality) [21]

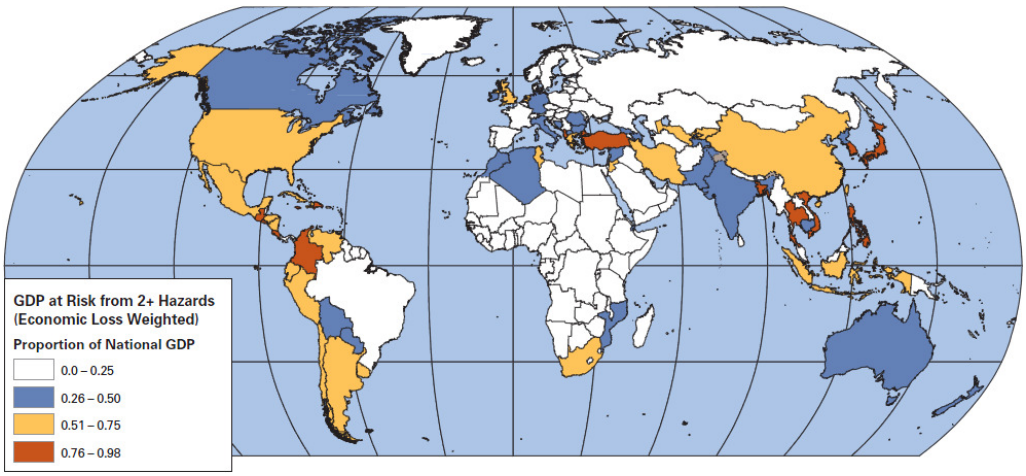

Figure 2.9 Highest Risk Areas from Two or More Hazards (Economic Losses) [21]

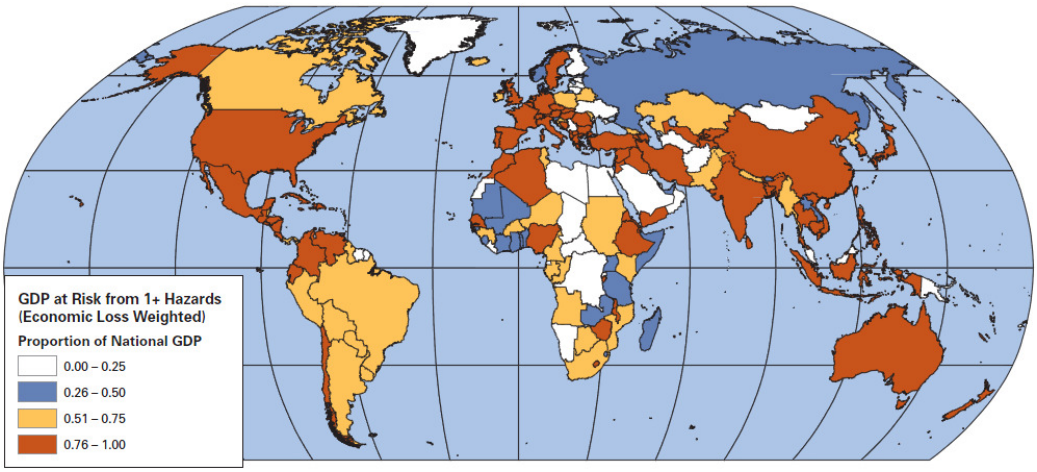

Figure 2.10 Highest Risk Areas from One or More Hazards (Economic Losses) [21]

Until vulnerability, and consequently risks, are reduced, countries with high proportions of population or GDP in hotspots are especially likely to incur repeated disaster-related losses and costs. Comparison of these maps with data on relief and reconstruction costs is instructive in this regard. Data on relief costs associated with natural disasters from 1992 to 2003 are available from the Financial Tracking System (FTS) of the United Nations Office for the Coordination of Humanitarian Affairs (OCHA) [123]. Total relief costs over this period are US$2.5 billion. Of this, US$2 billion went to just 20 countries, primarily for disasters involving the following hazards (listed in order of magnitude of the relief amount allocated): China (earthquakes and floods); India (earthquakes, floods, and storms); Bangladesh (floods); the Arab Republic of Egypt (earthquakes); Mozambique (floods); Turkey (earthquakes); Afghanistan (drought and earthquakes); El Salvador (earthquakes); Kenya (drought and floods); the Islamic Republic of Iran (earthquakes); Pakistan (drought and floods); Indonesia (drought, earthquakes, and floods); Peru (earthquakes and floods); Democratic Republic of Congo (volcanoes); Poland (floods); Vietnam (floods and storms); Colombia (earthquakes); Venezuela (floods); Tajikistan (droughts and floods); and Cambodia (floods). All of these countries except Egypt have more than half of their population in areas at relatively high risk from one or more hazards in Figure 2.8. The countries subject to multiple hazards in this list also are among those countries with at least one-fourth of their populations in areas at risk from two or more hazards in Figure 2.9. The correspondence with economic losses is not quite as strong in Figure 2.9 and Figure 2.10.

Total World Bank emergency lending from 1980 to 2003 was US$14.4 billion [112]. Of this, US$12 billion went to 20 countries, primarily for the following hazards

(listed in order of highest loan amount): India (drought, earthquakes, and storms); Turkey (earthquakes and floods); Bangladesh (floods and storms); Mexico (earthquakes and floods); Argentina (floods); Brazil (floods); Poland (floods); Colombia (earthquakes and floods); the Islamic Republic of Iran (earthquakes); Honduras (floods and storms); China (earthquakes and floods); Chile (earthquakes); Zimbabwe (drought); the Dominican Republic (storms); El Salvador (earthquakes); Algeria (earthquakes and floods); Ecuador (earthquakes and floods; Mozambique (drought and floods); the Philippines (earthquakes); and Vietnam (floods). All of these countries except Poland have half of their population in areas at relatively high mortality risk from one or more hazards in Figure 2.8, and all of them have at least half of their GDP in areas of relatively high economic risk from one or more hazards in Figure 2.10.

Recognizing the limitations of the global analysis, they undertook a number of case studies designed to investigate the potential of the hotspots approach at regional, national, and subnational scales, drawing on more detailed and reliable data sources as well as on expert knowledge concerning specific hazards and regions. Three case studies addressed specific hazards: storm surges, landslides, and drought. Three case studies addressed regional multihazard situations: Sri Lanka, the Tana River basin in Kenya, and the city of Caracas, Venezuela. The following are the key findings from the case studies:

1. Scale matters. Geographic areas that are identified as hotspots at the global scale may have a highly variable spatial distribution of risk at finer scales.

2. Scale affects data availability and quality. Hazard, exposure, and vulnerability data are available at subnational resolutions for individual countries and even cities, as the

analyses for Sri Lanka and Caracas show. More comprehensive, finer resolution, and better quality data permit more complete, accurate, and reliable identification of multihazard hotspots.

3. Scale affects the utility of the results. Better data resolution and a richer set of variables contribute to results that are more relevant for risk management planning at the national to local scale, as illustrated in the case study from Caracas. This is highly important, as decisions made at the local and national scales have perhaps the greatest potential to affect risk levels directly, whether positively or negatively.

4. The global- and local-scale analyses are complementary. In some instances, national-to-local level risk assessors and planners may be able to "downscale" global data for finer scale risk assessment to compensate for a lack of local data. Ideally, however, global analyses would be scaled up—generalized from more detailed, finer scale data. In practice, many barriers still remain. The global infrastructure for systematically assembling and integrating relevant data sets for disaster risk assessment at multiple scales remains inadequate. Nonetheless, the fact that relevant data sets can be obtained and integrated at various scales creates the hope that one day data can be collected and shared routinely to improve disaster risk assessment both globally and locally.

The Hotspots project has created an initial picture of the location and characteristics of disaster hotspots: areas at relatively high risk from one or more natural hazards. The findings of the analysis support the view that disasters will continue to impose high costs on human and economic development, and that disaster risk should be managed as an integral part of development planning rather than thought of strictly as a

humanitarian issue. The following paragraphs detail how disaster risk information can be useful for development policy and decision makers, and how it can be further developed in order to increase its usefulness.

The combination of human and economic losses, plus the additional costs of relief, rehabilitation, and reconstruction, makes disasters an economic as well as a humanitarian issue. Until vulnerability, and consequently risks, are reduced, countries with high proportions of population or GDP in hotspots are especially likely to incur repeated disaster-related losses and costs. Disaster risks, therefore, deserve serious consideration as an issue for sustainable development in high-risk areas.

The significance of high mortality and economic loss risks for socioeconomic development extends well beyond the initial direct losses to the population and economy during disasters. Covariate losses accompanying mortality, for example, include partial or total loss of household assets, lost income, and lost productivity. Widespread disaster-related mortality can affect households and communities for years, decades, and even generations.

In addition to mortality and its long-term consequences, both direct and indirect economic losses must be considered [112]. Direct losses are losses to assets, whereas indirect losses are the losses that accrue while productive assets remain damaged or destroyed. During disasters, both direct and indirect losses accumulate across the social, productive, and infrastructure sectors. The pattern of losses depends on the type of hazard and the affected sectors' vulnerabilities to the hazard. In large disasters, cumulative losses across sectors can have macroeconomic impacts.

Disasters impose costs in addition to human and economic losses. Costs include expenditures for disaster relief and recovery and for rehabilitation and reconstruction of damaged and destroyed assets. In major disasters, meeting these additional costs can require external financing or international humanitarian assistance. Disaster relief costs drain development resources from productive investments to support consumption over short periods. Emergency loans have questionable value as vehicles for long-term investment and contribute to country indebtedness without necessarily improving economic growth or reducing poverty. As disasters continue to occur, high-risk countries will continue to need high levels of humanitarian relief and recovery lending unless their vulnerability is reduced.

The Hotspots analysis has implications for development investment planning, disaster preparedness, and loss prevention. The highest risk areas are those in which disasters are expected to occur most frequently and losses are expected to be highest. This provides a rational basis for prioritizing risk-reduction efforts and highlights areas where risk management is most needed.

International development organizations are key stakeholders with respect to the global analysis. The analysis provides a scientific basis for understanding where risks are highest and why, as well as a methodological framework for regional- and local-scale analysis. The identified risks then can be evaluated further using more detailed data in the context of a region's or country's overall development strategy and priorities. This would serve development institutions and the countries in several ways to facilitate the development of better-informed investment strategies and activities.

Assistance Strategies: A development institution such as the World Bank may use the analysis at the global and/or regional level to identify countries that are at higher risk of disasters and "flag" them as priorities to ensure that disaster risk management is addressed in the development of a Country Assistance Strategy (CAS). While in some countries there can be a seemingly long list of urgent priorities to address in a CAS—e.g., reducing extreme poverty, fighting HIV/AIDS, promoting education, achieving macroeconomic stability—managing disaster risk should be considered an integral part of the development planning to protect the investments made rather than as a stand-alone agenda. The CAS should consider the consequences of unmitigated disaster risk in terms of possible tradeoffs with long-term socioeconomic goals.

Sector Investment Operations: In high-risk regions and countries, it is particularly important to protect investments from damage or loss, either by limiting hazard exposure or by reducing vulnerability. Risks of damage and loss should also be taken into account when estimating economic returns during project preparation. Investment project preparation, particularly in the high-risk areas identified in the global analysis, would benefit from including a risk assessment as a standard practice. This report's theory and methods can be translated easily into terms of reference for such assessments. Such assessments should identify probable hazards, as well as their spatial distribution and temporal characteristics (including return periods), and should evaluate vulnerabilities to the identified hazards that should be addressed in the project design.

Risk Reduction Operations: In high-risk countries and areas within countries, repeated, large-scale loss events can harm economic performance (Benson and Clay 2004). It may be impossible to achieve development goals such as poverty alleviation in

these areas without concerted efforts to reduce recurrent losses. Increasingly, risk and loss reduction are being seen as investments in themselves, and disaster-prone countries are demonstrating a willingness to undertake projects in which disaster and loss reduction are the principal aims. Such projects can include both hard and soft components: measures to reduce the vulnerability and exposure of infrastructure, as well as emergency funds and institutional, policy and capacity-building measures designed to increase the abilities of countries to manage disaster risks.

Contingency Financing: Emergency recovery and reconstruction needs after a major disaster may create a high demand for emergency financing. While such loans are usually appraised and approved relatively quickly, at times there can be delays in disbursing the funds, which increase the social and economic impacts of the disaster. Advance planning for recovery and resource allocation would allow for better targeting of resources toward investments that would restore economic activity quickly and relieve human suffering. This report's global disaster risk analysis provides a basis for identifying situations in which future emergency recovery loans are likely to be needed. This creates an opportunity for "preappraising" emergency loans, that is, designing a risk management strategy to guide the allocation of emergency reconstruction resources should such resources become necessary, or to arrange for other types of contingency financing with development banks.

The Hotspots project provides a common framework for improving risk identification and promoting risk management through a dialogue between organizations and individuals operating at various geographic scales. The methods and results provide useful tools for integrating disaster risk management into development efforts and should

be developed further. As a global analysis conducted with very limited local level participation and based on incomplete data, the results presented here should not provide the sole basis for designing risk management activities. The analysis does, however, provide a scientific basis for understanding where risks are highest and why, as well as a methodological framework for regional- and local scale analysis. The identified risks then can be evaluated further using more detailed data in the context of a region's or country's overall development strategy and priorities.

They have designed the Hotspots approach to be open-ended to allow additional studies to be incorporated on an ongoing basis. It provides a common framework for improving risk identification and promoting risk management through a dialogue between organizations and individuals operating at various geographic scales. The Hotspots analysis can be improved upon as a tool and developed in several directions.

Improve Underlying Databases. The first direction is to pursue the many opportunities in both the short and long term to improve the underlying databases for assessing disaster risks and losses. A range of new global scale data sets is currently under development, including a new global urban-extent database being developed by CIESIN in support of the Millennium Ecosystem Assessment. A joint project between the Earth Institute, the World Bank, and the Millennium Project will develop a much more detailed and complete database on subnational poverty and hunger. Much more comprehensive regional data sets will become available in specific areas of interest. On a regional scale, there are also much longer records of hazard events for specific hazards that could be harnessed to improve estimates of hazard frequency and intensity in high-risk areas [77]. Significant improvements could be made in characterizing flood, drought

and landslide hazards in particular. Existing data on disaster-related losses is being compiled into a multi-tiered system through which regularly updated historical data from multiple sources can be accessed. Additional work to link and cross-check existing data is needed, however, as is improvement in the assessment and documentation of global economic losses.

Undertake Case Studies. A second direction is to explore more fully the applicability and utility of the Hotspots approach to analysis and decision making at regional, national, and local scales. The initial case studies are promising, but are certainly not on their own sufficient to demonstrate the value of the overall approach or the specific data and methods under different conditions. More direct involvement of potential stakeholders would be valuable in extending the approach to finer scales of analysis and decision making. To be effective, efforts to improve risk identification in hotspot areas should be part of a complete package of technical and financial support for the full range of measures needed to manage disaster risks, including risk reduction and transfer.

Explore Long-term Trends. A third direction is to explore a key long-term issue: the potential effect of underlying changes in hazard frequency (for example, due to human-induced climatic change) coupled with long-term trends in human development and settlement patterns. To what degree could changes in tropical storm frequency, intensity, and position interact with continued coastal development (both urban and rural) to increase risks of death and destruction in these regions? Are agricultural areas, already under pressure from urbanization and other land use changes, likely to become more or less susceptible to drought, severe weather, or floods? Could other hazards such as

wildfires potentially interact with changing patterns of drought, landslides, deforestation, and land use to create new types of hotspots? Although some aspects of these questions have been addressed in the general context of research on climate change impacts, the interactions between climate change, the full range of hazards, and evolving human hazard vulnerability have not been fully explored [9][6].

Pursuing work in these directions will necessarily involve a wide range of institutions—national, regional and international, public and private sector, academic and operational. They hope that the Hotspots project has contributed a building block in the foundation of a global effort to reduce disaster-related losses by managing risks rather than by managing emergencies. They look forward to continuing collaboration with partners at all levels to put in place a global disaster risk management support system in order to mobilize the knowledge and resources necessary to achieve the goal.

2.4 Requirement Analysis in System Engineering [24]

2.4.1 System Engineering process inputs

The inputs to the process include the customer's requirements and the project constraints. Requirements relate directly to the performance characteristics of the system being designed. They are the stated life-cycle customer needs and objectives for the system, and they relate to how well the system will work in its intended environment.

Constraints are conditions that exist because of limitations imposed by external interfaces, project support, technology, or life cycle support systems. Constraints bound the development teams' design opportunities.

Requirements are the primary focus in the systems engineering process because the process's primary purpose is to transform the requirements into designs. The process develops these designs within the constraints. They eventually must be verified to meet both the requirements and constraints.

Requirements are categorized in several ways. The following are common categorizations of requirements that relate to technical management:

Customer Requirements: Statements of fact and assumptions that define the expectations of the system in terms of mission objectives, environment, constraints, and measures of effectiveness and suitability (MOE/MOS). The customers are those that perform the eight primary functions of systems engineering with special emphasis on the operator as the key customer. Operational requirements will define the basic need and, at a minimum, answer the following questions.

• Operational distribution or deployment: Where will the system be used?

• Mission profile or scenario: How will the system accomplish its mission objective?

• Performance and related parameters: What are the critical system parameters to accomplish the mission?

• Utilization environments: How are the various system components to be used?

• Effectiveness requirements: How effective or efficient must the system be in performing its mission?

• Operational life cycle: How long will the system be in use by the user?

• Environment: What environments will the system be expected to operate in an effective manner?

Functional Requirements: The necessary task, action or activity that must be accomplished. Functional (what has to be done) requirements identified in requirements analysis will be used as the toplevel functions for functional analysis.

Performance Requirements: The extent to which a mission or function must be executed; generally measured in terms of quantity, quality, coverage, timeliness or readiness. During requirements analysis, performance (how well does it have to be done) requirements will be interactively developed across all identified functions based on system life cycle factors; and characterized in terms of the degree of certainty in their estimate, the degree of criticality to system success, and their relationship to other requirements.

Design Requirements: The "build to," "code to," and "buy to" requirements for products and "how to execute" requirements for processes expressed in technical data packages and technical manuals. Derived Requirements: Requirements that are implied or transformed from higher-level requirement. For example, a requirement for long range or high speed may result in a design requirement for low weight.

Allocated Requirements: A requirement that is established by dividing or otherwise allocating a high-level requirement into multiple lower-level requirements. Example: A 100-pound item that consists of two subsystems might result in weight requirements of 70 pounds and 30 pounds for the two lower-level items.

The attributes of good requirements include the following:

•A requirement must be achievable. It must reflect need or objective for which a solution is technically achievable at costs considered affordable.

• It must be verifiable—that is, not defined by words such as excessive, sufficient, resistant, etc. The expected performance and functional utility must be expressed in a manner that allows verification to be objective, preferably quantitative.

• A requirement must be unambiguous. It must have but one possible meaning.

• It must be complete and contain all mission profiles, operational and maintenance concepts, utilization environments and constraints. All information necessary to understand the customer's need must be there.

• It must be expressed in terms of need, not solution; that is, it should address the "why" and "what" of the need, not how to do it.

• It must be consistent with other requirements. Conflicts must be resolved up front.

• It must be appropriate for the level of system hierarchy. It should not be too detailed that it constrains solutions for the current level of design. For example, detailed requirements relating to components would not normally be in a system-level specification.

2.4.2 Requirement Analysis of the System Engineering

Requirements analysis involves defining customer needs and objectives in the context of planned customer use, environments, and identified system characteristics to determine requirements for system functions. Prior analyses are reviewed and updated, refining mission and environment definitions to support system definition.

Requirements analysis is conducted iteratively with functional analysis to optimize performance requirements for identified functions, and to verify that

synthesized solutions can satisfy customer requirements. The purpose of Requirements Analysis is to:

• Refine customer objectives and requirements;

• Define initial performance objectives and refine them into requirements;

• Identify and define constraints that limit solutions; and

• Define functional and performance requirements based on customer provided measures of effectiveness.

In general, Requirements Analysis should result in a clear understanding of:

• Functions: What the system has to do,

• Performance: How well the functions have to be performed,

• Interfaces: Environment in which the system will perform, and

• Other requirements and constraints.

The understandings that come from requirements analysis establish the basis for the functional and physical designs to follow. Good requirements analysis is fundamental to successful design definition.

Typical inputs include customer needs and objectives, missions, MOE/MOS, environments, key performance parameters (KPPs), technology base, output requirements from prior application of SEP, program decision requirements, and suitability requirements.

Inputs converted to outputs consist of customer requirements, mission and MOEs (MNS, ORD), maintenance concept and other life-cycle function planning, and SE

outputs from prior development efforts.The controls for requirement analysis are laws and organizational policies and procedures, military specific requirements, utilization environments, and tech base and other constraints. The enablers to obtain the outputs are multi-disciplinary product teams, decision and requirements database including system/configuration item descriptions from prior efforts, and system analysis and control. This diagram is shown in the Figure 2.11.

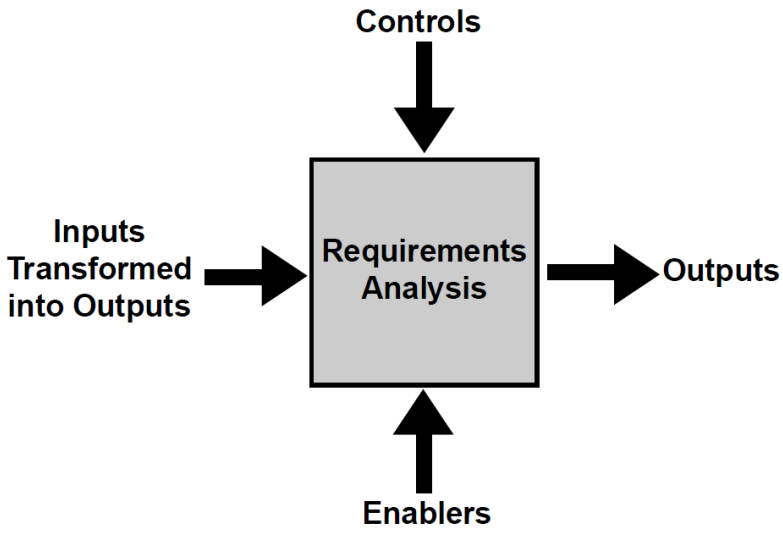

Figure 2.11. Inputs to Requirements Analysis [24]

Input requirements must be comprehensive and defined for both system products and system processes such as development, manufacturing, verification, deployment, operations, support, training and disposal. These are eight primary functions for input requirements analysis.

The operator customers have expertise in the operational employment of the product or item being developed. The developers like government and contractors are not necessarily competent in the operational aspects of the system under development.

Typically, the operator's need is neither clearly nor completely expressed in a way directly usable by developers. It is unlikely that developers will receive a well-defined problem from which they can develop the system specification. Thus, teamwork is necessary to understand the problem and to analyze the need. It is imperative that customers are part of the definition team.

On the other hand, customers often find it easier to describe a system that attempts to solve the problem rather than to describe the problem itself. Although these "solutions" may be workable to some extent, the optimum solution is obtained through a proper technical development effort that properly balances the various customer mission objectives, functions, MOE/MOS, and constraints. An integrated approach to product and process development will balance the analysis of requirements by providing understanding and accommodation among the eight primary functions.

Requirements Analysis is a process of inquiry and resolution. The following are typical questions that can initiate the thought process:

- What are the reasons behind the system development?
- What are the customer expectations?
- Who are the users and how do they intend to use the product?
- What do the users expect of the product?
- What is their level of expertise?
- With what environmental characteristics must the system comply?
- What are existing and planned interfaces?
- What functions will the system perform, expressed in customer language?

• What are the constraints (hardware, software, economic, procedural) to which the system must comply?

• What will be the final form of the product: such as model, prototype, or mass production?

This list can start the critical, inquisitive outlook necessary to analyze requirements, but it is only the beginning. A tailored process similar to the one at the end of this chapter must be developed to produce the necessary requirements analysis outputs.

2.4.3 REQUIREMENTS ANALYSIS OUTPUTS

The requirements that result from requirements analysis are typically expressed from one of three perspectives or views. These have been described as the Operational, Functional, and Physical views. All three are necessary and must be coordinated to fully understand the customers' needs and objectives. All three are documented in the decision database.

The Operational View addresses how the system will serve its users. It is useful when establishing requirements of "how well" and "under what condition." Operational view information should be documented in an operational concept document that identifies:

• Operational need definition,

• System mission analysis,

• Operational sequences,

• Operational environments,

• Conditions/events to which a system must respond,

• Operational constraints on system,

• Mission performance requirements,

• User and maintainer roles (defined by job tasks and skill requirements or constraints),

• Structure of the organizations that will operate, support and maintain the system

• Operational interfaces with other systems.

Analyzing requirements requires understanding the operational and other life cycle needs and constraints.

The Functional View focuses on WHAT the system must do to produce the required operational behavior. It includes required inputs, outputs, states, and transformation rules. The functional requirements, in combination with the physical requirements shown below, are the primary sources of the requirements that will eventually be reflected in the system specification. Functional View information includes:

• System functions

• System performance: qualitative, quantitative and timeliness

• Tasks or actions to be performed

• Inter-function relationships

• Hardware and software functional relationships

• Performance constraints

• Interface requirements including identification of potential open-system opportunities (potential standards that could promote open systems should be identified)

• Unique hardware or software

• Verification requirements (to include inspection, analysis/simulation, demo, and test).

The Physical View focuses on HOW the system is constructed. It is key to establishing the physical interfaces among operators and equipment, and technology requirements. Physical View information would normally include:

• Configuration of System: Interface descriptions, characteristics of information displays and operator controls, relationships of operators to system/ physical equipment, and operator skills and levels required to perform assigned functions.

• Characterization of Users: Handicaps (special operating environments), constraints (movement or visual limitations).

• System Physical Limitations: Physical limitations (capacity, power, size, weight), technology limitations (range, precision, data rates, frequency, language), government Furinished Equipment (GFE), Commercial-Off-the-Shelf (COTS), Nondevelopmental Item (NDI), reusability requirements, and necessary or directed standards.

In summary, an initial statement of a need is seldom defined clearly. A significant amount of collaboration between various life cycle customers is necessary to produce an acceptable requirements document. Requirements are a statement of the problem to be solved. Unconstrained and nonintegrated requirements are seldom sufficient for designing a solution. Because requirements from different customers will conflict, constraints will limit options, and resources are not unlimited; trade studies must be accomplished in order to select a balanced set of requirements that provide feasible solutions to customer needs.

The following section provides a list of tasks that represents a plan to analyze requirements. Part of this notional process is based on the 15 requirements analysis tasks

listed in IEEE P1220. This industry standard and others should be consulted when preparing engineering activities to help identify and structure appropriate activities.

As with all techniques, the student should be careful to tailor; that is, add or subtract, as suits the particular system being developed. Additionally, these tasks, though they build on each other, should not be considered purely sequential. Every task contributes understanding that may cause a need to revisit previous task decisions. This is the nature of all System Engineering activities.

First step is the preparation to establish and maintain decision database. When beginning a systems engineering process, be sure that a system is in place to record and manage the decision database. The decision database is an historical database of technical decisions and requirements for future reference. It is the primary means for maintaining requirements traceability. This database decision management system must be developed or the existing system must be reviewed and upgraded as necessary to accommodate the new stage of product development. A key part of this database management system is a Requirements Traceability Matrix that maps requirements to subsystems, configuration items, and functional areas. This must be developed, updated, and reissued on a regular basis. All requirements must be recorded. Remember: If it is not recorded, it cannot be an approved requirement.

The IEEE Systems Engineering Standard offers a process for performing Requirements Analysis that comprehensively identifies the important tasks that must be performed. These 15 task areas to be analyzed follow.

1. Customer expectations

2. Project and enterprise constraints

3. External constraints

4. Operational scenarios

5. Measure of effectiveness (MOEs)

6. System boundaries

7. Interfaces

8. Utilization environments

9. LIfe cycle

10. Functional requirements

11. Performance requirements

12. Modes of operation

13. Technical performance measures

14. Physical characteristics

15. Human systems integration

First task is to define and quantify customer expectations. They may come from any of the eight primary functions, operational requirements documents, mission needs, technology-based opportunity, direct communications with customer, or requirements from a higher system level. The purpose of this task is to determine what the customer wants the system to accomplish, and how well each function must be accomplished. This should include natural and induced environments in which the product(s) of the system must operate or be used, and constraints (e.g. funding, cost, or price objectives, schedule, technology, nondevelopmental and reusable items, physical characteristics, hours of operation per day, on-off sequences, etc.).

The second task is to identify and define constraints impacting design solutions. Project specific constraints can include:

• Approved specifications and baselines developed from prior applications of the Systems Engineering Process,

• Costs,

• Updated technical and project plans,

• Team assignments and structure,

• Control mechanisms, and

• Required metrics for measuring progress.

Enterprise constraints can include:

• Management decisions from a preceding technical review,

• Enterprise general specifications,

• Standards or guidelines,

• Policies and procedures,

• Domain technologies, and

• Physical, financial, and human resource allocations to the project.

Third task is to identify and define external constraints impacting design solutions or implementation of the Systems Engineering Process activities. External constraints can include:

• Public and international laws and regulations,

• Technology base,

• Compliance requirements: industry, international, and other general specifications, standards, and guidelines which require compliance for legal, interoperability, or other reasons,

• Threat system capabilities, and

• Capabilities of interfacing systems.

Forth task is to identify and define operational scenarios that scope the anticipated uses of system product(s). For each operational scenario, define expected:

• Interactions with the environment and other systems, and

• Physical interconnectivities with interfacing systems, platforms, or products.

Fifth task is to identify and define systems effectiveness measures that reflect overall customer expectations and satisfaction. MOEs are related to how well the system must perform the customer's mission. Key MOEs include mission performance, safety, operability, reliability, etc. MOSs are related to how well the system performs in its intended environment and includes measures of supportability, maintainability, ease of use, etc.

Sixth task is to define system boundaries including:

• Which system elements are under design control of the performing activity and which fall outside of their control, and

• The expected interactions among system elements under design control and external and/or higher-level and interacting systems outside the system boundary (including open systems approaches).

Seventh task is to define the functional and physical interfaces to external or higher-level and interacting systems, platforms, and/or products in quantitative terms (include open systems approach). Functional and physical interfaces would include mechanical, electrical, thermal, data, control, procedural, and other interactions. Interfaces may also be considered from an internal/external perspective. Internal interfaces are those that address elements inside the boundaries established for the system addressed. These interfaces are generally identified and controlled by the contractor responsible for developing the system. External interfaces, on the other hand, are those which involve entity relationships outside the established boundaries, and these are typically defined and controlled by the government.

Eighth task is to define the environments for each operational scenario. All environmental factors (natural or induced) which may impact system performance must be identified and defined. Environmental factors include:

- Weather conditions (e.g., rain, snow, sun, wind, ice, dust, fog),
- Temperature ranges,
- Topologies (e.g., ocean, mountains, deserts, plains, vegetation),
- Biological (e.g., animal, insects, birds, fungi),
- Time (e.g., dawn, day, night, dusk), and
- Induced (e.g., vibration, electromagnetic, chemical).

Ninth Task is to analyze the outputs of tasks 1-8 to define key life cycle process requirements necessary to develop, produce, test, distribute, operate, support, train, and dispose of system products under development. Use integrated teams representing the

eight primary functions. Focus should be on the cost drivers and higher risk elements that are anticipated to impact supportability and affordability over the useful life of the system.

Tenth task is to define what the system must accomplish or must be able to do. Functions identified through requirements analysis will be further decomposed during functional analysis and allocation.

Eleventh task is to define the performance requirements for each higher-level function performed by the system. Primary focus should be placed on performance requirements that address the MOEs, and other KPPs established in test plans or identified as interest items by oversight authorities.

Twelfth task is to define the various modes of operation for the system products under development. Conditions (e.g., environmental, configuration, operational, etc.) that determine the modes of operation should be included in this definition.

Thirteenth task is to identify the key indicators of system performance that will be tracked during the design process. Selection of TPMs should be limited to critical technical thresholds and goals that, if not met, put the project at cost, schedule, or performance risk. TPMs involve tracking the actual versus planned progress of KPPs such that the manager can make judgments about technical progress on a by-exception basis. To some extent TPM selection is phase dependent. They must be reconsidered at each systems engineering process step and at the beginning of each phase.

Forteenth task is to identify and define required physical characteristics (e.g., color, texture, size, weight, buoyancy) for the system products under development.

Identify which physical characteristics are true constraints and which can be changed, based on trade studies.

The last task is to identify and define human factor considerations (e.g., physical space limits, climatic limits, eye movement, reach, ergonomics) which will affect operation of the system products under development. Identify which human systems integration are constraints and which can be changed based on trade studies.

The follow-on tasks are related to the iterative nature of the Systems Engineering Process. These three tasks consists of to integrate requirements, to validate requirements, and verify requirements.

To integrate requirements, take an integrated team approach to requirements determination so that conflicts among and between requirements are resolved in ways that result in design requirements that are balanced in terms of both risk and affordability.

To validate requirements, validate that the derived functional and performance can be traced to the operational requirements, during Functional Analysis and Allocation.

To verify requirements, first, coordinate design, manufacturing, deployment and test processes. Second, ensure that requirements are achievable and testable. Third, verify that the design-to-cost goals are achievable. And last, verify that the functional and physical architectures defined during Functional Analysis/Allocation and Synthesis meet the integrated technical, cost, and schedule requirements within acceptable levels of risk.

2.5 Paradigm Shift of Navy Operational Vision [16]

Sea-based operations use revolutionary information superiority and dispersed, networked force capabilities to deliver unprecedented offensive power, defensive assurance, and operational independence to Joint Force Commanders. The 21st century sets the stage for tremendous increases in naval precision, reach, and connectivity, ushering in a new era of joint operational effectiveness. Innovative concepts and technologies will integrate sea, land, air, space, and cyberspace to a greater extent than ever before. In this unified battle space, the sea will provide a vast maneuver area from which to project direct and decisive power around the globe.

Future naval operations will use revolutionary information superiority and dispersed, networked force capabilities to deliver unprecedented offensive power, defensive assurance, and operational independence to Joint Force Commanders. Our Navy and its partners will dominate the continuum of warfare from the maritime domain—deterring forward in peacetime, responding to crises, and fighting and winning wars.

By doing so, U.S. Navy will continue the evolution of U.S. naval power from the blue-water, war-at-sea focus of the maritime strategy [111], through the littoral emphasis of "... From the Sea" [79] and "Forward ... from the Sea" [20], to a broadened strategy in which naval forces are fully integrated into global joint operations against regional and transnational dangers.

To realize the opportunities and navigate the challenges ahead, U.S. Navy must have a clear vision of how our Navy will organize, integrate, and transform. "Sea Power 21" is that vision. It will align our efforts, accelerate our progress, and realize the

potential of our people. "Sea Power 21" will guide our Navy as U.S. Navy defend our nation and defeat our enemies in the uncertain century. Sea Power 21 consists of three concepts. First, Sea Strike means projecting precise and persistent offensive power. Second, Sea Shield means projecting global defensive assurance. And last, Sea Basing means projecting joint operational independence.

Figure 2.12 Concepts of Sea Power 21 [105]

The events of 11 September 2001 tragically illustrated that the promise of peace and security in the new century is fraught with profound dangers: nations poised for conflict in key regions, widely dispersed and well-funded terrorist and criminal organizations, and failed states that deliver only despair to their people.

These dangers will produce frequent crises, often with little warning of timing, size, location, or intensity. Associated threats will be varied and deadly, including weapons of mass destruction, conventional warfare, and widespread terrorism. Future

enemies will attempt to deny us access to critical areas of the world, threaten vital friends and interests overseas, and even try to conduct further attacks against the American homeland. These threats will pose increasingly complex challenges to national security and future war fighting.

Previous strategies addressed regional challenges. Today, U.S. Navy must think more broadly. Enhancing security in this dynamic environment requires us to expand our strategic focus to include both evolving regional challenges and transnational threats. This combination of traditional and emerging dangers means increased risk to our nation. To counter that risk, our Navy must expand its striking power, achieve information dominance, and develop transformational ways of fulfilling our enduring missions of sea control, power projection, strategic deterrence, strategic sealift, and forward presence.

Three fundamental concepts lie at the heart of the Navy's continued operational effectiveness: Sea Strike, Sea Shield, and Sea Basing. Sea Strike is the ability to project precise and persistent offensive power from the sea; Sea Shield extends defensive assurance throughout the world; and Sea Basing enhances operational independence and support for the joint force. These concepts build upon the solid foundation of the Navy-Marine Corps team, leverage U.S. asymmetric advantages, and strengthen joint combat effectiveness.

U.S. Navy often cite asymmetric challenges when referring to enemy threats, virtually assuming such advantages belong only to our adversaries. "Sea Power 21" is built on a foundation of American asymmetric strengths that are powerful and uniquely ours. Among others, these include the expanding power of computing, systems

integration, a thriving industrial base, and the extraordinary capabilities of our people, whose innovative nature and desire to excel give us our greatest competitive advantage.

Sea Basing will enable to project joint operational independence. Operational maneuver is now, and always has been, fundamental to military success. As U.S. Navy look to the future, the extended reach of networked weapons and sensors will tremendously increase the impact of naval forces in joint campaigns. U.S. Navy will do this by exploiting the largest maneuver area on the face of the earth: the sea.

Sea Basing serves as the foundation from which offensive and defensive fires are projected, making Sea Strike and Sea Shield realities. As enemy access to weapons of mass destruction grows, and the availability of overseas bases declines, it is compelling both militarily and politically to reduce the vulnerability of U.S. forces through expanded use of secure, mobile, networked sea bases. Sea Basing capabilities will include providing Joint Force Commanders with global command and control and extending integrated logistical support to other services. Afloat positioning of these capabilities strengthens force protection and frees airlift-sealift to support missions ashore.

The predicted impacts of Sea Basing are pre-positioned warfighting capabilities for immediate employment, enhanced joint support from a fully netted, dispersed naval force, strengthened international coalition building, increased joint force security and operational agility, and minimized operational reliance on shore infrastructure. Sea Basing enables following Capabilities: Enhanced afloat positioning of joint assets, offensive and defensive power projection, command and control, integrated joint logistics, and accelerated deployment and employment timelines. In order to construct the Sea

Base, the following technologies are required: Enhanced sea-based joint command and control, heavy equipment transfer capabilities, intra-theater high-speed sealift, improved vertical delivery methods, integrated joint logistics, rotational crewing infrastructure, and international data-sharing networks.

Realization of the Sea Basing needs the following four steps: First, exploiting the advantages of sea-based forces wherever possible. Second, development of technologies to enhance on-station time and minimize maintenance requirements. Third, experiments with innovative employment concepts and platforms. And last, challenge of every assumption that results in shore basing of Navy capabilities

Netted and dispersed sea bases will consist of numerous platforms, including nuclear-powered aircraft carriers, multi-mission destroyers, submarines with Special Forces, and maritime pre-positioned ships, providing greatly expanded power to joint operations. Sea-based platforms will also enhance coalition-building efforts, sharing their information and combat effectiveness with other nations in times of crisis.

Sea Basing accelerates expeditionary deployment and employment timelines by pre-positioning vital equipment and supplies in-theater, preparing the United States to take swift and decisive action during crises. U.S. Navy intend to develop these capabilities to the fullest extent. Strategic sealift will be central to this effort. It remains a primary mission of the U.S. Navy and will be critical during any large conflict fought ashore. Moreover, U.S. Navy will build pre-positioned ships with at-sea-accessible cargo, awaiting closure of troops by way of high-speed sealift and airlift. Joint operational

flexibility will be greatly enhanced by employing pre-positioned shipping that does not have to enter port to offload.

Twenty-first-century operations will require greater efficiencies through the development of joint logistical support. This will include the provisioning of joint supplies and common ammunition, and the completion of critical repairs from afloat platforms. Providing these capabilities to on-scene commanders will significantly increase operational effectiveness and constitute a valuable addition to strategic basing support provided by friends and allies around the world.

Beyond its operational impact, the Sea Basing concept provides a valuable tool for prioritizing naval programs. Sea-based forces enjoy advantages of security, immediate employability, and operational independence. All naval programs should foster these attributes to the greatest extent feasible. This means transforming shore-based capabilities to sea-based systems whenever practical, and improving the reach, persistence, and sustainability of systems that are already afloat.

2.6 Monte-Carlo Simulation and Maximum Entropy Sampling

Monte Carlo simulation is a class of computational algorithms that rely on repeated random sampling to compute their results. Monte Carlo simulation is often used in computer simulations of physical and mathematical systems. These methods are most suited to calculation by a computer and tend to be used when it is infeasible to compute an exact result with a deterministic algorithm.[124] This method is also used to complement theoretical derivations.

Monte Carlo simulation is especially useful for simulating systems with many coupled degrees of freedom, such as fluids, disordered materials, strongly coupled solids, and cellular structures. They are used to model phenomena with significant uncertainty in inputs, such as the calculation of risk in business. They are widely used in mathematics, for example to evaluate multidimensional definite integrals with complicated boundary conditions. When Monte Carlo simulations have been applied in space exploration and oil exploration, their predictions of failures, cost overruns and schedule overruns are routinely better than human intuition or alternative "soft" methods.[50]

The modern version of the Monte Carlo simulation was invented in the late 1940s by Stanislaw Ulam, while he was working on nuclear weapon projects at the Los Alamos National Laboratory. It was named, by Nicholas Metropolis, after the Monte Carlo Casino, where Ulam's uncle often gambled.[66] Immediately after Ulam's breakthrough, John von Neumann understood its importance and programmed the ENIAC computer to carry out Monte Carlo calculations.

An early variant of the Monte Carlo simulation can be seen in the Buffon's needle experiment, in which π can be estimated by dropping needles on a floor made of parallel strips of wood. In the 1930s, Enrico Fermi first experimented with the Monte Carlo method while studying neutron diffusion, but did not publish anything on it.[53]

In 1946, physicists at Los Alamos Scientific Laboratory were investigating radiation shielding and the distance that neutrons would likely travel through various materials. Despite having most of the necessary data, such as the average distance a neutron would travel in a substance before it collided with an atomic nucleus, and how

much energy the neutron was likely to give off following a collision, the Los Alamos physicists were unable to solve the problem using conventional, deterministic mathematical methods. Stanislaw Ulam had the idea of using random experiments. He recounts his inspiration as follows:

The first thoughts and attempts I made to practice the Monte Carlo Method were suggested by a question which occurred to me in 1946 as I was convalescing from an illness and playing solitaires. The question was what are the chances that a Canfield solitaire laid out with 52 cards will come out successfully? After spending a lot of time trying to estimate them by pure combinatorial calculations, I wondered whether a more practical method than "abstract thinking" might not be to lay it out say one hundred times and simply observe and count the number of successful plays. This was already possible to envisage with the beginning of the new era of fast computers, and I immediately thought of problems of neutron diffusion and other questions of mathematical physics, and more generally how to change processes described by certain differential equations into an equivalent form interpretable as a succession of random operations. In 1946, I described the idea to John von Neumann, and U.S. Navy began to plan actual calculations. [27]

The work of von Neumann and Ulam required a code name. Von Neumann chose the name Monte Carlo. The name refers to the Monte Carlo Casino in Monaco where Ulam's uncle would borrow money to gamble.[50] Using lists of "truly" random random numbers was extremely slow, but von Neumann developed a way to calculate pseudorandom numbers, using the middle-square method. Though this method has been criticized as crude, von Neumann was aware of this: he justified it as being faster than

any other method at his disposal, and also noted that when it went awry it did so obviously, unlike methods that could be subtly incorrect.

Monte Carlo simulation was central to the simulations required for the Manhattan Project, though severely limited by the computational tools at the time. In the 1950s they were used at Los Alamos for early work relating to the development of the hydrogen bomb, and became popularized in the fields of physics, physical chemistry, and operations research. The Rand Corporation and the U.S. Air Force were two of the major organizations responsible for funding and disseminating information on Monte Carlo methods during this time, and they began to find a wide application in many different fields.

Uses of Monte Carlo simulation requires large amounts of random numbers, and it was their use that spurred the development of pseudorandom number generators, which were far quicker to use than the tables of random numbers that had been previously used for statistical sampling.

Maximum entropy sampling has been developed in the area of information theory and computer science. These studies are generally divided into two categories. First category is a sampling method by using Shanon entropy, and the other category is using Boltzman entropy.

Shannon entropy as a measure of information has been used in spatial design by Shewry and Wynn [95], where maximum entropy sampling (MES) was introduced as a criterion for the choice of experiments with the aim of maximizing the gain in

information for prediction at unsampled sites. This criterion was then adopted as one of the main methods for computer experiments [88].

The Shannon entropy of a random vector Γ, taking values on R^N and with density function of $p()$, is defined as

$$\text{Ent}(\Gamma) = E_\Gamma[-\log\{p(\Gamma)\}] \qquad \text{Eq. (2.1)}$$

if the expectation exists. Suppose that Γ can be decomposed into (Γs: $\Gamma\hat{s}$), where s represents the selected index set $s \subseteq \{1, \ldots, N\}$. The following decomposition appears in several forms in information theory [17]:

$$\text{Ent}(\Gamma) = \text{Ent}(\Gamma_s) + E_{\Gamma s}\{\text{Ent}(\Gamma_{\hat{s}} \mid \Gamma_s)\} \qquad \text{Eq. (2.2)}$$

Sebastini considered the Bayesian experimental design framework in its simplest form by applying Eq. (2.2) to the choice of experiment [92]. The procedure is following. Let Y represent a random n-vector in Ψ and Θ a random p-vector in Ω. Suppose that, given $\Theta = \theta$ and an experiment ξ, Y has a known distribution with probability density $p(y|\theta, \xi)$. Θ has a prior distribution with probability density $p(\theta)$, which is functionally independent of ξ. Thus, given ξ, the pair (Y, Θ) will have a joint distribution on Ψ x Ω. Then, suppose that ξ is to be chosen from a set of possible experiments E to acquire the maximum amount of information about Θ. The expected gain in information from ξ is

$$\text{Ent}(\Theta) - E_Y\{\text{Ent}(\Theta \mid Y, \xi)\} \qquad \text{Eq. (2.3)}$$

the expectation being over the marginal distribution of Y. If Ent(Θ) is not design dependent, which is an assumption made throughout this paper, the information theoretic

approach to the Bayesian choice of the experiment is to find ξ in E which minimizes the overall expected risk.

$$E_Y\{\mathrm{Ent}(\Theta \mid Y, \xi)\} \qquad \text{Eq. (2.4)}$$

An experiment ξ minimizes Eq. (2.4) most informative for Bayesian estimation of Θ, or more loosely optimal. The main result of this paper is in the following theorem.

Theorem 1. Suppose that the aim of the experiment is to acquire the maximum amount of information about Θ, and it is known a priori that the entropy of the joint distribution of Y, $\Theta|\xi$ is bounded and not functionally dependent on the design ξ, and that $\mathrm{Ent}(Y|\xi)$ and $E_Y\{\mathrm{Ent}(\Theta|Y,\xi)\}$ are bounded. Then, an experiment which maximizes the entropy of the marginal distribution of Y will be most informative for Θ.

Proof. Put $\Gamma_s = Y|\xi$ and $\Gamma_{\hat{s}} = \Theta$ in equation (2), so that the joint entropy of the observations Y and the parameter Θ can be decomposed as

$$\mathrm{Ent}(Y, \Theta|\xi) = \mathrm{Ent}(Y|\xi) + E_Y\{\mathrm{Ent}(\Theta|Y,\xi)\}. \qquad \text{Eq. (2.4)}$$

If all therms in Eq. 2.4 are bounded and the left-hand side is fixed in the sense that it does not depend on the experiment x, then the minimization of $E_Y\{\mathrm{Ent}(\Theta|Y,\xi)\}$ is achieved by maximizing $\mathrm{Eng}(Y|\xi)$.

This procedure is MES. It is pointed out in the paper that in many standard cases theorem 1 holds and MES can be applied. This is seen by using the information identity (2) again, interchanging the role of Θ and Y:

The assumption that Ent(Θ) is not design dependent, it is therefore enough to ensure that Ent($\Theta|Y,\xi$) does not depend on the design x for the term on the left-hand side not to depend on x. Summarizing we have the following theorem.

Theorem 2. Theorem 1 holds whenever Ent($\Theta|Y,\xi$) is not functionally dependent on the design ξ.

The MES principle yields the maximum increase of information that is achievable from the choice of the experiment. By using Eqs. (2.3) and (2.4) can be expressed as Ent(Y $|\xi$) – $E_\Theta\{$ Ent($\Theta|Y,\xi$)$\}$ and clearly, when $E_\Theta\{$ Ent($\Theta|Y,\xi$)$\}$ is not functionally dependent on ξ, MES applies [95].

JSDFS With fast-growing computer technology, Monte Carlo simulations have been very successful in studying various statistical systems including neural networks, problems in biology and chemistry, lattice-gauge theories, and optimization problems in various areas, not to mention the statistical physics in the study of phase transitions and critical phenomena. Calculation of entropy from simulation methods has been a very difficult task, since entropy is a function of the probability with which a typical equilibrium configuration of the system is sampled. Several methods have been suggested, and they have some advantages and disadvantages.

Almost all MC sampling algorithms are based on the idea of importance sampling, introduced by Metropolis et al [66]. The thermodynamic average <O> of an observable $O(x)$ can be estimated by [141]

$$O = \frac{\sum_{i=1}^{n} O(x_i) P^{-1}(x_i) \exp[-\beta H(x_i)]}{\sum_{i=1}^{n} P^{-1}(x_i) \exp[-\beta H(x_i)]} \qquad \text{Eq. (2.5)}$$

Where x_i represents a configuration at time i of a given system with a Hamiltonian H. β is the inverse temperature with $k_B = 1$, and $P(x)$ is a sampling probability. Equation 2.6 becomes exact in the infinite time limit, n → infinity. If $P(x)$ is chosen to be constant, very few samples contribute significantly to the sum in Eq. (2.5), and an enormously large value of n is required to get a reasonable estimate of <O>.

Importance sampling comes in if one chooses $P(x)$ as the Boltzmann weight exp[-$\beta H(x)$]. It is generally a good sampling algorithm, but it can fail to access all the possible equilibrium distributions of the partition function if there exists a large barrier between them (i.e., the required sample size n becomes too large). One confronts similar problems if one needs to use the histogram method [29] for a wide range of the coupling constant, say temperature T, due to the small number of samples away from the equilibrium position of the internal energy E.

Recently three approaches have been suggested to overcome these problems. The first one is the multi-histogram method [3][125], in which many histograms with overlapping distributions serve as connecting information bridges. This approach can widen the range of T [26][69], but is it not suited for sampling systems with a large barrier. The second approach is to use many micro-canonical ensembles. [4][5][61] This approach is used mostly to obtain the whole partition function numerically for relatively small systems. These two methods suffer from the following two common difficulties:

Errors propagate through the neighboring sets of data, requiring a systematic and elaborate study of error propagation, and many simulations at different temperatures are necessary. [125]

2.7 Evaluation and Selection of Candidates

The most suitable method to select the best one among candidates is Multi-Criteria Decision Making (MCDM). The International Society on Multiple Criteria Decision Making defines that Multi-Criteria Decision Making is the study of methods and procedures by which concerns about multiple conflicting criteria can be formally incorporated into the management planning process. [138]

Technique for Ordered Preference by Similarity to Ideal Solution (TOPSIS) is one of MCDM techniques that uses a ratio of Euclidean distances to rank designs. TOPSIS originated in a Ph.D. dissertation: Yoon, K. "Systems Selection by Multiple Attribute Decision Making" Ph.D. dissertation, Kansas State University, 1980. [114] TOPSIS is based on the concept that the chosen alternative should have the shortest geometric distance from the positive ideal solution and the longest geometric distance from the negative ideal solution. It is a method of compensatory aggregation that compares a set of alternatives by identifying weights for each criterion, normalising scores for each criterion and calculating the geometric distance between each alternative and the ideal alternative, which is the best score in each criterion. An assumption of TOPSIS is that the criteria are monotonically increasing or decreasing. Normalisation is usually required as the parameters or criteria are often of incongruous dimensions in multi-criteria problems.[115][116] Compensatory methods such as TOPSIS allow trade-offs between

criteria, where a poor result in one criterion can be negated by a good result in another criterion. This provides a more realistic form of modelling than non-compensatory methods, which include or exclude alternative solutions based on hard cut-offs.[38] It provides an indisputable preference order of solutions, describes customer preference in the form of weights for each criterion. As a result, the best alternative has shortest Euclidean distance to positive ideal solution and farthest away from negative-ideal solution. The steps of TOPSIS are as follows.

Step 1. Create an evaluation matrix consisting of m alternatives and n criteria, with the intersection of each alternative and criteria given as $(x_{ij})_{mxn}$.

Step 2. The matrix $(x_{ij})_{mxn}$ is then normalised to form the matrix $(r_{ij})_{mxn}$, using the normalisation method.

$$r_{ij} = \frac{x_{ij}}{pmax(v_j)} \qquad \text{Eq. (2.6)}$$

Where $pmax(v_j)$ is the maximum possible value of the indicator .

Step 3. Calculate the weighted normalized decision matrix

$$T = (t_{ij})_{m\times n} = (w_j r_{ij})_{m\times n} \qquad \text{Eq. (2.7)}$$

Where w_j is the original weight given to the indicator v_j.

Step 4. Determine the worst alternative A_w and the best alternative A_b:

$$A_w = \{\langle \max(t_{ij} | i = 1,2,) | j \in J_- \rangle, \langle \min(t_{ij} | i = 1,2,) | j \in J_+ \rangle\}$$

$$A_b = \{\langle \min(t_{ij} | i = 1,2,) | j \in J_- \rangle, \langle \max(t_{ij} | i = 1,2,) | j \in J_+ \rangle\} \qquad \text{Eq. (2.8)}$$

Where, J_+ is associated with the criteria having a positive impact, and J_- isassociated with the criteria having a positive impact.

Step 5. Calculate the L2-distance between the target alternative i and the worst condition A_w,

$$d_{iw} = \sqrt{\sum(t_{ij} - t_{wj})^2} \qquad \text{Eq. (2.9)}$$

and the distance between the alternative i and the best condition A_b

$$d_{ib} = \sqrt{\sum(t_{ij} - t_{bj})^2} \qquad \text{Eq. (2.10)}$$

where d_{iw} and d_{ib} are L2-norm distances from the target alternative to the worst and best conditions, respectively.

Step 6. Calculate the similarity to the best condition.

$$s_{ib} = \frac{d_{ib}}{d_{ib}+d_{iw}} \qquad \text{Eq. (2.11)}$$

$S_{ib} = 1$, if and only if the alternative solution has the worst condition

$S_{ib} = 0$, if and only if the alternative solution has the best condition.

Step 7. Rank the alternatives according to s_{ib}.

CHAPTER III

SIMULATION PROCESS

3.1 General Procedures

Analysis module for this research consists of seven parts; instability analysis, shipping lane estimation and sea state analysis, disembarkation analysis, operational analysis, overall effectiveness estimation, preliminary design, and the evaluation and selection of candidates. Figure 3.1 illustrates the flow of data and the sequence of analysis between these seven analysis components. As indicated in Figure 3.1, operational analysis and preliminary design components are developed by Beisecker and Koullias.[2][59] All the other analysis components are developed in this research. Instability analysis determines the likelihood and intensity of instability in a target region considering politicides and economic and environmental factors. Shipping lane and sea state analysis selects a shipping lane from the available U.S. navy base to the target region and calculates the corresponding distance. Furthermore, a distribution of Beaufort scale is assessed considering environmental and climatic aspects of regions where the selected shipping lane passes through. Disembarkation analysis determines widths and slopes of landable sections of the target region. Operational analysis calculates required army and supply with regard to time. Then global effectiveness is estimated using Monte-Carlo simulation and this estimation result allows preliminary design of a ship which satisfies all the requirements determined above. Furthermore, if the potential candidates exist, global effectiveness estimation allows comparison analysis of these candidates

using the multi-criteria decision making (MCDM) method and the most appropriate model can be selected.

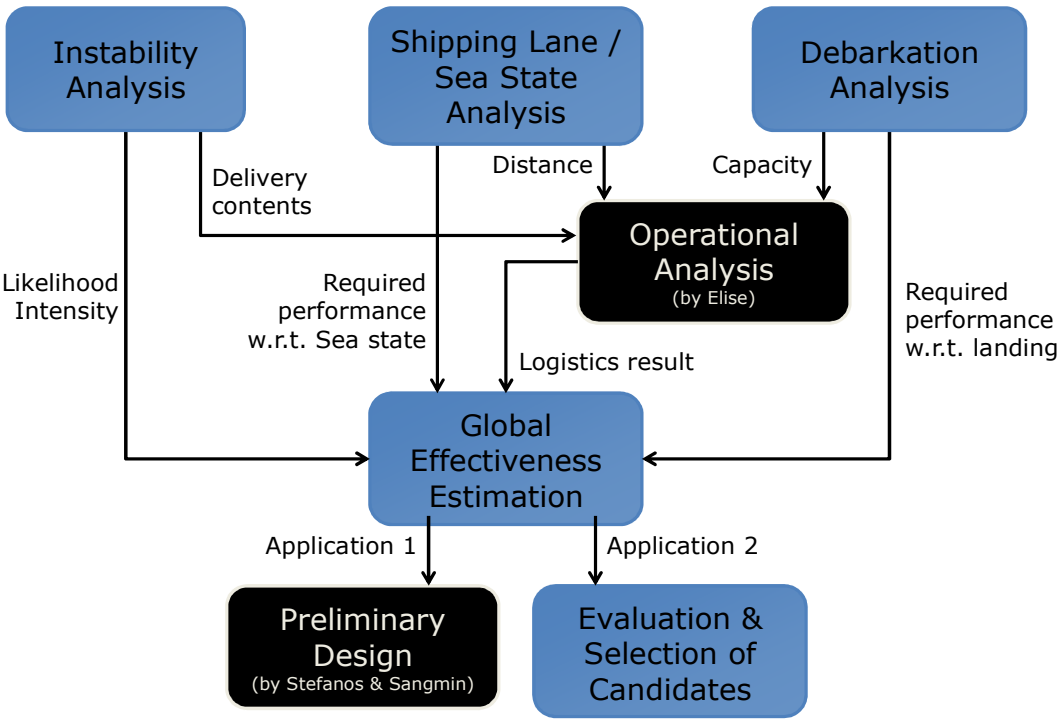

Figure 3.1 Seven Analysis Components of Analysis Module

3.2 Instability Analysis

3.2.1 The Socio-Economic and Political Instabilities

As mentioned before, O'Brien developed a set of macro-structural indicators to predict socio-economic and political instabilities in a country. His predictor thresholds were not made publicly available but the method described relies on a training and validation data sets. These are not readily available and are labor intensive to develop. He used Fuzzy Logic to train a model that predicted the level of instability in a country based on the high level (macro-structural) parameters that describe a country's situation.

[75][76] In essence his fuzzy logic model determines a membership function for the indicators and levels of conflict. It determines those membership functions using the training set (ranging from 1975 to 1984), and then compares the goodness of the model by using it to predict past events (from 1985 to 1999). The final integrated model results were then compared to the predictions made from 2000-2015 by the intelligence community.

The data used by O'Brien is not freely available, so for the purposes of this project a new dataset was integrated using publicly available data. Data included, e.g., CIA World Factbook, Freedom House and Heritage Foundation indices, and the World Water Organization. These data contain natural resources and it is no surprise since competition for natural resources is a well known trigger for war. Using the data obtained, a study was conducted to identify the level of correlation between the macro-level indicators and the likelihood of war. An additional data set for the number of conflicts in the area in the last 40 years was compiled for each country in the World and its distribution along each independent factor studied.

3.2.2 The Environmental Risks

The magnitude of the impact an environmental disaster can have is something that most people are well aware. Events like the 2010 Earthquake in Haiti as shoen in Figure 3.2, the 2004 Tsunami in the Indian Ocean, and the famines in Africa are just samples of the destruction and humanitarian impact these events can have. The World Bank and the University of Columbia developed a set of risk indices and datasets for each class of

natural hazard, i.e., Cyclones, Draught, Floods, Earthquakes, Volcanoes, and Landslides.[21]

These datasets were compiled from different sources and for that reason they were not necessarily consistent in their resolution or periods. The integrated datasets were reconciled and used to determine two different types of risk, mortality and economic loss. These two risk indices were assessed at a 2.5 degree by 2.5 degree grid using global census data from the Gridded Population of the World (GPW) project. [15] The concept of vulnerability for each region was incorporated by deriving coefficients of vulnerability of each level of risk for each type of natural disaster for each mayor area of the world. These coefficients were used to estimate how much of an impact a given disaster would have in a given area of the world, e.g., the 2010 Earthquake in Chile was 10 times stronger than the one in Haiti that same year but the number of casualties from the Haitian earthquake was 100 to 400 times higher. The discrepancy lies on the uncertainty around the true number of casualties from the Haitian earthquake of 2010.

The study aggregated the mortality and economic loss risk for all the different hazards throughout the world. The mortality risks indicate what magnitude of response and the likelihood that a response to that area of the world would have to occur. As with all the data integrated into the decision supporting tool, the environmental hazard risk datasets can be modified by the user.

Figure 3.2 Earthquake in Haiti (2010) [72]

3.3 Shipping Lane Estimation and Sea State Analysis

3.3.1 Shipping Lane Estimation between Points of Embarkation and Debarkation

To estimate shipping lanes between points of embarkation and debarkation, available embarkation and disembarkation points have to be identified. Figure 3.3 illustrates possible embarkation points for MEC; from Sea Ports of Embarkation (SPOEs) (in green), to the location of the Maritime Prepositioned Groups (MPGs) (in yellow), to Intermediate Staging Bases (ISBs) in red and yellow. There are three major factors that increase the difficulty of the assessment of potential embarkation points; (1) these possible points of embarkation are not a static set, (2) they are not all equally suited to stage any type of operation, and (3) potential points of embarkation can be located at a number of friendly countries as well. The first concern lies on the fact that some countries are rescinding their contracts with the Unit States and disallowing it to base their military

forces on their sovereign territories (e.g., Uzbekistan). There is a high degree of uncertainty as to which bases will be open when, since political swaying has a large impact on a country's will to host US military forces. The second concern centers around the fact that capabilities of available bases are not equal, e.g., some are not big enough to stage a sea-based-supported Mayor Combat Operation (MCO) from. The third concern is somewhat related to the first concern in an opposite way. The fact that the points of embarkation can be located at a number of friendly countries increases the potential embarkation points, which is beneficial but increases the uncertainty related to the points of embarkation.

The point of disembarkation is even more complex to address than the point of embarkation. In this case, the analysis has to incorporate local instabilities and destabilization factors and the willingness of the US and its allies to act in those areas of the world. Instabilities can be due to a myriad of reasons, political, socio-economic, military, environmental, and etc. The willingness of the US to intervene has to do with the popular sentiment at the time, the US' interest in the region at the time, and the fortitude of the alliances. For the purposes of this research a series of risk factors are developed to address (1) the socio-econo-political instabilities, (2) the resources in the area, and (3) the natural disasters.

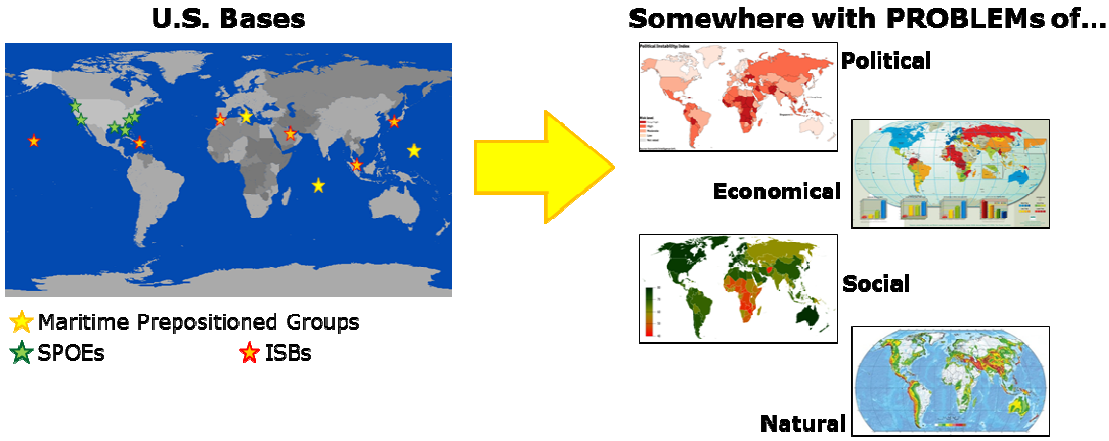

Figure 3.3 Points of Embarkation and Debarkation [1]

3.3.3 Sea State Analysis

State of the sea during shipping is one of essential factors in design of a ship. In this research, Beaufort scale is used to indicate the sea state along a selected shipping lane. Thirteen Beaufort scale numbers from 0 to 12 are used to describe the distributions of wind speed, wave heights, and current heights and the corresponding confidence level is determined. Details of wind speed and wave heights corresponding to each Beaufort scale number is shown in chapter 6. The sea state analysis results are crucial to determine the required performance of a ship such as a draft depth, loading time and unloading time.

3.4 Disembarkation Analysis

This analysis describes coastline analysis model developed by ASDL, including existing SRTM data and estimation method based on the Fractal theory. It was identified and obtained by ASDL developed models. The applications of these models are given along with visualization integrated strategic analysis tool. Main demands for Coastline Analysis can be categorized into two parts: the length of available coastline and the area

for deploying. Figure 3.4 illustrates an example of landing operation. This shows the need of coastline for landing and the area for deploying. The first requirement is the length of the coastline for landing which is shallow enough for navy crafts to land because the length of shallow coastline is the measure of how many navy craft can land at the same time. The second requirement is the size of the area of deploying. The area of deploying should be large enough such that MEC can deploy the delivery and turn around to come back.

Figure 3.4 Landing Operation [45]

3.5 Operational Analysis

For the operational analysis, the code developed by Beisecker has been used in this study. Beisecker's work can quantitatively assess the impacts of new capabilities and

vessels at the systems-of-systems level. Her methodology is able to investigate diverse, disruptive technologies acting on multiple elements within the system-of-systems architecture. Furthermore, the method is capable of capturing the complex interactions between elements and the architecture and is able to assess the impacts of new systems. [2] Beisecker identified six gaps in the previous methods including the need to break the problem into sub-problems in order to incorporate a heterogeneous, interacting fleet, dynamic loading, and dynamic routing. The identified gaps were investigated and methods were recommended to address these gaps to enable overall operational analysis across scenarios. Scenarios were fully defined by a scheduled set of demands, distances between locations, and physical characteristics that could be treated as input variables. Details of the operational analysis method developed by Beisecker are discussed in Chapter 8.

3.6 Global Effectiveness Estimation

As mentioned above Monte-Carlo Simulation is used for global effectiveness estimation. To estimate global effectiveness two distributions are determined; the distribution of distances without the weighing and the weighed distances. These distributions can be studied as probability density functions or they can be integrated to obtain the cumulative distribution function (CDF) which can help address the question "how often will my MEC be able to deploy directly from an SPOE, ISB to the Area of Operations (AOO). This analysis can also aid in comparing different sized MECs using payload range curves.

3.7 Preliminary Design of Medium Exploratory Connector

A typical ship design spiral is shown in Figure 3.6. Sizing and synthesis is directly dependent on resistance and powering, as well as weights and geometry, thus these two phases of the spiral are of primary importance. Hull definition and hydrostatics provide an additional level of fidelity to the tool, i.e., resistance calculations can be improved by incorporating a hull model in the tool. In addition, a graphical display of the hulls provides a form of visual debugging for the design iterations. Although the exact hull definition is not known, it can be deduced from previous designs. Hydrostatics is calculated from the hull definition. Arrangements and structures are not important at this point; only the physical size and performance of the ship is important. These two phases are generally tackled in the detailed design phase of the spiral. Stability (initial stability) is incorporated as a simple check to see if generated designs are stable based on a historical rule of thumb. Stability requires knowledge of the location of all components in the ship and their weights and is best left for the detailed design phase. An improved stability model will be incorporated in the future, but this requires some effort in the Arrangements department.

The sizing and synthesis approach based on Raymer suffers from several deficiencies. The first difficulty stems from the historical nature of the approach. The empty weight fraction is based on historical data and the solution is sensitive to this choice. A small body of experience exists that is associated with SESs, the majority of which are under 200 ltons. To develop larger designs, this approach must extrapolate to the next order of magnitude in size and weight. Extrapolation is generally a poor design approach. The physics for the vessel in Koullias are included as a resistance polar. However, this physics-based approach relies on historical data for the various coefficients

and dimensional quantities, such as drag coefficients, efficiencies, fuel consumption, and cushion densities. In addition, only the major aerodynamic/hydrodynamic resistance components with known, simple analytical expressions at superhump Froude numbers are included. The development of new vessels where no experience exists requires a detailed, physics-based approach that will in general be iterative. A historical aspect is necessary in the design tool for the following reasons: to provide a starting point for the designs; to provide a substitute for information that is not yet available at the conceptual design phase; to provide a nominal setting for some variable that is not required and thus assumed to always function correctly and to converge the initial guesses on the weights.

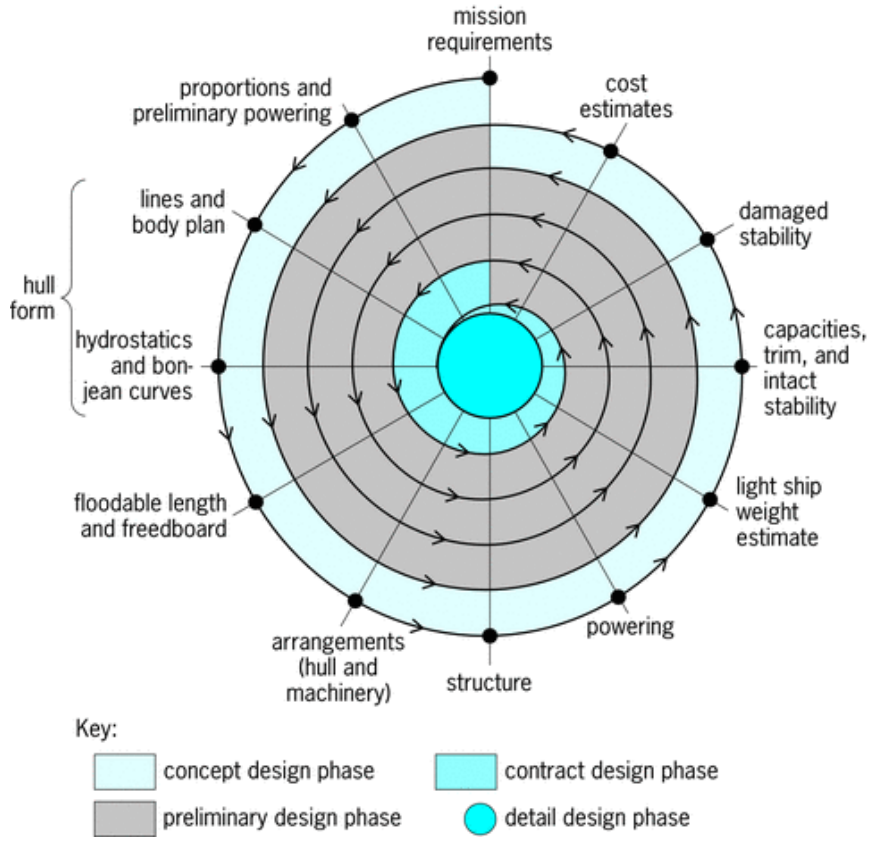

Figure 3.5 Basic design spiral, showing the iterative ship design process [126]

Figure 3.5 depicts the iterative process used in generate designs. The design process is initiated with the requirements of speed, payload, range, and sea state, some dimensional parameters to define the general shape of the ship, and a guess on the lightship and full load displacements. The geometry module computes the ship particulars, based on a physical arguments and some historical rules of thumb, and communicates them to the mission module. The mission module calls the resistance module to determine the fuel required for the current design. The mission module then communicates back to the geometry module the computed weights, and if they do not agree to the initial weight guesses within some tolerance, the process repeats until there is convergence. A process which translates a set of owner's requirements into the drawings, specifications, and other technical data necessary to actually build a ship. Naval architects lead the process, but engineers and designers with many other skills contribute. These other skills include marine engineering, structural design, and production engineering. The ship design process is iterative, and is subdivided into several phases during which the design is developed in increasing degrees of detail. Typically, the owner's requirements specify the mission that the new ship must perform and define such parameters as required speed, fuel endurance, and cargo weight and capacity.

3.8 Evaluation and Selection of Candidates

Based on the aforementioned analyses results, this research suggests the guideline to select the best candidates of conceptual naval assets. This decision making procedure includes various criteria such as range, payload, speed, landing ability and acquisition cost. The most suitable method to select the best one among candidates is Multi-Criteria Decision Making (MCDM). In this research, The Technique for Order of Preference by

Similarity to Ideal Solution (TOPSIS) is employed in order to solve multiple conflicting criteria can be formally incorporated into the management planning process. TOPSIS is based on the concept that the chosen alternative should have the shortest geometric distance from the positive ideal solution and the longest geometric distance from the negative ideal solution. Finally, this study provides the environment to support decision making by using MCDM.

CHAPTER IV

HYPOTHESES

The literature review produceds a series of questions since the research confronts the technical challenges and the limitations of previous models. These research questions are broken down into five topics that define the gaps in current methods and models. The three key analysis gaps are instability analysis concerning natural disasters, geological analysis at the disembarkation point, and global effectiveness analysis of newly designed Navy ships. In addition, there are three technical challenges: uncertainties in instability, providing real-time information, and interactive decision-making support. These analysis gaps and technical challenges raise the five questions posed and addressed later in this section. This section presents each question, how the research questions will be answered and what theory should be included. A series of hypotheses will be proposed based on a literature study of tools and techniques from other fields that may prove suitable to answer the research questions. Each research question will lead to a hypothesis. All hypotheses are defined as testable and falsifiable contents. They will be proved in following chapters.

The first topic comes from the question: “what is the most suitable way to characterize a scenario?”. Since not all scenarios are equally likely, the discrete event simulation needs a method to estimate likelihood and the importance of each scenario. Deploying the military inherently suggests that the region is not peaceful. The region may be unstable due to an event such as a riot, military coup, disorder by natural disaster, conflict of religion or other cause of unrest. These causes of unrest are related to political,

social, economic and environmental factors. The probabilistic instability index calculated by the socio-economic, political and natural disaster factors provides an indication of how likely any country or region is to become unstable and therefore require assistance from the United States.

In other words, the purpose of this topic is to improve the accuracy of instability analysis. The core concept behind this question is: "what is going to happen and where it is going to be?". In the previous studies by O'Brien, the instability analysis is estimated based on the socio-economic and political environment. However, the tsunami Indonesia in 2004 and the earthquake in Haiti in 2010 show that U.S. military also needs to consider humanitarian operations due to natural disasters in its analysis. Furthermore, this type of instability depends on the natural characteristics of the region, not on the characteristics of the country. The proposed instability analysis method includes two sets of databases: factors inregard to countries and factors inregard to the region. Therefore, the instability index by the new method is aproperty of the region, not the country. The first hypothesis is defined as follows.

Hypothesis 1: ***By including natural disaster, the simulation of scenario becomes more realistic.***

This hypothesis addresses the previously stated research question: "What is the most suitable way to characterize a situation?". The previous study was based on the socio-economic and political environment would not detect the need for a humanitarian operation to relieving damage from a natural disaster such as a tsunami or earthquake. As

a result, the instability analysis based on the location with a natural disaster index will capture the incidence efficiently.

The second topic builds off on this improved instability analysis. Since military assets have a long development time, the discrete event simulation needs an assessment of the likelihood of a given scenario in the near future in order to estimate the usability of these proposed assets. This need concerns the question "how does one forecast instability in the near future?". Two forecasting methods can be applied. The first method is to forecasts the future instability based on the present instability factors. The second method estimates the future instability based on the forecasted instability factors. In the case unstable regions, it is almost impossible to accurately forecast these factors. However, this research is focused on the unstable regions. Therefore, the former method should be employed. This forecasting method is meaningful only if the following hypothesis is true.

Hypothesis 2: ***Historical regressions of the impact of socioeconomic political and environmental conditions on a regional instability produce accurate prediction for the near future of 20 years. In addition, probabilistic causation models accurately capture factor interactions with minimal information.***

The third research topic origininates in the need of making the discrete event simulation representative. In other words, the purpose of this question is to identify a method to estimate the effectiveness and usability of military assets when it moves to any place in the world from the available naval base. The conventional discrete event simulation makes computational experiments of a single or a few scenario-based analyses. These analyses results are insufficient to be representative for all global situations. The

best method to represent overall global scenarios must consider the entire world area. However, this method is inefficient and requires an unreasonably large amount of time. One of the best alternatives is a Monte-Carlo simulation which samples a number of random experimental points. Unfortunately, another problem, the question of how many experiments should be conducted, arises if a Monte-Carlo simulation is used directly. The number of experiments cannot be decided at the beginning. Therefore, this subtopic requires an algorithm that terminates a Monte-Carlo simulation when the random distribution reasonably covers the entire global area. In response, an adaptive Monte-Carlo simulation was developed which will stop when the distribution of results converges upon an acceptable point resolution. Also, by using the sampling method with maximum entropy, the most efficient set of additional experimental points can be used. Accordingly, the adaptive Monte-Carlo simulation with maximum entropy concept ensures the minimum required accuracy and efficiently captures the global effectiveness of the MEC. For this topic, the following hypothesis must be proved.

Hypothesis 3: ***An adaptive Monte-Carlo Simulation with maximum entropy concept accurately and efficiently captures the global effectiveness distribution of the MEC.***

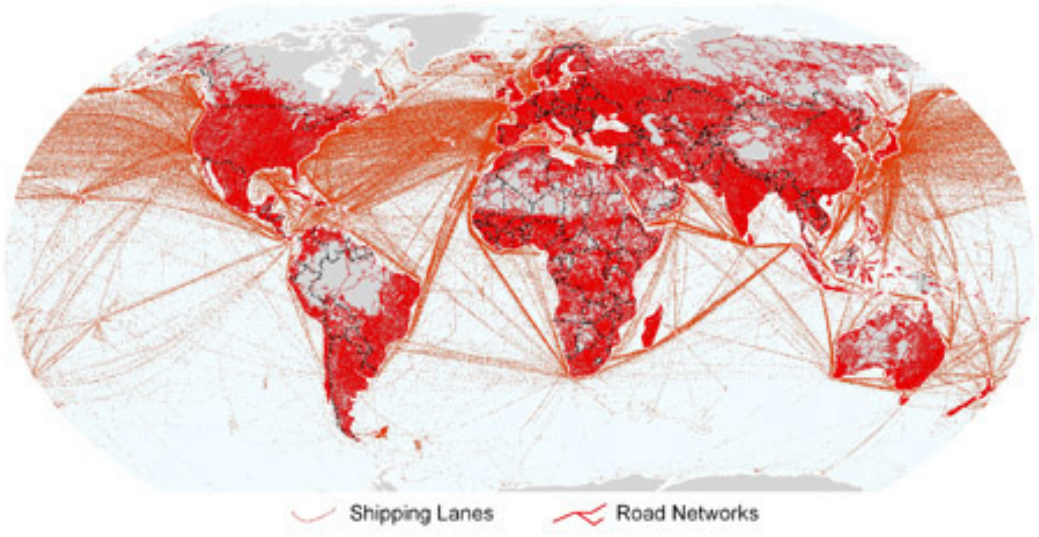

Figure 4.1 Superposition of Shipping Lanes [54]

The next research topic is concerned with developing a technique to find a shipping lane as quickly as possible. In order to estimate the global effectiveness, an enormous number of simulations are required because of the repetitive nature of Monte-Carlo simulations. Therefore, the shipping lane estimation should be done in the minimum amount of time. So far, many kind of methods have been developed, however, most of them include the calculation procedure to find the shortest path. The time of calculation to find shortest shipping lane makes Monte-Carlo simulations significantly computationally expensive. This fact drives the question about the most efficient method for finding realistic maritime routes between any two points on the globe. Superposition of shipping lanes in Figure 4.1 shows that shipping lanes overlap in many important points. These points exist at ocean bottlenecks. To reduce the time to find a path and calculate distance, pre-calculated tables based on those important points, can be used.. By making the pre-calculated sheet of shipping lanes based on the minimum set of bottle points, no calculation is needed. It means that Monte-Carlo simulation and real-time

display can be enabled. In order to use these advantages, The following hypothesis must be true.

Hypothesis 4: A *minimum set of bottle neck points can estimate reasonable shipping distances.*

The final research topic comes from the study to improve the accuracy of discrete event simulation. The geological condition highly effects the operational analysis. The width of coastline defines the maximum number of simultaneous disembarkations, and the coastline should include enough space for the landing craft to turn back. Also, the slope of coastline is one of main constraints on performance. Therefore, by adding geological analysis, more realistic simulation would be enabled. However, the current landing condition in the discrete event simulation model does not use a real geological database. Accordingly, another question is how to model and assess the debarkation points efficiently. The geological analysis for width, space and slope of coastline is relatively straight forward. By analyzing the disembarkation points with a high resolution geographical database, the actual values of the coastal slope and the available area beyond coastline can be calculated. So, if we have appropriate high resolution database, a single geographical analysis is not a problem. However, two technical problems arise when we use highest reolution geological database (SRTM). First technical problem is that SRTM covers only the region between the latitude 60N and 60S. This means that SRTM database does not include the region close to both polar areas. The second technical problem is the size of this database. The required storage size is more than two gigabytes. The calculation of geological is computationally expensive because this time for calculation is proportional to second-order of resolution. The fractal

theory will solve these two problems at the same time. To prove the usability of fractal theory, the following hypothesis must be true.

Hypothesis 5: ***Using the principle of coastal self-similarity and low resolution geographical data, we can accurately estimate the available coastline for unimproved beach landings for a given MEC climb angle.***

CHAPTER V

INSTABILITY ANALYSIS

The system development process of system engineering can be devided into three stages: Concept development, engineering development and post development stage. Concept development stage consists of three phases again: Needs analysis, concept exploration and concept definition as shown in Figure 5.1. The first step of developing new naval asset is to define the requirements for a new system and these requirements can be found and quantified by the study of mission areas and mission types. For example, the range of new asset should be higher than distance from the navy base to the target and the payload depends on the type of mission.

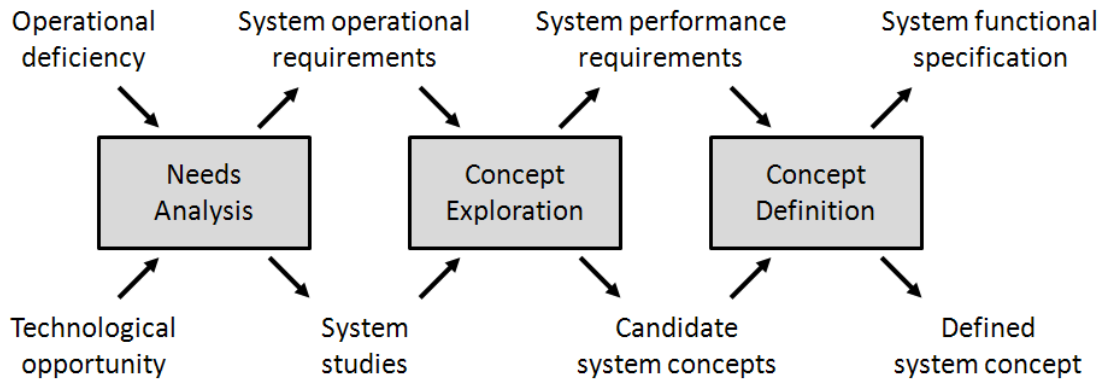

Figure 5.1 Concept Development Phases in Systems Engineering [127]

To quantify the system operational requirements, the analysis to predict where the mission will be needed. Because of the long term service life of vessels, the stochastic approach is one of most suitable candidates. In this research, probability causation model can estimate the likelihood of U.S. intervention and this procedure consists of three

stages: The likelihood of instability, the probability to solve the conflict without aid, and the probability of U.S. intervention.

The first stage is to quantify the magnitude of the instability in each region/country. In past researched showed the political, economic and social factors can predict how unstable the country is. Also, natural disasters are considered as main factors to make the society unstable. By the statistical regression model, this stage estimates the duration of conflicts in the service life of vessels.

The second stage is to quantify the probability that the country can solve the conflicts without the aid of other countries or organizations, when the unstable situation occurs. GDP and GDP per capita are seleted to estimate this probability. Most of countries, which have high GDP per capita, can prepare military assets to cope with conflicts and the equipments to resolve the emergency by natural disasters. However, the magnitude of assets also highly depends on the GDP of each country. In the case of Kuwait, it has pretty high GDP per capita but relatively low GDP. As a result, Kuwait needed the aid from other countries when Iraq intervened.

The last stage is to quantify the probability that U.S. will provide the support when the country needs an aid. This is mainly from the relation between countries, and the treaties can reflect the relation. Therefore, the factors for third probability are the number of treaties of defense, mutual security, peace corps, terrorism, disaster assistance and humanitarian assistance. These three sequential probabilistic approaches and procedures are explained in the following chapters.

5.1 Socio-Economic and Political Instabilities

Sean O'Brien developed a set of macro-structural indicators to predict socio-economic and political instabilities in the countries in his seminal work [75][76]. His detailed predictor thresholds were not made publicly available but his method described depends on a training and validation data sets. These are not readily available and are labor intensive to develop. O'Brien used Fuzzy Logic [11] to train a model that predicted the level of instability in a country based on the high level macro-structural parameters that describe a country's situation. In essence, O'Brien's fuzzy logic model identifies a membership function for the indicators and levels of conflict. It determines those membership functions using the training set ranging from 1975 to 1984, and then compares the goodness of the model by using it to predict past events from 1985 to 1999. The final integrated model results were then compared to the predictions made from 2000 to 2015 by the intelligence community.

The database used by O'Brien is not publicly open, so for the purposes of this research, a new database was integrated based on the publicly available data. The database includes information from CIA World Factbook [14], Freedom House [33], Heritage Foundation indices [41], and the World Water Organization [113]. These data contain natural resources and it is no surprise since competition for natural resources is a well known trigger for war.

Based on the database obtained, a study was conducted to identify the level of correlation between the macro-level indicators and the likelihood of war. An additional data set for the number of conflicts in the area in the last 60 years was compiled for each country in the world and its distribution along each independent factor studied. For this

thesis, total eight macro-structural parameters are considered as factors for military conflicts, based on O'Brien's research. The standard for military conflicts is defined as the event of war organized continuing use of force. This definition is exactly same as the level four of conflict in Kosimo database [121]. The importance of each indicator can be estimated by comparing orthogonal estimates calculated statistically [52][73][96]. The results for eight parameters are presented in Figure 5.2. The results indicate that the probability of conflict is most highly correlated with GDP per capita and oil production. Civil liberty, economic freedom and infant mortality show the level of next group of significance, while political right, life expectancy and youth bulge indicate relatively less effects on the historical conflicts.

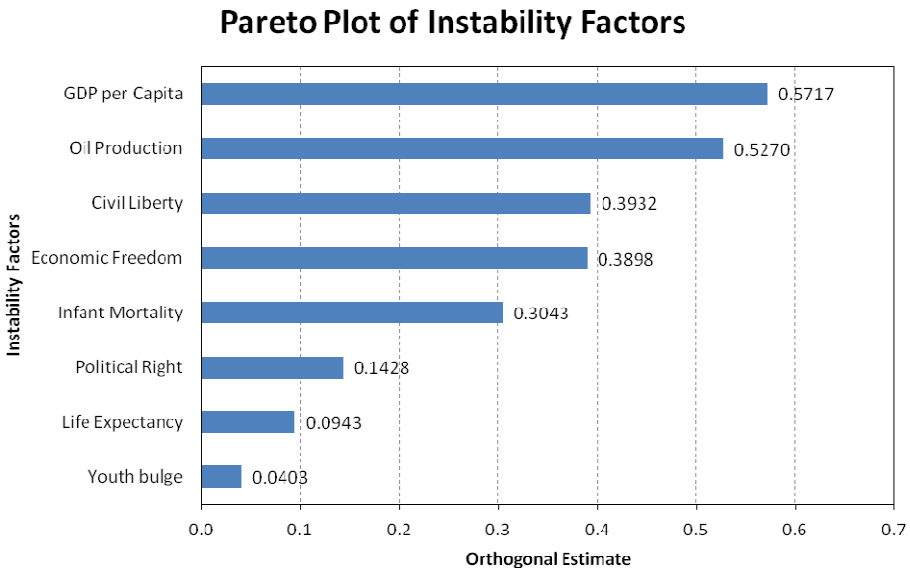

Figure 5.2 Pareto Plot of the factors for conflicts

5.1.1 Regression Model of Socio-Economic and Political Instabilities

The most important parameter of conflicts is GDP per capita. The orthogonal estimate of GDP per capita is calculated as 0.5717. The data of GDP per capita refers

CIA world fact book [14]. The probability with regard to GDP per capita is shown in Figure 5.3. Overall, the result indicates that the numbers of conflicts are in inverse proportion to GDP per capita. The numbers of samples in each category are in the range from 19 to 32 except the first graph of the range under 4,000 and the fifth graph of the range between 16,000 and 20,000. The number of samples for the first graph is 73 because this section includes many of countries in Africa, Asia and small island countries. The number of samples for the fifth graph is 13 and it is the minimum number of samples. Exceptionally, the section for the range from 20,000 to 30,000 shows relatively higher result. This is caused by the conflicts of Israel against the countries in Middle East.

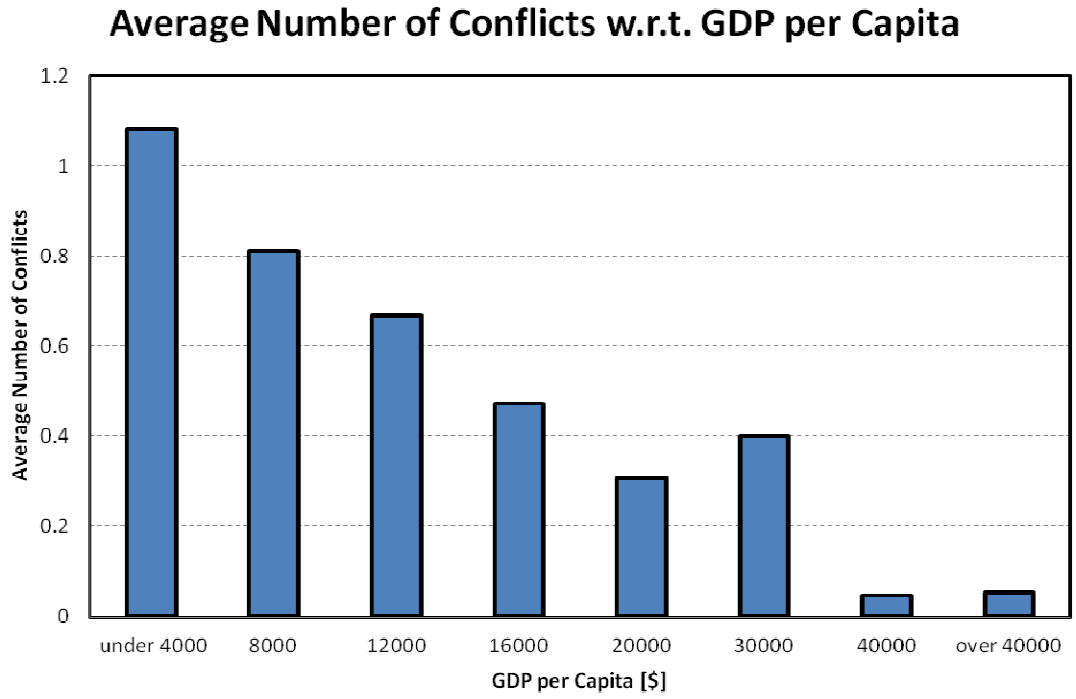

Figure 5.3 Average numbers of conflicts with regard to GDP per capita

In order to acquire the fitting line for the average number of conflicts, Weibull distribution is applied. Original Weibull distribution is as follows: [70]

$$f(x;\lambda,k) = \frac{\kappa}{\lambda}\left(\frac{x}{\lambda}\right)^{\kappa-1} e^{-\left(\frac{x}{\lambda}\right)^{\kappa}}, \text{if } x \geq 0 \qquad \text{Eq. (5.1)}$$

$$= 0, \text{if } x < 0$$

Because Weibull distribution is for probability that the summation is always one, for this research, Weibull distribution needs to be modified in order to show the appropriate numbers. The modified Weibull distribution is as follows:

$$f(x;\lambda,k) = A\frac{\kappa}{\lambda}\left(\frac{Bx}{\lambda}\right)^{\kappa-1} e^{-\left(\frac{Bx}{\lambda}\right)^{\kappa}}, \text{if } x \geq 0 \qquad \text{Eq. (5.2)}$$

$$= 0, \text{if } x < 0$$

By using this modified Weibull distribution, the fitting line for the average number of conflicts can be estimated. The equation for the fitting line is described in Eq. (5.3). To check the accuracy, R square and R square adjust are one of the most important indicator. The R square value is estimated as 0.95124, and R square adjust value is estimated as 0.93174. These values are both over 0.9 and these values can be regarded as excellent fitting model considering the unpredictable and complicated properties of conflict causes. The result of fitting is compared in Figure 5.4. Except one section caused by Israel, most of area shows well-matching prediction.

$$f1(x;\lambda,k) = 1.0743(5.714 \cdot 10^{-5}\, x)^{-0.06731} e^{-\left(5.714 \cdot 10^{-5}\, x\right)^{0.93269}} \qquad \text{Eq. (5.3)}$$

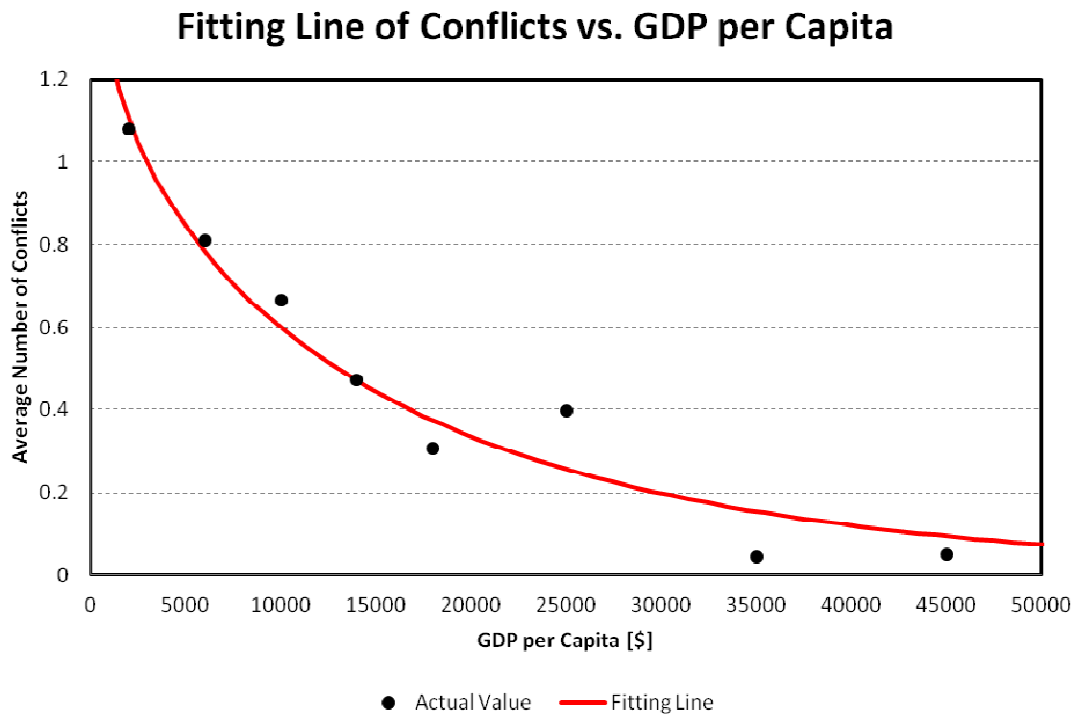

Figure 5.4 Fitting line of the number of Conflicts with regard to GDP per capita

The second important factor of instability is the amount of oil production of each country. The data of oil production refers CIA world fact book [14].The orthogonal estimate of oil production is calculated as 0.5270. The average numbers of conflicts with regard to oil production is shown in Figure 5.5. Overall, the result indicates that the numbers of conflicts are in logarithmically proportion to oil production. The numbers of samples in each category are 58 countries for the section with no oil production, 44 countries for the range under 10,000 BBL per day, 14 countries for the range between 10,000 and 100,000 BBL per day, 17 countries for the range between 100,000 and 1,000,000 BBL per day, and 48 countries for the range over 1,000,000 BBL per day. Especially, the section for highest oil production shows less average number of conflicts

than the second highest range. This phenomenon is caused by the stable countries with large amount oil production such as the United States, Saudi Arabia, and Norway.

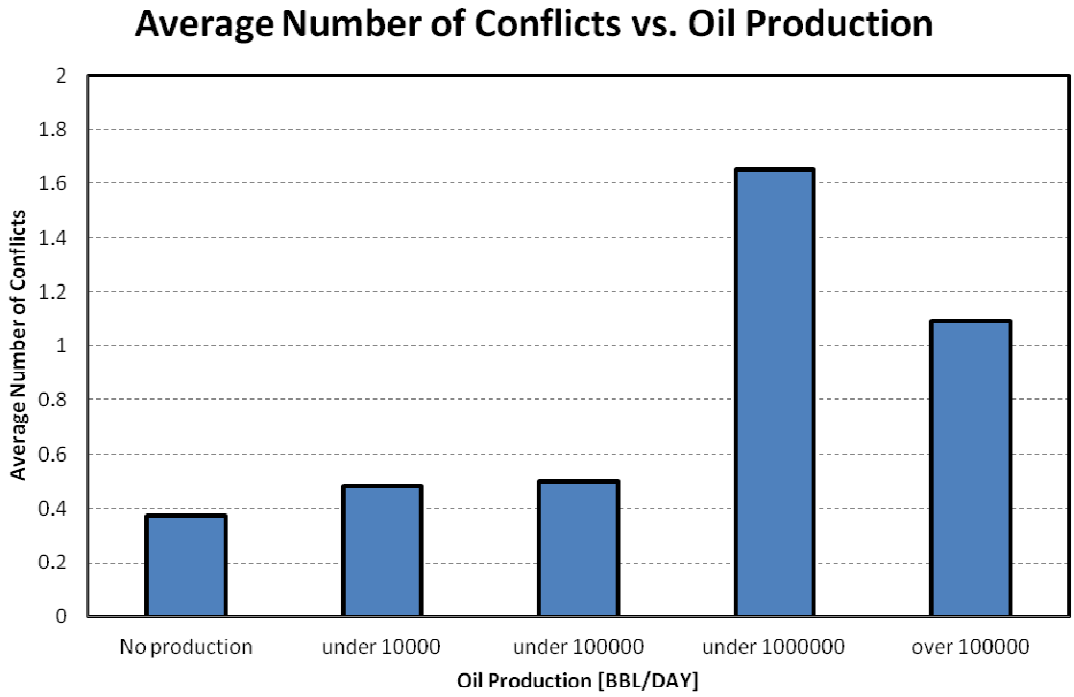

Figure 5.5 Average numbers of conflicts with regard to oil production

To make the response surface model, the Weibull distribution is employed again. However, in order to fit the asymmetric original distribution, the Weibull distribution is modified in the different method from the case of GDP per Capita. This modified Weibull distribution is as follows:

$$f(x;\lambda,k) = \frac{\kappa}{\lambda}\left(\frac{A-B(\log x-C)}{\lambda}\right)^{\kappa-1} e^{-\left(\frac{A-B(\log x-C)}{\lambda}\right)^{\kappa}} + D \qquad \text{Eq. (5.4)}$$

The fitted response surface model is described in Eq. (5.5). The R square value is estimated as 0.99504, and R square adjust value is estimated as 0.99009. These values are over 0.99 and these values can be regarded significantly excellent considering the

geographically different situation of the countries with conflict. The result of fitting is compared in Figure 5.6. Generally, most of area shows well-matching prediction.

$$f2(x) = 3.5047\left(2.4230 - 0.3483(\log[\text{Oil production}] - 3)\right)^{4.0482} \cdot e^{-\left(2.4230 - 0.3483(\log[\text{Oil production}] - 3)\right)^{5.0482}} + 0.4301 \quad \text{Eq. (5.5)}$$

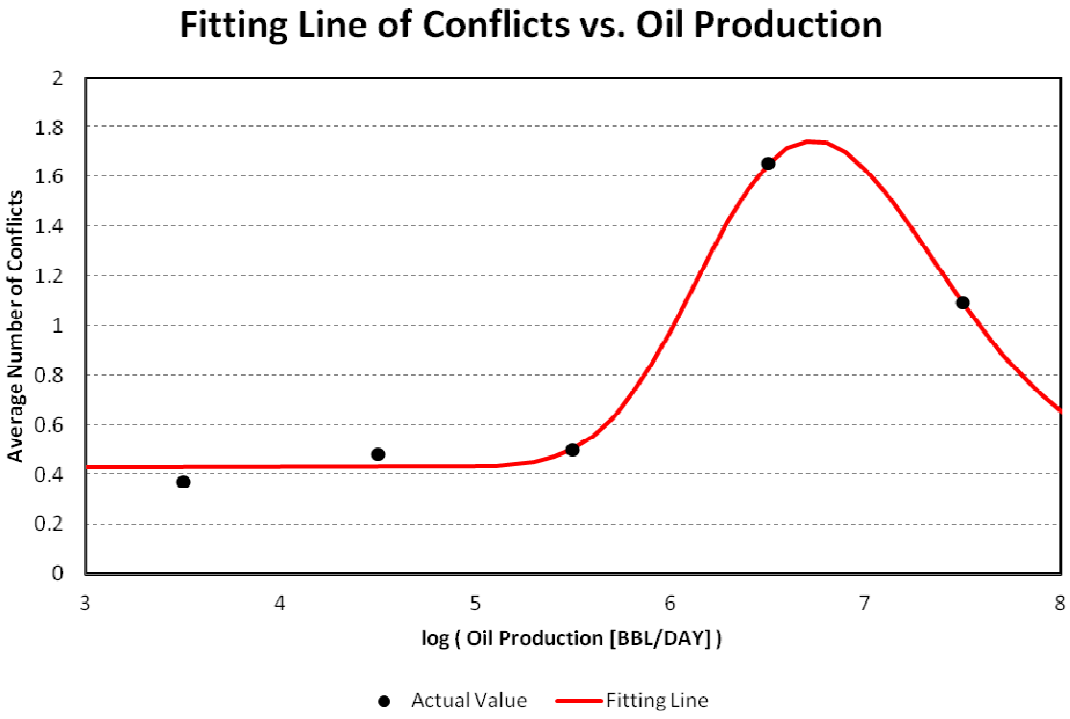

Figure 5.6 Fitting line of the number of Conflicts with regard to oil production

The third important factor of instability is the degree of civil liberty index of each country. The data of civil liberty refers freedom house which is an independent watchdog organization dedicated to the expansion of freedom around the world [33]. Higher index of civil liberty means that the country allows more restricted civil liberty to their citizen. The orthogonal estimate of civil liberty is calculated as 0.3932. The average numbers of conflicts with regard to civil liberty is shown in Figure 5.7. Overall, the result indicates that the numbers of conflicts are in proportion to civil liberty index. The numbers of

samples in each category are 51 countries for level 1 civil liberty index, 29 countries for level 2 civil liberty index, 32 countries for the level 3 civil liberty index, 28 countries for level 4 civil liberty index, 32 countries for level 5 civil liberty index, 15 countries for level 6 civil liberty index, and 8 countries for level 7 civil liberty index.

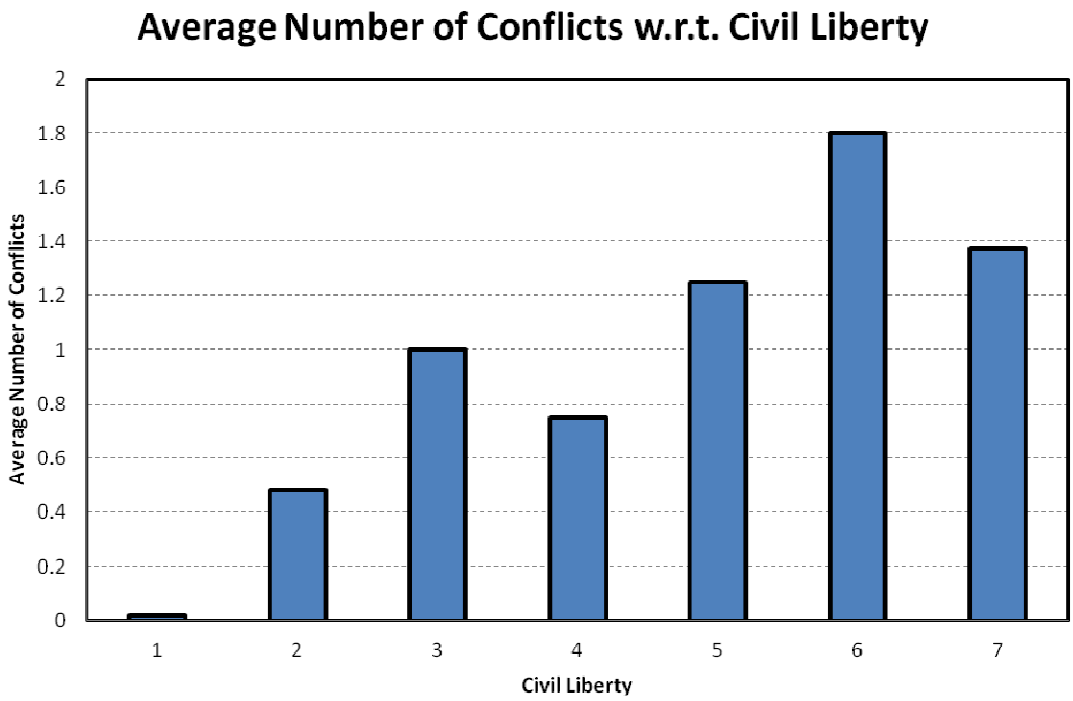

Figure 5.7 Average numbers of conflicts with regard to civil liberty

To make the response surface model, the linear approximation is employed. The formulation for linear approximation is as follows:

$$f(x) = Ax + B \qquad \text{Eq. (5.6)}$$

The fitted response surface model is described in Eq. (5.7). The R square value is calculated as 0. 814082, and R square adjust value is calculated as 0. 776899. These values are around 0.8 and these values can be regarded reasonable considering the limited

sample size of the countries with conflict. The result of fitting is compared in Figure 5.8. Generally, most of area shows well-matching prediction too.

$$f3(x) = 0.2482378 \cdot \text{Infant Mortality} - 0.039042 \qquad \text{Eq. (5.7)}$$

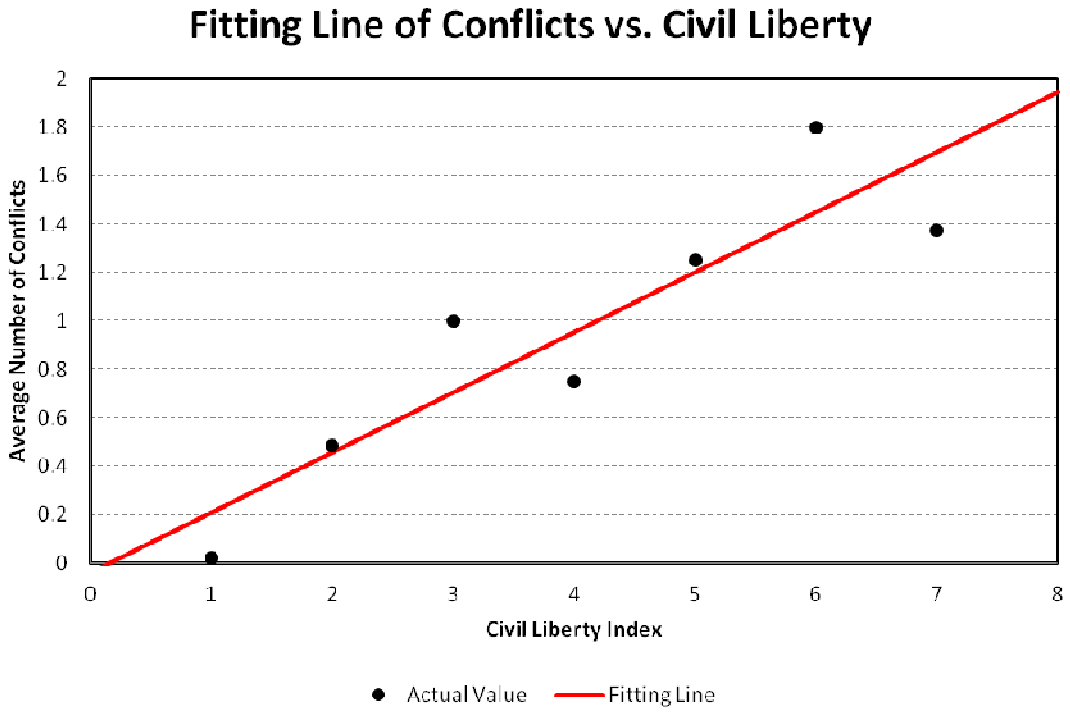

Figure 5.8 Fitting line of the number of Conflicts with regard to civil liberty

The fourth important factor of instability is the degree of economic freedom index of each country. The data of economic freedom refers freedom house whose mission formulate and promote conservative public policies based on the principles of free enterprise, limited government, individual freedom, traditional American values, and a strong national defense [41]. Lower index of economic freedom means that the country allows more restricted economic freedom to their citizen. The orthogonal estimate of economic freedom is calculated as 0.3898. The average numbers of conflicts with regard to economic freedom is shown in Figure 5.9. Overall, the result indicates that the

numbers of conflicts are in proportion to civil liberty index. The numbers of samples in each category are 51 countries for level 1 civil liberty index, 29 countries for level 2 civil liberty index, 32 countries for the level 3 civil liberty index, 28 countries for level 4 civil liberty index, 32 countries for level 5 civil liberty index, 15 countries for level 6 civil liberty index, and 8 countries for level 7 civil liberty index.

The result that is not intuitive is the distribution for Economic Freedom Index (EFI). The results indicate that if the country has very low levels of EFI, it has lower probability of undergoing a military instability than if it receives a mid-range EFI. A possible explanation for this is that countries that are between free markets and highly controlled economies are more likely to become unstable. It is not surprising that they would be more likely to experience conflict than the free markets, but it is unexpected that they would be more likely to experience conflict than the more autocratic economies.

To make the response surface model, the linear approximation is employed. The formulation for cubic polynomial approximation is as follows:

$$f(x) = Ax^3 + Bx^3 + Cx + D \qquad \text{Eq. (5.8)}$$

The fitted response surface model is described in Eq. (5.9). The R square value is calculated as 0. 955379, and R square adjust value is calculated as 0.888448. These values are around 0.9 and these values can be regarded excellent considering the limited sample size of the countries with conflict. The result of fitting is compared in Figure 5.10. Generally, most of area shows significantly well-matching prediction.

$$f(x) = 0.143\ 10^{-4}\ \mathrm{EFI}^3 - 0.00122\ \mathrm{EFI}^2 - 0.00154\ \mathrm{EFI} + 2.410 \qquad \text{Eq. (5.9)}$$

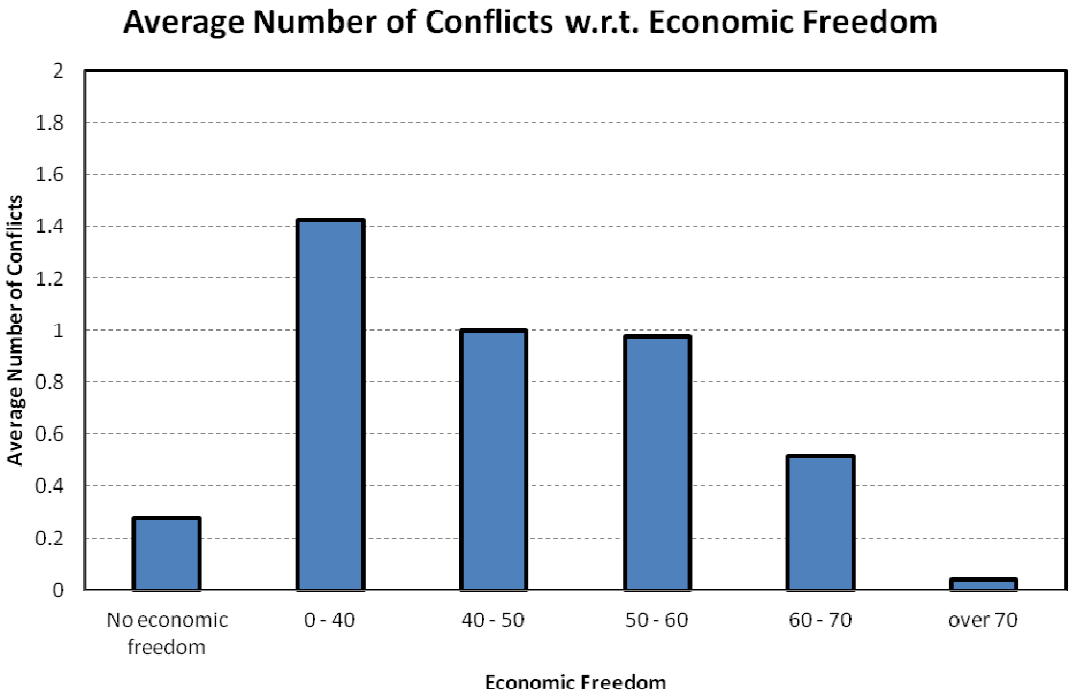

Figure 5.9 Average numbers of conflicts with regard to economic freedom index

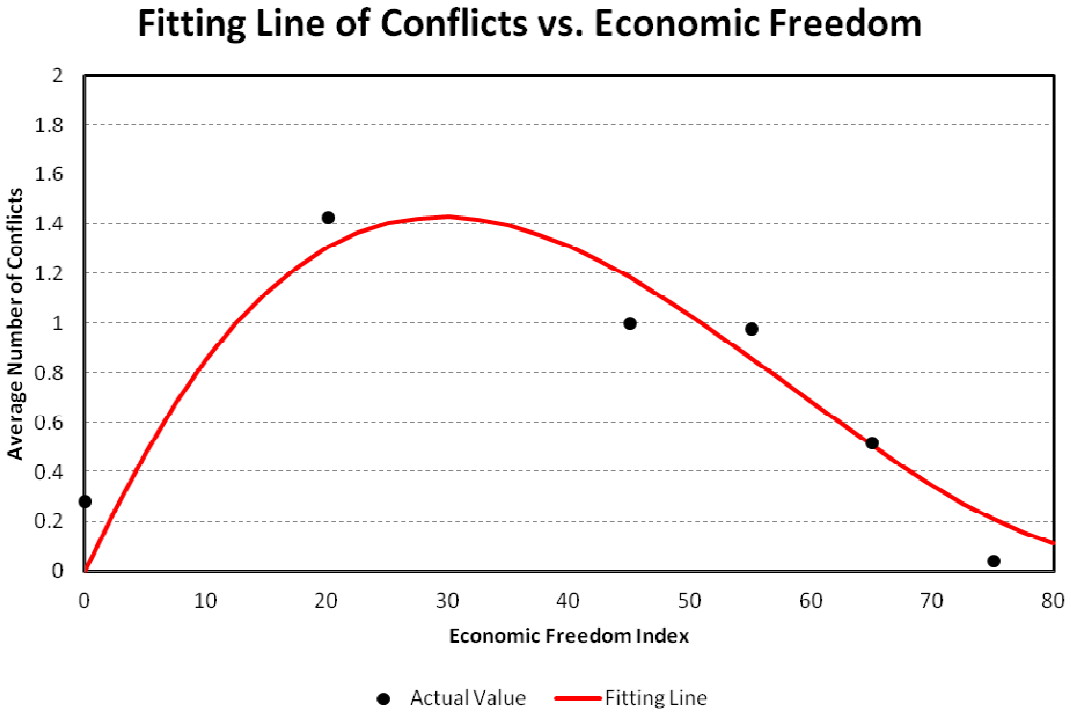

Figure 5.10 Fitting line of the number of Conflicts with regard to economic freedom index

The fifth important factor of instability is the degree of infant mortality of each country. The data of oil production refers CIA world fact book [14]. The orthogonal estimate of infant mortality is calculated as 0.3043. The average numbers of conflicts with regard to infant mortality is shown in Figure 5.11. Overall, the result indicates that the numbers of conflicts are in proportion to infant mortality. The numbers of samples in each category are 143 countries for the range under 25 death per one thousand infants, 38 countries for the range between 25 and 50 death per one thousand infants, 26 countries for the range between 50 and 75 death per one thousand infants, 15 countries for the range between 75 and 100 death per one thousand infants, and 9 countries for the range over 100 death per one thousand infants. More than half of countries have the infant mortality under 25 death per one thousand infants.

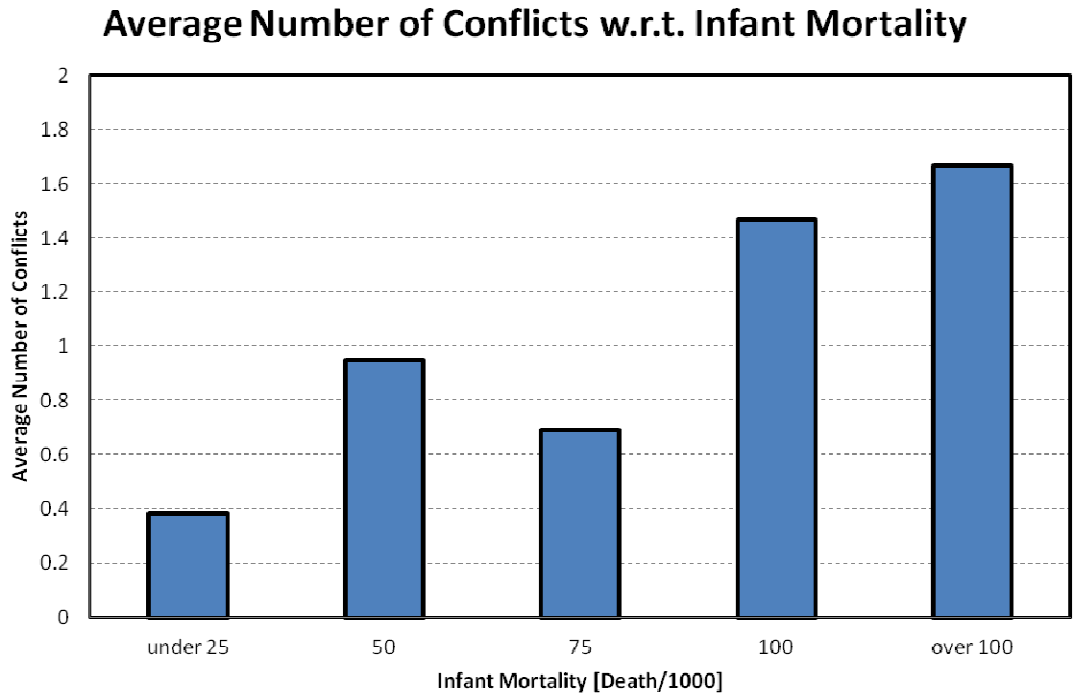

Figure 5.11 Average numbers of conflicts with regard to infant mortality

To make the response surface model, the linear approximation is employed. The formulation for linear approximation is as follows:

$$f(x) = Ax + B \qquad \text{Eq. (5.10)}$$

The fitted response surface model is described in Eq. (5.11). The R square value is calculated as 0.838838, and R square adjust value is calculated as 0.785118. These values are around 0.8 and these values can be regarded reasonable considering the limited sample size of the countries with conflict. The result of fitting is compared in Figure 5.12. Generally, most of area shows well-matching prediction too.

$$f(x) = 0.0123336 \cdot \text{Infant Mortality} + 0.2606748 \qquad \text{Eq. (5.11)}$$

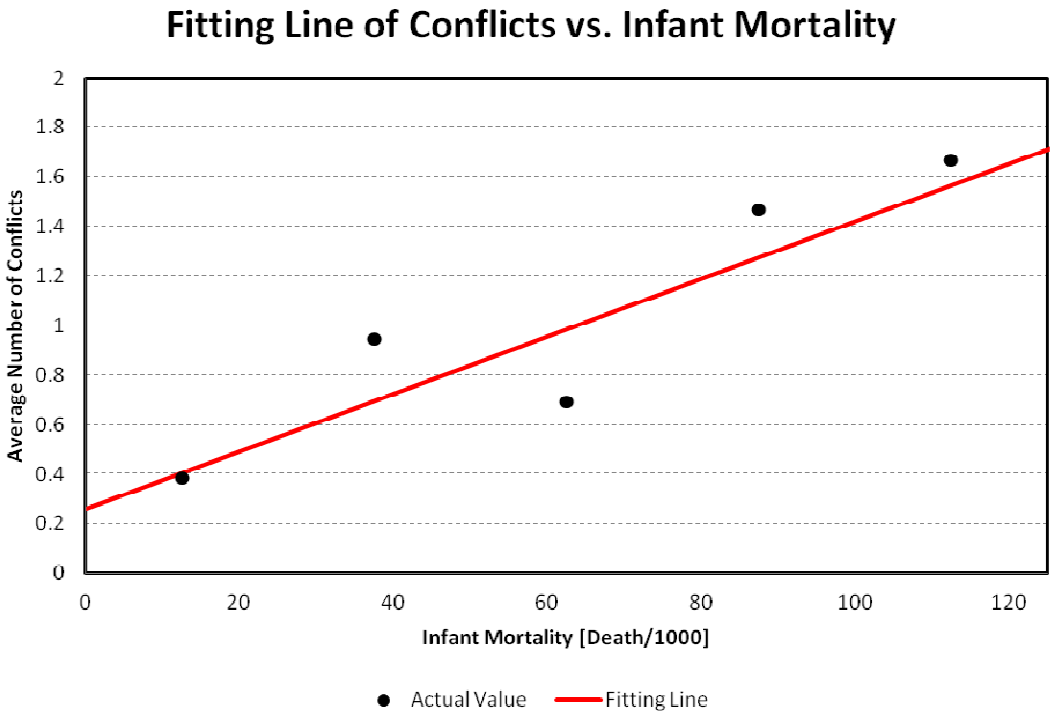

Figure 5.12 Fitting line of the number of Conflicts with regard to infant mortality

The sixth important factor of instability is the degree of political right index of each country. The data of political right refers freedom house which is an independent watchdog organization dedicated to the expansion of freedom around the world [33]. Higher index of political right means that the country allows more restricted political right to their citizen. The orthogonal estimate of political right is calculated as 0.1428. The average numbers of conflicts with regard to political right is shown in Figure 5.13. Overall, the result indicates that the numbers of conflicts are in proportion to political right index. The numbers of samples in each category are 9 countries for level 1 civil liberty index, 21 countries for level 2 civil liberty index, 14 countries for the level 3 civil liberty index, 22 countries for level 4 civil liberty index, 21 countries for level 5 civil liberty index, 24 countries for level 6 civil liberty index, and 35 countries for level 7 civil liberty index.

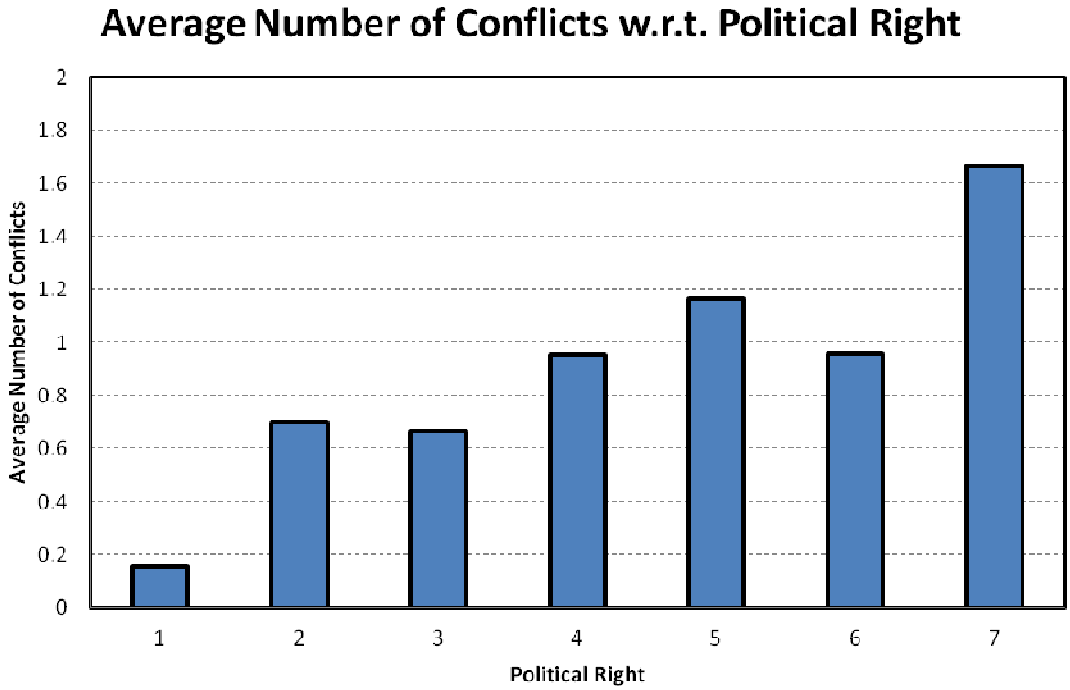

Figure 5.13 Average numbers of conflicts with regard to political right

To make the response surface model, the linear approximation is employed. The fitted response surface model is described in Eq. (5.12). The R square value is calculated as 0. 74732, and R square adjust value is calculated as 0.696784. These values are around 0.8 and these values can be regarded reasonable considering the limited sample size of the countries with conflict. The result of fitting is compared in Figure 5.14. Generally, most of area shows well-matching prediction too.

$$f3(x) = 0.1654599 \cdot \text{Political right} + 0.2039678 \qquad \text{Eq. (5.12)}$$

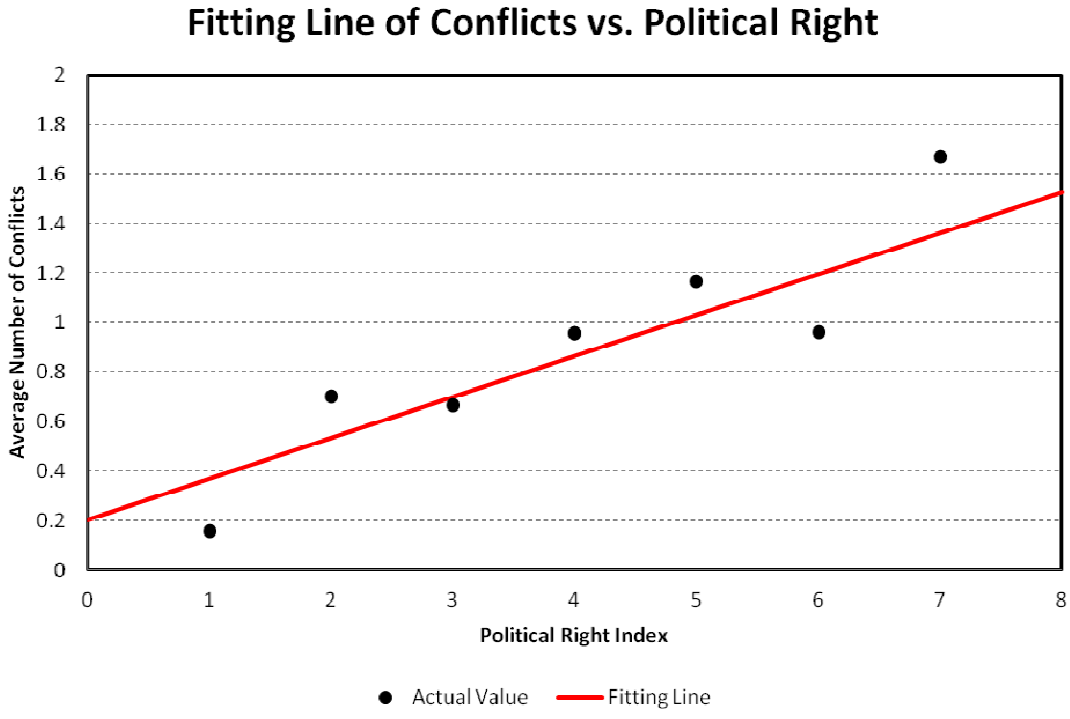

Figure 5.14 Fitting line of the number of Conflicts with regard to political right

The seventh important factor of instability is the degree of life expectancy of each country. The data of oil production refers CIA world fact book [14]. The orthogonal estimate of life expectancy is calculated as 0.0943. The average numbers of conflicts with

regard to life expectancy is shown in Figure 5.15. Overall, the result indicates that the numbers of conflicts are in inverse proportion to life expectancy. The numbers of samples in each category are 17 countries for the range under 50 years, 24 countries for the range between 50 and 60 years, 38 countries for the range between 60 and 70 years, 58 countries for the range between 70 and 75 years, 66 countries for the range between 75 and 80 years, and 20 countries for the range over 80 death years.

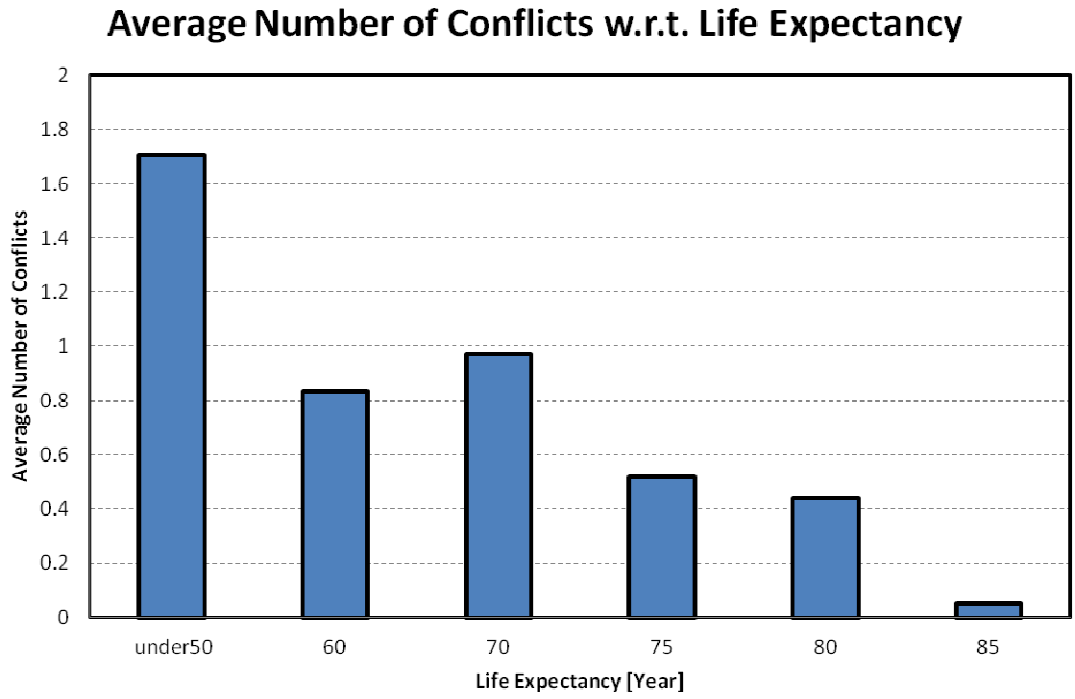

Figure 5.15 Average numbers of conflicts with regard to life expectancy

To make the response surface model, the linear approximation is employed. The fitted response surface model is described in Eq. (5.13). The R square value is calculated as 0. 881034, and R square adjust value is calculated as 0. 851292. These values are over 0.85 and these values can be regarded reasonable considering the limited sample size of

the countries with conflict. The result of fitting is compared in Figure 5.16. Generally, most of area shows well-matching prediction too.

$$f3(x) = -0.037502 \cdot \text{Life expectancy} + 3.2377689 \qquad \text{Eq. (5.13)}$$

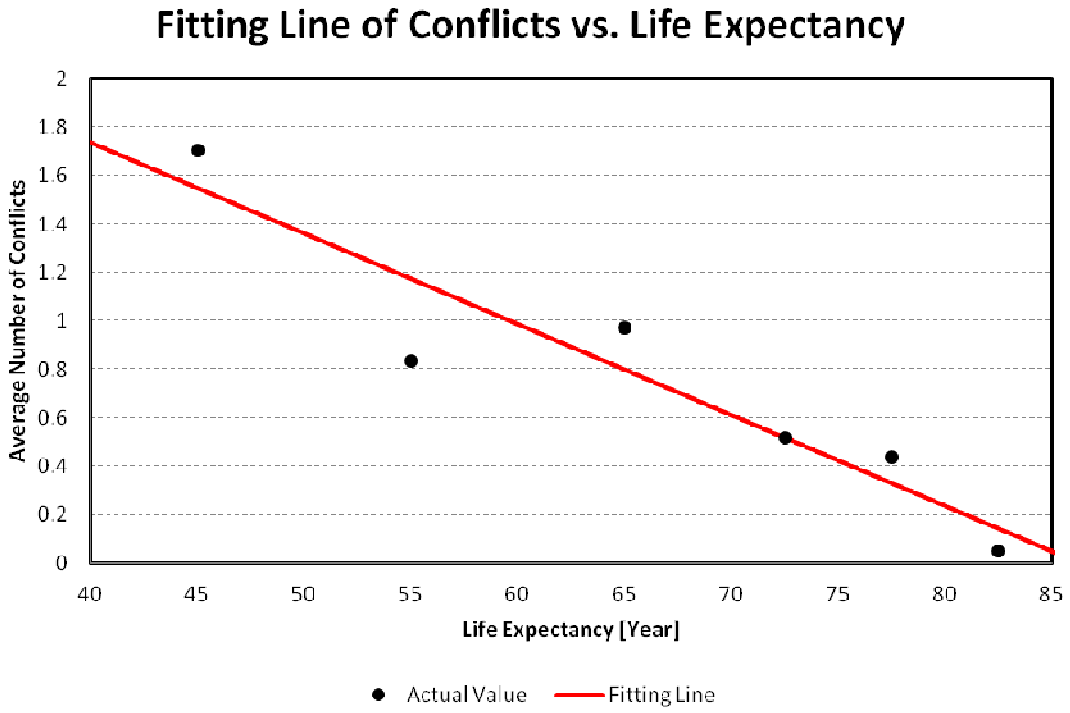

Figure 5.16 Fitting line of the number of Conflicts with regard to life expectancy

The least important factor of instability is the degree of youth bulge of each country. The youth bulge is defines as the ration of population ages 15 to 29 to those ages 30 to 54. The data of youth bulge refers U.S. Bureau of the Census, International Database [108]. The orthogonal estimate of youth bulge is calculated as 0.0403. The average numbers of conflicts with regard to youth bulge is shown in Figure 5.17. Overall, the result indicates that the numbers of conflicts are in proportion to youth bulge. The numbers of samples in each category are 1 country for the range under 0.5, 11 countries for the range between 0.5 and 0.6, 10 countries for the range between 0.6 and 0.7, 14

countries for the range between 0.7 and 0.8, 37 countries for the range between 0.8 and 1.0, 40 countries for the range between 1.0 and 1.25, and 33 countries for the range over 1.25.

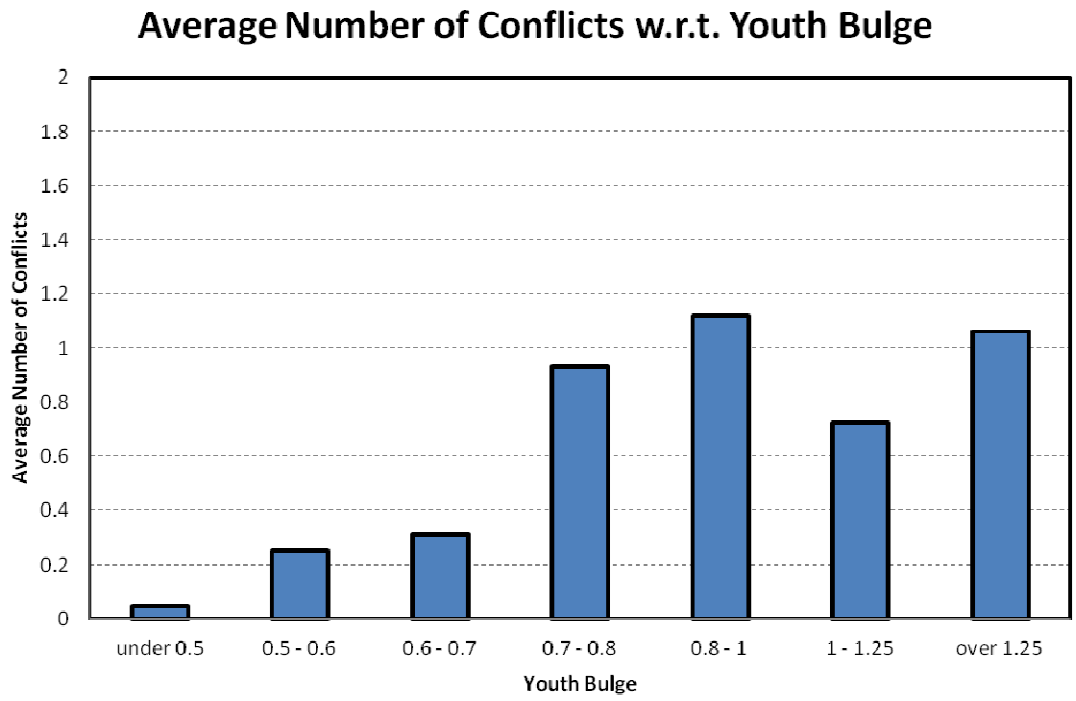

Figure 5.17 Average numbers of conflicts with regard to youth bulge

To make the response surface model, the linear approximation is employed. The fitted response surface model is described in Eq. (5.14). The R square value is calculated as 0. 575119, and R square adjust value is calculated as 0. 490143. These values are over 0.85 and these values can be regarded reasonable considering the limited sample size of the countries with conflict. The result of fitting is compared in Figure 5.18. Generally, most of area shows well-matching prediction too.

$$f3(x) = 0.8663668 \cdot \text{Youth bulge} - 0.047175 \qquad \text{Eq. (5.14)}$$

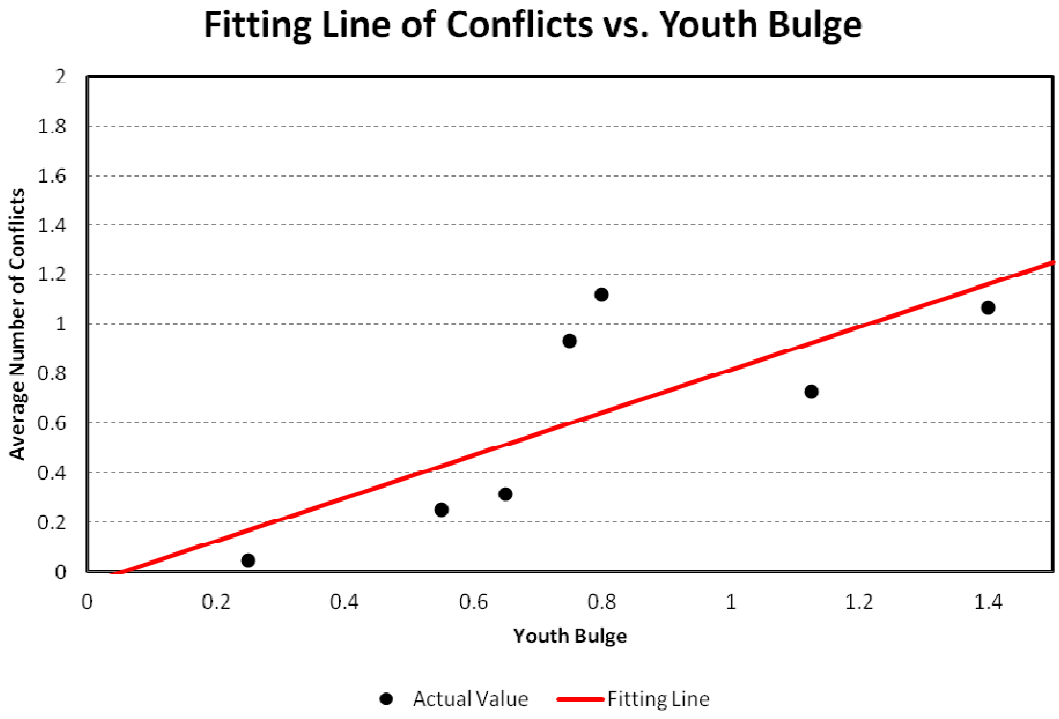

Figure 5.18 Fitting line of the number of Conflicts with regard to youth bulge

Intutively, some of factors can have correlation with other factors. Figure 5.19 describes those relations. Most of factors shows relatively weak correlation except that of political right index and civil liberty. Maximum level of Conflict in KOSIMO database is shown in Figure 5.20. Red colored countries had the military conflict of KOSIMO level 4. Orange colored countries had the military conflict of KOSIMO level 3. Yellow colored countries had the military conflict of KOSIMO level 2. Light green colored countries had the military conflict of KOSIMO level 1. Green colored countries had no military conflict.In addition, based on the Socio-Economic and Political factors, instability indices can be estimated as shown in Figure 5.21. Generally, the countries known as unstable

situation are displayed in red and orange colors. This figure implies the current situation of each country is pretty different from historic unstability.

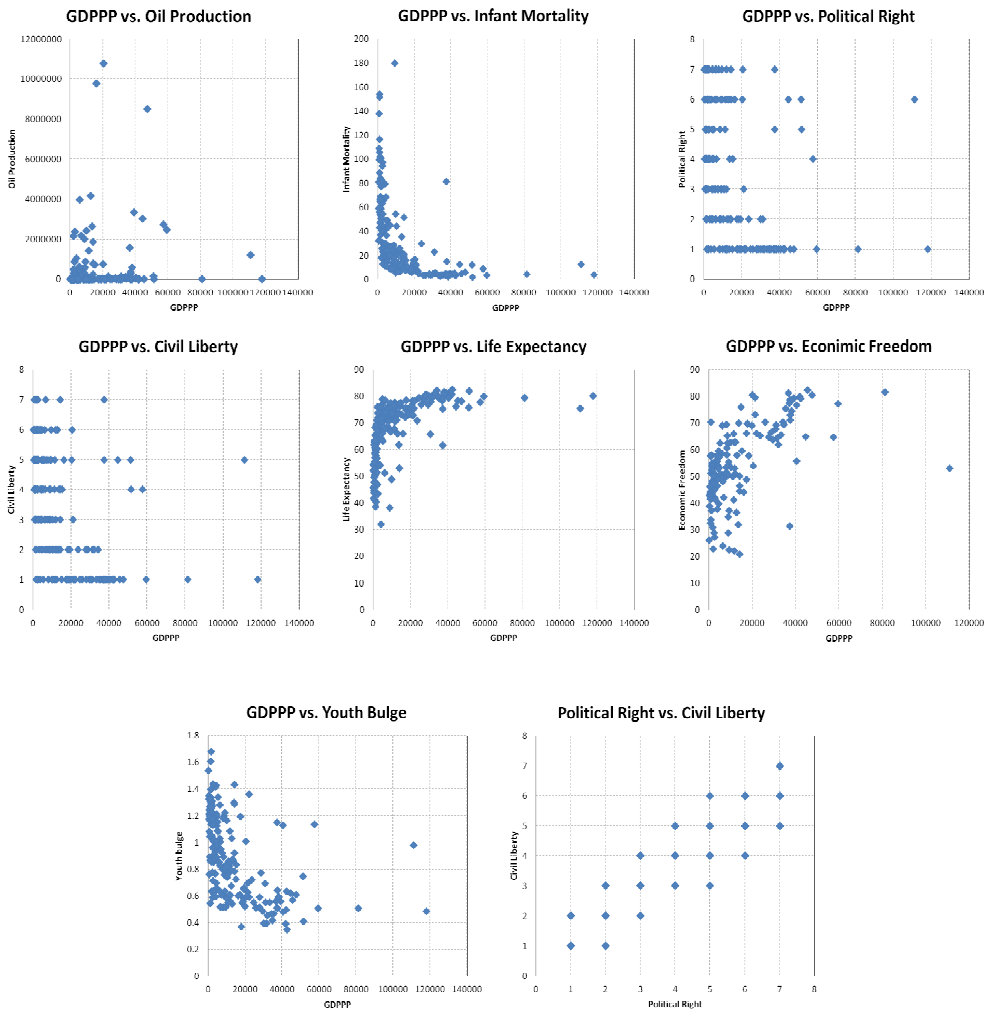

Figure 5.19 Correlation between factors

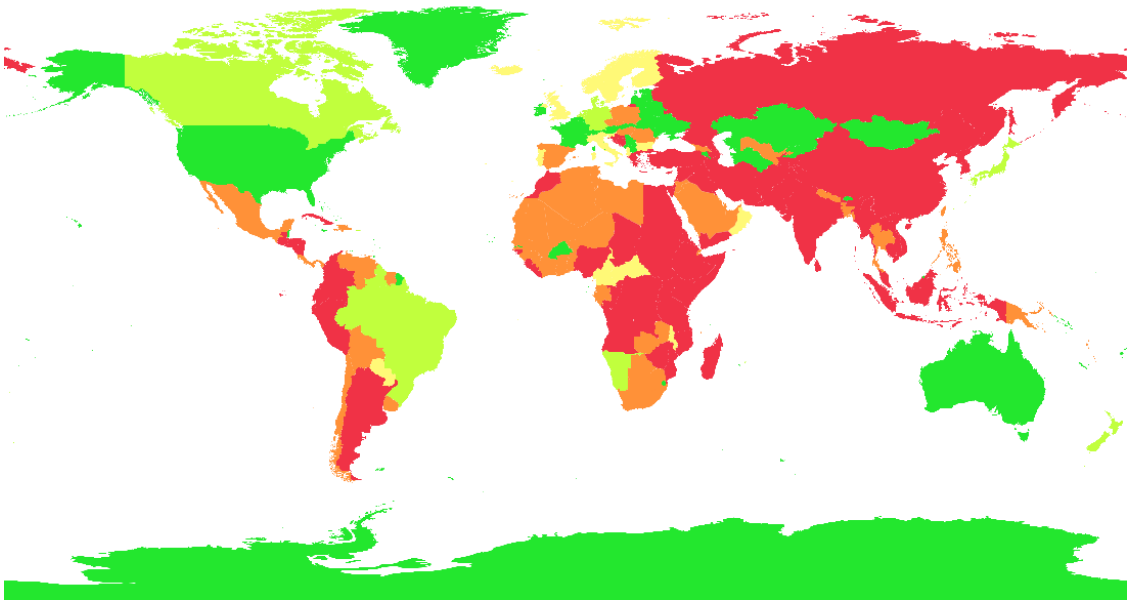

Figure 5.20 Maximum level of Conflict in KOSIMO database

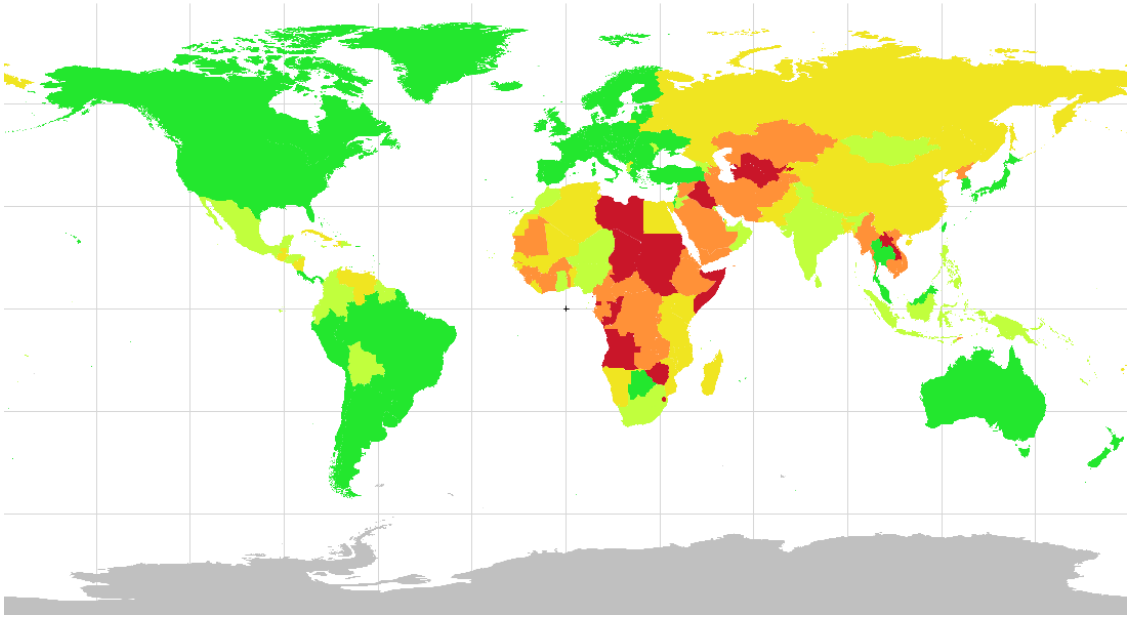

Figure 5.21 Instability Index Predicted by Socio-Economic and Political factors

5.1.2 Time-evolving Probability of Socio-Economic and Political Instabilities

Figure 5.22 shows the average commualtive duration of the conflicts of the countries which GDP per capita are less than $5,000 from 1950 to 2000. The graph shows the linear relation between time and duration in 50 years and it can be regarded as stochastic tendency. This regression results can quantify the usability of the vessels with regard to the service life. For example, the vessel with 20 years service life can be used for average 1.8 years to the countries with GDP per capita less than $5000, while the vessel with 40 years service life can be used for average 4.6 years to the countries in the same category.

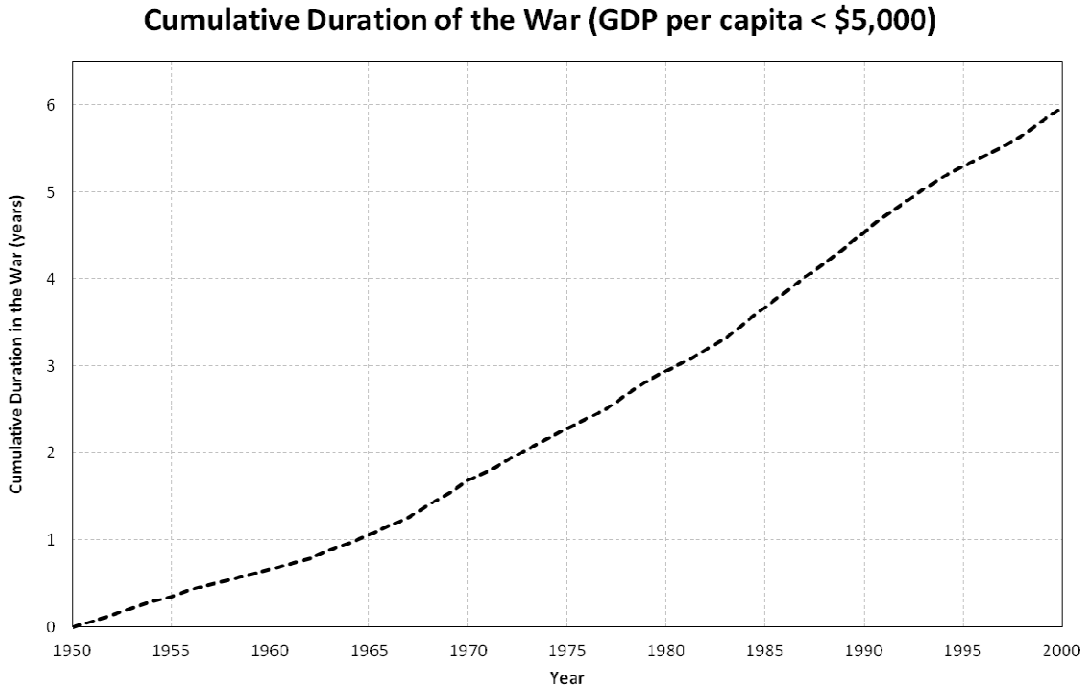

Figure 5.22 Cumulative duration of the conflicts from 1950 to 2000

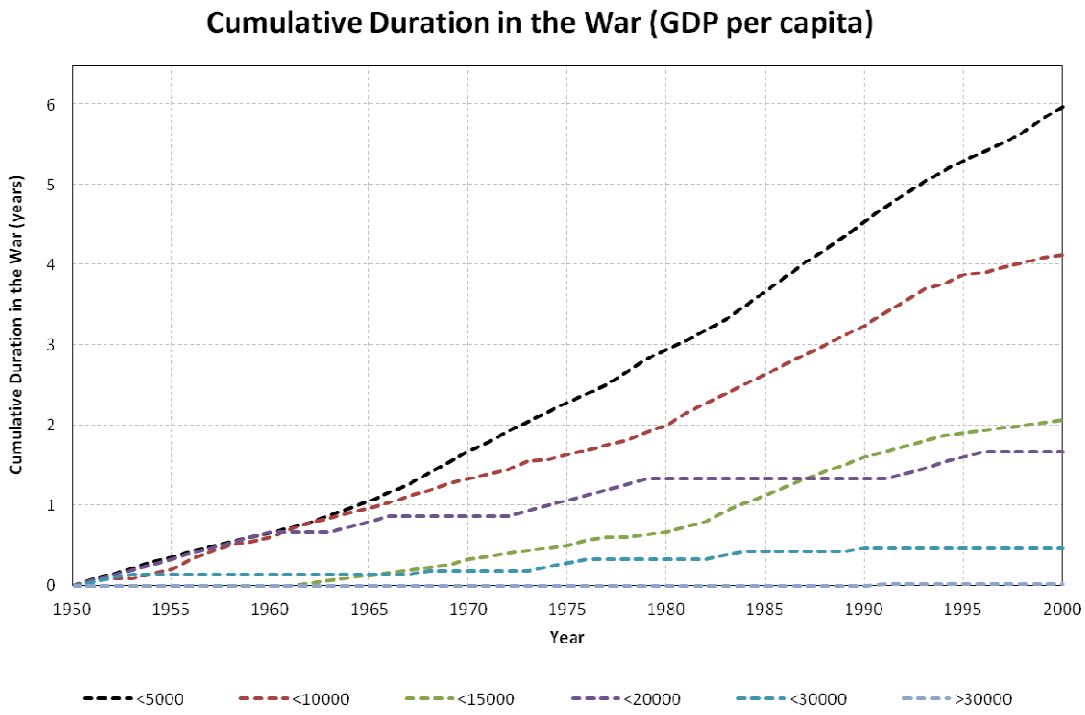

Figure 5.23 Cumulative Duration in the War (GDP per capita)

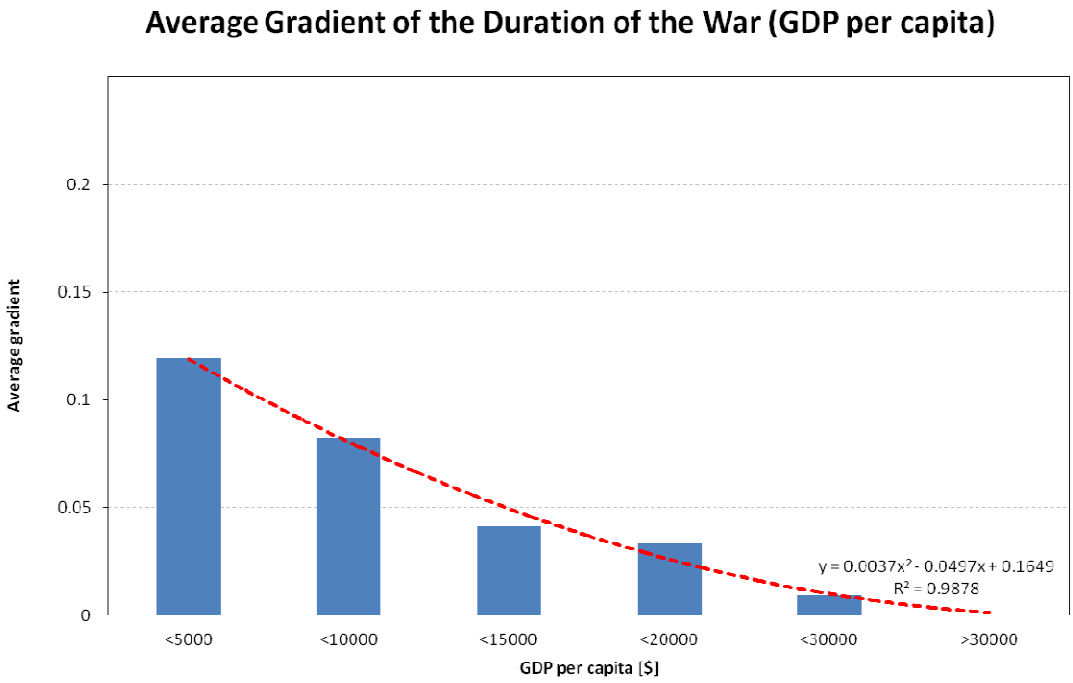

Figure 5.24 Average Gradient of the Duration of the War (GDP per capita)

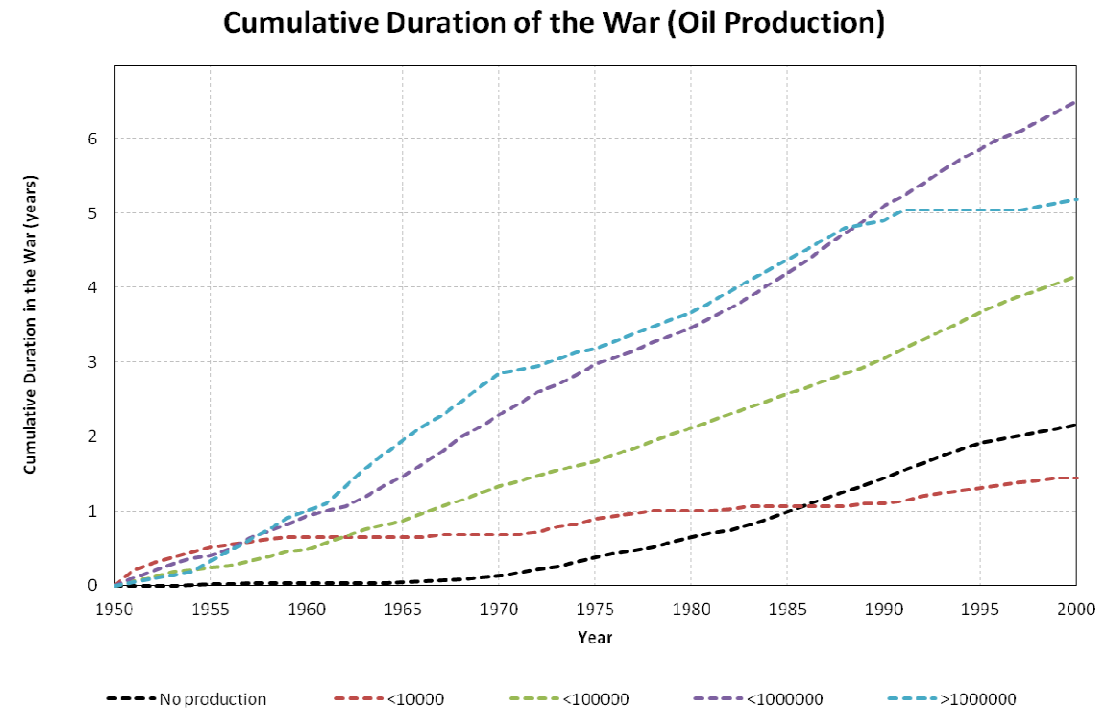

Figure 5.25 Cumulative Duration in the War (Oil Production)

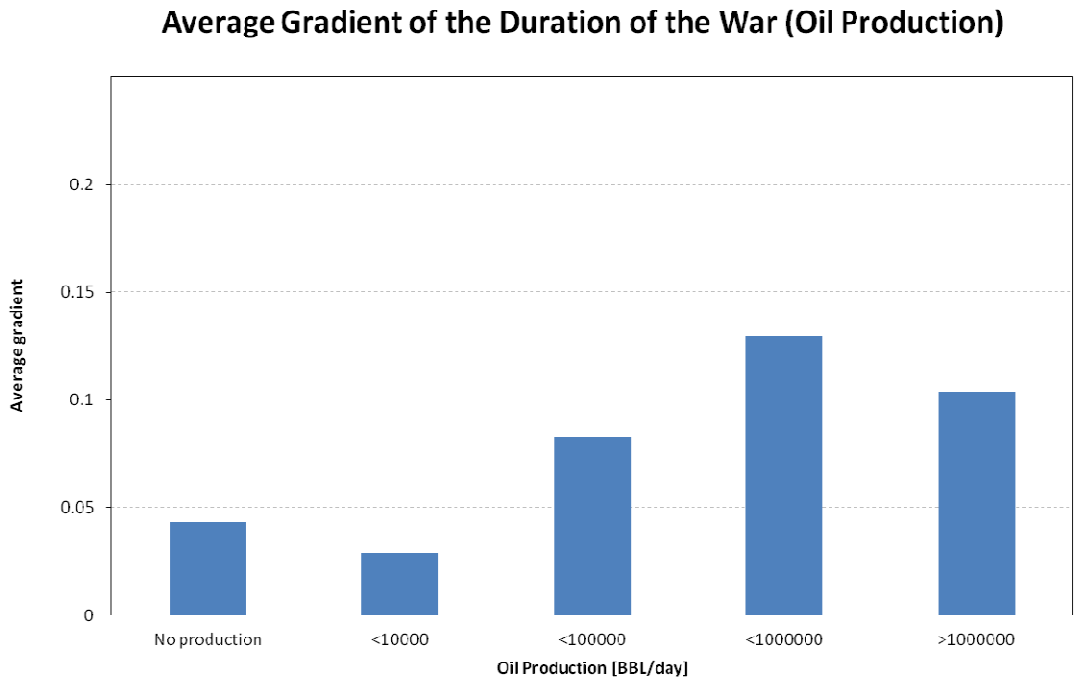

Figure 5.26 Average Gradient of the Duration of the War (Oil Production)

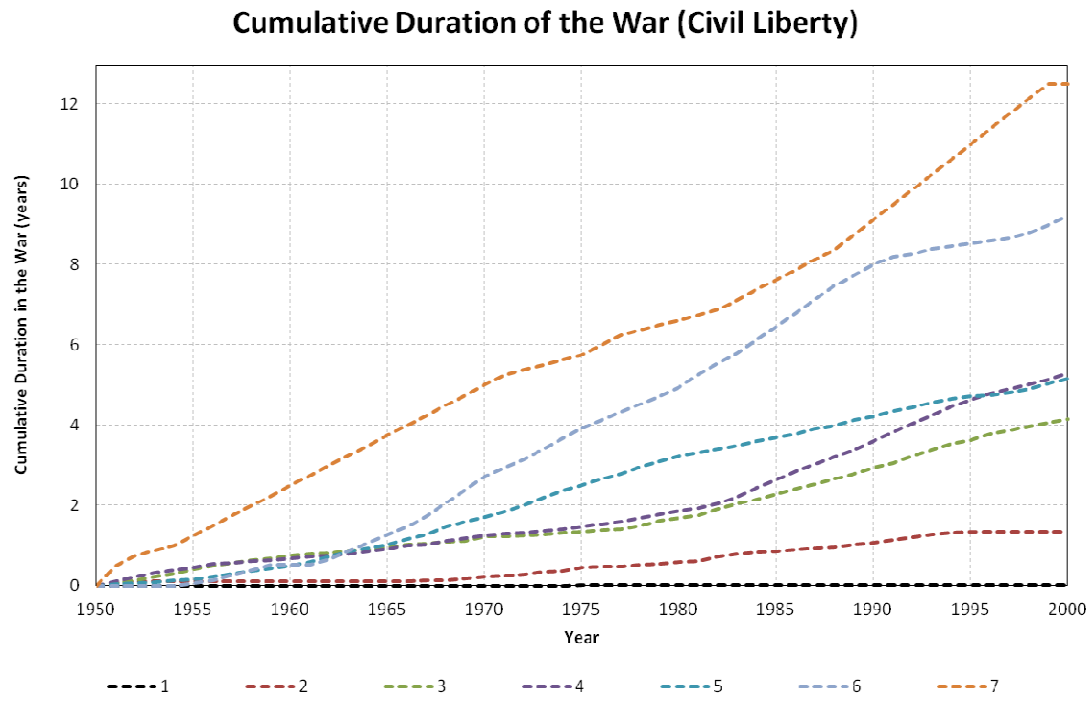

Figure 5.27 Cumulative Duration in the War (Civil Liberty)

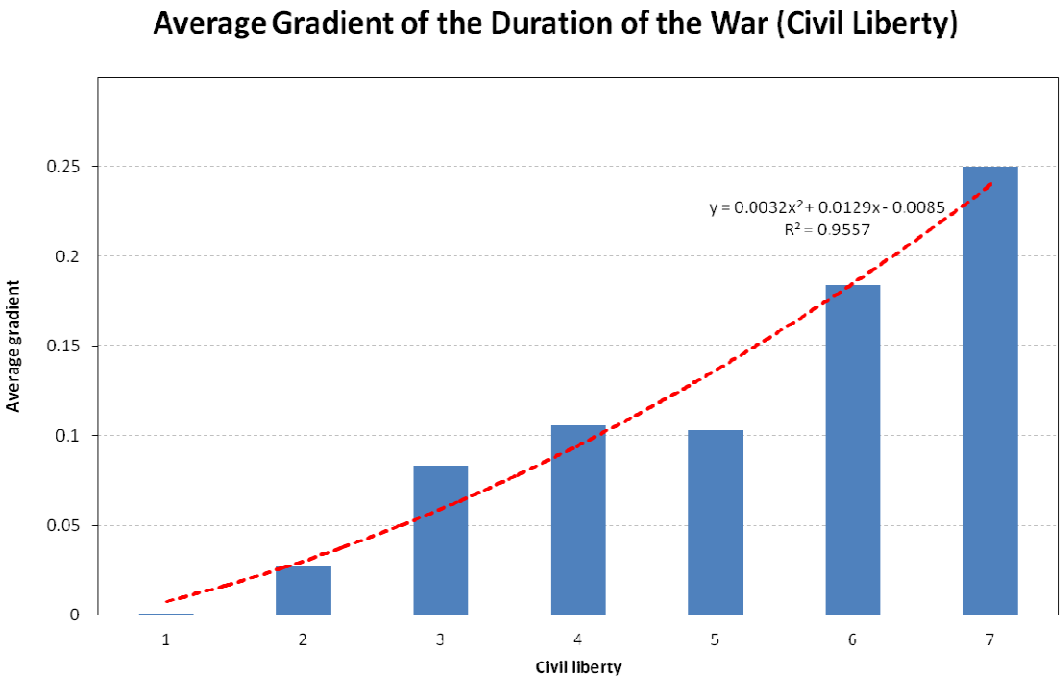

Figure 5.28 Average Gradient of the Duration of the War (Civil Liberty)

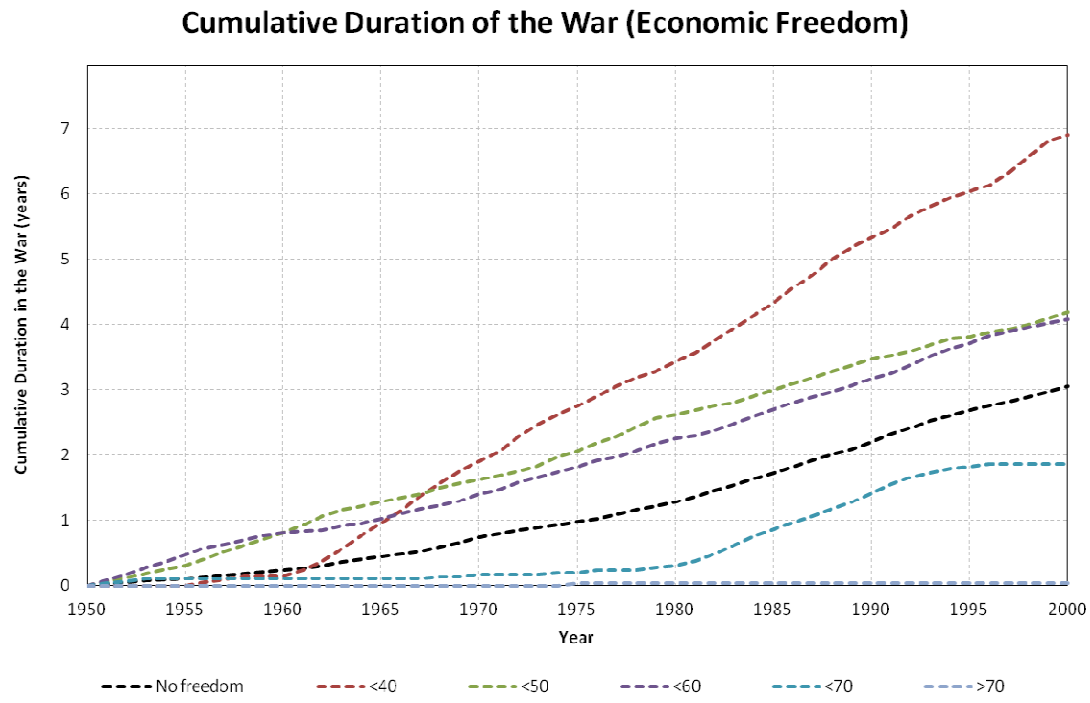

Figure 5.29 Cumulative Duration in the War (Economic Freedom)

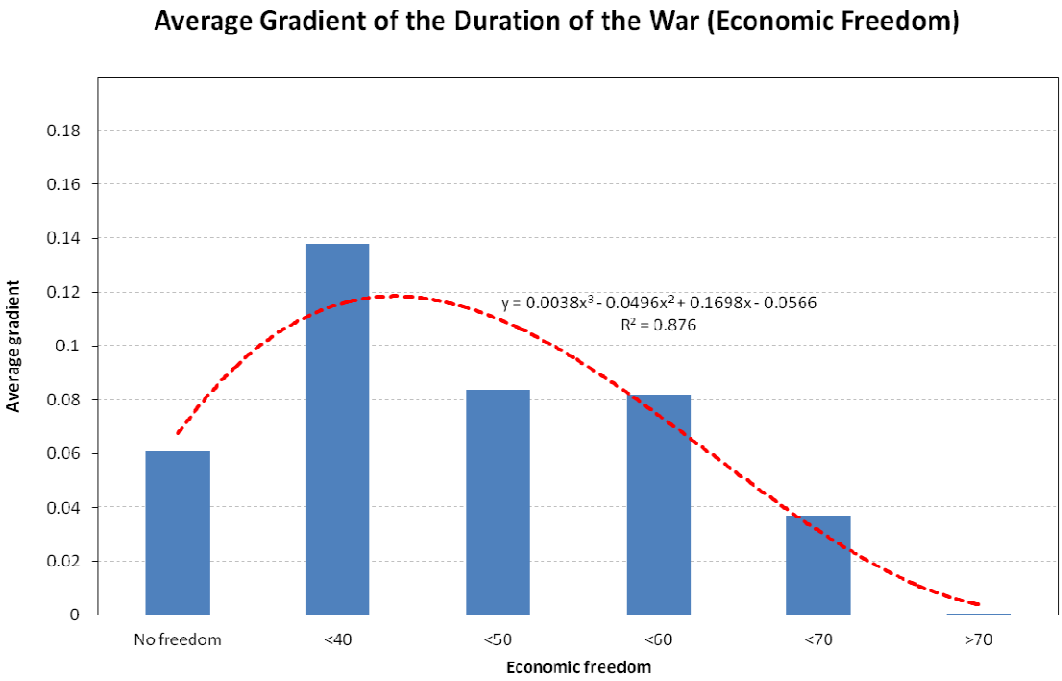

Figure 5.30 Average Gradient of the Duration of the War (Economic Freedom)

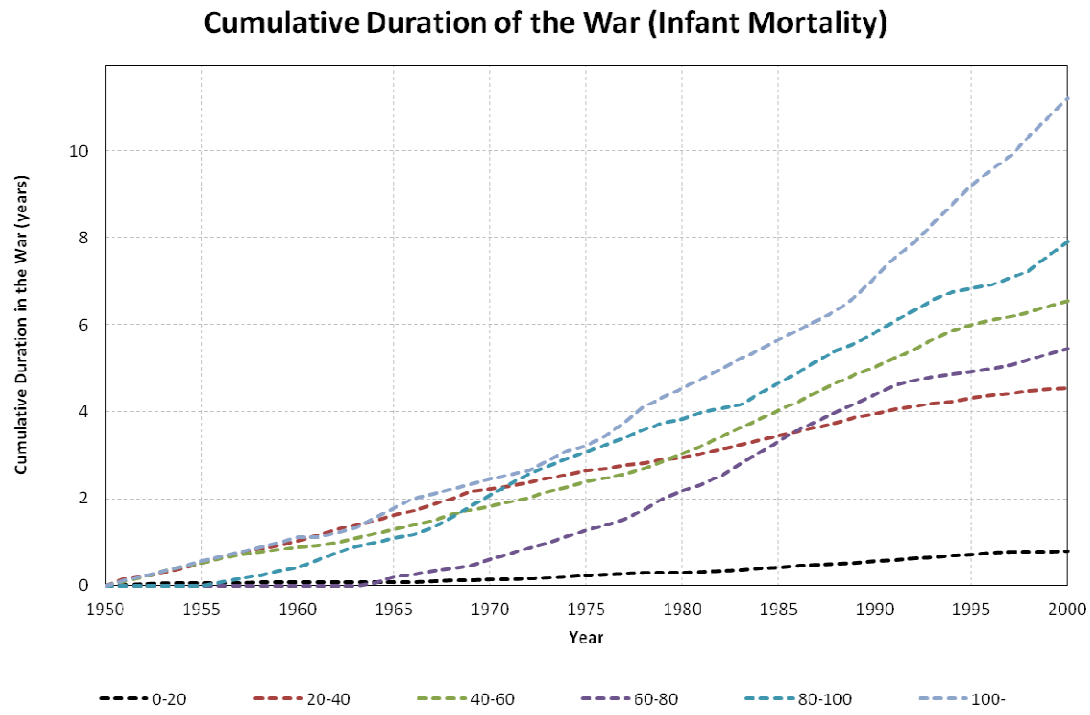

Figure 5.31 Cumulative Duration in the War (Infant Mortality)

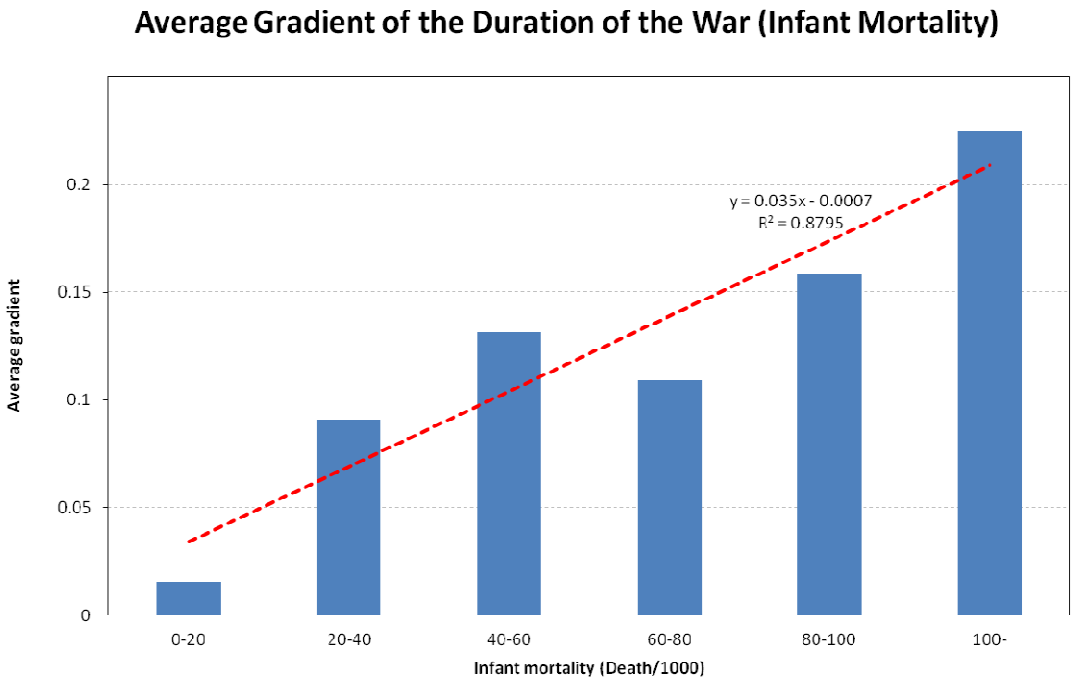

Figure 5.32 Average Gradient of the Duration of the War (Infant Mortality)

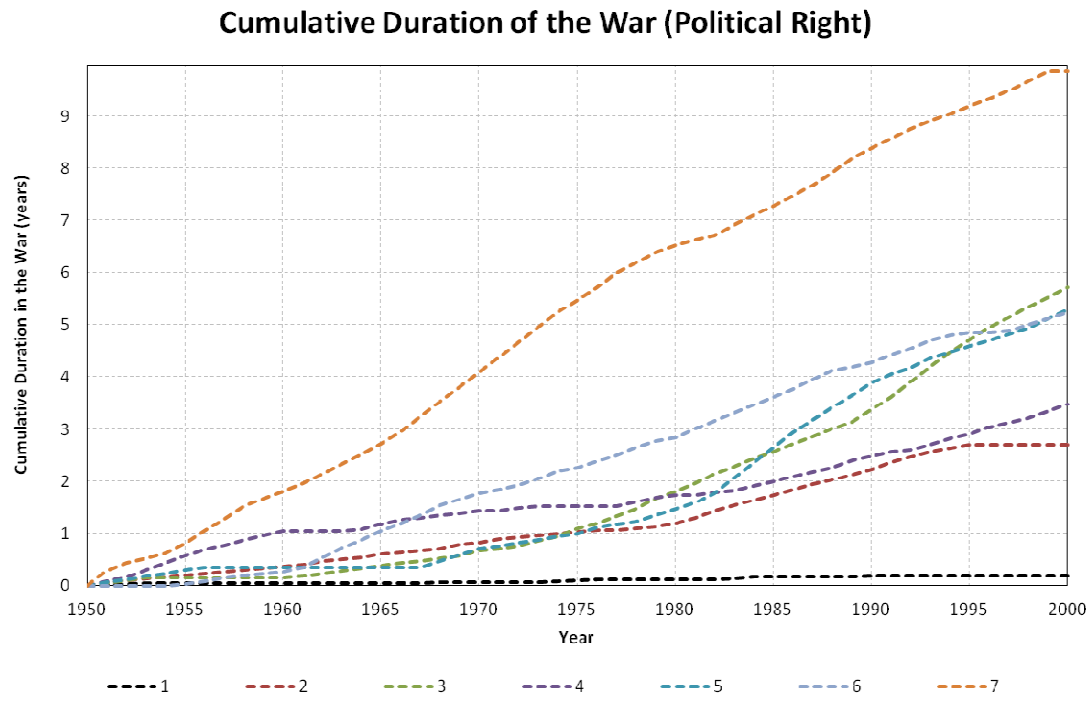

Figure 5.33 Cumulative Duration in the War (Political Right)

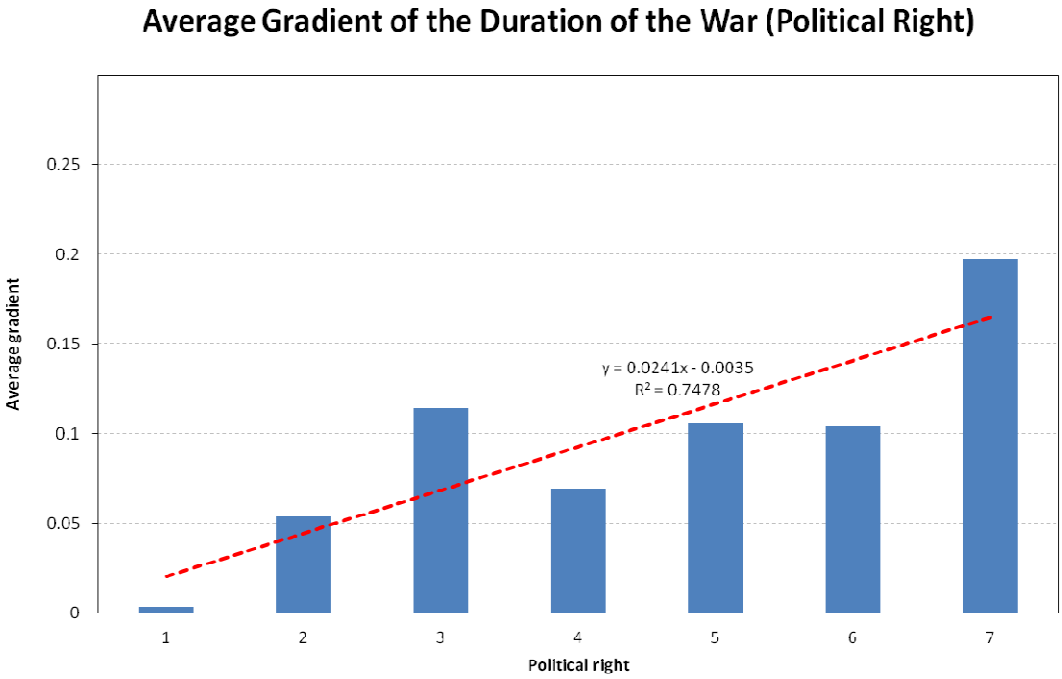

Figure 5.34 Average Gradient of the Duration of the War (Political Right)

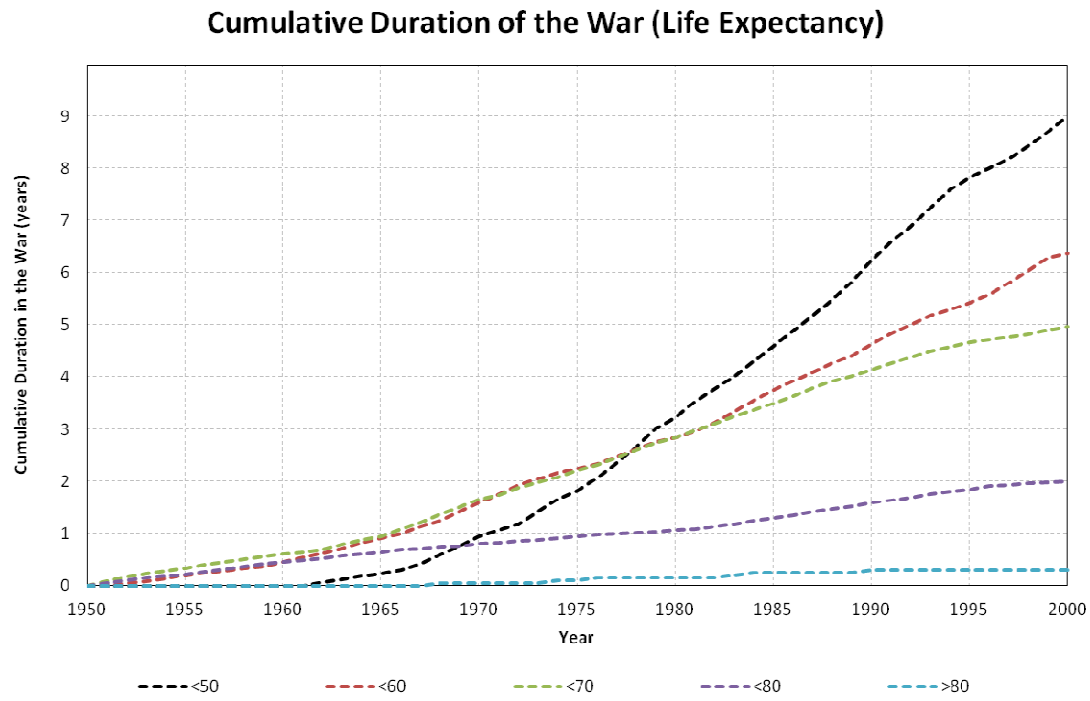

Figure 5.35 Cumulative Duration in the War (Life Expectancy)

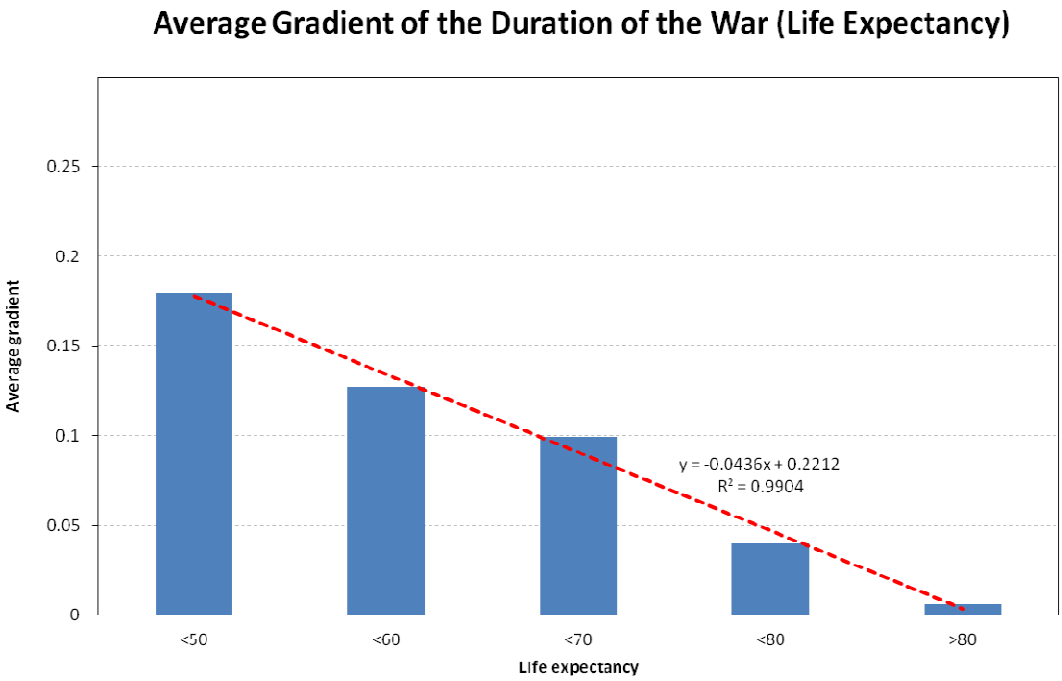

Figure 5.36 Average Gradient of the Duration of the War (Life Expectancy)

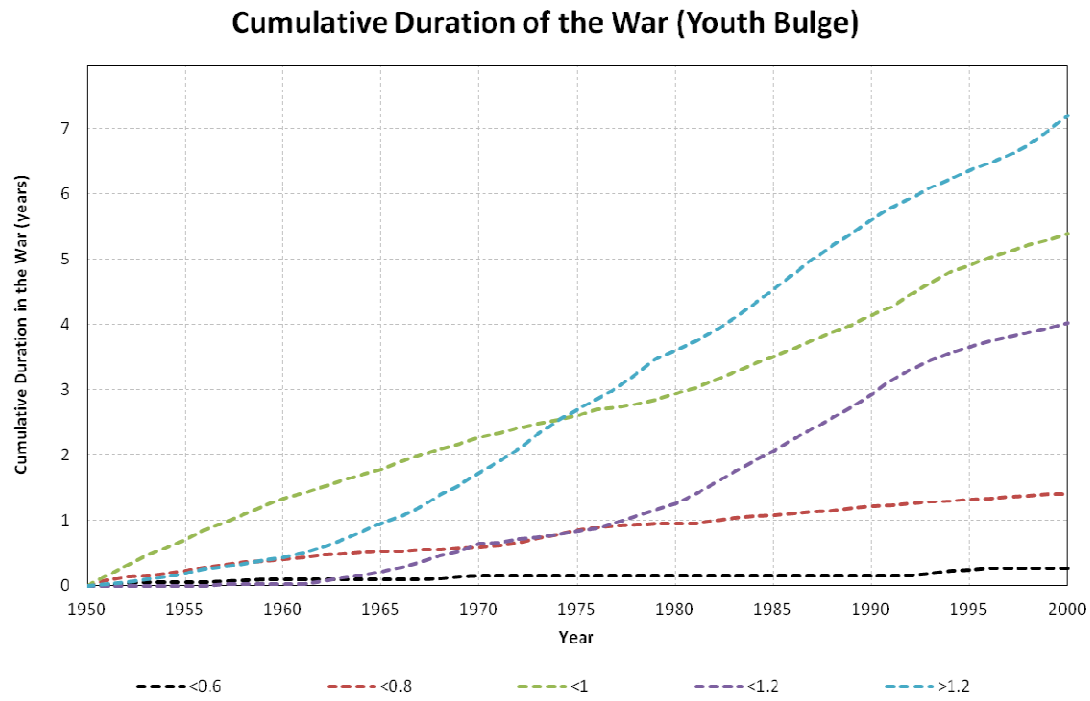

Figure 5.37 Cumulative Duration in the War (Youth Bulge)

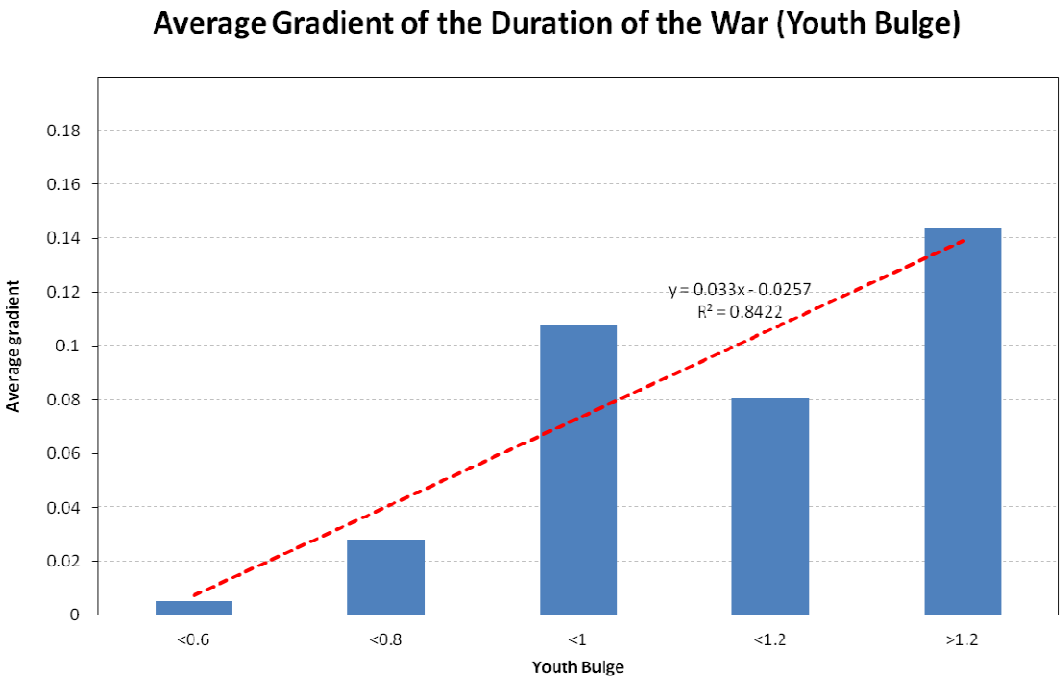

Figure 5.38 Average Gradient of the Duration of the War (Youth Bulge)

5.2 Environmental Risks

Most people are well aware that the magnitude of the impact an environmental disaster can have is something that. Natural Disasters like the earthquake in Haiti in 2010, the tsunami in the Indian Ocean in 2004, and the famines in Africa are representative samples of the destruction and humanitarian impact these events can have. Hypothesis 1 can be intuitively justified by considering that more than 10,000 U.S. military personal had been to distribute food and water, and provide security for the relief effort because of the earthquake of Haiti in 2010.

The World Bank and the University of Columbia developed a set of risk indices and datasets for each class of natural hazard, i.e., Cyclones, Draught, Floods, Earthquakes, Volcanoes, and Landslides.[21] Figure 5.39 depicts the mortality risk due to drought for the entire world. Notice that sub-Saharan Africa has the highest level of risk for deaths due to drought, and the regions in yellow have the intermediate levels of risk, and the regions in blue had the lowest, white indicates no risk. The reader is reminded that this figure only details the risk due to drought.

These datasets were compiled from different sources and for that reason they were not necessarily consistent in their resolution or periods. The integrated datasets were reconciled and used to determine two different types of risk, mortality and economic loss. These two risk indices were assessed at a 2.5' x 2.5' grid using global census data from the Gridded Population of the World (GPW) project.[15] The concept of vulnerability for each region was incorporated by deriving coefficients of vulnerability of each level of risk for each type of natural disaster for each mayor area of the world. These coefficients

were used to estimate how much of an impact a given disaster would have in a given area of the world, e.g., the 2010 Earthquake in Chile was 10 times stronger than the one in Haiti that same year but the number of casualties from the Haitian earthquake was 100 to 400 times higher. The discrepancy lies on the uncertainty around the true number of casualties from the Haitian earthquake of 2010.

The study aggregated the mortality and economic loss risk for all the different hazards throughout the world. The mortality risk for all hazards is presented in Figure 5.40. These risks indicate what magnitude of response and the likelihood that a response to that are of the world would have to occur. As with all the data integrated into the decision support tool, the environmental hazard risk datasets can be modified by the user.

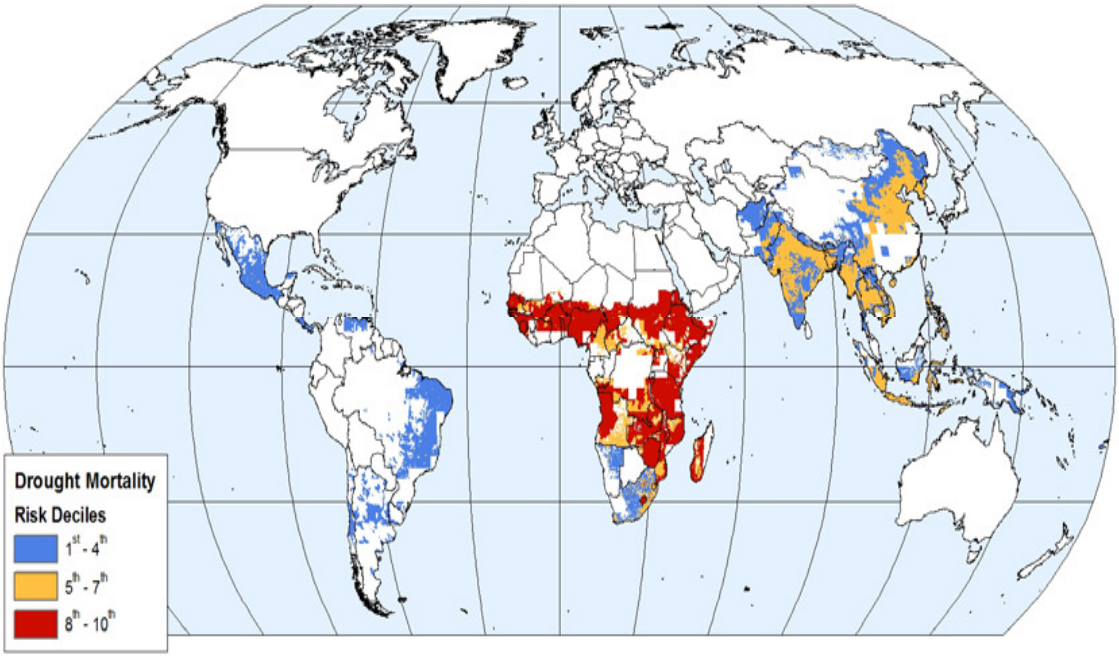

Figure 5.39 Drought Mortality Risk [21]

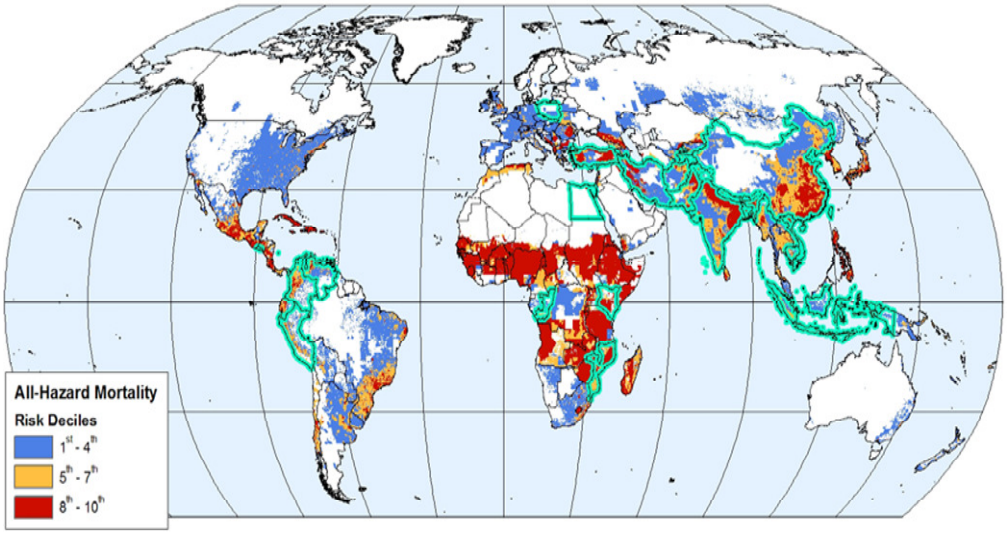

Figure 5.40 All Hazard Mortality Risk [21]

Figure 5.41 shows the difference of instability indices when the natural disaster factors are involved. The instability indices has been increased, especially in the case of Haiti and Philippine.

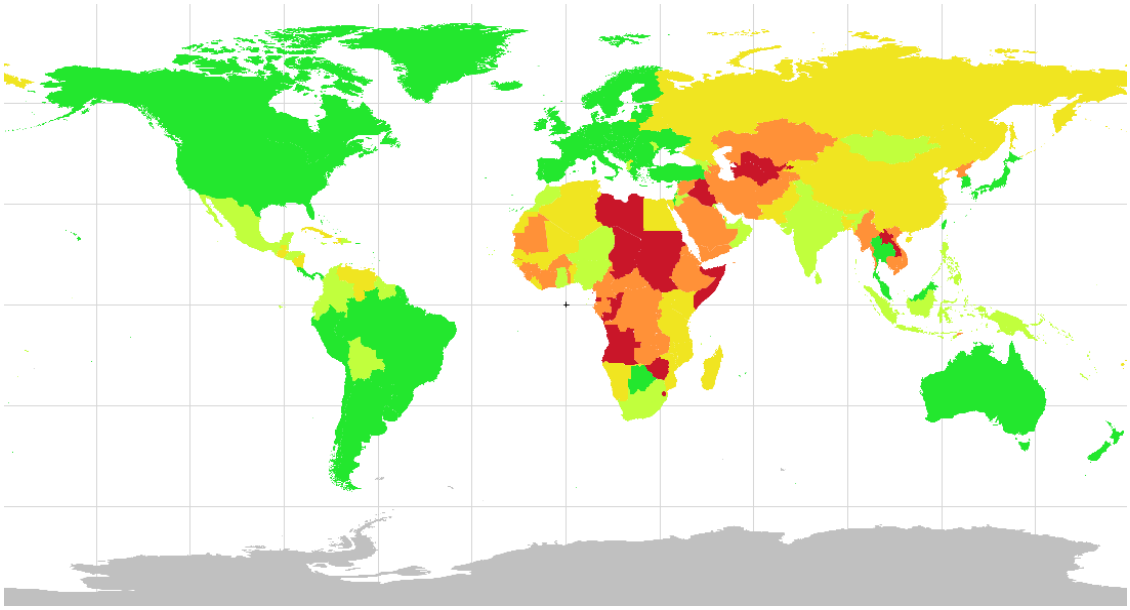

(a) Instability Indices without Natural Disaster

Figure 5.41 Comparison of Instability Indice

(b)

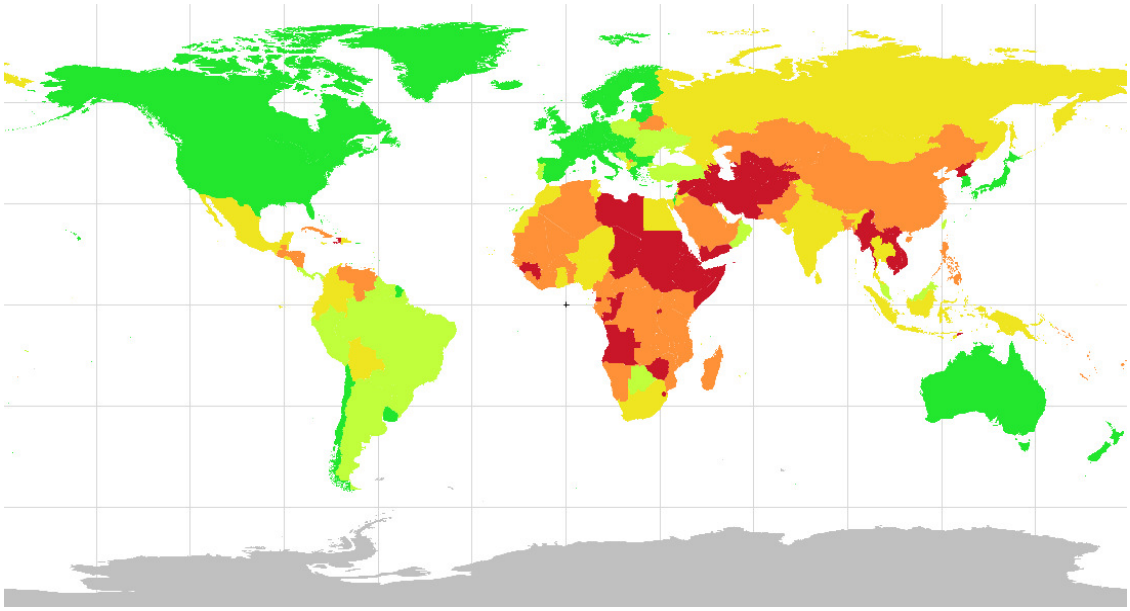

(b) Instability Indices with Natural Disaster

Figure 5.41 Comparison of Instability Indices (continued)

5.3 Forecasting Instability

Two methods can be applied. The first one is to forecast the instability in the future based on the present instability factors. The other is to estimate the instability in the future based on the forecasted instability factors. Many organization such as United Nations Statistics Division provide the forecasting data of various social, economic and political factors, and environmental forecasting can be provided by the research center such as Tyndall Centre for Climate Change Research. [128][107] The second method seems to predict the instability indices in the future. Figure 5.42 shows the prediction of infant mortality by United Nations Statistics Division. However, two problems are included in the second method. First, most forecasting results show optimistic future in spite of the uncertainty of conflicts and natural disaster. Second, In the case of factors in

unstable region, it is almost impossible to accurately forecast those factors. As a matter of fact, this research is focusing on the unstable regions. Therefore, this research employs the forecasting method to predict instability in the future based on the present instability factors..

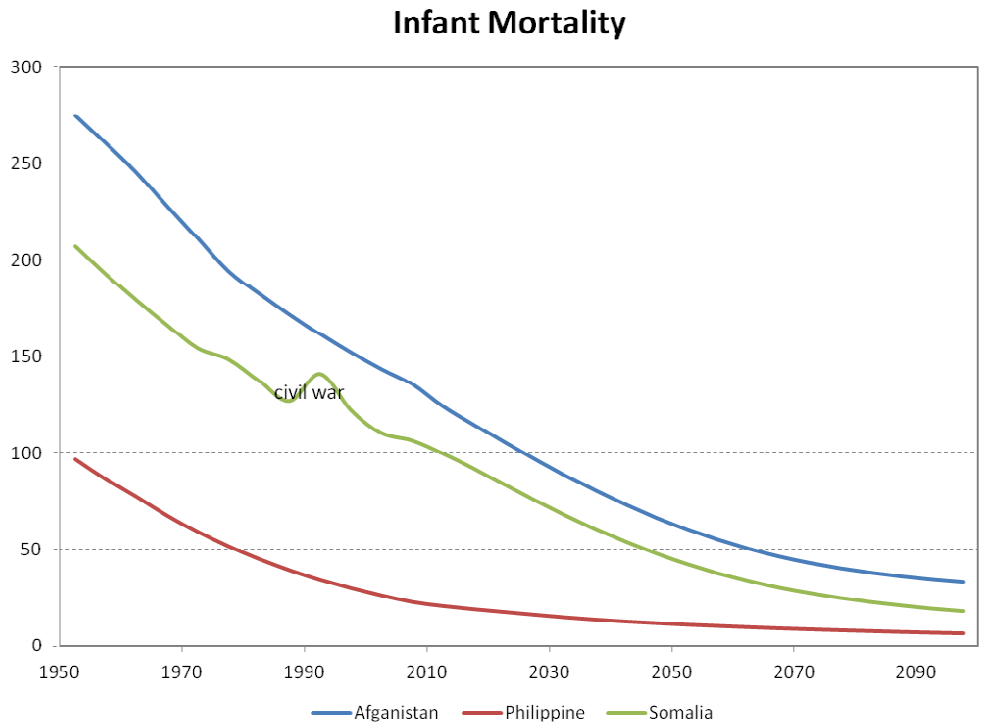

Figure 5.42 Forecasting of Infant Mortality [128]

5.4 Probability of the ability to solve the conflict without Intervention

The second probability to estimate the likelihood of dispatch can be calculated by the measure that the country can solve the conflicts without the aid of other countries or organizations, when the unstable situation occurs. GDP and GDP per capita can be considered most important factors to estimate this probability. Generally, the countries can have an extra budget if they have high GDP per capita. In other words, most of countries, which have high GDP per capita, can prepare military assets to cope with

conflicts and the equipments to resolve the emergency by natural disasters. However, high GDP per capita does not mean high defense budget all the time, especially when the magnitude of country is relatively low. For example, Kuwait has pretty high GDP per capita but relatively low GDP. As a result, Kuwait needed the aid from other countries when Iraq invaded Kuwait in 1990.

The first step of quantification is the statistical analysis of number of conflicts with regard to the factors, GDP per capita and GDP. The cumulative graph of GDP per capita is depicted in Figure 5.43 and that of GDP is depicted in Figure 5.45. Because this statistical graphs do not show smooth function, the fitting line by exponential functions can obtain noiseless smooth results. The second step is to acquire the function of relation between the probability of ability to solve the conflicts without intervention and each factor. The results are described in Figure 5.44 and 5.46. The probability to need the aid of other countries is inversely proportional to both of GDP per capita and GDP. The probability with regard to GDP has the threshold on \$30,000,000,000 while GDP per capita has smooth effect. The 2nd order polynomial regression model of relation between the probability and GDP per capita is derived as in Eq. (5.15). The R square value of this regression model is 0.9778.

$$7.180 \cdot 10^{-10}\mathrm{GDPPP}^2 - 3.495 \cdot 10^{-5}\mathrm{GDPPP} + 0.824 \qquad \text{Eq. (5.15)}$$

The exponential regression model of relation between the probability and GDP also is derived as in Eq. (5.16). The R square value of this regression model is 0.9420.

$$1.214 \cdot 10^{9}\mathrm{GDP}^{-1} - 3.891 \cdot 10^{18}\mathrm{GDP}^{-2} + 9{,}479 \cdot 10^{27}\mathrm{GDP}^{-3} + 0.664$$

Eq. (5.16)

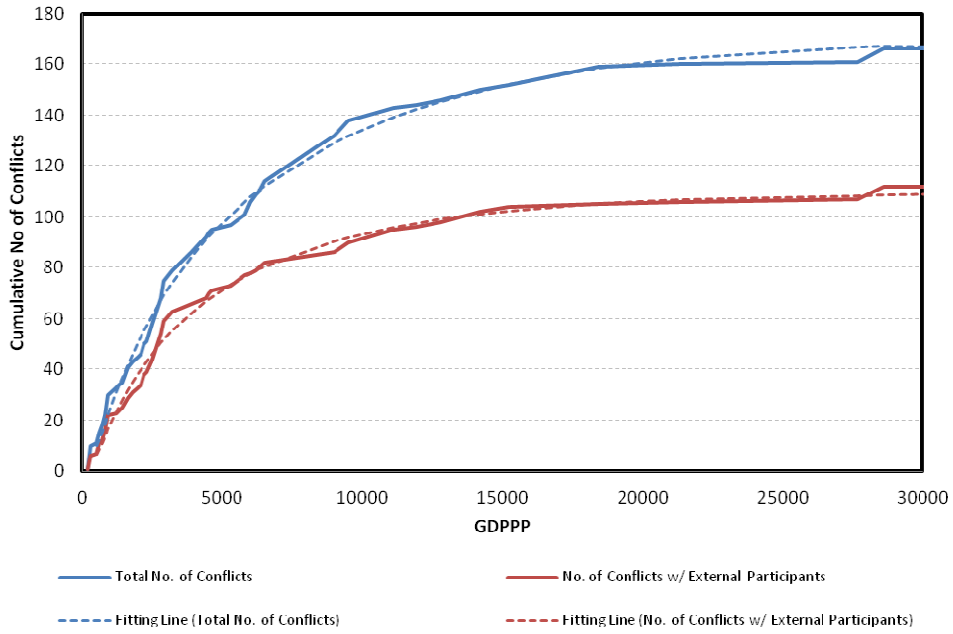

Figure 5.43 Cumulative Historical Data of Total Number of Conflicts and the Number of Conflicts with External Participants with regard to GDP per capita

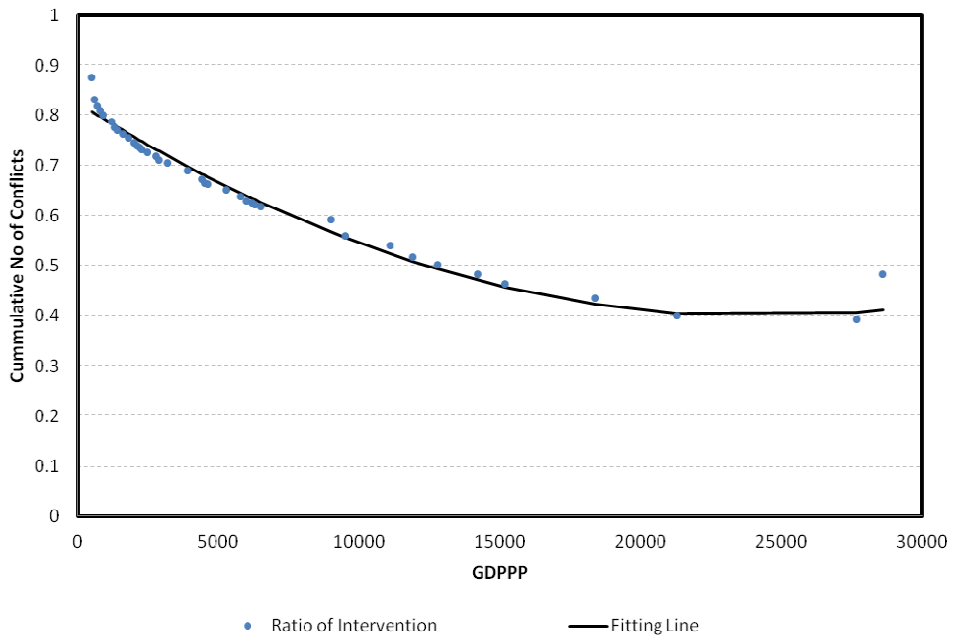

Figure 5.44 The Ratio of Conflicts with External Participants with regard to GDP per capita

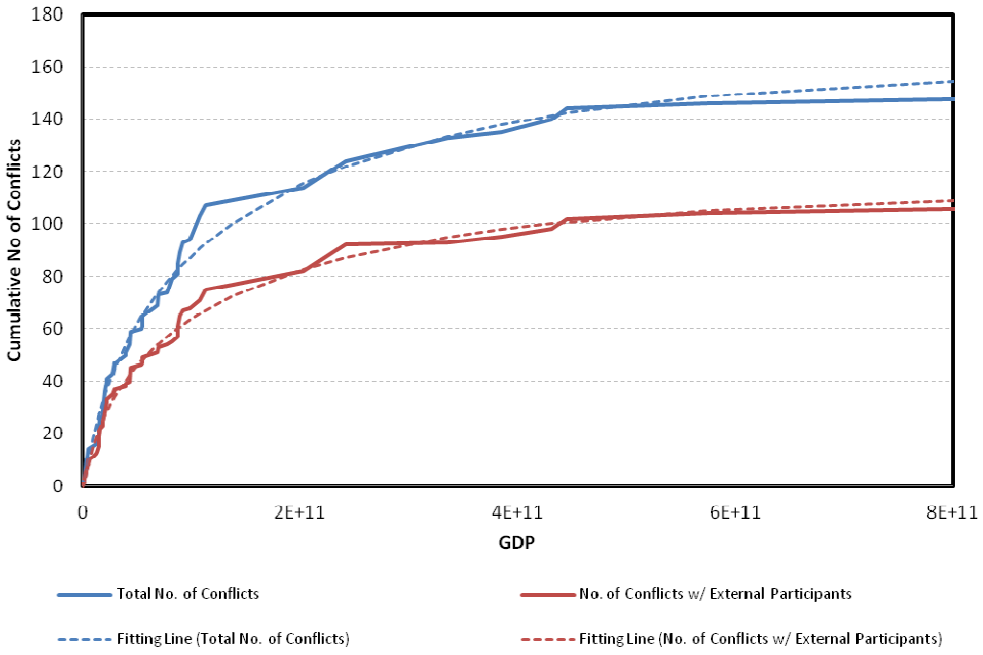

Figure 5.45 Cumulative Historical Data of Total Number of Conflicts and the Number of Conflicts with External Participants with regard to GDP

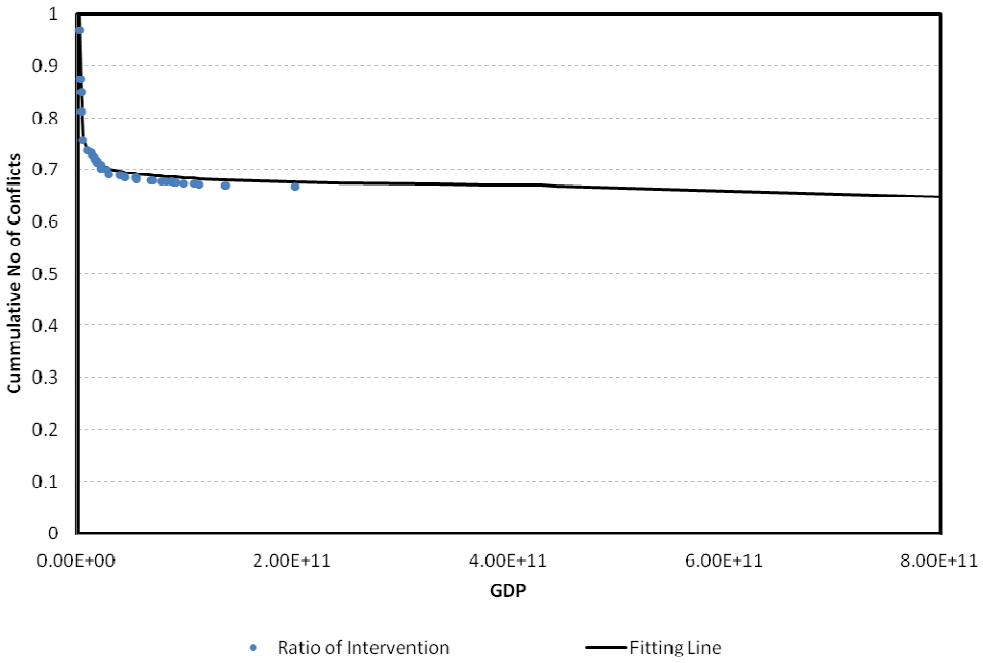

Figure 5.46 The Ratio of Conflicts with External Participants with regard to GDP

5.5 Probability of U.S. intervention

The last probability of the probabilistic causation model is to quantify the probability that U.S. will provide the support when the country can not solve the unstable situation by itself. Because this is mainly from the relation between countries, the treaties between U.S. and each country can reflect this relation. Therefore, the factors for third probability are the number of treaties of defense, mutual security, peace corps, terrorism, disaster assistance and humanitarian assistance.

This stage needs to be categorized into two cases. First case is the third probability about socio-economic and political instability and the other case is the third probability about unstable situation from natural disasters. The factors for the former case are the number of treaties of defense, mutual security peace corps and terrorism. Currently effective treaties with a few countries are shown in Table 5.1.

Table 5.1 Number of Treaties: Military [104]

Country	Defense	Mutual Security	Peace Corps	Terrorism
China			1	
France	34	1		
Austria	2	1		
Brazil	11		1	
Cyprus	1	1	1	
Haiti	5		1	
Israel	16	1		1
Kenya	3		1	
Korea, South	47	1		
Luxembourg	9	1	1	
San Marino				
Turkey	20	1	1	
Venezuela	4		1	
Zambia	2	1		

At first, if U.S. has the treaty of mutual defense, the intervention of the U.S. will be followed. Therefore, the third probability is one. If not, the probability can be estimated by the numbers of the other three kind of treaties. Statistical analysis shows the relation between the past U.S. interventions and the treaties of defense and peace corps. Unfortunately, the treaties of terrorism can not be analyzed independently, because four countries with the treaties of terrorism were never involved to any type of conflicts. Therefore, the treaty of terrorism is assumed as a type of the treaty of defense in this research. The relation between the past U.S. interventions and the treaties of defense and peace corps has the shape of step function with threshold. If the number of the treaties of defense is lower or same as five, the probability of U.S. intervention is 33.3%. If it is higher than five, this probability increases to 57.9%. Likewise, if the country has the treaty of peace corps with U.S., this probability is 35.7%. If not, this probability increases to 41.7% as well.

In the case of humanitarian mission, the factors can be the treaties of disaster assistance, peace corps and humanitarian assistance. Currently effective treaties with a few countries are shown in Table 5.2. However, because historical data is not enough to analyze statistically in this case, it is assumed that if the country has the one of those treaties with the U.S., the probability of U.S. intervention is 0.6, or the probability is 0.4.

Table 5.2 Number of Treaties: Natural Disasters [104]

Country	Disaster Assistance	Peace Corps	Humanitarian Assistance
Afghanistan		1	
Burma			
Iran	1	1	
Sudan			1

5.6 Instability Analysis in the Decision Supporting Tool (DESTINA)

In this research, JMP is used to develop an interactive decision supporting tool which allows necessary simulations required in the current research. JMP is a statistical analysis tool which supports the use of a scripting language. Therefore, this software provides benefits in terms of an efficient analysis of the enormous amount of database required in this research. Instability factor, causation with instability and weights for each factor mentioned in Sections 5.1 are the inputs used in DESTINA as shown in Figure 5.47.

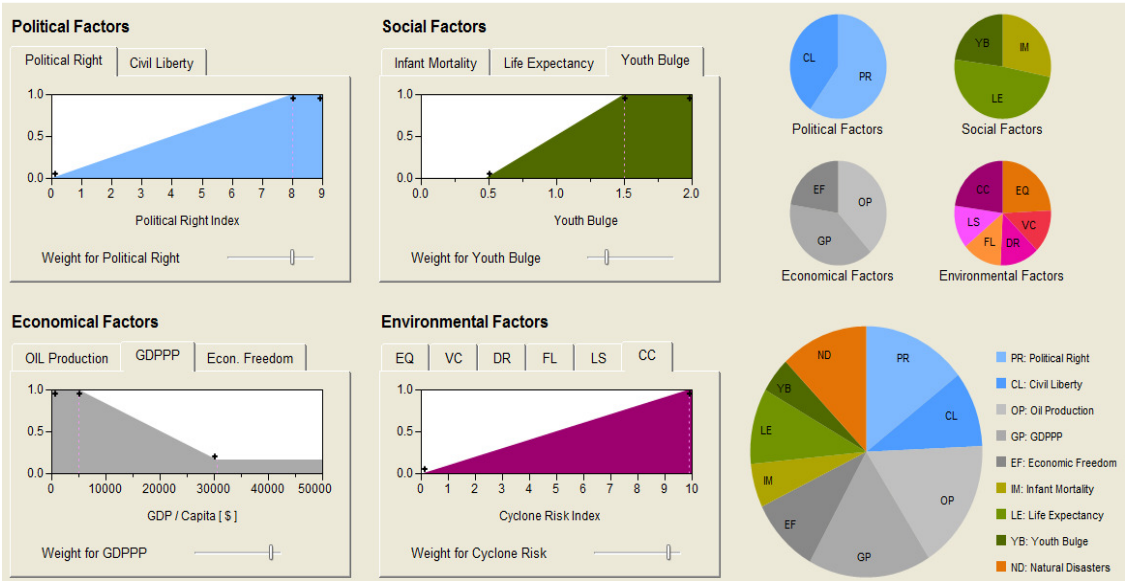

Figure 5.47 Input GUI of Instability Analysis in DESTINA

When a target region is selected, DESTINA provides instability analysis result as shown in Figure 5.48. On the left hand side, general information about the target region is displayed. The radar chart shown in the center demonstrates how instability index is calculated based on each factor considered in the analysis and on the right hand side at the bottom, information about the nearest U.S. base is provided.

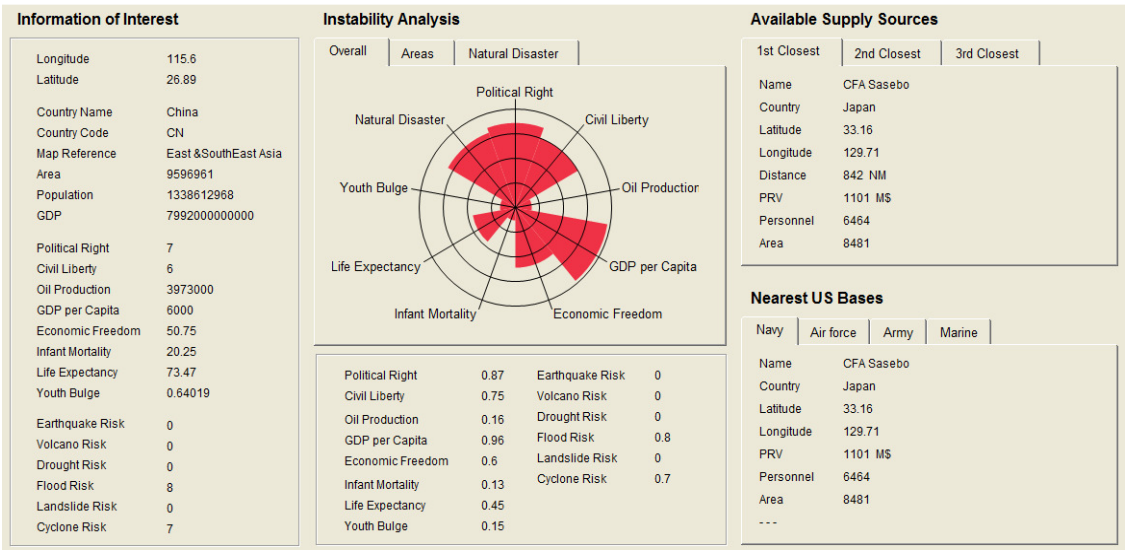

Figure 5.48 Output Display of Instability Analysis in DESTINA

Furthermore DESTINA provides a dynamic map as shown in Figure 5.49. This dynamic map can display instability indices re-calculated in real time as the given instability causation and weights are changed. The dynamic map of DESTINA consists of six layers as shown in Figure 5.50 and each of these layers can be turned on or off. Detailed explanation of DESTINA is described in the chapter 12.

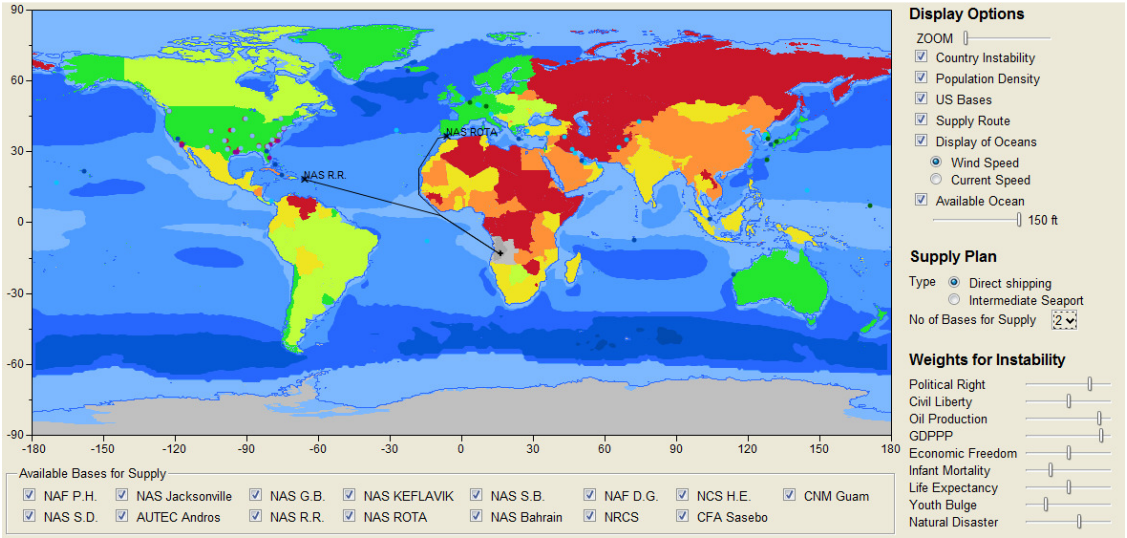

Figure 5.49 Dynamic Map of Instability Analysis in DESTINA

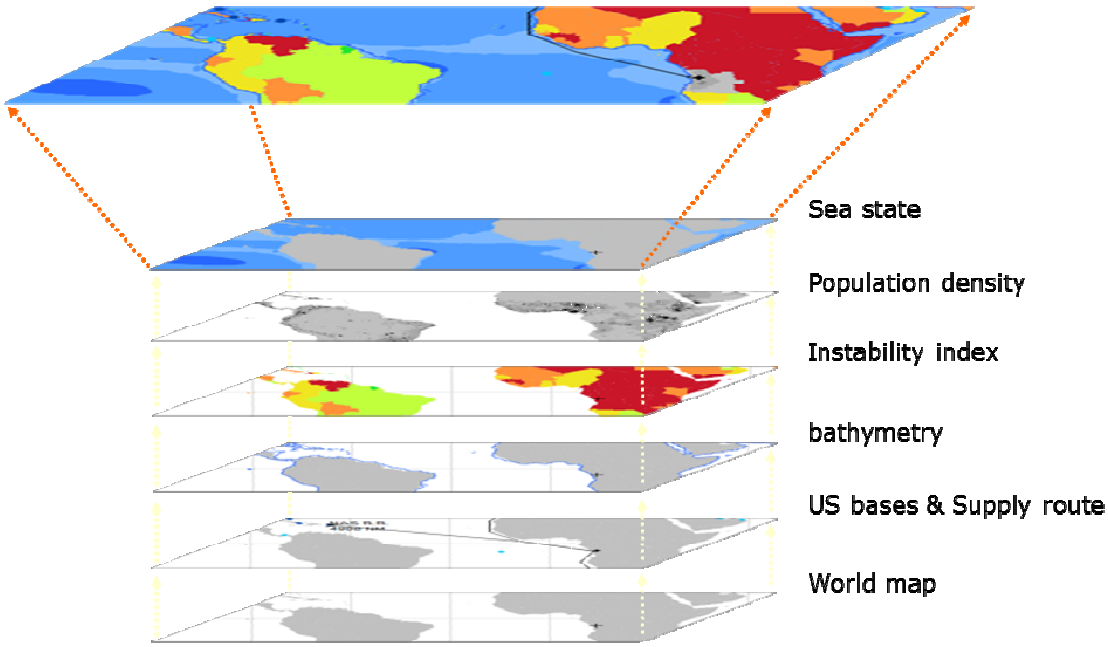

Figure 5.50 Layers of Dynamic Map in DESTINA

CHAPTER VI

SHIPPING LANE ESTIMATION AND SEA STATE ANALYSIS

6.1 Shipping Lane Estimation from Embarkation to Disembarkation

Figure 6.1 depicts possible embarkation points for MEC; from Sea Ports of Embarkation (SPOEs) in purple, to Intermediate Staging Bases (ISBs) in dark blueThe number of ISBs depicted is a small subset of the possible numbers, and in the cases of the Pacific and Indian Ocean MPGs, they are located at mayor ISBs, Guam and Diego Garcia, respectively. The figure may seem deceptive in that the question of where embarkation will take place is well defined. Three factors difficult this assessment: (1) these possible points of embarkation are not a static set, (2) they are not all equally suited to stage any type of operation, and (3) it may be possible to stage and operation from a friendly country. The first concern lies on the fact that countries are rescinding their contracts with the Unit States and disallowing it to base their military forces on their sovereign territories (e.g., Uzbekistan). The second concern centers around the fact that some bases are more or less capable, e.g., some are not big enough to stage a sea-based-supported Mayor Combat Operation (MCO) from, in essence, not all these bases were created equal.

The sources used for this research are available in the open literature and range from data published by defense research groups such as Globalsecurity.org and FAS.org, the Department of Defense like the US Base Structure Report, and geospatial data, for example, Google Earth. Nonetheless, there is a high degree of uncertainty as to which bases will be open when, since political swaying has a large impact on a country's will to

host US military forces. This is not to say that there are no contracts with the host countries, but these contracts lapse and must be renewed, something that is not always approved by the host nation. The perceived threat also has an impact on the location of these bases, for example, most bases were distributed along Western Europe and the Far East prior to 1990, and after the fall of the Soviet Union and the escalation of the conflicts in the Middle East, a large portion of them distributed throughout the Middle East and Central Asia.

Table 6.1 contains the list of Intermediate Staging Bases and Sea Ports of Embarkation used for this analysis. The intent of the tool created here was not to develop a rigid set of ISBs and SPOEs, but allow the user to modify this list in the future by either adding or removing SPOEs or ISBs. These bases are shown in Figure 6.1.

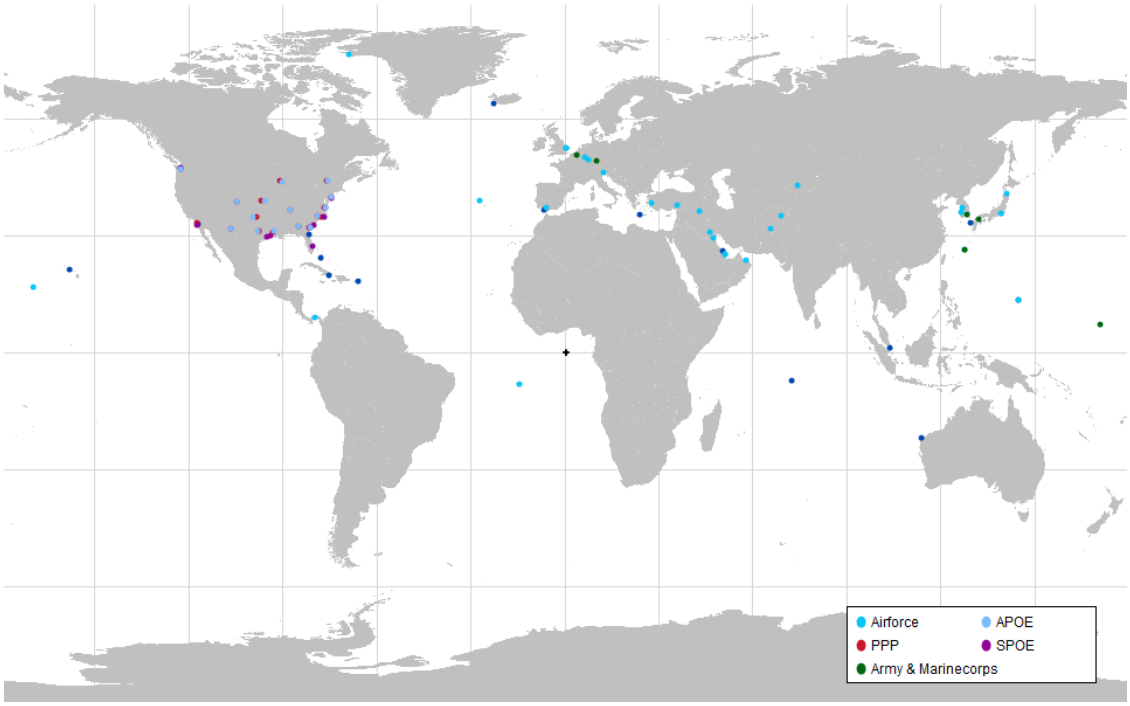

Figure 6.1 Possible Embarkation Points for Naval Operation

Table 6.1 Sea Ports of Embarkation and Intermediate Staging Bases [1]

Name	Branch	Country	Latitude	Longitude
MCB CAMP S D BUTLER OKINAWA	USMC	Japan	26.33º	127.8º
MCAS IWAKUNI	USMC	Japan	34.15º	132.18º
PWC PEARL HARBOR	USN	USA	21.45º	-158º
EDWARDS AIR FORCE BASE	USN	USA	35.29º	-118.91º
NAS NORTH ISLAND SAN DIEGO	USN	USA	33.02º	-116.85º
NAS JACKSONVILLE	USN	USA	30.21º	-81.69º
NAVUNSEAWARCENDET AUTEC ANDR	USN	Bahamas	24.43º	-77.95º
GUANTANAMO BAY	USN	Cuba	19.9º	-75.15º
NAVSTA ROOSEVELT ROADS	USN	Puerto Rico	18.29º	-65.84º
NAS KEFLAVIK	USN	Iceland	64.01º	-22.57º
NAVSTA ROTA	USN	Spain	36.62º	-6.35º
NAVSUPPACT SOUDA BAY	USN	Crete	35.5º	24.15º
ADMINSUPPU SWA	USN	Bahrain	26.22º	50.58º
AL UDEID AIR BASE	USN	Qatar	25.26º	51.45º
DIEGO GARCIA	USN	BIOT	-7.32º	72.42º
NAVREGCONTRCTR	USN	Singapore	1.35º	103.9º
NAVCOMMSTA H E HOLT EXMOUTH	USN	Australia	-21.93º	114.13º
COMFLEACT SASEBO	USN	Japan	33.17º	129.72º
COMNAVMARIANAS GUAM	USN	Guam	13.47º	144.78º
PORT OF TACOMA, WA	SPOE	USA	47.27º	-122.41º
PORT OF SAN DIEGO, CA	SPOE	USA	32.69º	-117.14º
PORT OF GALVESTON, TX	SPOE	USA	29.68º	-95º
PORT OF BEAUMONT, TX	SPOE	USA	29.86º	-93.94º
PORT OF SAVANNAH, GA	SPOE	USA	32.13º	-81.15º
PORT OF JACKSONVILLE, FL	SPOE	USA	27.18º	-80.23º
PORT OF CHARLESTON, SC	SPOE	USA	32.85º	-79.95º
PORT OF MOREHEAD CITY, NC	SPOE	USA	34.72º	-76.7º
PORT OF HAMPTON ROADS, VA	SPOE	USA	37.08º	-76.34º
PORT OF NEW YORK/NEW JERSEY	SPOE	USA	39.49º	-74.45º

The point of disembarkation is even more complex to address than the prior one. In this case, the analysis has to incorporate local instabilities and destabilization factors and the willingness of the US and its allies to act in those areas of the world. Instabilities can be due to a myriad of reasons, political, socio-economic, military, environmental, etc. The willingness of the US to intervene has to do with the popular sentiment at the time, the US' interest in the region at the time, and the fortitude of the alliances. For the purposes of this research a series of risk factors will be developed to address (1) the socio-econo-political instabilities, (2) the resources in the area, and (3) the natural disasters.

6.2 Navigation Course Planning

The definition of an efficient shipping lane can reduce travel time and fuel cost. It is therefore imperative that operators select the best route possible, and if a tool was to simulate the route taken by naval assets, it should mimic an operator's decision making as closely as possible. The essential elements to defining a good route are the origin (in this case an SPOE or ISB), the destination (in this case the area of operations), the environmental conditions, the commercial shipping in the area, and the topographical characteristics of the globe.

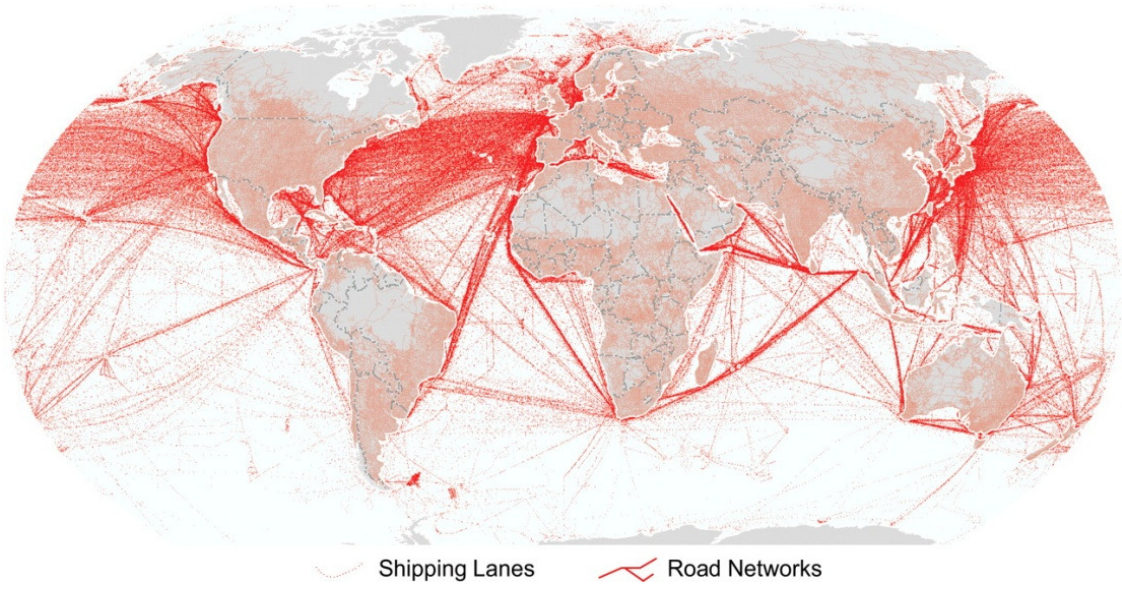

Figure 6.2 Shipping lanes [54].

Figure 6.2 shows the most common routes taken by commercial ships. The map highlights the most common origins and destinations but also the points used to circumnavigate the world. The map clearly demonstrates the connectivity of the points and how it is constrained by continents and islands. This connectivity can be considered to be a graph, a mathematical representation of pairwise relations, in this case, which points are connected to one another. A graph in turn can be translated into matrix form, which is referred to as the adjacency matrix of the graph. An example graph and adjacency matrix is presented in Figure 6.3. Figure 6.4 depicts the points (depicted as black crosses) used to generate the shipping lanes for the entire globe.

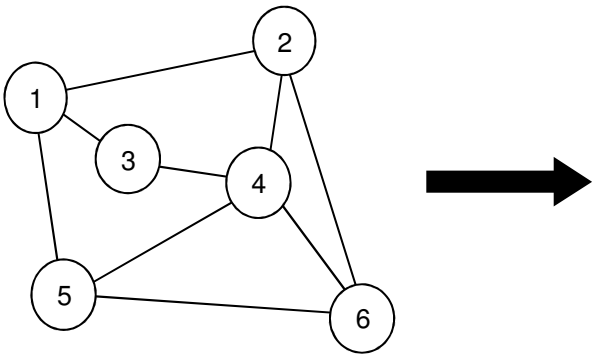

	1	2	3	4	5	6
1		1	1		1	
2				1		1
3				1		
4					1	1
5						1
6						

Figure 6.3 Graph and Associated Adjacency Matrix

Path finding is a computationally expensive enterprise, which grows exponentially with the number of possible points. In this application, there are 151 points used, therefore the matrix use to compute the world shipping lanes has the size of 151 by 151. In order to enable near-real-time results, the possible routes were pre-calculated for the different ISBs and SPOEs. These routes and their associated shipping distance are included in the tool as a database. This database is queried by the tool when a user selects an AOO, the query uses the destination to find the closest base to the point, e.g., [1] describes the case where the user selected point 25 as the destination, the tool will then use the points described under “route” and know that the closes base is base “203” and the distance is 5892. Using this method, the user can obtain a route in real-time. The downside of this method is that if new bases are added, additional entries to the database must be added. At this stage, the tool requires this to be done separately and for the data to be added to the database. Future versions are envisioned to allow the tool to accept additional points of origin and then recalculate the shipping routes automatically.

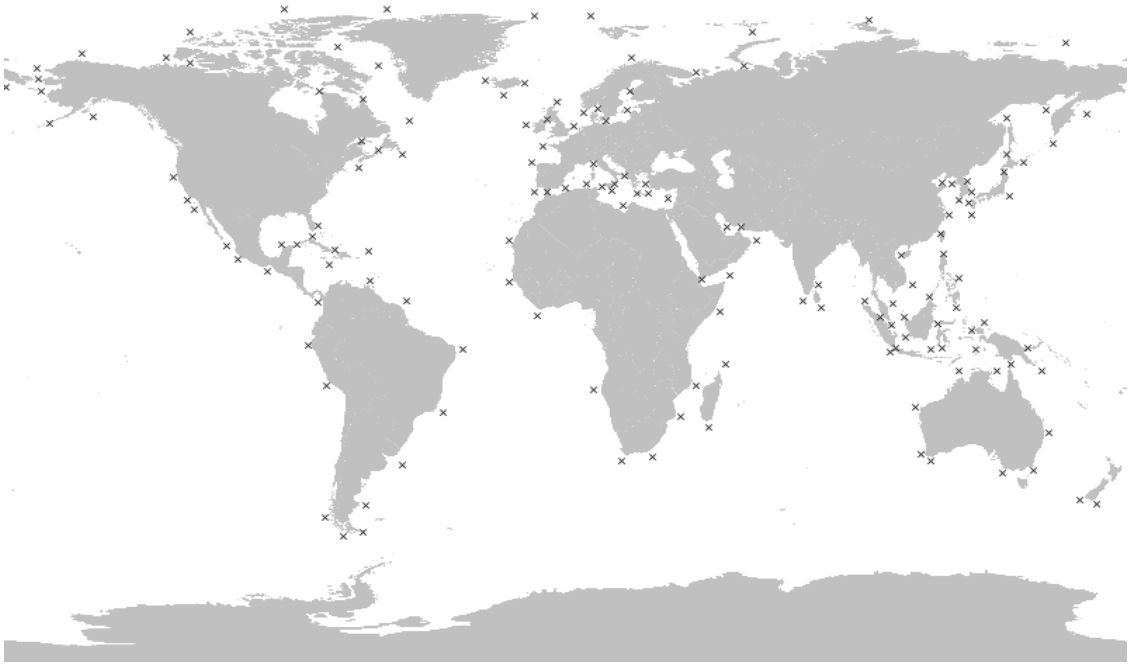

Figure 6.4 Connection Points for Shipping Route Planning

Table 6.2 Pre-calculated Route Example.

Start Point	Routing Points								Navy Base	Distance (nm)
25	13	203	203	203	203	203	203	203	203	5892
25	13	202	202	202	202	202	202	202	202	5981
25	201	201	201	201	201	201	201	201	201	6392
25	30	34	42	45	46	43	207	207	207	6447
25	30	34	42	45	46	43	36	28	206	7088
25	30	34	42	45	46	49	55	209	209	7097
25	30	34	42	45	46	43	36	205	205	7269
25	30	34	73	82	88	213	213	213	213	7553
25	30	34	42	45	46	43	36	204	204	7579
25	217	217	217	217	217	217	217	217	217	7946

One additional consideration has to be discussed with regards to the routing algorithm. It is possible that the closest ISB or SPOE might not be available because of a

variety of reasons, e.g., the base cannot support that type of operation, simultaneous military operations may not allow for that base to be used, or the foreign nation has rescinded its contract with the US armed forces and does no longer allow US forces to be stationed within its borders. To consider this kind of problem, the user can decide at any point during the analysis which ISBs are available. Figure 6.5 depicts this using an example. In this example, the user chose the AOO to be within the borders of the country Gabon. The closest ISB from which to stage the operation is Naval Station (NAVSTA) Rota in Spain. The figure on the left depicts the route taken by the assets, circumnavigating the coast of northwestern Africa to reach their destination in off of the coast of Gabon. If the user was the deselect NAVSTA Rota as a possible origin for the operation of interest, the tool would automatically choose the next closest base, in this case NAVSTA Roosevelt Roads in Puerto Rico.

Figure 6.5 Automatic Route Considering Available Bases

One of the options under the shipping lanes check box is the option to use an intermediate port between the location of interest and the naval base. A limited database of seaports was compiled, attempting to limit the number of possible seaports, by overall size and maximum draft. Once the, nearest intermediate seaport is calculated, a path is

plotted approximately following the coastline from the port to the nearest point on the coastline to the point of interest. This calculation is not done in real time, since it is computationally expensive, though not as much as the aforementioned shipping lane algorithm. In order to simplify the calculation, the world coastline was discretized into about 2200 points. For each one of these points a path is calculated to the nearest port by iterating along the coast from coast point to coast point, until the seaport is reached. Two paths are calculated, one starting clockwise from the initial point, and one starting counter clockwise, the shortest path is chosen. This was put into a look-up table so that the paths can be plotted in real time when the tool is in use.

Another available option is the supply from multiple sources. Considering requirement and ability of each source, many of sources can be chosen up to three. The number of required sources should be decided based on the information of each base. Because this is manually selected in the current version, this option will be upgraded to be done automatically. In the Figure 6.6, three supply routes by using intermediate seaport are described.

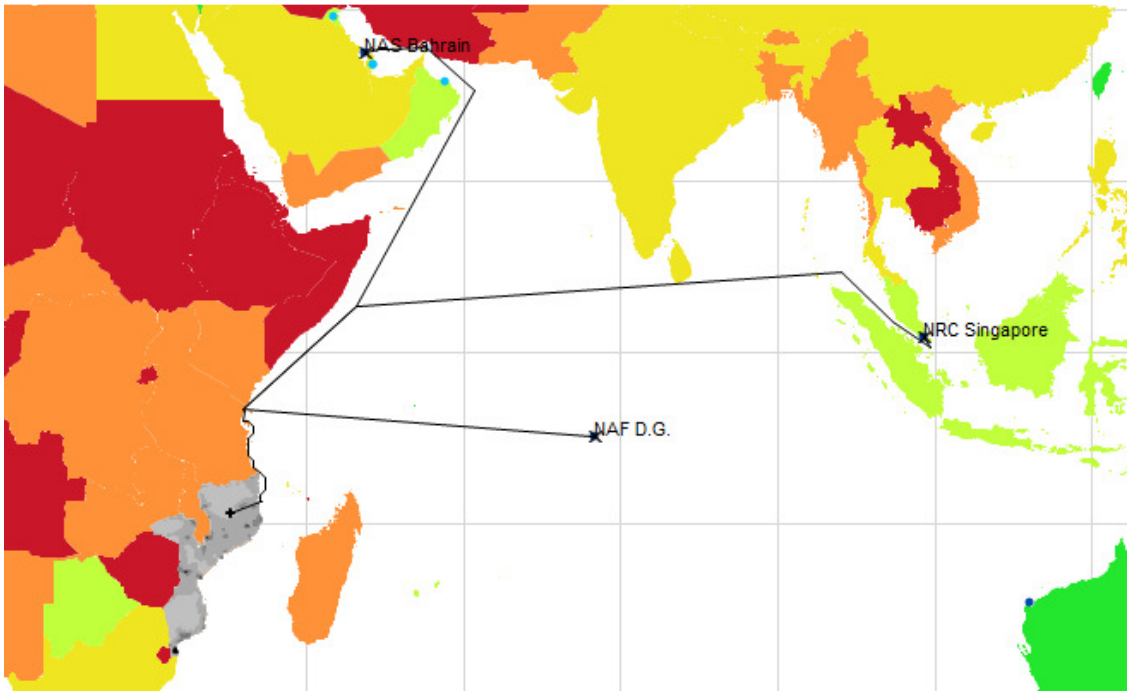

Figure 6.6 Shipping lane by using intermediate seaport and multiple sources

For a selected target region, DESTINA determines a shipping lane from the nearest available U.S. navy base to the target and calculates the corresponding distance. Among a various types of methodologies that have been developed to find a shipping lane, a method using a pre-calculated sheet based on 82 bottleneck points is selected in the current research. By using this method, a shipping lane can be determined efficiently in real time and Monte-Carlo simulation used to calculate the overall effectiveness of MEC is possible within a reasonable time frame.

When the sailing distance is determined by using the pre-calculated sheet, Errors associated with the shipping length are within 5 percent as shown in Table 6.3. As mentioned in Hypothesis 5, this error is in reasonable range considering it does not need any calculation. Therefore, the benefits from savings in analysis time and applications of

various design methodologies are more substantial than the slight reduction in the accuracy of the shipping lane due to the use of the pre-calculated sheet. [85]

Table 6.3 Accuracy of Shipping Lane Distance by Pre-calculated sheet

Embarkation		Debarkation		Distance by DESTINA [NM]	Actual Distance [NM]	Error [%]
Apra	Guam	Tokyo	Japan	1376	1374	0.15
San Diego	US	Sydney	Australia	6533	6533	0.00
Rota	Spain	Luanda	Angola	4037	3854	4.75
San Juan	Puerto Rico	cape town	South Africa	5887	5772	1.99
Jacksonville	US	Buenos Aires	Argentine	6033	5761	4.72
Reykjavik	Iceland	Dakar	Senegal	3021	2988	1.10

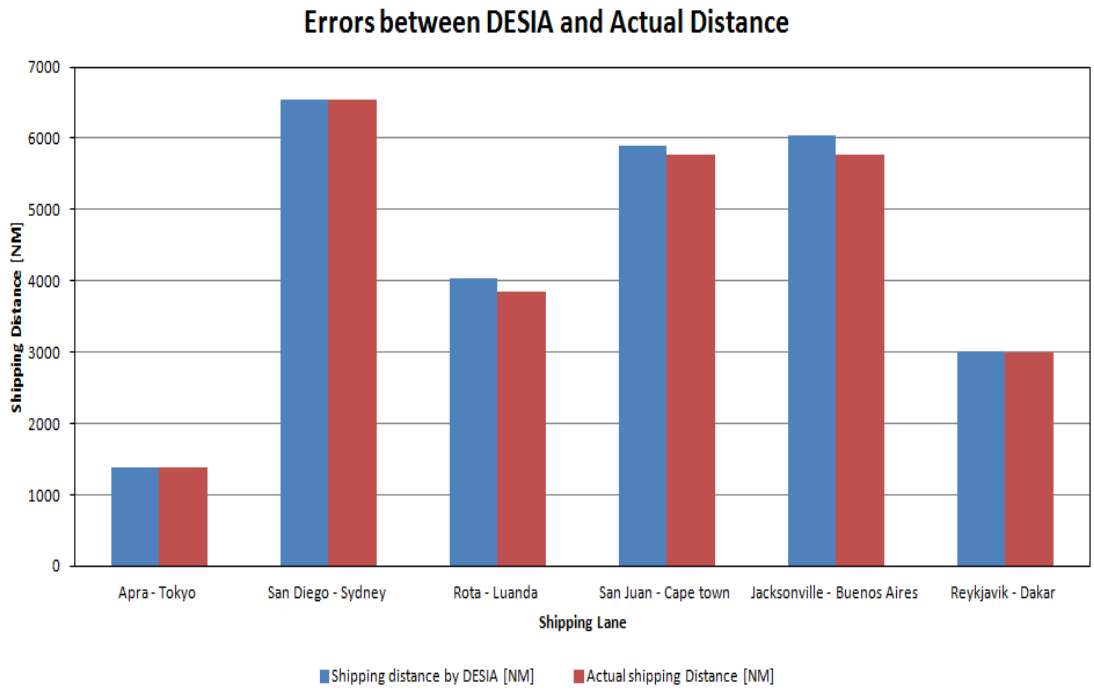

Figure 6.7 Comparison of Shipping Distance by Pre-calculated Table and Actual Values

Figure 6.8 Errors of Shipping Distance by Pre-calculated Table

6.3 Sea State Analysis along Shipping Lane

Beaufort scale was devised in 1805 by Francis Beaufort (later Rear Admiral Sir Francis Beaufort), an Irish-born Royal Navy officer, while serving on HMS Woolwich. The scale that carries Beaufort's name had a long and complex evolution, from the previous work of others, including Daniel Defoe the century before, to when Beaufort was a top administrator in the Royal Navy in the 1830s when it was adopted officially and first used during the voyage of Charles Darwin on HMS Beagle. [65] In the early 19th century, naval officers made regular weather observations, but there was no standard scale and so the weather observations could be very subjective, e.g., one man's "stiff breeze" might be another's "soft breeze". Beaufort succeeded in standardizing the scale.

The initial scale of thirteen classes (zero to twelve) did not reference wind speed numbers but related qualitative wind conditions to effects on the sails of a man-of-war, then the main ship of the Royal Navy, from "just sufficient to give steerage" to "that which no canvas sails could withstand". At zero, all sails would be up; at six, half of the sails would have been taken down; and at twelve, all sails would be stowed away.

The scale was made a standard for ship's log entries on Royal Navy vessels in the late 1830s and was adapted to non-naval use from the 1850s, with scale numbers corresponding to cup anemometer rotations. In 1916, to accommodate the growth of steam power, the descriptions were changed to how the sea, not the sails, behaved and extended to land observations. Rotations to scale numbers were standardized only in 1923. George Simpson, C.B.E. (Later Sir George Simpson), Director of the UK Meteorological Office, was responsible for this and for the addition of the land-based descriptors. The measure was slightly altered a few decades later to improve its utility for meteorologists. Currently, many countries have abandoned the scale and use the metric system based units, m/s or km/h, instead, but the severe weather warnings given to the public are still approximately the same as when using the Beaufort scale.

The Beaufort scale was extended in 1946, when Forces 13 to 17 were added. [90] However, Forces 13 to 17 were intended to apply only to special cases, such as tropical cyclones. [129] Nowadays, the extended scale is only used in Taiwan and mainland China, which are often affected by typhoons.

Wind speed on the 1946 Beaufort scale is based on the empirical formula: [63]

$$v = 0.836\, B^{1.5}\ m/s \qquad \text{Eq. (6.1)}$$

Where v is the equivalent wind speed at 10 meters above the sea surface and B is Beaufort scale number. For example, B = 9.5 is related to 24.5 m/s which is equal to the lower limit of "10 Beaufort". Using this formula the highest winds in hurricanes would be 23 in the scale.

Table 6.4 Beaufort Scale with Corresponding Wind Speed and Wave Heights. [64]

Beaufort number	Description	Wind speed (Knot)	Wave height (ft)
0	Calm	< 1	0
1	Light air	1 – 2	0 – 1
2	Light breeze	3 – 6	1 – 2
3	Gentle breeze	7 – 10	2 – 3.5
4	Moderate breeze	11 – 15	3.5 – 6
5	Fresh breeze	16 – 20	6 – 9
6	Strong breeze	21 – 26	9 – 13
7	High wind, moderate gale, near gale	27 – 33	13 – 19
8	Gale, fresh gale	34 – 40	18 – 25
9	Strong gale	41 – 47	23 – 32
10	Strom, whole gale	48 – 55	29 – 41
11	Violent storm	56 – 63	37 – 52
12	Hurricane force	≥ 64	≥ 46

Currently, hurricane force winds are sometimes described as Beaufort scale 12 through 16, very roughly related to the respective category speeds of the Saffir–Simpson Hurricane Scale, by which actual hurricanes are measured, where Category 1 is equivalent to Beaufort 12. However, the extended Beaufort numbers above 13 do not match the Safire–Simpson Scale. Category 1 tornados on the Fujita and TORRO scales also begin roughly at the end of level 12 of the Beaufort scale but are indeed independent scales although the TORRO scale wind values are based on the 3/2 power law relating

wind velocity to Beaufort force. [62] Table 6.4 summarizes descriptions of Beaufort number and corresponding wind speed and wave heights. It should be noted that wave heights shown in Table 6.4 are for conditions in the open ocean, not along the shore.

In addition, average sea state along shipping lane can be analyzed. The sea state data includes three categories: wind speed, current speed, and wave height. Sea state analysis is indispensible to design the ship, because the wave height is critical to decide maximum draft and all three data effect on the mission range and cruise speed. The distribution is shown as Figure 6.9. The distribution of wind speed is known as being similar to Weibull distribultion approximately. [86]

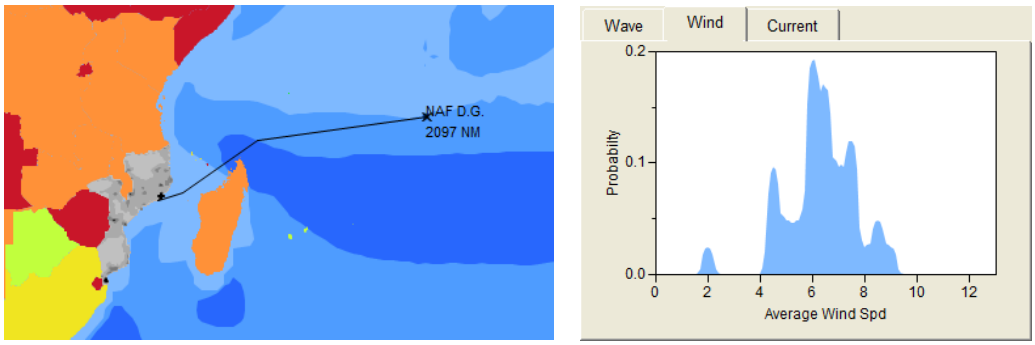

Figure 6.9 Sea state analysis along the shipping lane

6.4 Shipping Lane Estimation and Sea State Analysis in the Decision Supporting Tool

DESTINA provides various options in the assessment of shipping lanes. Figure 6.10 illustrates various options available in DESTINA such as simultaneous shipping from multiple sources, selection of availabilities of different bases, and shipping through the intermediate seaport nearest to the target region. These options improve reality and variability of scenarios which allows more reliable and realistic analysis results.

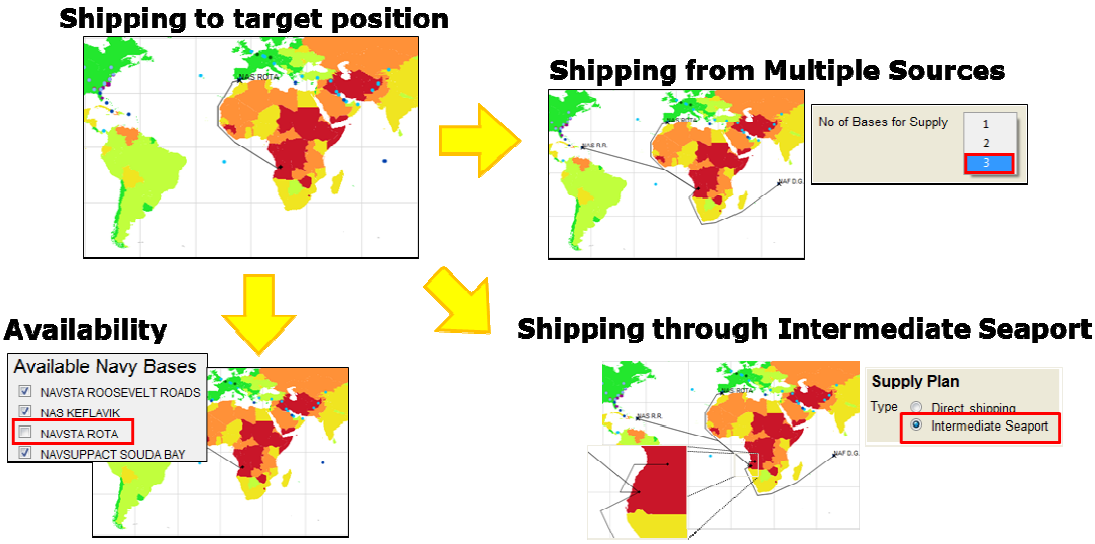

Figure 6.10 Various Options Available in DESTINA

State of the sea during shipping is one of essential factors in design of a ship. DESTINA assesses wind speed, wave heights, and current speed along the given shipping lane and indicates them using Beaufort scale. Then the requirements of the ship can be identified based on the confidence level determined by the Beaufort scale. The sea state of a given shipping lane obtained by the process described above is essential to determine the required performance of a ship along the selected shipping lane such as a draft depth. Figure 6.11 shows analysis results of sea state for a given shipping lane and the corresponding Beaufort scale with the confidence level obtained in DESTINA.

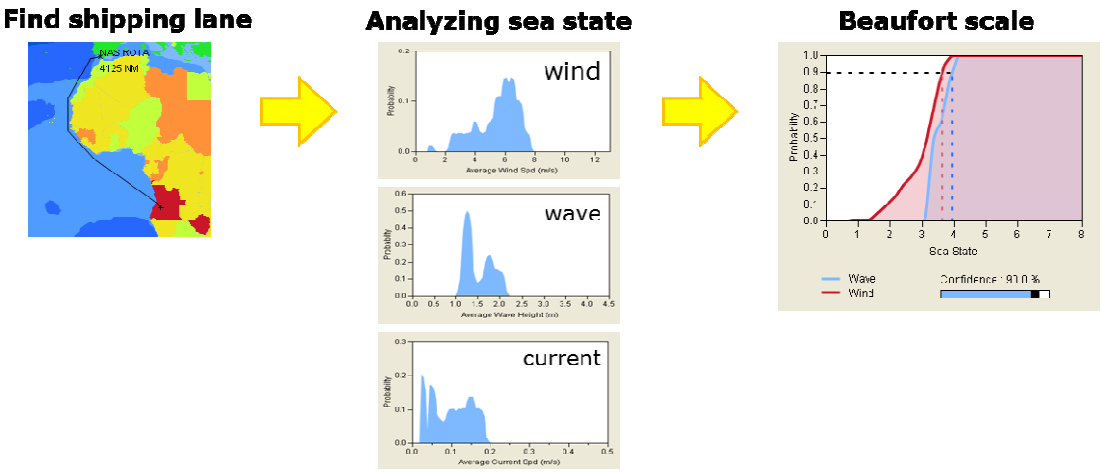

Figure 6.11 Sea State Analysis in DESTINA

CHAPTER VII

DISEMBARKATION ANALYSIS

7.1 Demand for Coastline Analysis

This section describes coastline analysis model development, including existing SRTM data and estimation method based on Fractal theory. The applications of these models are given along with visualization integrated strategic analysis tool. Main demands for Coastline Analysis can be categorized into two parts: the length of available coastline and the area for deploying, which are shown in Figure 7.1. The first requirement is the length of coastline shallow enough, because it is the measure of how many navy craft can land at the same time. The second requirement is how large the area is. : MEC can deploy the delivery and turn around to come back.

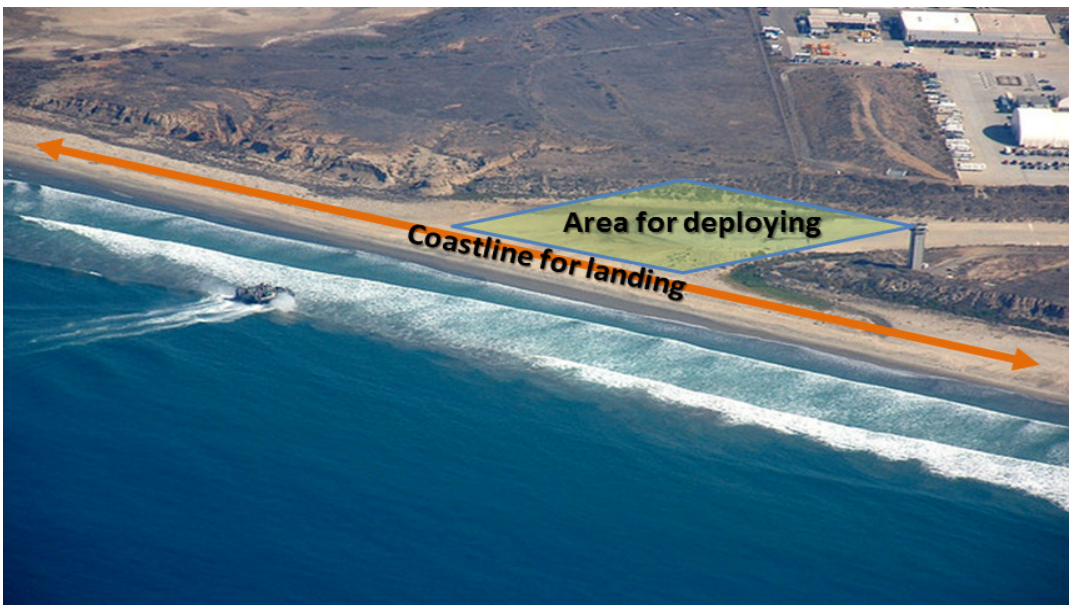

Figure 7.1 Coastline for Landing and Area for Deploying and Turning [46]

7.2 Fractal Theory for Coastline Analysis

French mathematician Benoît Mandelbrot published “How Long Is the Coast of Britain? Statistical Self-Similarity and Fractional Dimension” in Science in 1967 [130]. In this paper Mandelbrot discussed self-similar curves that have Hausdorff dimension between 1 and 2. These curves are examples of fractals, although Mandelbrot did not use this term in the paper, as he did not coin it until 1975. The paper is one of Mandelbrot's first publications on the topic of fractals.

The paper examined the coastline paradox: the property that the measured length of a stretch of coastline depends on the scale of measurement. Empirical evidence suggested that the smaller the increment of measurement, the longer the measured length becomes. If one were to measure a stretch of coastline with a yardstick, one would get a shorter result than if the same stretch were measured with a 30cm (one-foot) ruler. This was because one would be laying the ruler along a more curvilinear route than that followed by the yardstick. Figure 7.2 shows an example where the measured length of coastline is longer if the size of the measurement is smaller. The empirical evidence suggested a rule which, if extrapolated, showed that the measured length increased without limit as the measurement scale decreased towards zero.

Figure 7.2 Coastline Length With Regard To Measurement Size

This discussion implied that it was meaningless to talk about the length of a coastline; some other means of quantifying coastlines were needed. Mandelbrot discussed an empirical law discovered by Lewis Fry Richardson, who observed that the measured length L(G) of various geographic borders was a function of the measurement scale G. Collecting data from several different examples, Richardson conjectured that L(G) could be closely approximated by a function of the form:

$$L(G) = MG^{1-D} \qquad \text{Equation 7.1}$$

where M is a positive constant and D is a constant, called the dimension, greater than or equal to 1. Intuitively, if a coastline looks smooth it should have dimension close to 1; and the more irregular the coastline looks the closer its dimension should be to 2. The examples in Richardson's research have dimensions ranging from 1.02 for the coastline of South Africa to 1.25 for the West coast of Britain.

Mandelbrot then described various mathematical curves, related to the Koch snowflake, which were defined in such a way that they were strictly self-similar. Mandelbrot showed how to calculate the Hausdorff dimension of each of these curves, each of which had a dimension D between 1 and 2 (he also mentioned but did not give a construction for the space-filling Peano curve, which had a dimension exactly 2). He noted that the approximation of these curves with segments of length G had lengths of the form G^{1-D}. The resemblance with Richardson's law was striking. Note that the paper did not claim that any coastline or geographic border actually had fractional dimension. Instead, he noted that Richardson's empirical law was compatible with the idea that

geographic curves, such as coastlines, could be modeled by random self-similar figures of fractional dimension.

Near the end of the paper Mandelbrot briefly discussed how one might approach the study of fractal-like objects in nature that looked random rather than regular. For this he defined statistically self-similar figures and said that these were encountered in nature.

The study is important because it is a turning point in Mandelbrot's early thinking on fractals. It is an example of the linking of mathematical objects with natural forms that was a theme of much of his later work.

7.3 Coastline Analysis

To analyze coastline, this module uses Shuttle Radar Topography Mission (SRTM) data which includes height information with 6000 by 6000 resolution for 5 degree squares as shown in Figure 7.3 [109]. From the data, it estimates the gradient of each point on the coastline. Because this database has only the height numbers, the pre-procedures are required to calculate the gradient. First, the water region needs to be identified if it is ocean or lake. It is solved by the process to confirm it is directly connected to the given point as ocean or not. Second, the direction to land is also defined as one of 16 basic directions based on the shape of coastline. Finally, there are meaningless small peninsulas to land because they do not have enough space behind the landing points. These points are removed from the candidate of coastline.

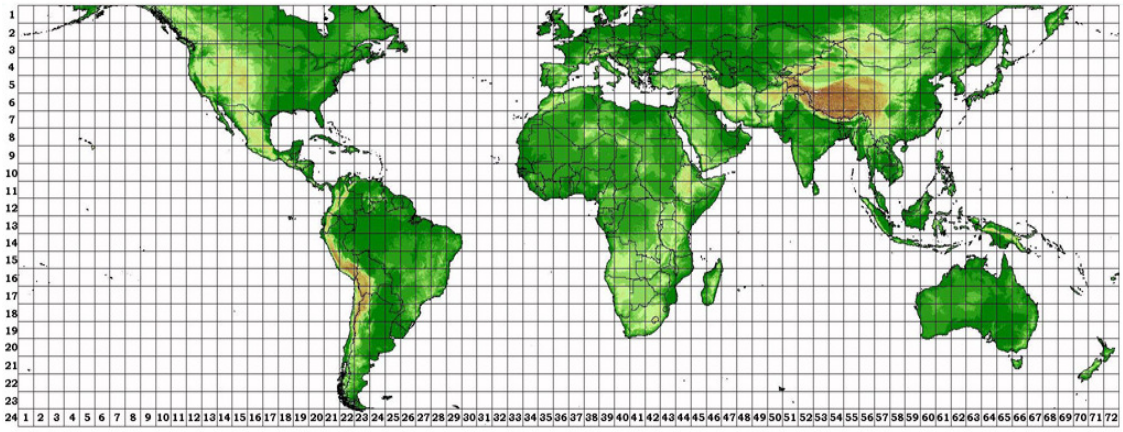

Figure 7.3 SRTM Data Grid [42]

Next step is to estimate the gradient of coastline. The points of coastline can be defines as the points of boundary next to the points of ocean. And two gradient data are calculated; the gradient of the coastline itself and the average gradient of 500m along the landing direction. The first gradient is required for availability for landing and the second is for deploying and turning back. Then, the overall availability of coastline points is determined based on two constraints. Based on the performance of MEC, the constraints are given as the maximum gradient of coastline and the average gradient of 1500 ft along the landing direction. The last procedure is to calculate the length of consecutive points. This length is related to the maximum number of landing at the same time and it can provide the environment for the operational analysis. General procedure of the Algorithm for consecutive available coastline based on SRTM database is shown in Figure 7.4.

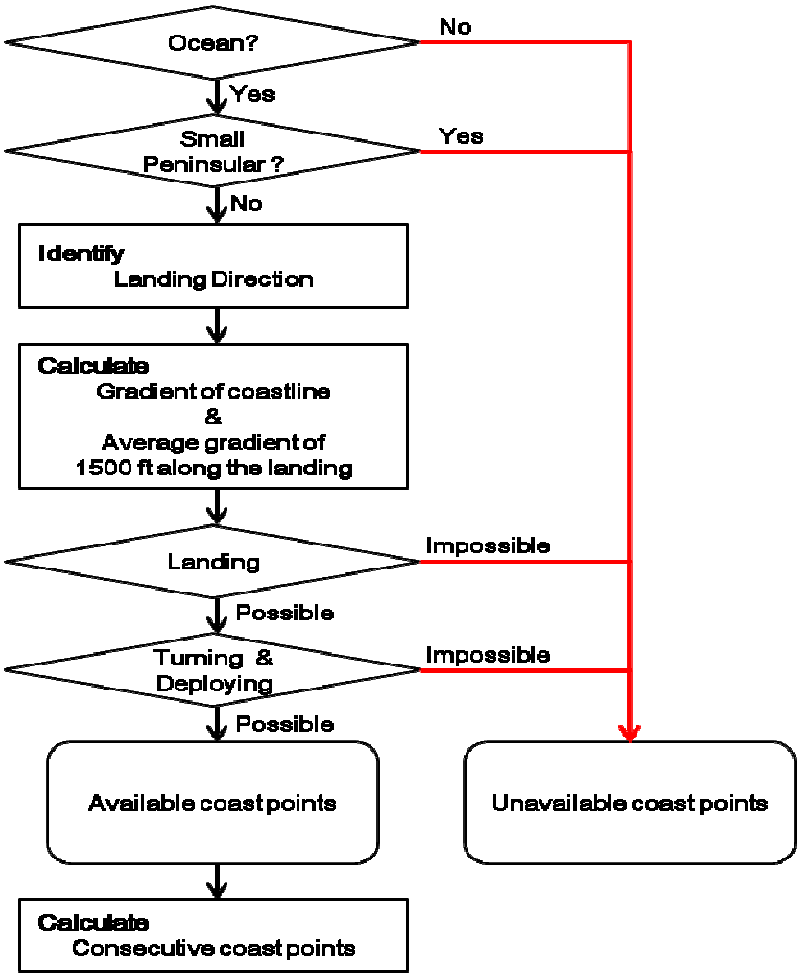

Figure 7.4 General Procedure of the Algorithm for Consecutive Available Coastline

Two examples are attached by using the developed tool above. In the analysis result of northwest coastline in Oregon, the first example is shown in the Figure 7.5. The left figure is 3D graph of the region from Google Earth and the right figure is the analysis result [37]. The criteria for gradients of coastline and landing area are 5 %. Black coastline is the appropriate region to land and deploy, and the yellow coastline is not suitable region. It shows that precipices are displayed as yellow line and beach area is possible to land. As the result, the longest available coastline is the beach in the left part and its length is 9.88 miles.

Figure 7.5 Analysis Result of Northwest Coastline in Oregon [37]

The second example in Figure 7.6 is the analysis result of southwest coastline in Chile. This example describes the ability to analyze complex coastline without errors. The shown area is the longitude -75 to -74.75 and latitude -50.25 to -50. The criteria for gradients of coastline and landing area are 5% as well. Likewise, Black coastline is the appropriate region to land and deploy, and the yellow coastline is not suitable region. As the result, the longest available coastline is the beach in the left part and its length is 11.78 miles in the top center of figure.

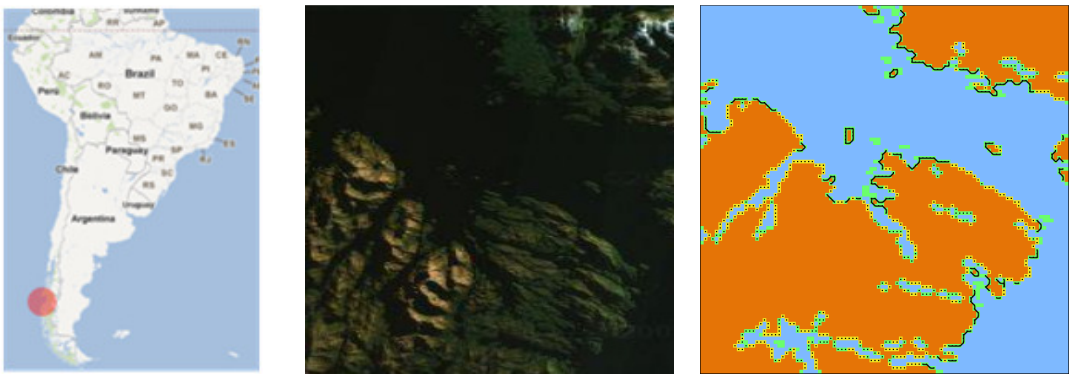

Figure 7.6 Analysis result of southwest coastline in Chile [37]

7.4 Fractal relation for the limited SRTM data

SRTM data provide highly detailed height and bathymetry. However, it does not include the region of latitude over 60 north and under 60 south which are shown as blue in Figure 7.7. Therefore, this module needs a different method to calculate the available coastline of those regions with same or similar accuracy.

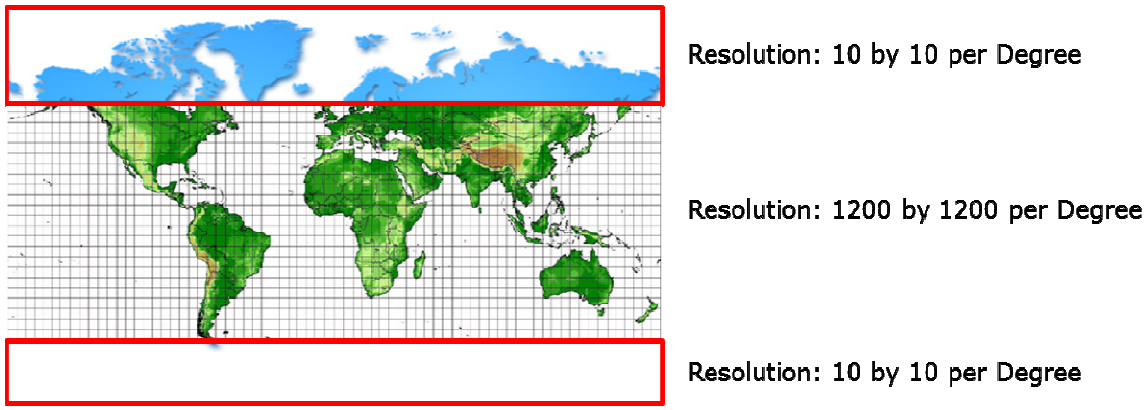

Figure 7.7 Missing Part of SRTM Database [42]

The fractal relation based on the self-similarity of coastline is one of solutions to calculate with similar accuracy. This fractal relation can be formulated as following.

$$L(G) = MG^{1-D}$$

Here, L is measured length, G is measurement scale, and the other M and D are constants. To confirm the Fractal relation, the length of coastline is estimated based on the different measurement scales in the 10 by 10 degree region that includes Italy. This area and the measured length are described in Figure 7.8. For reference, the coastline of Italy is 7600 km in CIA World Factbook.

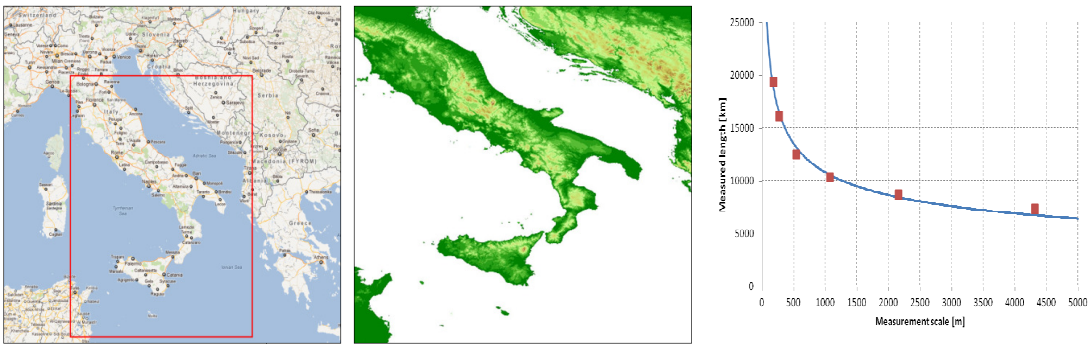

Figure 7.8 Fractal Relation of Coastline Length of Italy [43]

As the result of the length from six different measurement scales, we can estimate the approximate relation of the coastline as following.

$$L(G) = 99685.8\ G^{-.32144} \quad [km] \qquad \text{Equation 7.2}$$

For now, the fractal relation is identified that it can fit values and trend overall area. Vice versa, from the part of points in the low resolution, the value of other points in high resolution can be estimated. To validate this assumption, new fractal relation is extracted from two points in low resolution region, and four approximated values in high resolution can be estimated from this fractal relation. The result is described in Figure 7.9. Two red circle points are the basis for fractal relation and four black points are actual values of coastline length at each point. The blue dotted line means extrapolation by fractal relation. This extrapolation line is pretty close to the actual values and follows its trend. Until the point A (measurement scale 540 m), extrapolation line is almost similar to the actual points and the range between the point A and B is 75% of unknown area in the higher resolution region. The exact values of actual and estimated length are shown in Table 7.1. Aforementioned before, the errors at 540m and 1080m are less than 3%.

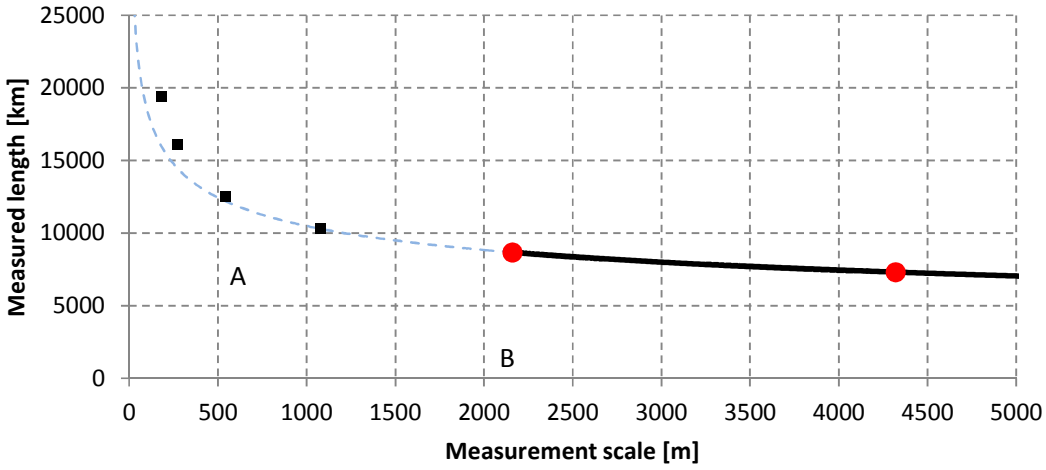

Figure 7.9 Fractal Relation of Coastline Length

Table 7.1 Comparison of Actual and Estimated Values for Coastline Length of Italy

Measurement scale [m]	Actual length [km]	Estimated length [km]	Error [%]	Ratio to Smallest low resolution
1080	10339.9	10287.4	-0.5	0.500
540	12510.7	12205.3	-2.4	0.250
270	16124.4	14480.6	-10.2	0.125
180	19401.7	16003.5	-17.5	0.083

The second example is the northern coastline in Brazil shown in Figure 7.10. This coastline is relatively smooth and shallow. Likewise, this extrapolation line is pretty close to the actual values and follows its trend as well. The exact values of actual and estimated length are shown in Table 7.2.

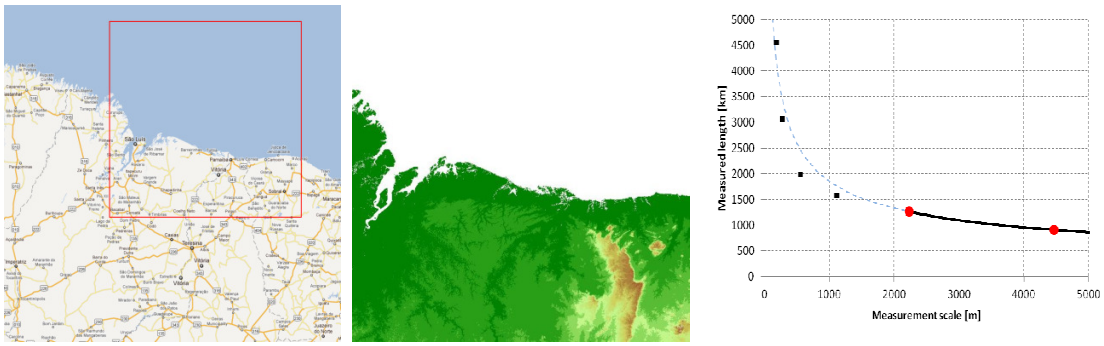

Figure 7.10 Fractal Relation of Coastline Length of Brazil [43]

Table 7.2 Comparison of Actual and Estimated Values for Coastline Length of Brazil

Measurement scale [m]	Actual length [km]	Estimated length [km]	Error [%]	Ratio to Smallest low resolution
1116	1579.8	1765.7	-11.8	0.500
558	1986.2	2471.3	-24.4	0.250
279	3068.1	3472.6	-13.2	0.125
186	4566.4	4207.8	7.85	0.083

The last example is the east coastline in North Korea as shown in Figure 7.11. This coastline is relatively complicated and the slope is pretty high. Likewise, this extrapolation line is pretty close to the actual values and follows its trend as well. The exact values of actual and estimated length are shown in Table 7.3. The normalized graph of three examples discussed above is shown in Figure 7.12.

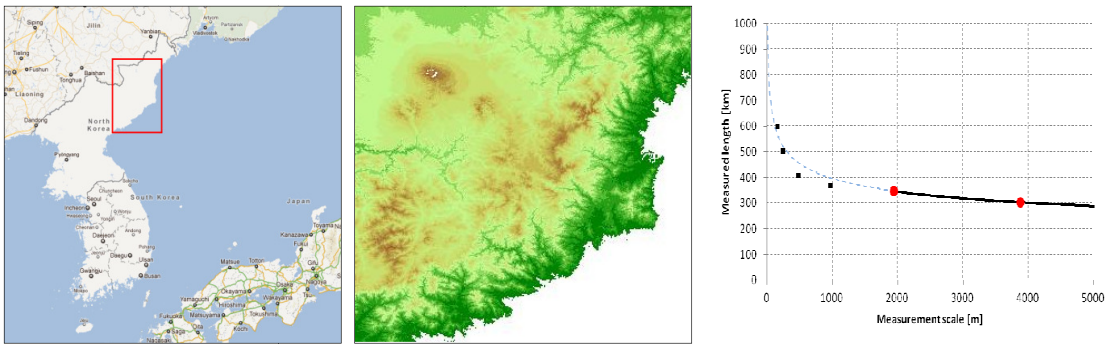

Figure 7.11 Fractal Relation of Coastline Length of North [43]

Table 7.3 Comparison of Actual and Estimated Values for Coastline of North Korea

Measurement scale [m]	Actual length [km]	Estimated length [km]	Error [%]	Ratio to Smallest low resolution
970	368.7	395.7	-7.3	0.500
485	410.4.7	457.9	-11.6	0.250
243	502.6	524.2	-4.3	0.125
162	599.8	566.0	5.64	0.083

Likewise, we can estimate the values around polar area, the by using extrapolation. Currently, available height data base of Polar area is 10 by 10 per each square degree. Comparing to SRTM data that provides 1200 by 1200 per square degree, the resolution gap is highly different. The formulation can be obtained in the low resolution part, and the length of coastline can be estimated by extrapolation to the high resolution part under the assumption that the proportion of available coastline is constant in the point. From those results, we can justify Hypothesis 5.

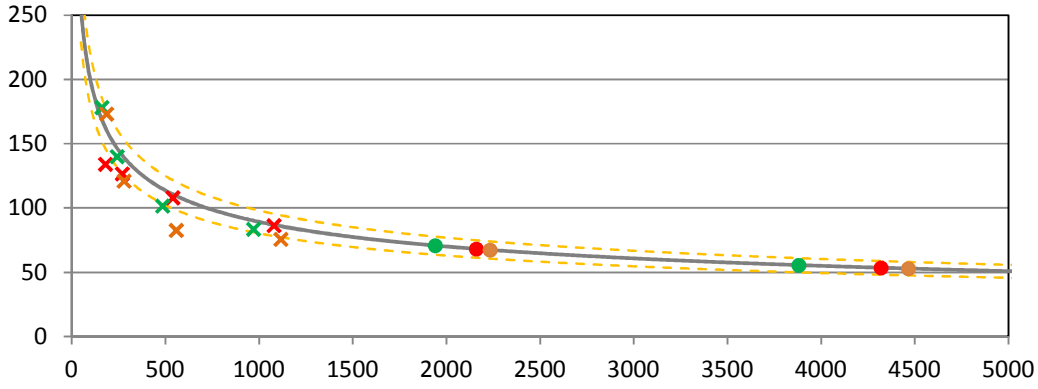

Figure 7.12 Normalized Results of Three Examples

7.5 Disembarkation Analysis in the Decision Supporting Tool

Coastline analysis can provide the length of available coastline at the given position to the operational analysis. Also, the criterion for landing availability is based on the maximum climbing angle that is calculated by the sizing and synthesis module. The integration of these tools is shown in Figure 7.13.

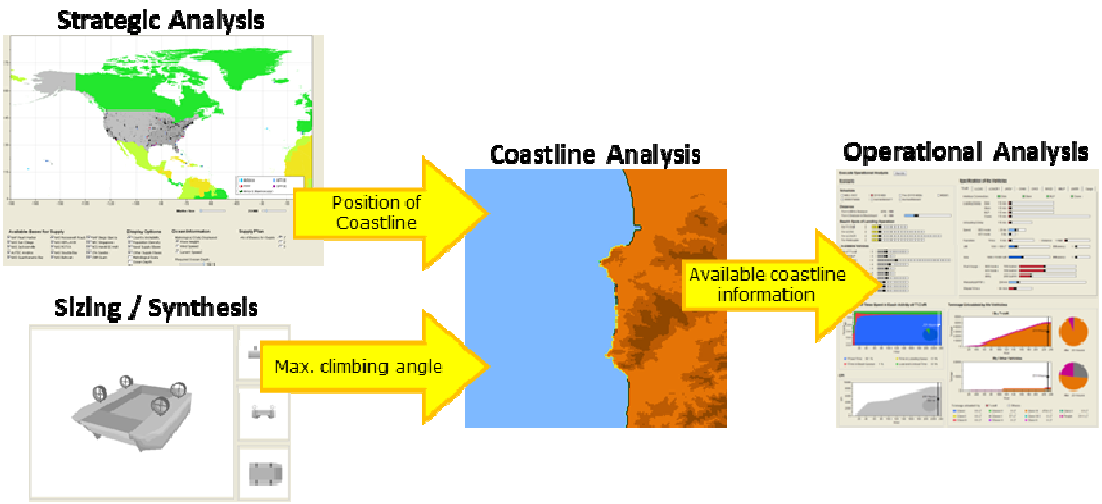

Figure 7.13 Disembarkation Analysis in DESTINA

CHAPTER VIII

OPERATIONAL ANALYSIS

8.1 Operational Analysis

Beisecker conducted research on the effectiveness of the Medium Exploratory Connector (MEC), an Office of Naval Research (ONR) innovative naval prototype. [2] The US Navy is shifting to power projection from the sea which stresses the capabilities of its current fleet and exposes a need for a new surface connector. The design of complex systems in the presence of changing requirements, rapidly evolving technologies, and operational uncertainty continues to be a challenge. Furthermore, the design of future naval platforms must take into account the interoperability of a variety of heterogeneous systems and their role in a larger system-of-systems context. To date, methodologies to address these complex interactions and optimize the system at the macro-level have lacked a clear direction and structure and have largely been conducted in an ad-hoc fashion. Traditional optimization has centered around individual vehicles with little consideration of the impact on the overall system. A key enabler in designing a future connector is the ability to rapidly analyze technologies and perform trade studies using a system-of-systems level approach. The objective of Beisecker was to develop a process that can quantitatively assess the impacts of new capabilities and vessels at the systems-of-systems level. This new methodology must be able to investigate diverse, disruptive technologies acting on multiple elements within the system-of-systems architecture. Illustrated through a test case for a Medium Exploratory Connector (MEC), the method must be capable of capturing the complex interactions between elements and the

architecture and must be able to assess the impacts of new systems. Based on a review of current methods, six gaps were identified, including the need to break the problem into sub-problems in order to incorporate a heterogeneous, interacting fleet, dynamic loading, and dynamic routing. For the robust selection of design requirements, analysis was performed across multiple scenarios, which required the method to include parametric scenario definition.

The identified gaps were investigated and methods were recommended to address these gaps to enable overall operational analysis across scenarios. Scenarios were fully defined by a scheduled set of demands, distances between locations, and physical characteristics that could be treated as input variables. Introducing matrix manipulation into discrete event simulations enabled the abstraction of sub-processes at an object level and reduced the effort required to integrate new assets. Incorporating these linear algebra principles enabled resource management for individual elements and abstraction of decision processes. Although the run time was slightly greater than traditional if-then formulations, the gain in data handling abilities enabled the abstraction of loading and routing algorithms.

The loading and routing problems were abstracted and solution options were developed and compared in Beisecker. [2] Realistic loading of vessels and other assets was needed to capture the cargo delivery capability of the modeled mission. The dynamic loading algorithm was based on the traditional knapsack formulation where a linear program was formulated using the lift and area of the connector as constraints. The schedule of demands from the scenarios represented additional constraints and the reward equation. Cargo available was distributed between cargo sources thus an assignment

problem formulation was added to the linear program, requiring the cargo selected to load on a single connector to be available from a single load point.

Dynamic routing allowed a reconfigurable supply chain to maintain a robust and flexible operation in response to changing customer demands and operating environment. Algorithms based on vehicle routing and computer packet routing were compared across five operational scenarios, testing the algorithms ability to route connectors without introducing additional wait time. Predicting the wait times of interfaces based on connectors en route and incorporating reconsideration of interface to use upon arrival performed consistently, especially when stochastic load times were introduced, was expandable to a large scale application. This algorithm selects the quickest load-unload location pairing based on the connectors routed to those locations and the interfaces selected for those connectors. A future connector could have the ability to unload at multiple locations if a single load exceeds the demand at an unload location. The capability for multiple unload locations was considered a special case in the calculation of the unload location in the routing. To determine the unload location to visit, a traveling salesman formulation was added to the dynamic loading algorithm. Using the cost to travel and unload at locations balanced against the additional cargo that could be delivered, the order and locations to visit were selected. Predicting the workload at load and unload locations to route vessels with reconsideration to handle disturbances could include multiple unload locations and created a robust and flexible routing algorithm. The incorporation of matrix manipulation, dynamic loading, and dynamic routing enabled the robust investigation of the design requirements for a new connector. The robust process used shortfall, capturing the delay and lack of cargo delivered, and fuel usage as

measures of performance. The design parameters for the MEC, including the number available and vessel characteristics such as speed and size were analyzed across four ways of testing the noise space. The four testing methods were: a single scenario, a selected number of scenarios, full coverage of the noise space, and feasible noise space. The feasible noise space was defined using uncertainty around scenarios of interest. The number available, maximum lift, maximum area, and surface effect ship (SES) speed were consistently design drivers. There was a trade-off in the number available and size along with speed. When looking at the feasible space, the relationship between size and number available was strong enough to reverse the number available, to desiring fewer and larger ships. The secondary design impacts came from factors that directly impacted the time per trip, such as the time between repairs and time to repair. As the noise sampling moved from four scenario to full coverage to feasible space, the option to use interfaces were replaced with the time to load at these locations and the time to unload at the beach gained importance. The change in impact could be attributed to the reduction in the number of needed trips with the feasible space. The four scenarios had higher average demand than the feasible space sampling, leading to loading options being more important. The selection of the noise sampling had an impact of the design requirements selected for the MEC, indicating the importance of developing a method to investigate the future naval assets across multiple scenarios at a system-of-systems level.

8.2 Inputs and OutputsOperational Analysis

Inputs and outputs of operational analysis are described in the following tables.

Table 8.1 Input List of Operational Analysis

Input list		Min	Max
General	Schedules	1	6
	Sea Base Distance (nmi)	20	200
	Num of ISBs	1	3
	Distance to ISB 1 (nmi)		
	Distance to ISB 2 (nmi)		
	Distance to ISB 3 (nmi)		
	Number of MEC	0	10
	Number of MLPs	0	5
	Number of LCACs	0	30
	Number of LCACR	0	10
	Number of LMSR	0	5
	Number of Cargo ships	0	5
	Number of JHSVs	0	10
	Number of CH46	0	10
	Number of CH53	0	10
	Number of MV-22s	0	10
	MEC Beach Spots	0	10
	LCAC Beach Spots	0	15
	LCACR Beach Spots	0	20
	Helo Beach Spots	0	15
Interfaces	Interface Connection (Side)		0,1
	Interface Connection (Stern)		0,1
	Interface Connection (Crane)		0,1
	Interface Connection (Helo)		0,1
	LMSR Speed	10	30
	Interface Connection (Side)		0,1
	Interface Connection (Stern)		0,1
	Interface Connection (Crane)		0,1
	Interface Connection (Helo)		0,1
	Cargo1 Speed	10	30
	Number of CH46 carried in transit	0	4
	Number of CH53carried in transit	0	4
	Interface Connection (Side)		0,1
	Interface Connection (Stern)		0,1
	Interface Connection (MLP)		0,1
	Interface Connection (Crane)		0,1
	Loading Delay_Side (min)	15	600

Table 8.1 Input List of Operational Analysis (continued)

Input list		Min	Max
Interfaces	Loading Delay_Stern (min)	15	600
	Loading Delay_MLP (min)	15	600
	Loading Delay_Crane (min)	15	1200
	Unloading Delay (min)	15	300
MEC	SES Speed (kts)	20	50
	ACV Speed (kts)	3	15
	Transition Time (min)	5	90
	MEC Transition Distance (nmi)	1	10
	MEC Max Lift(LT)	200	1000
	MEC Lift eff	0	1
	MEC Max Area(sqft)	5000	15000
	MEC Area eff	0	1
	Fuel Usage in SES mode (gal/hr)	700	1500
	Fuel Usage in ACV mode (gal/hr)	700	1500
	Fuel Usage idling (gal/hr)	200	1500
	MEC reliability	200	1200
	MEC repair time	90	300
MLP	MLP Connection Time (min)	30	240
	MLP Disconnect Time (min)	30	240
	MLP Speed (kts)	10	30
	MLP Time to Offload LCACs	15	60
	MLP Time to Load LCACs	15	60
	MLP Time to Offload LCACRs	15	60
	MLP Time to Load LCACRs	15	60
	Fuel Usage cruising (gal/hr)	700	1500
	Fuel Usage idling(gal/hr)	200	1500
LCAC	LCAC round trip range (nmi)	15	50
	LCAC Loading Time (min)	15	300
	LCAC Unloading Time (min)	15	120
	LCAC Speed (kts)	30	50
	LCACs per MLP	1	8
	LCAC Max Lift(LT)	20	100
	LCAC Lift Eff	0	1
	LCAC Max Area(sqft)	200	1000
	LCAC Area Eff	0	1
	Fuel Usage cruising (gal/hr)	700	1500
	Fuel Usage idling(gal/hr)	200	1500

Table 8.1 Input List of Operational Analysis (continued)

Input list		Min	Max
LCACR	LCACR round trip range (nmi)	15	100
	LCACR Loading Time (min)	15	450
	LCACR Unloading Time (min)	15	300
	LCACR Speed (kts)	30	50
	LCACRs per MLP	1	4
	LCACR Max Lift(LT)	40	300
	LCACR Lift Eff	0	1
	LCACR Max Area(sqft)	400	3000
	LCACR Area Eff	0	1
	Fuel Usage cruising (gal/hr)	700	1500
	Fuel Usage idling(gal/hr)	200	1500
JHSV	JHSV Unloading Time (min)	10	120
	JHSV Loading Time (min)	10	120
	JHSV Speed (kts)	10	50
	JHSV Max Lift(LT)	200	1000
	JHSV Lift Eff	0	1
	JHSV Max Area (sqft)	1000	10000
	JHSV Area Eff	0	1
	Fuel Usage cruising (gal/hr)	400	1500
	Fuel Usage idling(gal/hr)	100	1500
CH46	CH46 unloading time (min)	10	60
	CH46 internal loading time (min)	10	60
	CH46 sling loading time (min)	10	60
	CH46 speed (kt)	100	200
	CH46 Max Lift internal (LT)	2	8
	CH46 Max Lift sling(LT)	2	8
	CH46 Lift Eff	0	1
	CH46 Max Area internal (sqft)	100	200
	CH46 Max Area sling (sqft)	50	500
	CH46 Area Eff	0	1
	Fuel Usage clean (gal/hr)	100	500
	Fuel Usage sling load (gal/hr)	100	500
	Fuel Usage idling(gal/hr)	50	500
CH53	CH53unloading time (min)	10	60
	CH53 internal loading time (min)	10	60
	CH53 sling loading time (min)	10	60
	CH53 speed (kt)	100	200

Table 8.1 Input List of Operational Analysis (continued)

Input list		Min	Max
	CH53 Max Lift internal (LT)	10	25
	CH53 Max Lift sling(LT)	10	25
	CH53 Lift Eff	0	1
	CH53 Max Area internal (sqft)	150	300
	CH53 Max Area sling (sqft)	150	500
	CH53 Area Eff	0	1
	Fuel Usage clean (gal/hr)	500	1000
	Fuel Usage sling load (gal/hr)	500	1000
	Fuel Usage idling(gal/hr)	300	1000
MV22	MV22 land on MLP?		0,1
	MV22 use helo landing spot?		0,1
	MV22 Unloading Time MLP (min)	15	120
	MV22 Loading Time (min)	15	120
	MV22 Unloading Time Helo spot (min)	15	120
	MV22 Speed (kts)	200	300
	MV22 Max Lift(LT)	5	25
	MV22 Lift Eff	0	1
	MV22 Max Area (sqft)	50	500
	MV22 Area Eff	0	1
	Fuel Usage cruising (gal/hr)	400	1000
	Fuel Usage idling(gal/hr)	100	750
Reliability	LCAC reliability	200	1200
	LCAC repair time	90	300
	LCACR reliability	200	1200
	LCACR repair time	90	300
	JHSV reliability	200	1200
	JHSV repair time	90	300
	CH46 reliability	50	900
	CH46 repair time	90	300
	CH53 reliability	50	900
	CH53 repair time	90	300
	MV22 reliability	50	900
	MV22 repair time	90	300

Table 8.2 Output List of Operational Analysis

Column No	Variable	Column No	Variable
1	Time	24	Cargo by others: Class 2
2	T_craft.numunloaded	25	Cargo by others: Class 3
3	T_craft.travel	26	Cargo by others: Class 4
4	T_craft.beachqueue	27	Cargo by others: Class 5
5	T_craft.SBqueue	28	Cargo by others: Class 6
6	T_craft.load	29	Cargo by others: Class 7
7	LCAC.numunloaded	30	Cargo by others: Class 8
8	LCACR.numunloaded	31	Cargo by others: Class 9
9	CH46.numunloaded	32	Cargo by others: Class 10
10	CH53.numunloaded	33	Total CPI
11	Cargo by MEC: etc	34	num.average(MEC.load_wts)
12	Cargo by MEC: Class 1	35	num.average(MEC.load_areas)
13	Cargo by MEC: Class 2	36	num.average(LCAC.load_wts)
14	Cargo by MEC: Class 3	37	num.average(LCAC.load_areas)
15	Cargo by MEC: Class 4	38	num.average(LCACR.load_wts)
16	Cargo by MEC: Class 5	39	num.average(LCACR.load_areas)
17	Cargo by MEC: Class 6	40	num.average(CH46.load_wts)
18	Cargo by MEC: Class 7	41	num.average(CH46.load_areas)
19	Cargo by MEC: Class 8	42	num.average(CH53.load_wts)
20	Cargo by MEC: Class 9	43	num.average(CH53.load_areas)
21	Cargo by MEC: Class 10	44	time - first cargo delivered
22	Cargo by others: etc	45	---
23	Cargo by others: Class 1	46	Total Cargo delivered

Table 8.3 Class of Cargo [36]

Class	Description	Consumer Class
Class I	Subsistence (food), gratuitous (free) health and comfort items.	Troops
Class II	Clothing, individual equipment, tent-age, organizational tool sets and kits, hand tools, unclassified maps, administrative and housekeeping supplies and equipment.	Troops
Class III	Petroleum, Oil and Lubricants (POL) (package and bulk): Petroleum, fuels, lubricants, hydraulic and insulating oils, preservatives, liquids and gases, bulk chemical products, coolants, deicer and antifreeze compounds, components, and additives of petroleum and chemical products, and coal.	Equipment
Class IV	Construction materials, including installed equipment and all fortification and barrier materials.	Troops
Class V	Ammunition of all types, bombs, explosives, mines, fuzes, detonators, pyrotechnics, missiles, rockets, propellants, and associated items.	Equipment
Class VI	Personal demand items (such as health and hygiene products, soaps and toothpaste, writing material, snack food, beverages, cigarettes, batteries, alcohol, and cameras—nonmilitary sales items).	Troops
Class VII	Major end items such as launchers, tanks, mobile machine shops, and vehicles.	Equipment
Class VIII	Medical material (equipment and consumables) including repair parts peculiar to medical equipment. (Class VIIIa – Medical consumable supplies not including blood & blood products; Class VIIIb – Blood & blood components (whole blood, platelets, plasma, packed red cells, etc.).	Troops
Class IX	Repair parts and components to include kits, assemblies, and sub-assemblies (repairable or non-repairable) required for maintenance support of all equipment.	Equipment
Class X	Material to support nonmilitary programs such as agriculture and economic development (not included in Classes I through IX).	Civilians

8.3 Operational Analysis in the Decision Supporting Tool

To perform operation analysis, the code developed by Beisecker is integrated with other modules in DESTINA. Figure 8.1 shows the input part of the graphical user interface (GUI) of DESTINA. Various scenarios such as peace-keeping and humanitarian operation and various vehicles such as cargo ships including MEC and helicopters can be used to perform realistic simulation using DESTINA.

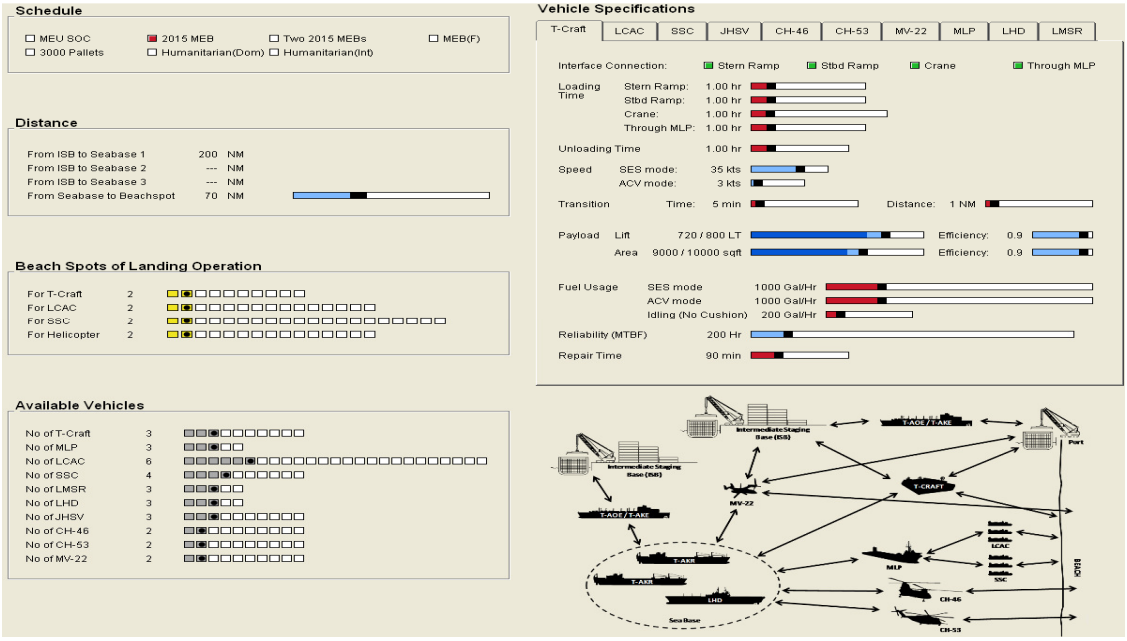

Figure 8.1 Input GUI of Operational Analysis in DESTINA

Figure 8.2 shows an example of operational analysis results in DESTINA based on the given input. The operational analysis results, e.g., combat power index and cargo unloading progress are shown with regard to time measured from the day of an incident, e.g., an earthquake.

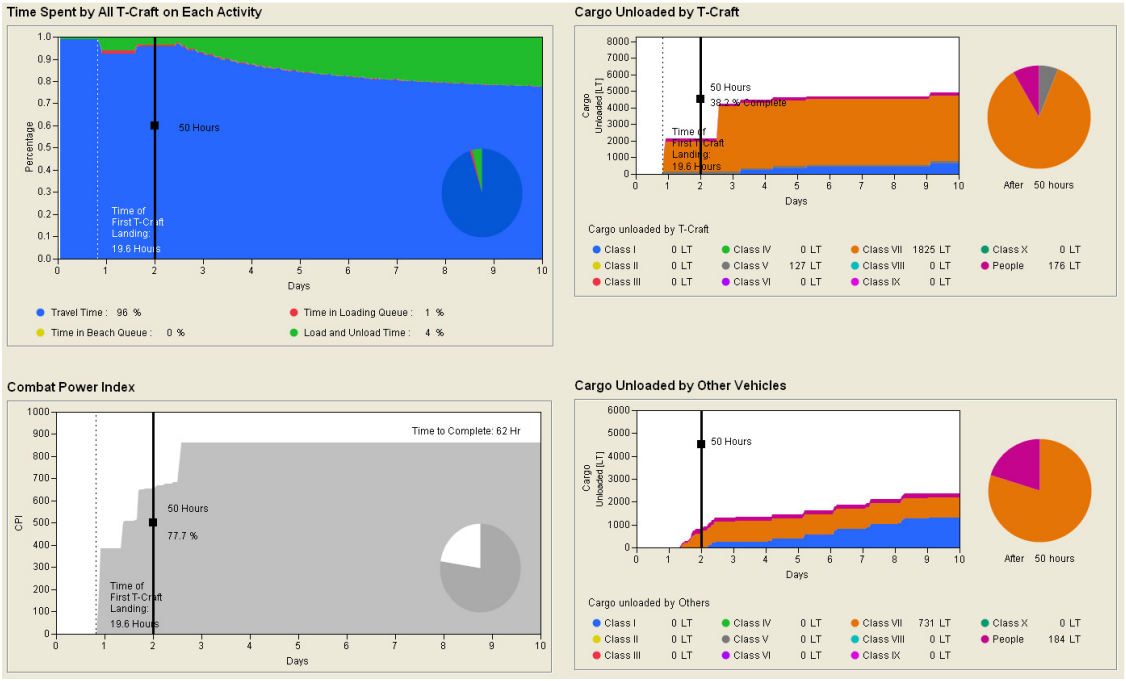

Figure 8.2 Output Display of Operational Analysis in DESTINA

CHAPTER IX

GLOBAL EFFECTIVE ESTIMATION

9.1 Adaptive Monte-Carlo Simulation

Hypothesis 3 presents that adaptive Monte-Carlo simulation with maximum entropy concept accurately and efficiently captures the global effectiveness distribution of the MEC. Figure 9.1 shows the procedure of convergence with regard to the number of experiments in Monte-Carlo simulation. Adaptive Monte-Carlo simulation will be stopped when the convergence satisfies the condition that the user defines. By using adaptive numbers of experiments, Monte-Carlo simulation can get reliable statistical results in the minimum time. And how to capture the global effectiveness is explained in the next example.

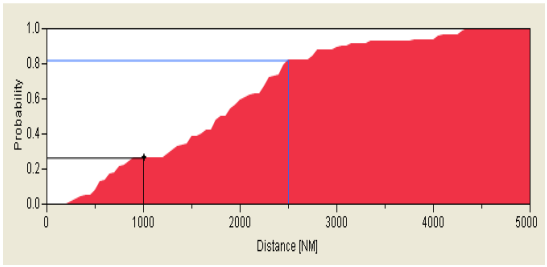

(a) 100 experiments

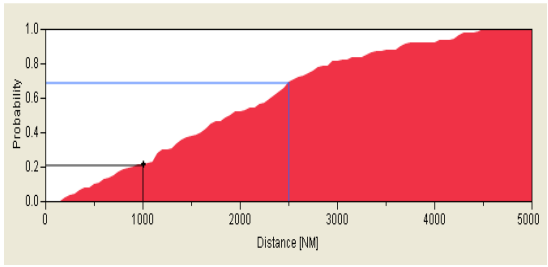

(b) 200 experiments

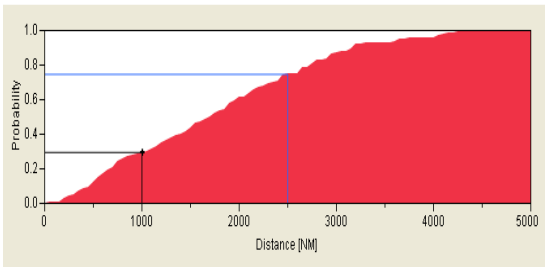

(c) 300 experiments

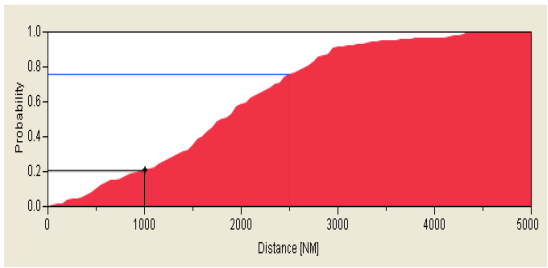

(d) 400 experiments

Figure 9.1 Convergence of Monte-Carlo Simulation by Number of Experiments

9.2 Sampling Method with Maximum Entropy Concept

Maximum entropy sampling has been developed in the area of information theory and computer science. These studies are generally divided into two categories. First category is a sampling method by using Shanon entropy, and the other category is using Boltzman entropy. In this research, instead of simplified concept of entropy, original entropy for constant volume thermodynamics is used because the sampling points in this research has more analogies with the entropy concept in thermodynamics as shown in Table 9.1.

Table 9.1 Analogies of Entropy Concept

Thermodynamics	This research
Heat sources	Sampling points
Specific heat	Area
Temperature	Representative index
Number of moles	Population density
Temperature of Heat source	Reliability of information

In the case of entropy for constant volume in thermodynamics, the equation for changed entropy is as follows. [139]

$$\Delta S_V = nc_v \ln \frac{T_f}{T_i} \qquad \text{Eq. (9.1)}$$

Where, C_v is specific heat, T is temperature and n is number of moles of gas. Sampling points can be regarded as heat sources and the power of heat sources can be quantified from the reliability of the information at those points. In this research, the

reliability of information is assumed as all same level, so all power is quantified as unit magnitude. Then, the temperature distribution out of sampling points means the reliability of information and this is the measure of representation of overall data regression. the temperature distribution can be calculated by Fourier's law.

$$\frac{dQ}{dt} = -kA\frac{dT}{dx} \qquad \text{Eq. (9.2)}$$

Because the information of sampling points is estimated based on the current situation, temperature distribution can be regarded as reaching the convergence. The solution of 2 dimensional stationary condition for Fourier's law is as follows.

$$T(x,y) = k((x - x_s)^2 + (y - y_s)^2) \qquad \text{Eq. (9.3)}$$

Then, finally the entropy of sampling has the following equation.

$$\Delta S = \iint n \ln \frac{T_{final}(x,y)}{T_{initial}(x,y)}\, dx\, dy \qquad \text{Eq. (9.4)}$$

The procedure of selection of additional points is described in Figure 9.2. Initial temperature distribution by original sampling points is shown in Figure 9.2(a) and the candidates of additional points are displayed in Figure 9.2(b). After calculating the change of entropy about each candidate, the maximum change of entropy can be found. Then, the point to make the maximum change of entropy is selected as an additional point. Figure 9.2(c) shows the final temperature distribution after selecting an additional point. This selection of a point implies where the sampling points is most sparse as well and the impact of an additional point can be maximized. Therefore, this procedure provides better efficiency and reduce the computational cost. In addition, this technique enable Monte-Carlo simulation to get the required information in the minimum time.

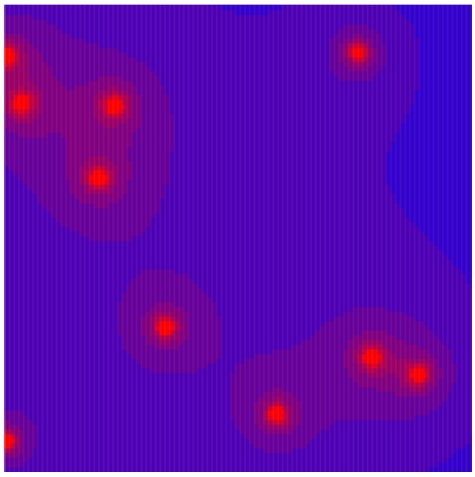

(a) Original temperature distribution

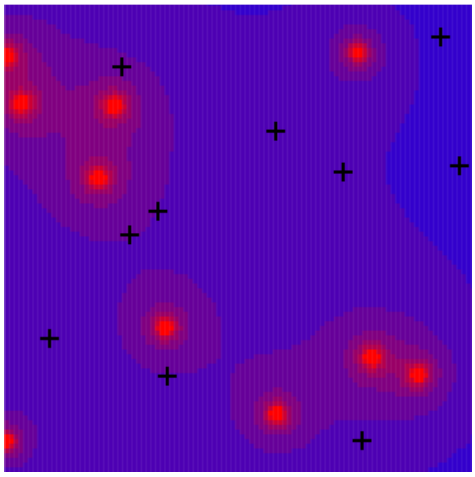

(b) Available additional points

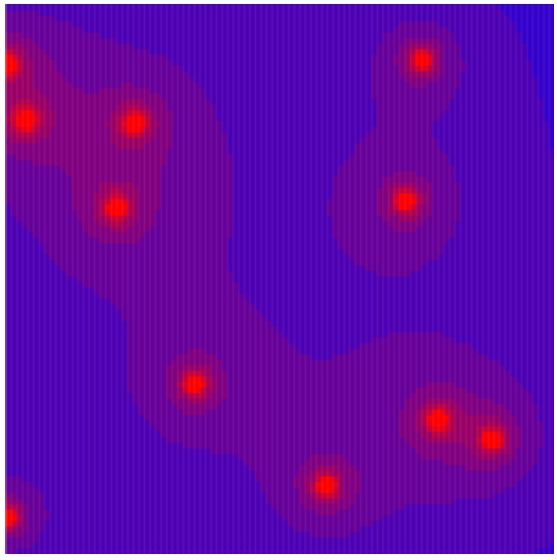

(c) New temperature distribution by adding a new point

Figure 9.2 Procedure to Add Point by Maximum Entropy

In this research, the likelihood of dispatch is the essential goal of statistical analysis. Even though one area has high instability by some factors like natural disasters, the need to dispatch can be extremely low if the population there is significantly small. Consequently, the population density is one of important weight for the result and this can be reflected to the solving procedure.

On the assumption that top center has more population as shown in the Figure 9.3, the solution considering the weight of population density becomes different from the previous solution. Figure 9.4 shows the procedure and the difference of two solutions are compared in Figure 9.5.

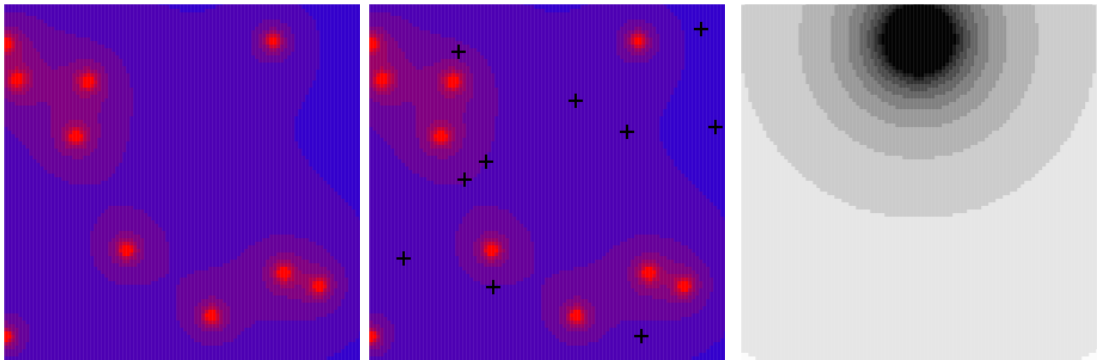

(a) Original distribution (b) Available Points (c) Weighting Distribution

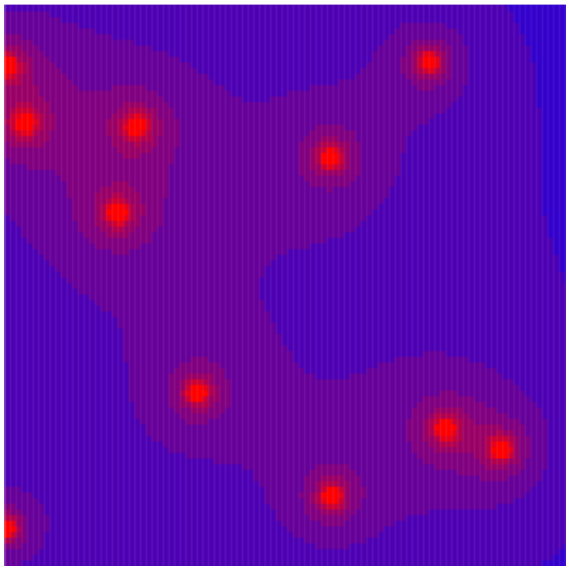

(c) New temperature distribution by adding a new point

Figure 9.3 Selection of Additional Point by Maximum Entropy and Weighting

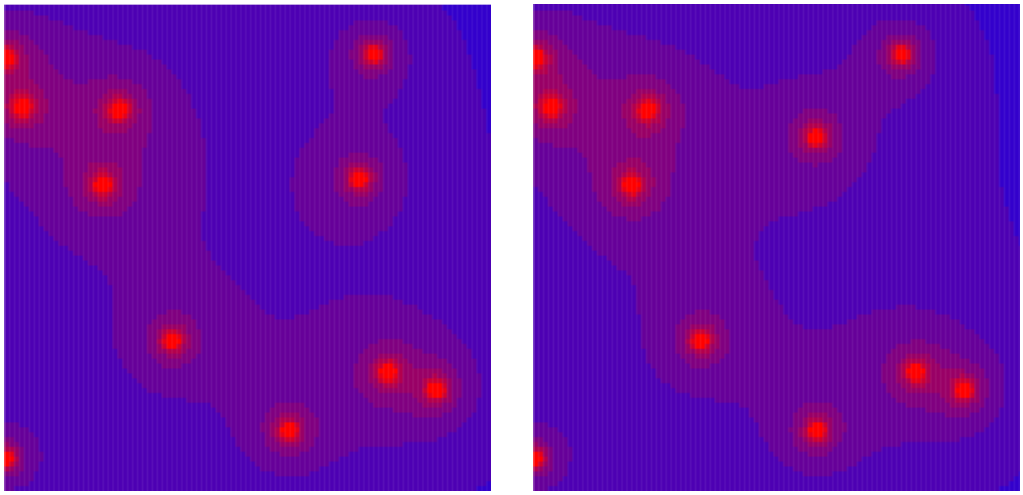

Figure 9.4 Comparison of Additional Points with regard to Weighting

The procedure of adaptive sampling method is depiced in the Figure 9.5. The standard deviations keeps similar values along the procedure. To compare the coverage by sampling points, average distance to the closest point is used. If the numbers of sampling points are same, the higher value means better coverage as show in Figure 9.6. The comparison is described in Figure 9.7.

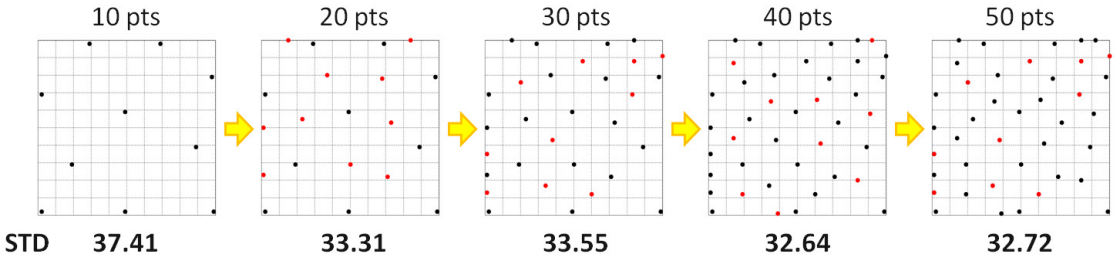

Figure 9.5 Standard Deviation Values with regard to Sampling Points

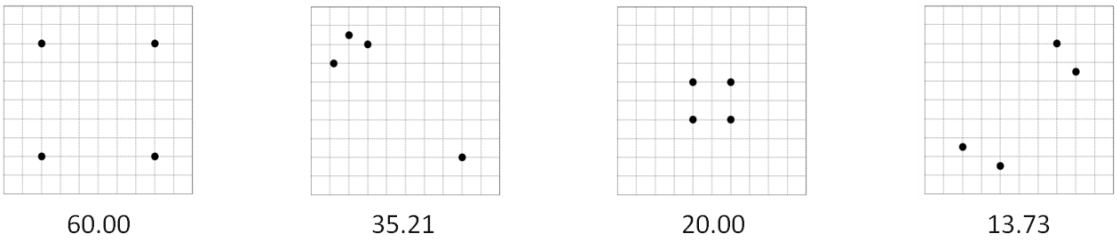

Figure 9.6 Measure of the Coverage by Sampling Points

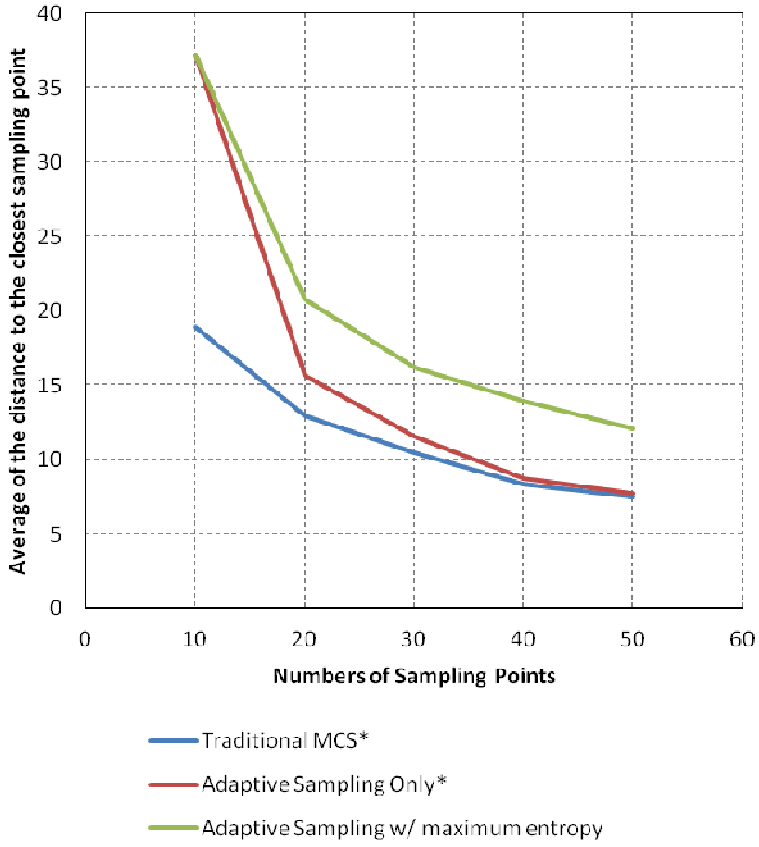

Figure 9.7 Comparison of Sampling Methods

9.3 Global Effectiveness Estimation

In the first example, a Monte-Carlo Simulation was executed to analyze the possible distributions of range the MEC will have to operate under. The set of existing ISBs and SPOEs was used as the starting position for MEC. The political instability factors were varied within the ranges depicted in Table 9.2. For this study only these six instability criteria were analyzed. The distances from the closest ISB/SPOE to each country remains constant despite the result of the Monte-Carlo Simulation (i.e., the distance between Diego Garcia and Madagascar will not change if the threshold for political rights and its weight changes) and were therefore only computed once for each

country. This distance was weighed by the instability calculated for each Monte-Carlo Run. For example if a country had zero instability, its distance was not included in the set of possible distances MEC would have to travel. If a country had an instability criteria of 80% versus a country which had an instability criteria of 40%, its distance would be included twice as many times as the country with the instability criteria of 40%, effectively weighing that distance more prominently in the distribution.

Table 9.2 Monte-Carlo Simulation Inputs for the DESTINA

Type	Variables	Unit	Min	Max	Input Values to SAT
Thresholds	Oil Production / Capita	BBL/Day-Person	0	0.05	No Modification
	GDP / Capita	$	0	50000	No Modification
	Infant Mortality	Death/1000	0	200	No Modification
	Life Expectancy	Years	0	90	No Modification
	Political Right	N/A	1	7	No Modification
	Civil Liberty	N/A	1	7	No Modification
Weights	Oil Production / Capita	Day-Person/BBL	0	1	Value / Sum of Weights
	GDP / Capita	1/$	0	1	Value / Sum of Weights
	Infant Mortality	1000/Death	0	1	Value / Sum of Weights
	Life Expectancy	1/Years	0	1	Value / Sum of Weights
	Political Right	N/A	0	1	Value / Sum of Weights
	Civil Liberty	N/A	0	1	Value / Sum of Weights

The results from this Monte-Carlo Simulation are depicted in Figure 9.8 and 9.9. The two distributions presented are the distribution of distances without the weighing in Figure 9.6 and the weighed distances in Figure 9.7. These distributions may look similar for both cases but there are some subtle differences. The unweighed distances peak higher to the left, while the weighed have higher values in the range between 2,000nmi and 3,750nmi. This can be an indication that countries that in the future may display higher levels of instability are further away from the existing ISBs, a result that is not completely unexpected. Nonetheless, these results are not fully indicative of what regions may or may not be stable in the future.

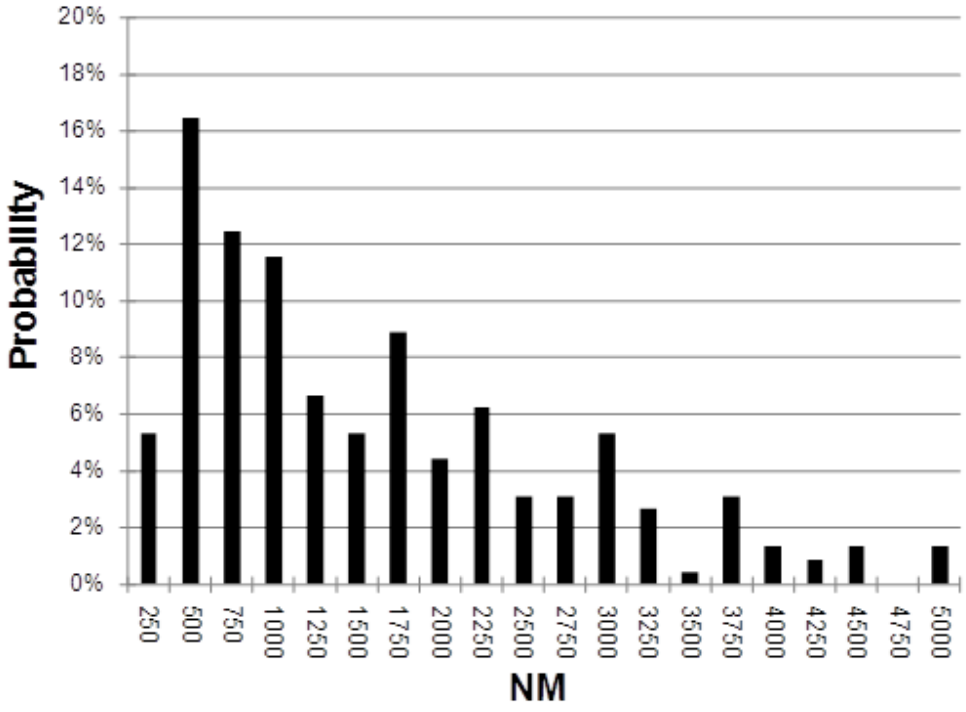

Figure 9.8 Distributions of distances between the ISBs and the Sea Base

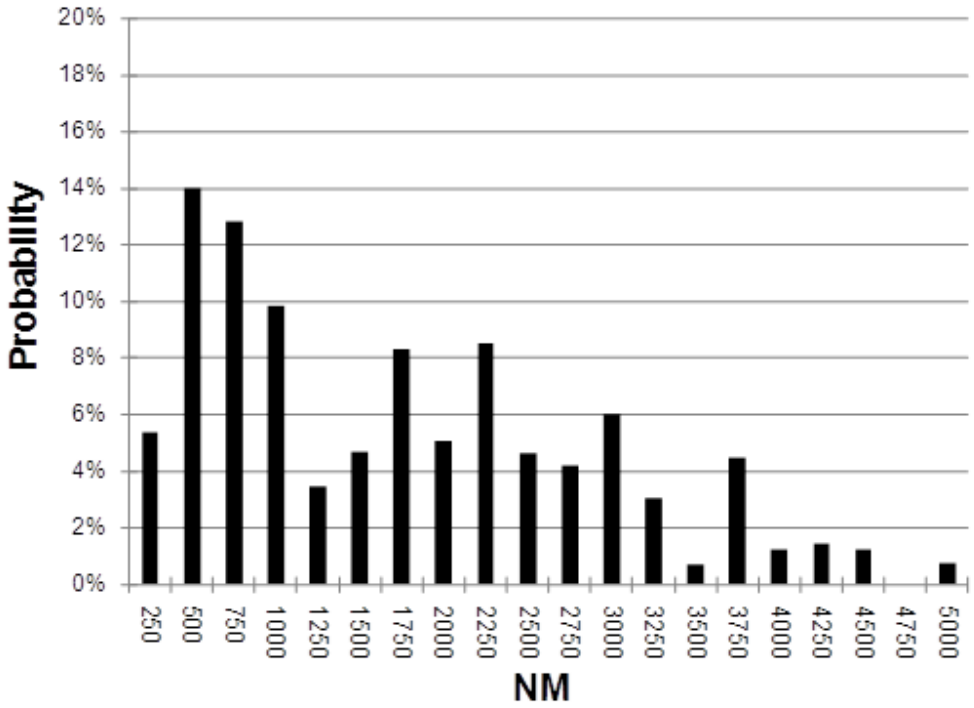

Figure 9.9 Distributions of distances Weighed by Instability Index

These distributions can be studied as probability density functions, or as they can be integrated to obtain the cumulative distribution function (CDF) as depicted in Figure 9.10. The two distributions presented are the distribution of distances without the weighing at the top and the weighed distances at the bottom. This format of CDF can help address the question about how often will my MEC be able to deploy directly from an SPOE, ISB to the Area of Operations (AOO). For example, from the current available navy bases, 95% coastline area in the world is under the distance 3741.1 NM. When we weigh the distance by the instability index, 95% coastline area in the world is under the distance 3733.5 NM. This distance distribution can provide the requirement of range for the new design of navy vessels.

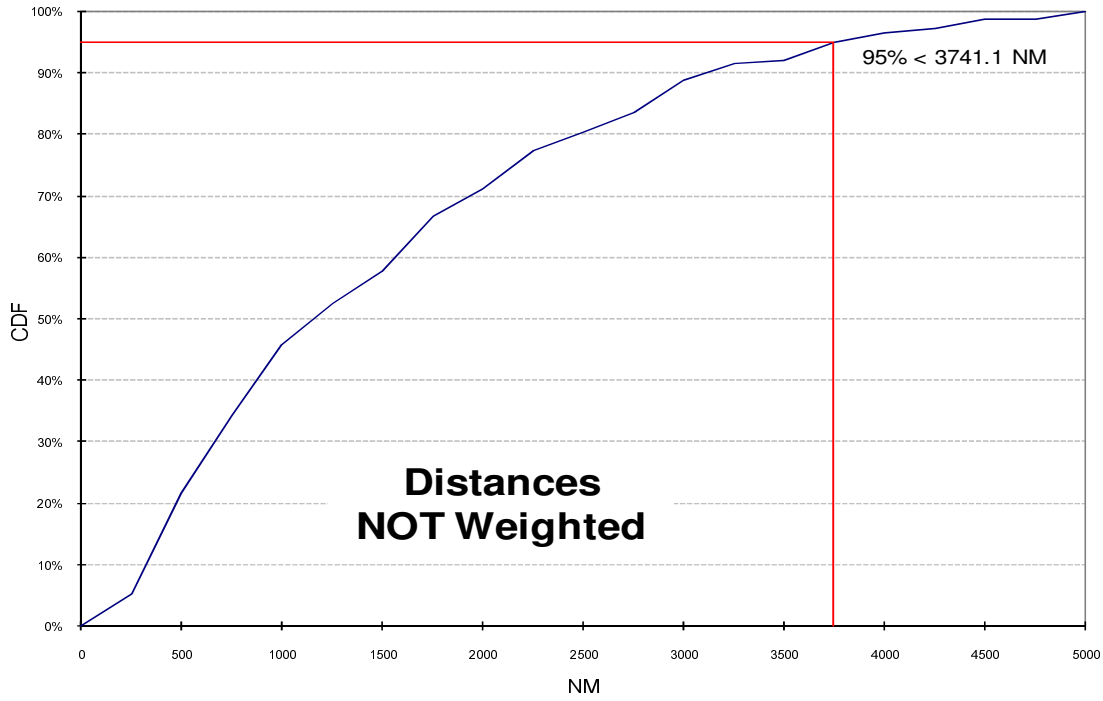

(a) Comulative Density Function of Shipping Distance

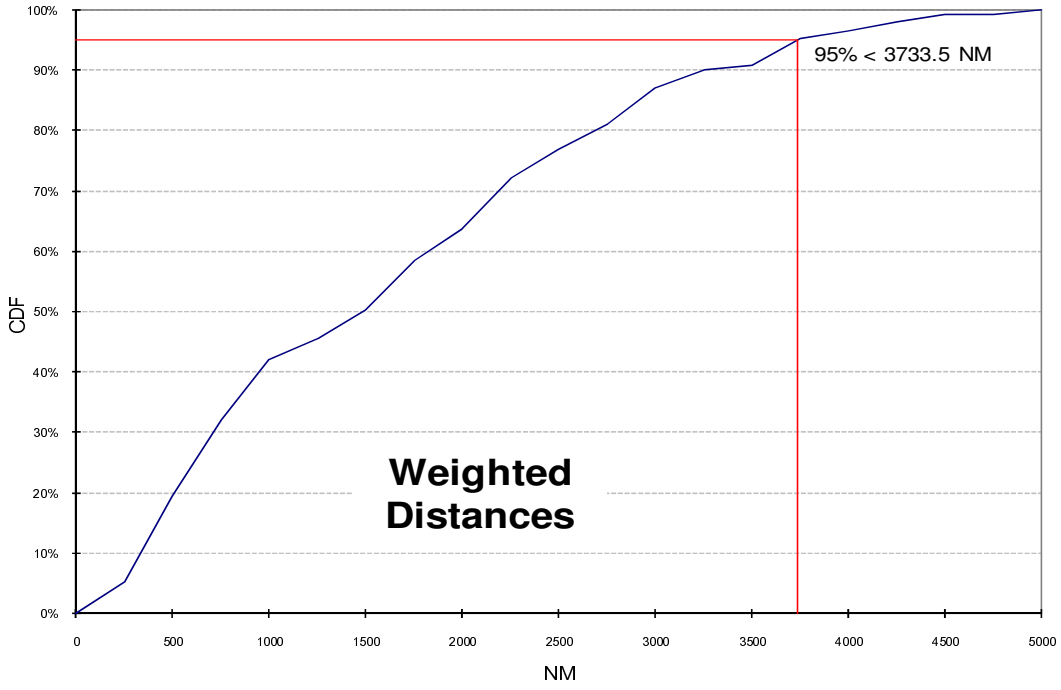

(a) Comulative Density Function of Shipping Distance with Weighting

Figure 9.10 Probabilistic Range Analysis

This analysis can also aid in comparing different sized MECs. Aircraft cargo and range is often analyzed as a payload-range curve, a limiting curve for the maximum payload that can be carried for a given range. The sections of the payload range curve can be defined by a maximum range for maximum payload and a maximum payload for maximum range. Figure 9.11 depicts the payload range curve for three different MECs (on the left) and the confidence of how much payload would be carried to the AOO by each MEC. The three MEC depicted are the objective (in blue) and threshold (in red) MECs described in the MEC Broad Agency Announcement (BAA), and a parametric MEC (in green) that can be used to compare to the other two. In this case the parametric MEC was made to be an intermediate size MEC with all MEC having a maximum range without payload of 2,500nmi as required by the BAA.

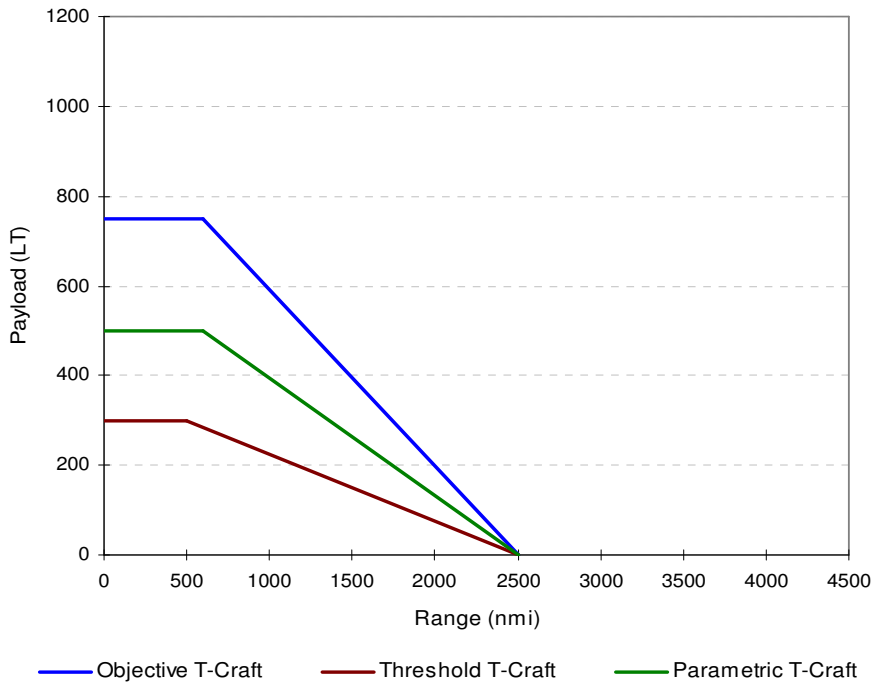

Figure 9.11 the payload range curve for three candidates of MEC

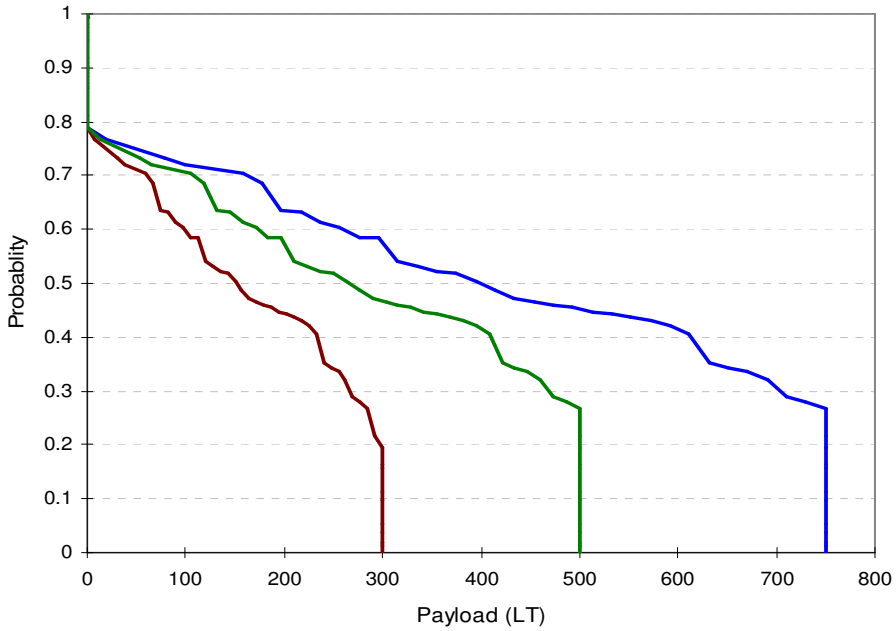

Figure 9.12 Probabilistic Analysis on Payload Delivered After Transit to AOO

The results from Figure 9.12 can be used as follows. For a given payload to be carried on the first deployment of the MEC, the probability that at least that much payload will be carried can be obtained by observing the probability at which the required payload intercepts the probability curve. For example, Figure 9.13 depicts the case where a minimum of 200LT are to be carried by MEC on its deployment from an ISB or SPOE. This figure states that the threshold MEC will carry that much payload 44% of the times, while the objective MEC would carry that much payload 63.5% of the times. The intermediate MEC would carry that much payload 57% of the times.

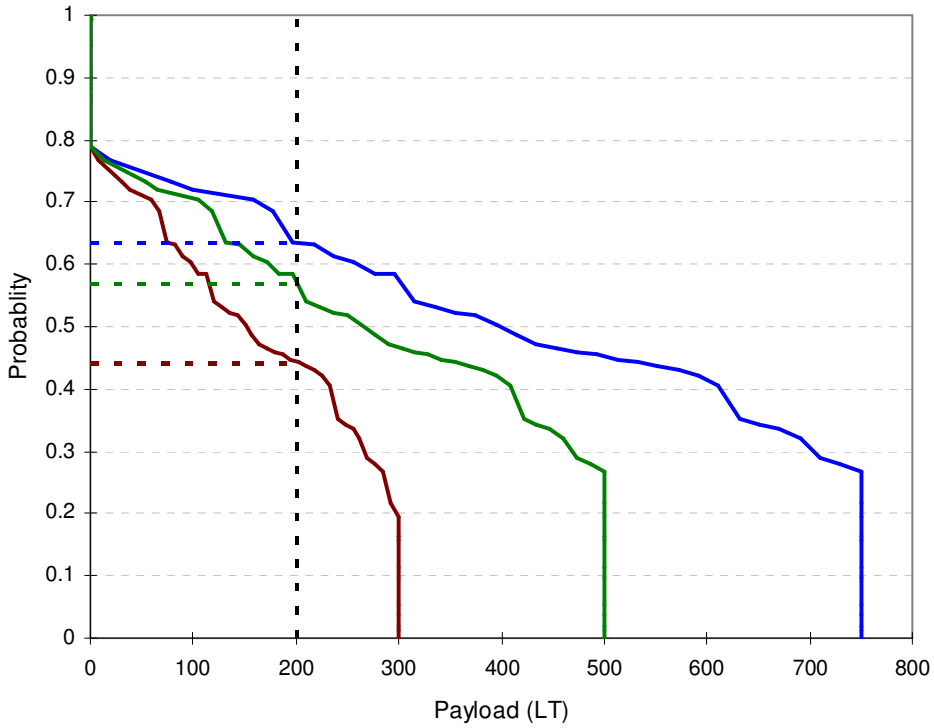

Figure 9.13 Probability of Carrying at Least 200 LT in the Initial Deployment

This analysis can be extended to other MEC designs, for example, a MEC that can carry 1000LT for 600nmi and has a maximum unrefueled range of 3,500nmi. Figure 9.15 depicts the comparison of this new MEC against the objective and the threshold MEC. For a minimum of 200LT, this new MEC would be able to bring that much payload 86.5% of the times. For a minimum of 300LT, the smallest MEC would be able to carry that much payload 20% of the times it was deployed, while the objective MEC would be able to do so 58% of the times and the larger MEC 80% as shown in Figure 9.16.

This ability of MEC to self-deploy and carry a minimum amount of payload would have different values for different missions. If MEC was to support a landing operation in support of Mayor Combat Operations, its ability to carry a large amount of payload on its initial leg might not be as useful as if it was responding to a humanitarian operation. The rationale for this example is as follows: If MEC was to deploy faster than

the assault wave, or before the bulk of the supply forces arrive, it would operate in a high threat environment for which it was not meant to operate. On the other hand, if MEC was to deploy with humanitarian aid, it could respond faster than the other assets and help alleviate the situation. The impact that 200LT or 300LT would have on a humanitarian disaster would have to be gauged by the decision maker. This is the rationale for not assigning value to these capabilities of MEC, the tool is meant to support decision makers with quantitative analysis where quantitative analysis is feasible.

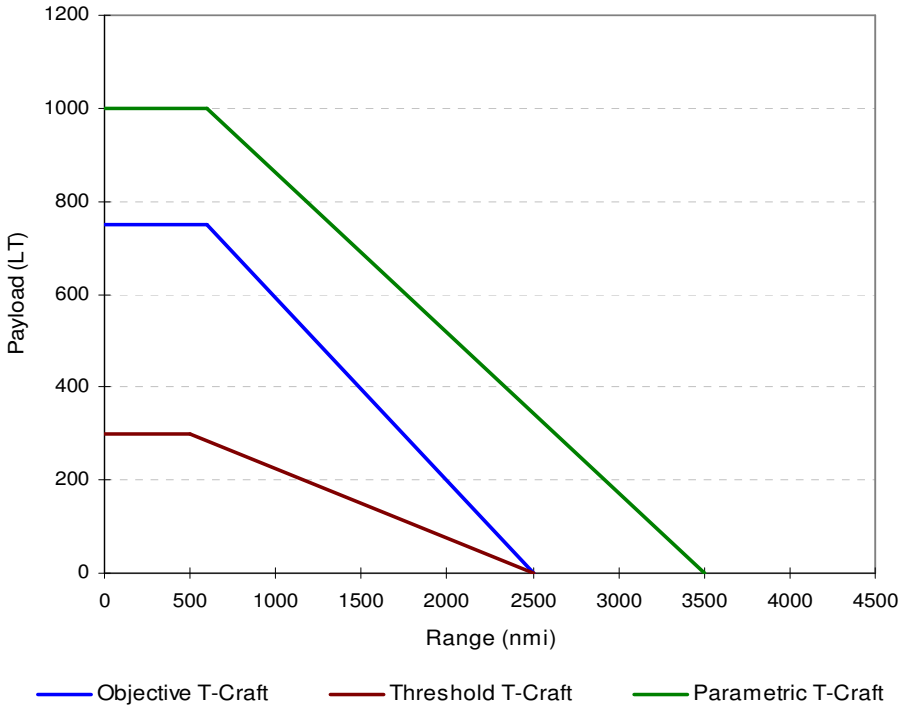

Figure 9.14 the payload range curve for Larger candidates of MEC

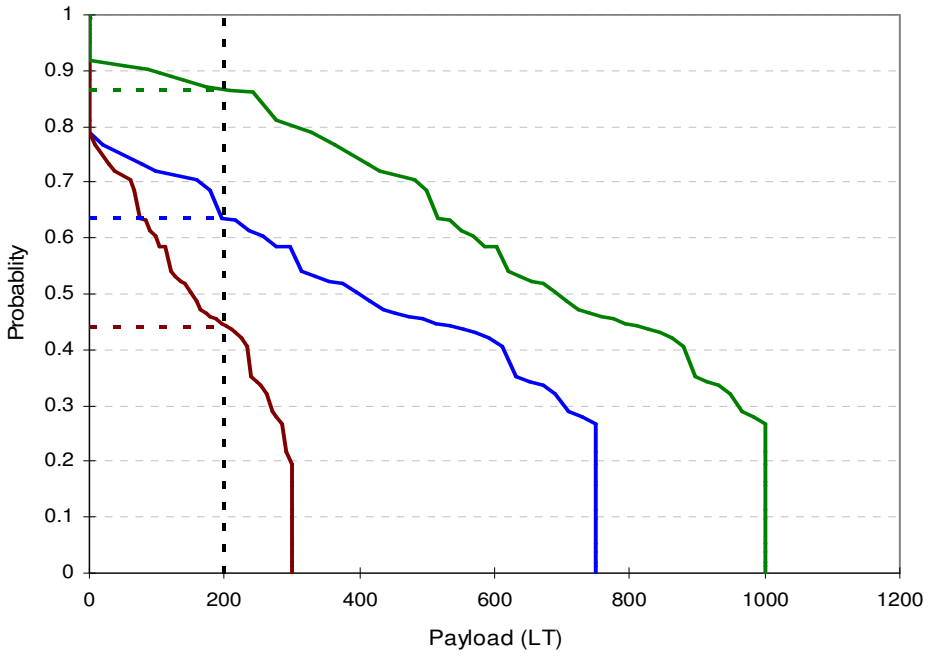

Figure 9.15 Example of Larger MEC with Extended Range

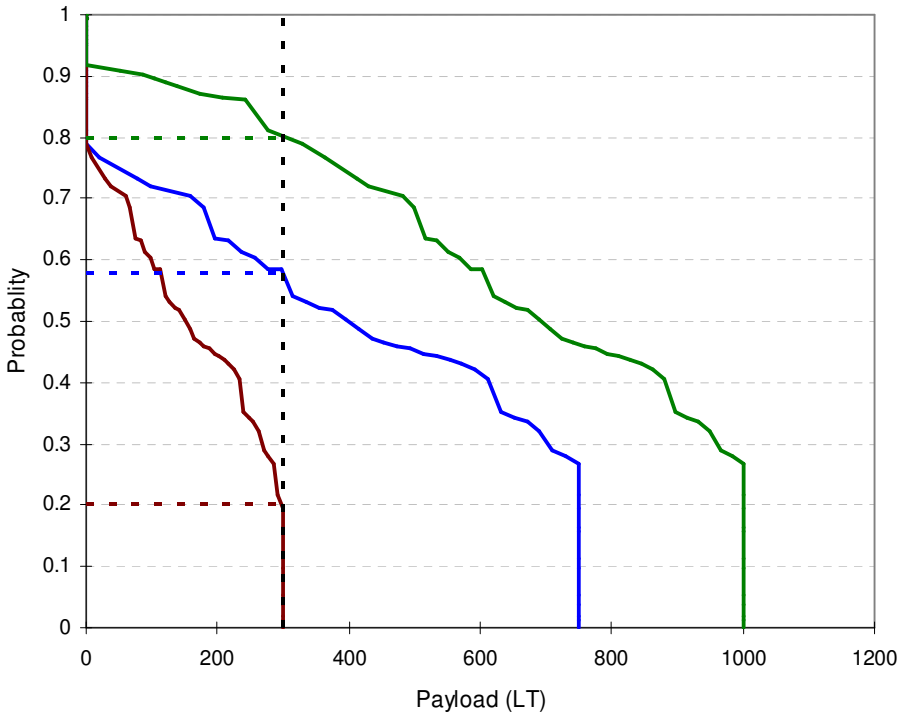

Figure 9.16 Probability of each MEC carrying a minimum of 300LT

9.4 Probabilistic Logistic Utility Index

To verify the effectiveness of vessels, the fair measure for comparison is required. In this research, Probabilistic Logistic Utility (PLU) is suggested as a measure of probability of direct shipping with regard to required payload. This PLU is calculated from the linear mapping of payload-range relation and statistical distribution of distance. Therefore, PLU can provide the quantified measure of the global effectiveness estimation. The procedure to calculate PLU is described in Figure 9.17.

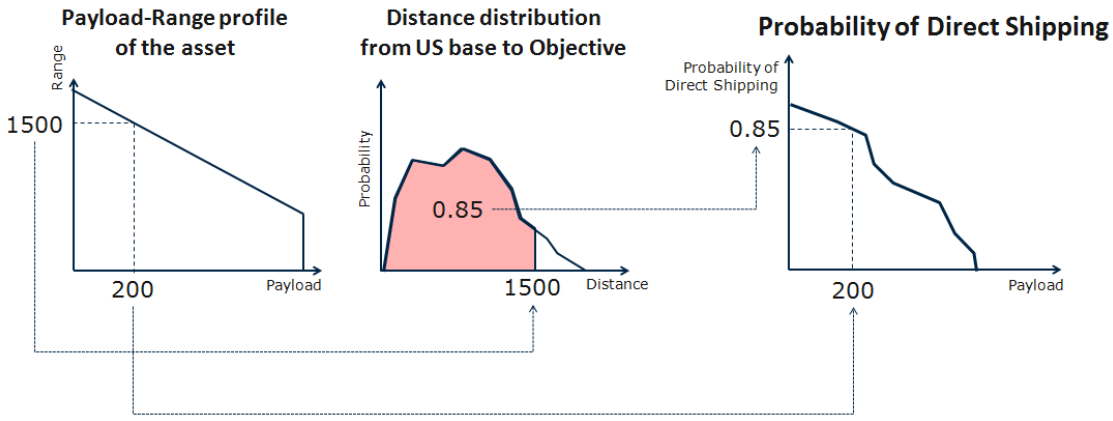

Figure 9.17 Linear Mapping for Probability of Direct Shipping

In other words, Probabilistic Logistic Utility (PLU) is the measure of probability of direct shipping with regard to required payload. In reality, two requirement for logisitics can be applied first: minimum required payload and minimum probability of direct shipping. Therefore, It is formulated as follows:

$$PLU = \int_{PL_{min}}^{PL_{max}} [PDS - PDS_{req}] \, d\,PL \qquad \text{Eq. (9.5)}$$

Where, PLU: Probabilistic Logistic Utility

PL_{min}: minimum required payload

PL_{max}: maximum required payload

PDS: probability of direct shipping

PDS_{min}: minimum required probability of direct shipping

The comparison based on PLU is shown in Figure 9.18. First candidate is capable of carrying 500 LT and its maximum range is 2500 NM. Second candidate can carry 450 LT and its maximum range is 3500 NM. Briefly, the candidate 1 has better maximum payload but the candidate 2 has better maximum range. By calculateing PLU, the global effectiveness index can be estimated as 192.74 and 217.19. It means that the candidate 2 has more serviceable globally.

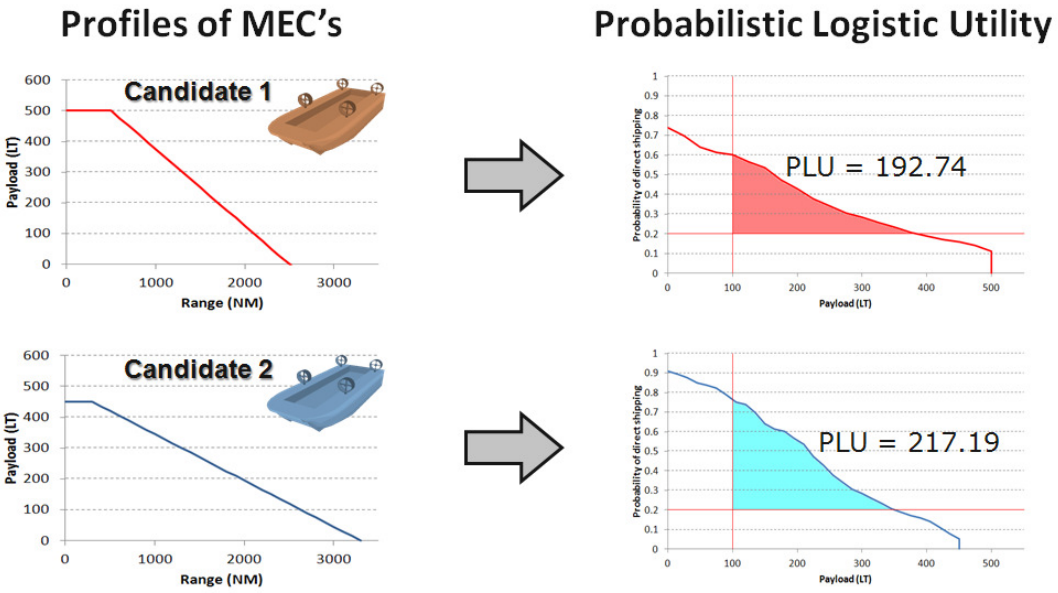

Figure 9.18 Probabilistic Logistic Utility Index of Two MECs

9.5 Filters of Countries

To provide higher degree of freedom for decision makers, this decision support method includes filters which block the likelihood of U.S. intervention in specific countries selected by users as shown in Figure 9.19. This function can supply the scenarios more similar to the actual situation.

Figure 9.19 Filters of Countries

9.6 Global Effectiveness Estimation in the Decision Supporting Tool

The DESTINA was used to demonstrate its functionality. The idea behind the tool itself is to provide decision makers with an intuitive real-time decision support tool to allow them to test different concepts and understand what impact they would have on the

effectiveness of MEC and the entire sea-based logistics force. Figure 9.20 shows a screen shot of the Monte-Carlo Simulation Module in DESTINA.

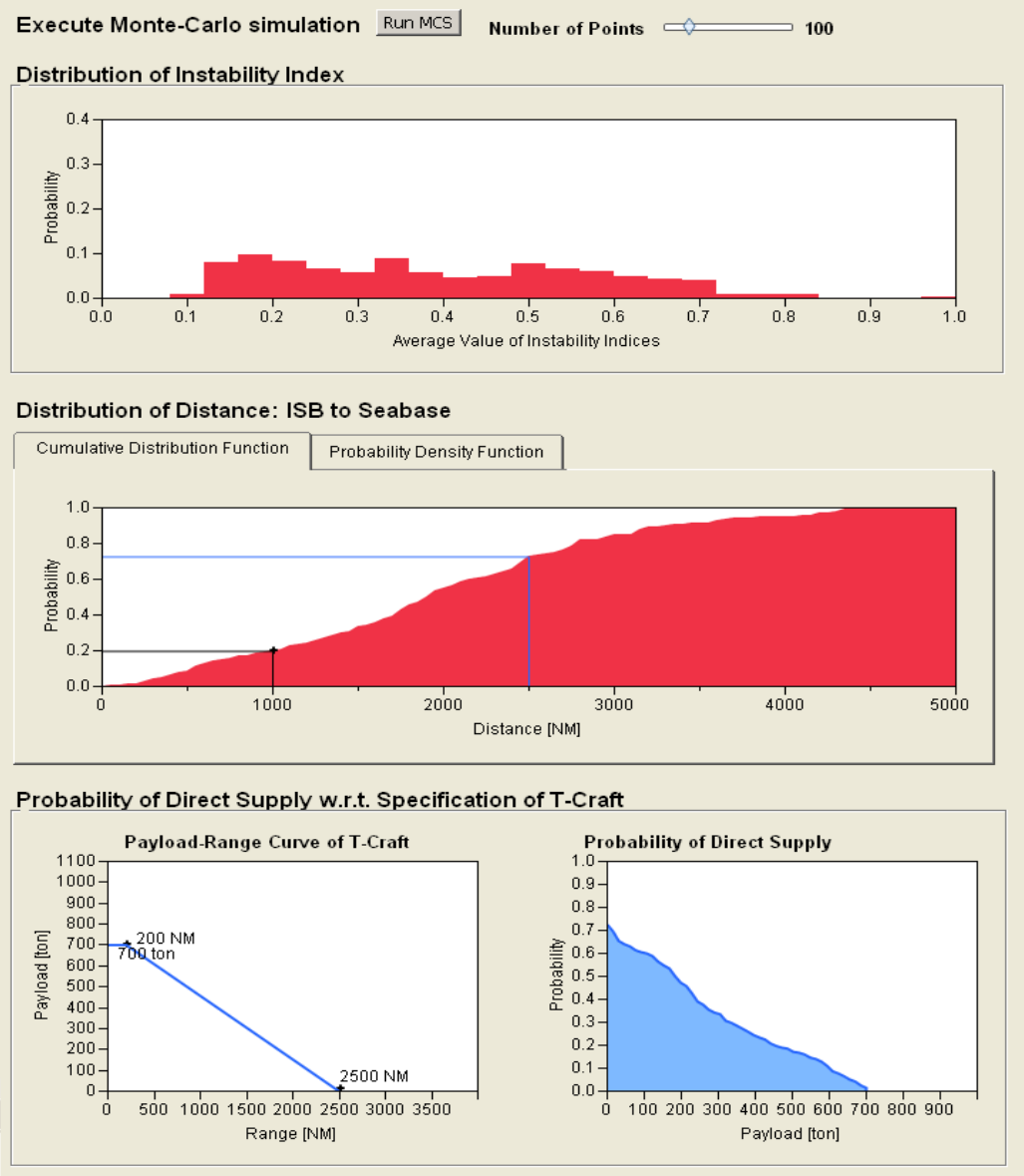

Figure 9.20 Monte-Carlo Simulation in DESTINA

CHAPTER X

PRELIMINARY DESIGN OF MEDIUM EXPLORATORY CONNECTOR

10.1 Preliminary Design of Medium Exploratory Connector

The sizing and synthesis approach based on Raymer suffers from several deficiencies. The first difficulty stems from the historical nature of the approach. The empty weight fraction is based on historical data and the solution is sensitive to this choice. A small body of experience exists that is associated with SESs, the majority of which are under 200 ltons. To develop larger designs, this approach must extrapolate to the next order of magnitude in size and weight. Extrapolation is generally a poor design approach. The physics for the vessel in Koullias are included as a resistance polar. However, this physics-based approach relies on historical data for the various coefficients and dimensional quantities, such as drag coefficients, efficiencies, fuel consumption, and cushion densities. In addition, only the major aerodynamic/hydrodynamic resistance components with known, simple analytical expressions at superhump Froude numbers are included. The development of new vessels where no experience exists (revolutionary designs) requires a detailed, physics-based approach that will in general be iterative. A historical aspect is necessary in the design tool for the following reasons: to provide a starting point for the designs; to provide a substitute for information that is not yet available at the conceptual design phase; to provide a nominal setting for some variable that is not required and thus assumed to always function correctly; and to converge the initial guesses on the weights. Figure 10.1 depicts the iterative process used in generate

designs. The design process is initiated with the requirements of speed, payload, range, and sea state, some dimensional parameters to define the general shape of the ship, and a guess on the lightship and full load displacements. The geometry module computes the ship particulars, based on a physical arguments and some historical rules of thumb," and communicates them to the mission module. The mission module calls the resistance module to determine the fuel required for the current design. The mission module then communicates back to the geometry module the computed weights, and if they do not agree to the initial weight guesses within some tolerance, the process repeats until there is convergence. [34]

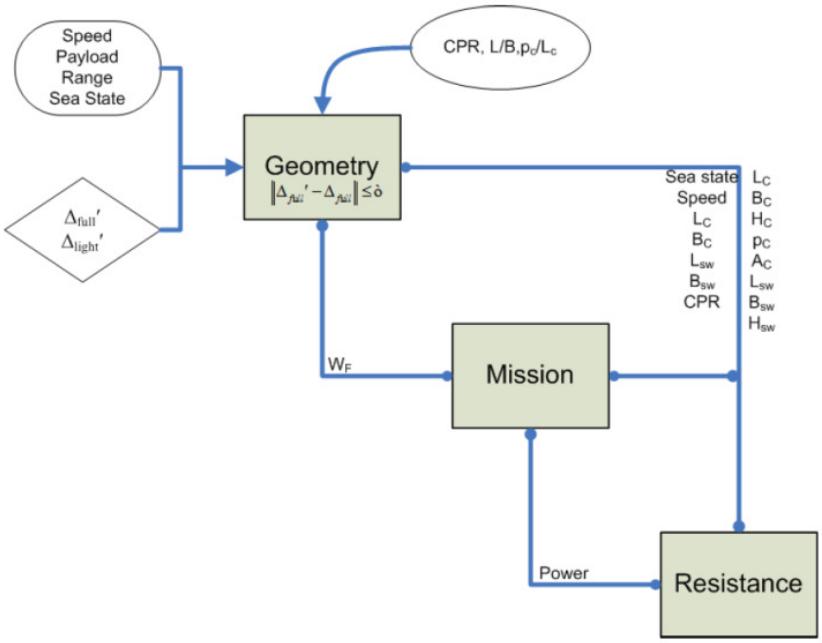

Figure 10.1 Iterative Process of General Designs [59]

A typical ship design spiral is shown in Figure 10.2. Sizing and synthesis is directly dependent on resistance and powering, as well as weights and geometry, thus these two phases of the spiral are of primary importance. Hull definition and hydrostatics

provide an additional level of fidelity to the tool, i.e., resistance calculations can be improved by incorporating a hull model in the tool. In addition, a graphical display of the hulls provides a form of visual debugging for the design iterations. Although the exact hull definition is not known, it can be deduced from previous designs. Hydrostatics is calculated from the hull definition. Arrangements and structures are not important at this point; only the physical size and performance of the ship is important. These two phases are generally tackled in the detailed design phase of the spiral. Initial stability is incorporated as a simple check to see if generated designs are stable based on a historical rule of thumb. Stability requires knowledge of the location of all components in the ship and their weights and is best left for the detailed design phase. An improved stability model will be incorporated in the future, but this requires some effort in the Arrangements department. [67][106]

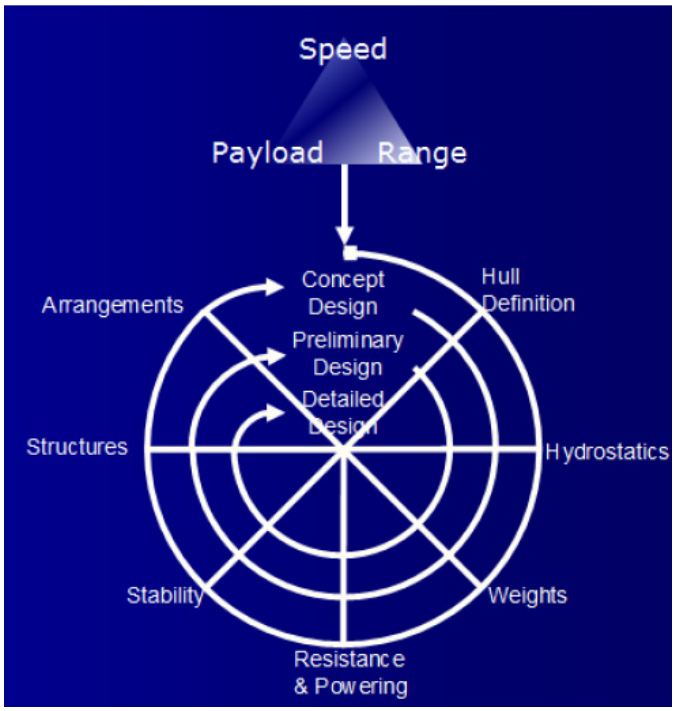

Figure 10.2 Typical Ship Design Spiral [59]

10.2 Surrogate Model of Medium Exploratory Connector

In Chapter 3, preliminary design procedure is discussed. However, repetitive sizing and synthesis process requires a certain amount of time. Because DESTINA is a design supporting tool, it is more important to support decision makers in real time rather than provide a high fidelity model which takes substantial time to complete. To achieve this, DESTINA includes a response surface model (RSM) obtained by neural network using the results of design of experiments from an analyzer developed by Koullias. [59] Figure 10.3 illustrates this procedure for sizing and synthesis in DESTINA.

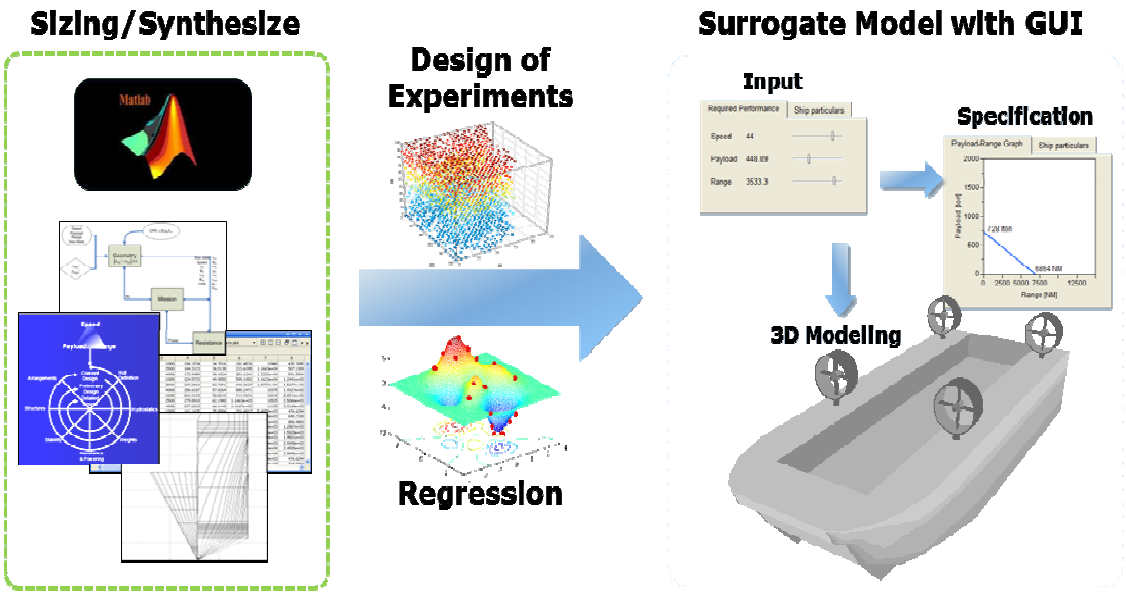

Figure 10.3 Procedure for Sizing and Synthesis in DESTINA

Parametric design of MEC on the different kinds of input variable is observed in the part of sizing tool. This tool has a visualized 3D modeling of open or closed deck MEC. The input variables that influenced a shape of MEC were collected from historical ship data, and applied to make surrogate model of air cushion length (L_c) and beam (B_c)

of MEC which was used to draw 3D modeling of MEC. Also, estimated cost of single MEC was calculated by coast analysis.

To visualize the sensitivities of the cushion length (L_c) and beam (B_c) to the input variables used in this study, the JMP prediction profiler was used, seen in Figure 10.4. The plots show the sensitivity of the result to variations in the input. Inquiring into the trends, cushion length (L_c) and beam (B_c) are sensitive to the speed, the payload, and the range of MEC. These inputs was called required performance input in this study, and was input parameter of MEC 3D modeling, seen in Figure 10.4.

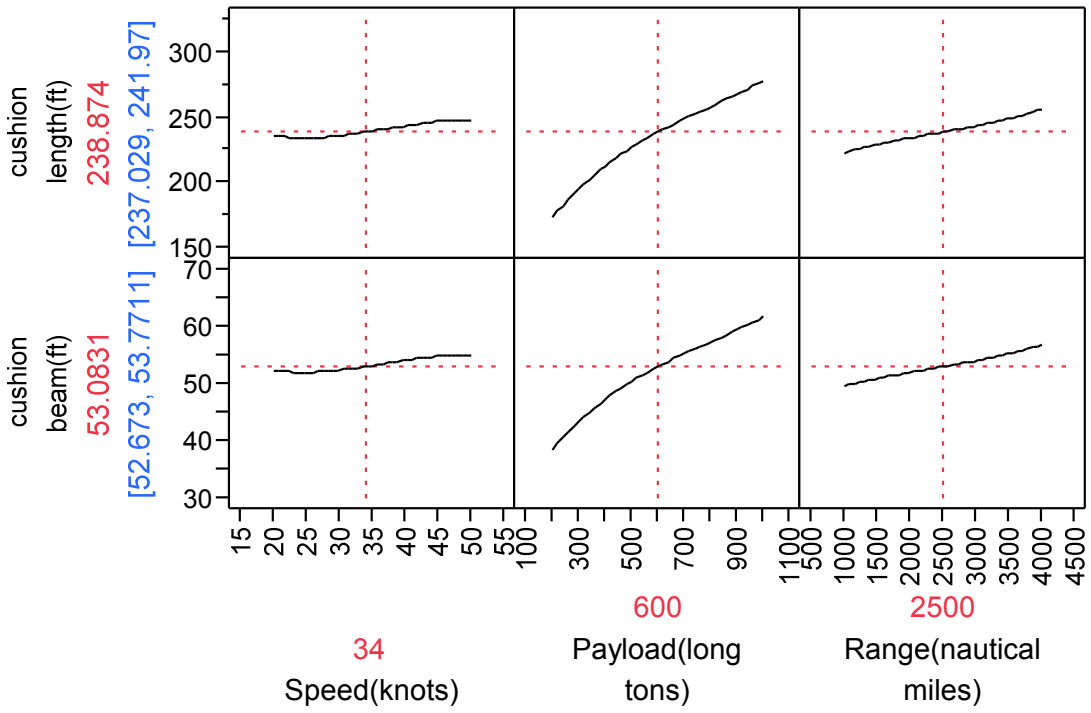

Figure 10.4 Prediction Profiler

The surrogate models were assumed 3rd polynomial and used standard least square fitting. Goodness of surrogate models was checked by using three statistical ways, such as the R^2 and the adjusted R^2 values, the Actual by predicted plot, and the residual

by predicted plots. The R^2 and the adjusted R^2 values, the actual by predicted plots and residual by predicted plots are used to check the goodness of surrogate models of cushion length (L_c) and beam (B_c). The R^2 value is a measure of how much variability is accounted for by a model. The adjusted R^2 value measures the variation accounted for by the explanatory variables. As a rule of thumb, both statistics have to be greater than 0.8. The R^2 and the adjusted R^2 values are greater than 0.997 and 0.995, respectively. A high value of the R^2 and the adjusted R^2 indicate that the constructed model is in the ball park.

The Actual by predicted plot shows the actual values of the response plotted against the predicted equation for the response based on the assumed functional form. The data has an even distribution along the perfect fit line which is a red solid line, and 95% confidence curves which are red dashed lines are closed to the perfect fit line, seen in Figure 10.5. This indicates that the regressed equations are sufficiently modeling the behavior of the supplied data and the errors for that data point are small.

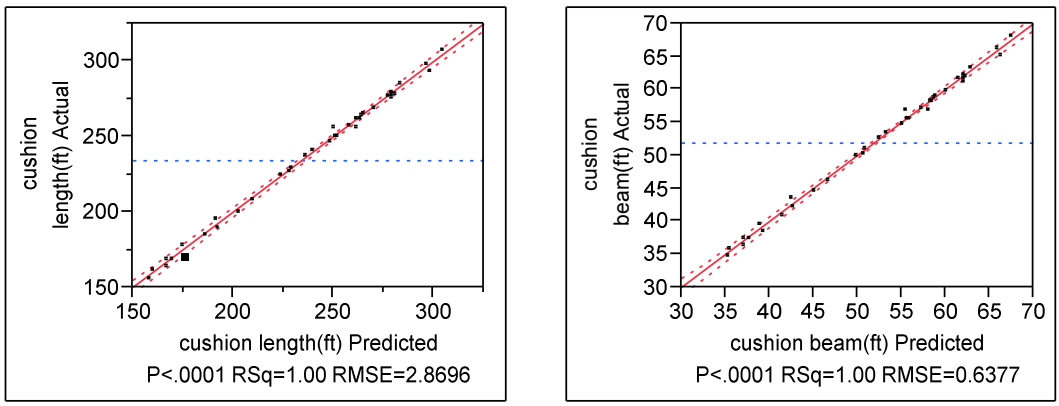

Figure 10.5 Actual by Predicted Plot

The residual by predicted plots result in a random scattering of the data points about zero with no distinguishable pattern and a small magnitude relative to the predicted value, seen in Figure 10.6. The meaning of this pattern is that the assumed 3nd order model may be valid.

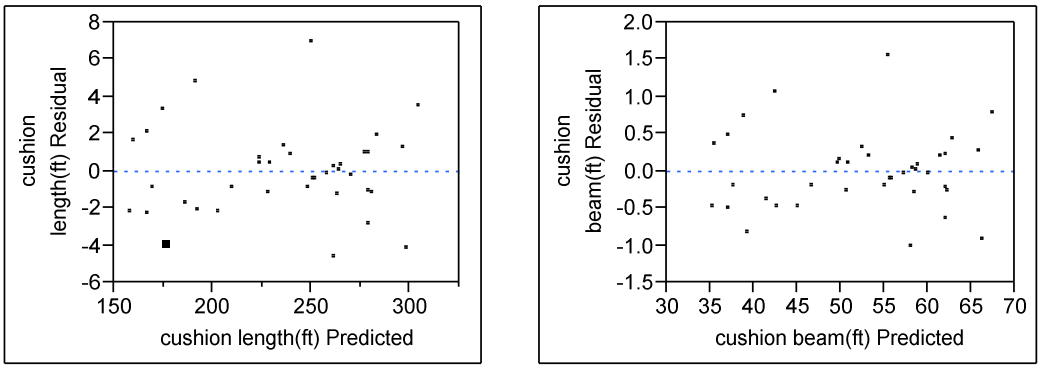

Figure 10.6 Residual by Predicted Plot

The surrogate models of max payload, max range, and gross weight were made using same inputs. Also, validity of surrogate models was confirmed in the same way. The actual by predicted plots of these three are seen in Figure 10.7.

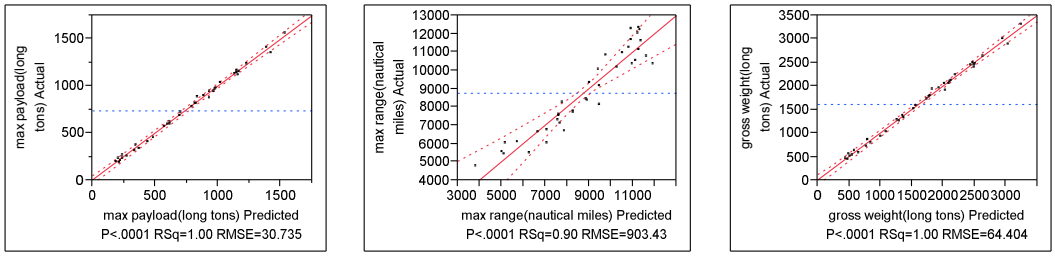

Figure 10.7 Actual by Predicted Plot of Max. Payload, Max. Range, and Gross weight

These surrogate models are recalculated when the input in DESTINA is changed. Outputs of surrogate models are a graph of payload to range and ship particulars. And these outputs are automatically updated by reestimating the surrogate models. The samples of surrogate models by neural net is as follows.

maximum range = 6040.91

-8.2491.54*Squish(0.13-0.00*VACV-0.13*VSES+0.01*BSH+0.02*HC+0.00*LC+0.01*BC+0.21*CPR)
-155906.60*Squish(4.51-0.00*VACV-0.06*VSES-0.57*BSH-0.21*HC+0.01*LC+0.03*BC-0.21*CPR)
-203804.21*Squish(-6.33-0.00*VACV-0.23*VSES-0.00*BSH+0.01*HC+0.02*LC+0.01*BC-0.38*CPR)
+171231.99*Squish(-5.21-0.00*VACV+0.65*VSES-0.02*BSH-0.02*HC-0.03*LC-0.00*BC-0.81*CPR)
+121883.11*Squish(-3.58+0.00*VACV+0.04*VSES-0.20*BSH+0.08*HC-0.01*LC+0.19*BC+3.53*CPR)
-8004.09*Squish(-6.82+0.00*VACV-0.06*VSES+0.25*BSH-0.01*HC-0.01*LC-0.04*BC+7.80*CPR)
+152117.75*Squish(5.32+0.00*VACV-0.68*VSES+0.03*BSH+0.02*HC+0.03*LC+0.00*BC+1.07*CPR)
+148863.37*Squish(4.94-0.00*VACV-0.06*VSES-0.55*BSH-0.23*HC+0.01*LC+0.02*BC-0.22*CPR)
-323377.29*Squish(1.49+0.00*VACV+0.13*VSES-0.01*BSH-0.01*HC-0.00*LC-0.00*BC-0.34*CPR)
-4739.23*Squish(-0.23+0.00*VACV+0.08*VSES-0.12*BSH-0.05*HC-0.00*LC+0.01*BC-3.20*CPR)

Eq. (10.1)

prime mover power for Catamaran =4049323

-2154729*Squish((-4.07)-0.00*VACV+0.38*VSES-0.02*BSH-0.03*HC-0.02*LC-0.01*BC-0.08*CPR)
-5236072.75*Squish(3.75-0.00*VACV-0.34*VSES-0.00*BSH+0.00*HC+0.02*LC+0.01*BC+0.08*CPR)
+5556359.55*Squish((-4.97)-0.00*VACV+0.01*VSES+0.08*BSH+0.05*HC-0.00*LC-0.00*BC-0.43*CPR)
-838577.59*Squish(2.92+0.00*VACV-0.01*VSES-0.07*BSH-0.05*HC+0.01*LC-0.01*BC-0.42*CPR)
-3178226.16*Squish((-3.50)+0.00*VACV+0.31*VSES+0.02*BSH+0.02*HC-0.02*LC-0.01*BC-0.06*CPR)
+3181810.50*Squish(4.51+0.00*VACV-0.01*VSES-0.12*BSH-0.03*HC+0.00*LC+0.01*BC+1.48*CPR)
-3819440.57*Squish(0.51+0.00*VACV+0.06*VSES-0.05*BSH-0.04*HC-0.00*LC+0.01*BC-0.77*CPR)
-951107.92*Squish(0.20-0.00*VACV-0.07*VSES+0.07*BSH+0.08*HC+0.00*LC-0.01*BC+0.87*CPR)
-2544785.88*Squish((-0.56)-0.00*VACV-0.06*VSES+0.02*BSH+0.02*HC+0.01*LC-0.01*BC+0.64*CPR)
+2811175.66*Squish(2.49+0.00*VACV+0.00*VSES-0.05*BSH-0.04*HC+0.00*LC-0.00*BC-0.52*CPR)

Eq. (10.2)

lift power for SES Mode = 742180.58

+593292.11*Squish(5.30-0.00*VACV+0.00*VSES-0.05*BSH+0.03*HC-0.01*LC+0.02*BC-1.96*CPR)
-307821.13*Squish((-4.72)-0.00*VACV-0.00*VSES-0.08*BSH+0.07*HC+0.00*LC-0.02*BC+2.05*CPR)
-1029254.06*Squish(6.26+0.00*VACV-0.00*VSES-0.05*BSH-0.05*HC-0.00*LC+0.03*BC-3.15*CPR)
+599416.23*Squish((-0.07)+0.00*VACV-0.00*VSES-0.03*BSH-0.02*HC-0.00*LC+0.02*BC-0.08*CPR)
-385153.45*Squish(1.84+0.00*VACV-0.00*VSES-0.01*BSH-0.00*HC-0.00*LC+0.01*BC-3.32*CPR)
+587567.36*Squish(0.91-0.00*VACV+0.00*VSES+0.01*BSH+0.02*HC+0.00*LC+0.00*BC-2.37*CPR)
-414366.25*Squish(2.38+0.00*VACV+0.00*VSES-0.04*BSH-0.04*HC-0.00*LC+0.02*BC-0.61*CPR)
-159734.46*Squish(0.93-0.00*VACV+0.00*VSES-0.04*BSH-0.01*HC+0.00*LC+0.01*BC-2.92*CPR)
-506333.89*Squish((-0.81)+0.00*VACV+0.00*VSES+0.01*BSH+0.01*HC+0.00*LC+0.01*BC+0.84*CPR)

Eq. (10.3)

Power to drive thrust fans in SES Mode on flat land = -285893

+39191.12*Squish(5.24-0.36*VACV+0.00*VSES+0.06*BSH+0.01*HC+0.00*LC-0.01*BC+0.57*CPR)
-1188893.75*Squish(10.64-0.16*VACV+0.00*VSES-0.09*BSH-0.10*HC+0.01*LC-0.05*BC-0.40*CPR)
-1740377.89*Squish((-6.39)+0.78*VACV+0.00*VSES-0.02*BSH-0.03*HC-0.03*LC-0.01*BC-0.61*CPR)
+3111644*Squish((-18.37)+0.14*VACV-0.00*VSES+0.08*BSH+0.08*HC-0.03*LC+0.20*BC+0.32*CPR)
+88049.72*Squish((-5.93)+0.14*VACV-0.00*VSES+0.05*BSH+0.04*HC+0.00*LC+0.01*BC-0.22*CPR)
+2554793*Squish(12.74-0.14*VACV+0.00*VSES-0.08*BSH-0.09*HC+0.02*LC-0.10*BC-0.31*CPR)
-1120391.94*Squish(5.88-0.74*VACV-0.00*VSES+0.03*BSH+0.05*HC+0.03*LC+0.01*BC+0.69*CPR)
+640759.24*Squish((-7.25)+0.85*VACV+0.00*VSES+0.01*BSH-0.01*HC-0.04*LC-0.02*BC-0.45*CPR)
-1653552*Squish((-26.02)+0.14*VACV-0.00*VSES+0.07*BSH+0.08*HC-0.05*LC+0.33*BC+0.35*CPR)

Eq. (10.4)

Fuel Weight = 4481.30

+16831.52*Squish((-10.05)+0.00*VACV-0.24*VSES+0.16*BSH+0.10*HC-0.05*LC+0.09*BC+9.77*CPR)
+3913.71*Squish((-8.07)+0.00*VACV-0.11*VSES+0.13*BSH+0.10*HC-0.03*LC+0.04*BC+8.27*CPR)
+21258.74*Squish(9.17-0.00*VACV+0.12*VSES-0.13*BSH-0.08*HC+0.03*LC-0.05*BC-8.20*CPR)
-14790.75*Squish(8.34-0.00*VACV-0.00*VSES-1.24*BSH-0.37*HC+0.01*LC+0.11*BC-1.58*CPR)
-14752.62*Squish((-8.40)+0.00*VACV+0.00*VSES+1.24*BSH+0.38*HC-0.01*LC-0.11*BC+1.53*CPR)
-18604.38*Squish((-4.78)+0.00*VACV+0.00*VSES+0.10*BSH-0.01*HC+0.00*LC-0.00*BC-0.03*CPR)
-28837.80*Squish(4.73-0.00*VACV-0.00*VSES-0.08*BSH-0.03*HC-0.00*LC+0.00*BC-0.01*CPR)
+17725.80*Squish(5.69-0.00*VACV+0.00*VSES-0.09*BSH-0.06*HC+0.00*LC+0.01*BC-0.39*CPR)

Eq. (10.5)

Metacentric Height =

2736.61+0.27*Squish(7.86-0.14*VACV-0.07*VSES+0.07*BSH+0.00*HC+0.00*LC-0.02*BC-3.68*CPR)
+409.45*Squish((-7.11)+0.00*VACV+0.00*VSES+0.05*BSH+0.02*HC+0.00*LC-0.01*BC+5.19*CPR)
+1943.83*Squish(8.70-0.00*VACV-0.00*VSES-0.08*BSH-0.08*HC-0.00*LC+0.02*BC-3.58*CPR)
+133.89*Squish(2.61+0.00*VACV+0.00*VSES-0.06*BSH+0.02*HC-0.00*LC-0.01*BC-2.30*CPR)
-5433.17*Squish(4.21-0.00*VACV-0.00*VSES-0.06*BSH+0.01*HC-0.00*LC-0.02*BC+2.11*CPR)
+645.30*Squish(38.49-0.00*VACV+0.00*VSES-0.08*BSH-0.01*HC-0.00*LC-0.02*BC-35.67*CPR)
-603.47*Squish((-3.43)+0.00*VACV+0.00*VSES+0.11*BSH-0.05*HC-0.00*LC+0.04*BC-3.79*CPR)
-403.16*Squish((-0.82)-0.00*VACV+0.00*VSES+0.02*BSH+0.01*HC+0.00*LC+0.02*BC-3.84*CPR)
-515.76*Squish((-2.60)-0.00*VACV+0.00*VSES+0.01*BSH-0.04*HC+0.01*LC+0.03*BC-5.45*CPR)

Eq. (10.6)

Lightship Displacement = -15384.50

+78253.49*Squish((-1.37)+0.00*VACV+0.23*VSES-0.02*BSH-0.02*HC-0.02*LC+0.01*BC-0.58*CPR)
-64315.27*Squish((-1.15)+0.00*VACV+0.00*VSES+0.04*BSH+0.04*HC+0.00*LC-0.01*BC+1.11*CPR)
+36226.12*Squish(0.64+0.00*VACV-0.22*VSES+0.05*BSH+0.04*HC+0.01*LC-0.01*BC+1.29*CPR)
+13760.89*Squish((-2.12)+0.00*VACV+0.00*VSES+0.08*BSH+0.06*HC+0.00*LC-0.02*BC+1.87*CPR)
+12776.60*Squish((-1.83)+0.00*VACV+0.00*VSES+0.09*BSH+0.10*HC+0.00*LC-0.02*BC+2.68*CPR)
-82109.56*Squish(3.33+0.00*VACV+0.00*VSES-0.03*BSH-0.03*HC+0.00*LC+0.00*BC-0.65*CPR)
+175438.95*Squish(4.73+0.00*VACV+0.23*VSES-0.09*BSH-0.07*HC+0.03*LC-0.06*BC-4.01*CPR)
-42044.63*Squish((-2.01)+0.00*VACV+0.24*VSES+0.00*BSH+0.00*HC-0.02*LC+0.01*BC+0.02*CPR)
-40549.32*Squish(13.50+0.00*VACV+0.11*VSES-0.20*BSH-0.15*HC+0.03*LC-0.01*BC-10.34*CPR)
-62609.94*Squish(3.36+0.00*VACV+0.28*VSES-0.10*BSH-0.07*HC+0.02*LC-0.06*BC-4.14*CPR)

Eq. (10.7)

Range = 36040.91

-82491.54*Squish(0.13-0.00*VACV-0.13*VSES+0.01*BSH+0.02*HC+0.00*LC+0.01*BC+0.21*CPR)
-155906.60*Squish(4.51-0.00*VACV-0.06*VSES-0.57*BSH-0.21*HC+0.01*LC+0.03*BC-0.21*CPR)
-203804.21*Squish((-6.33)-0.00*VACV-0.23*VSES-0.00*BSH+0.01*HC+0.02*LC+0.01*BC-0.38*CPR)
+171231.99*Squish((-5.21)-0.00*VACV+0.65*VSES-0.02*BSH-0.02*HC-0.03*LC-0.00*BC-0.81*CPR)
+121883.11*Squish((-3.58)+0.00*VACV+0.04*VSES-0.20*BSH+0.08*HC-0.01*LC+0.19*BC+3.53*CPR)
-8004.09*Squish((-6.82)+0.00*VACV-0.06*VSES+0.25*BSH-0.01*HC-0.01*LC-0.04*BC+7.80*CPR)
+152117.75*Squish(5.32+0.00*VACV-0.68*VSES+0.03*BSH+0.02*HC+0.03*LC+0.00*BC+1.07*CPR)
+148863.37*Squish(4.94-0.00*VACV-0.06*VSES-0.55*BSH-0.23*HC+0.01*LC+0.02*BC-0.22*CPR)
-323377.29*Squish(1.49+0.00*VACV+0.13*VSES-0.01*BSH-0.01*HC-0.00*LC-0.00*BC-0.34*CPR)
-4739.23*Squish((-0.23)+0.00*VACV+0.08*VSES-0.12*BSH-0.05*HC-0.00*LC+0.01*BC-3.20*CPR)

Eq. (10.8)

Where, VACV: ACV speed,

VSES: SES speed,

BSH: Sidehull beam,

HC: Cushion height,

LC: Cushion length,

BC: Cushion beam,

CPR: Cushion pressure ration

$$\text{Squish}(x) = \frac{1}{1 + e^{-x}}$$

Another output of required performance input was surrogate model of cost. Cost of MEC was influenced by shape of MEC. For cost analysis, thecost model of exponential with 2 way interactions was used. It was researched by Chi Yon Ting in Navy Post-graduate School (NPS). [102] Input variables of cost model are displacement(D), length, and crew of MEC, seen in the following equation. These input values were also changed when the shape of MEC was changed. The result of cost analysis in the sizing tool is displayed in DESTINA as well.

$$\text{Cost} = 11.38\, e^{0.00082\,D + 0.0069\,L - 0.002\,C} \times e^{-1.2\times10^{-5}\,D\,L} \qquad \text{Eq. (10.9)}$$

Where, D: displacement,

L: length,

C: crew

Three dimensional modeling of MEC was composed of an air cushion, a side hull, a deck, and fans. Air cushion length and beam were result of surrogate models. The side hull, deck and fan size was the proportion to the air cushion size. Cushion height was half of cushion beam. Hull height was 1.8 times of cushion height. Hull beam was equal to cushion beam. Hull length is 1.1 times of cushion length. Fan diameter is half of cushion beam.

10.3 Preliminary Design in the Decision Supporting Tool

The final outcome of sizing tool is displayed in 3D modeling of MEC seen in Figure 10.8. This modeling gives visual result of shape when speed, range, and payload of MEC are changed. That is to say, user expects the shape of MEC on a certain mission. Default shape of 3D modeling of MEC is open deck. Closed deck shape is selected from

sizing input tab of deck shape. Also, the model has the option of open or closed deck shape with a lamp. The ship particular inputs, such as hull rate that was the proportion of hull beam to cushion beam, fan diameter, length of bow was changed by slider bar in DESTINA. Figure 10.8 shows sizing input and output and a 3D modeling based on the sizing and synthesis results in DESTINA.

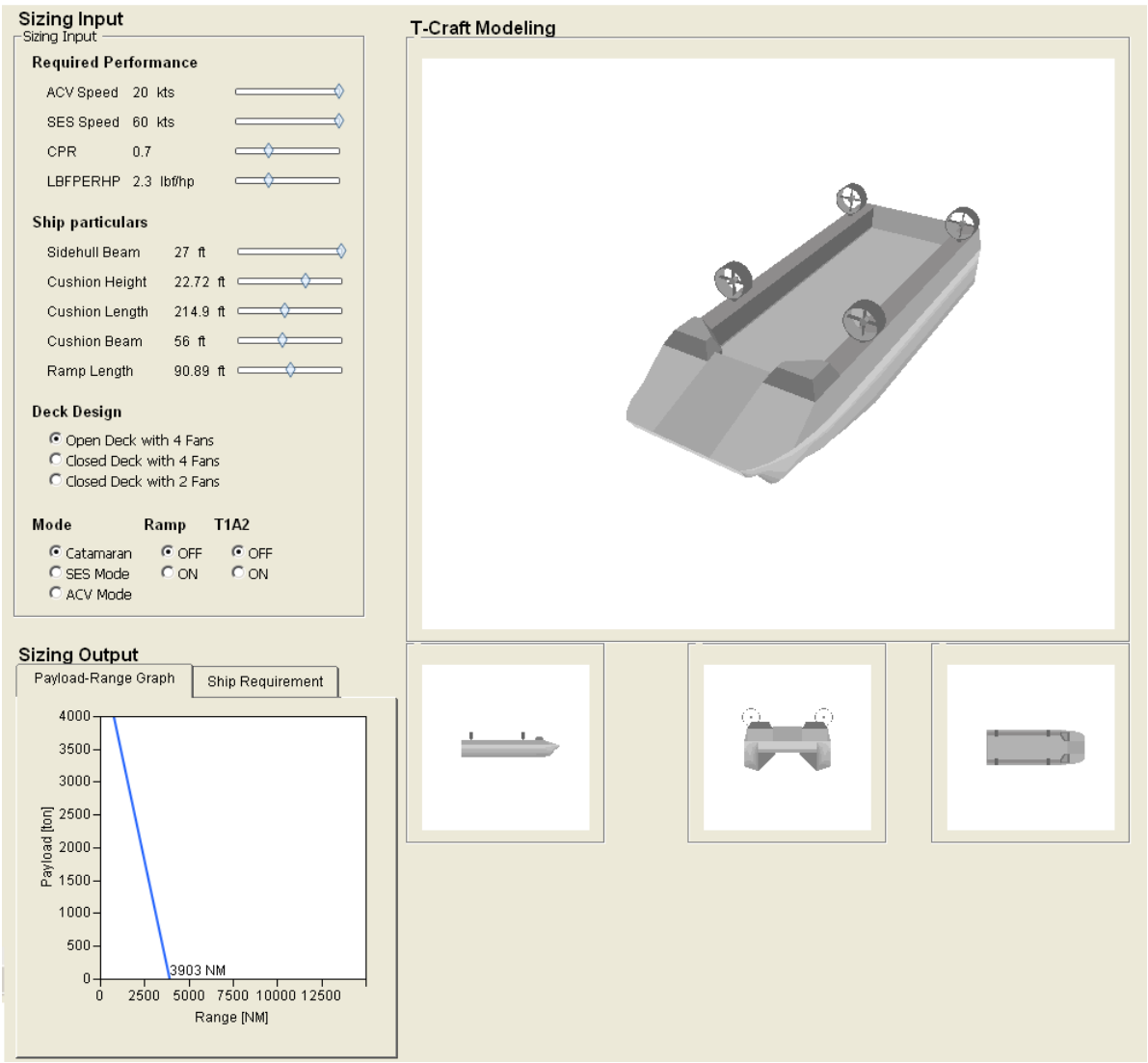

Figure 10.8 Sizing and Synthesis Module in DESTINA

CHAPTER XI

EVALUATION AND SELECTION OF CANDIDATES

11.1 Multi-Criteria Decision Making Method

The most suitable method to select the best one among candidates is Multi-Criteria Decision Making (MCDM). The International Society on Multiple Criteria Decision Making defines that Multi-Criteria Decision Making is the study of methods and procedures by which concerns about multiple conflicting criteria can be formally incorporated into the management planning process. [138]

Technique for Ordered Preference by Similarity to Ideal Solution (TOPSIS) is one of MCDM techniques that uses a ratio of Euclidean distances to rank designs. TOPSIS originated in a Ph.D. dissertation: Systems Selection by Multiple Attribute Decision Making. [114] It provides an indisputable preference order of solutions, describes customer preference in the form of weights for each criterion. As a result, the best alternative has shortest Euclidean distance to positive ideal solution and farthest away from negative-ideal solution. The steps of TOPSIS are as follows.

Step 1: form alternatives and evaluation criteria from QFD and Morphological matrix

Step 2: create decision matrix by grouping the objective and subjective evaluation criteria

Step 3: Quantify qualitative criteria

Step 4: Nondimensionalize the attribute values

Step 5: Establish relative importance of the criteria by assigning weighted values

Step 6: Determine if the attributes are a “benefit” or a “cost”

Step 7: create positive ideal solution from the maximum of the benefit and minimum of cost

Step 8: create negative ideal solution from the minimum of the benefit and maximum of cost

Step 9: calculate the separation values of each alternative from ideal solutions measured by the n-dimensional Euclidean distance

Step 10: calculate the relative closeness of each alternative to the ideal solutions

Step 11: Select the best alternative by selecting the closest to 1.00

11.2 Multi-Criteria Decision Making Method in the Decision Supporting Tool

Except the application module for the preliminary design, DESTINA includes another application module for evaluation and selection. The environment to compare candidates is provided by other modules mentioned before. This module can compare and evaluate maximum three candidates by Multi-Criteria Decision Making method. Among Multi-Criteria Decision Making methods, Technique for Ordered Preference by Similarity to Ideal Solution (TOPSIS) is launched in DESTINA. TOPSIS provides an indisputable preference order of solutions based on the Euclidean distance to positive ideal solution. Figure 6.38 shows the module for evaluation and selection in DESTINA.

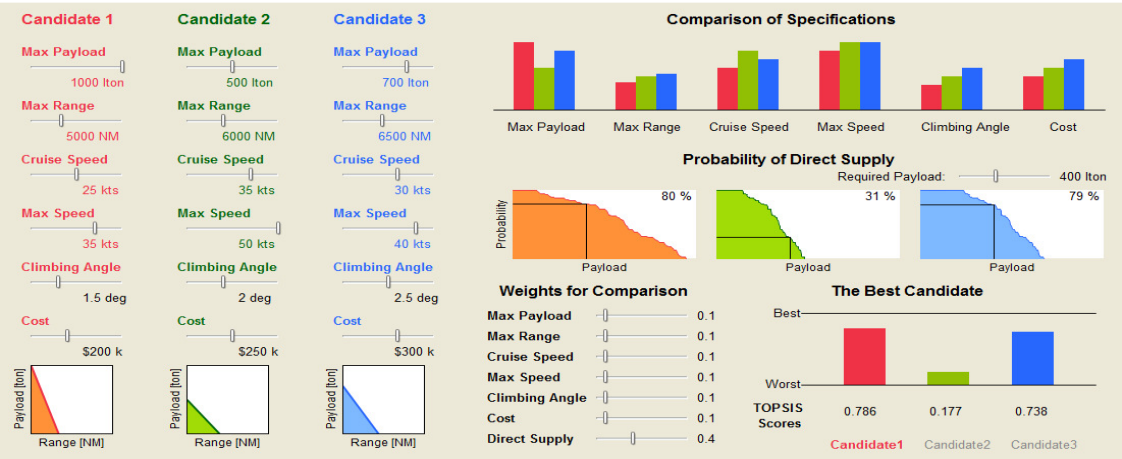

Figure 11.1 Evaluation and Selection Module in DESTINA

CHAPTER XII

SIMULATION

This chapter show the procedure from the requirement analysis to the estimation of usuability. Assumed scenario is the peace corps mission in Angola. For this scenario, 2015 MEB is selected as a mission type. 2015 MEB has 14,484 personnel, organized into a Sea Base Echelon, a Forward Base Echelon, and a Sustained Operations Ashore Echelon. Major equipment of 2015 MEB also include three squadrons of JSF, a squadron of EA-18G, and a squadron of light attack helicopters. The Sustained Operation Ashore Echelon normally operates from the continental United States. However, it is assumed to operate from the closest U.S. Navy base in this scenario. [131] [132]

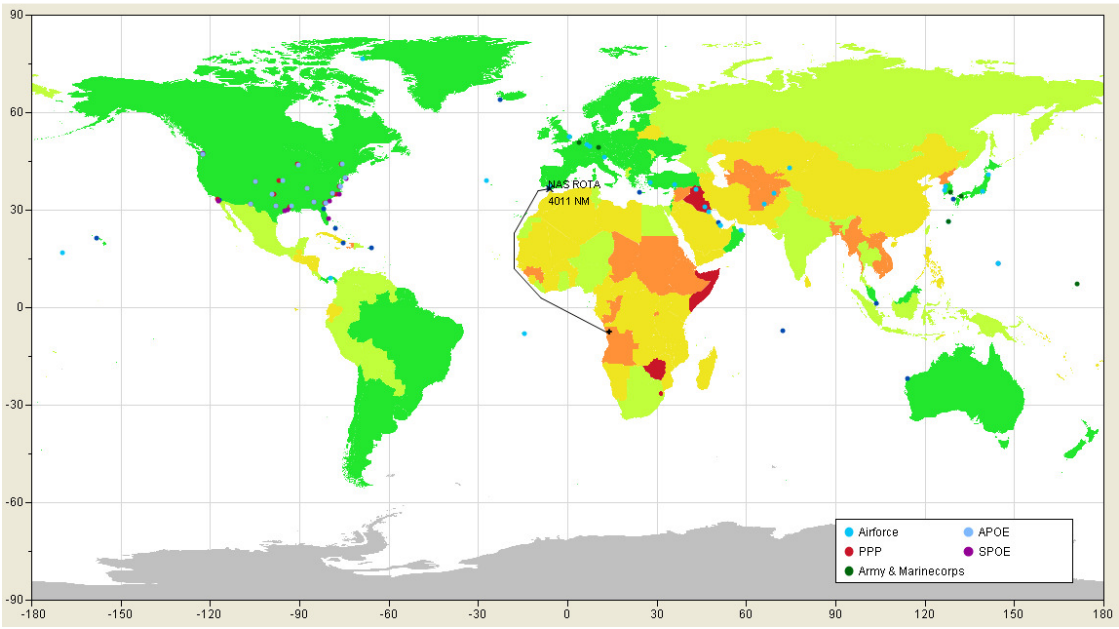

Figure 12.1 Shipping Route from NAS Rota to Angola

At first, the position of conflicts manually can be selected as the coastline of Angola here. Then, shipping route and distance are displayed in the map as shown in Figure 12.1. Also, the information of selected area in Figure 12.2 is described at the right side of the map.

Longitude (deg.)	13.84
Latitude (deg.)	-7.56
Country Name	Angola
Country Code	AO
Map Reference	Africa
Area (Mil. Sqft)	1.25
Population (Mil.)	12.8
GDP (2010 M$)	112800
Political Right	6
Civil Liberty	5
Oil Production (BBL/1000)	2015
GDP per Capita (2010 $)	9000
Economic Freedom	29
Infant Mortality (Death/1000)	180.21
Life Expectancy (Years)	38.2
Youth Bulge	1.22661
Earthquake Risk Index	0
Volcano Risk Index	0
Drought Risk Index	9
Flood Risk Index	0
Landslide Risk Index	0
Cyclone Risk Index	0

Figure 12.2 Information of Selected Mission Area

Along the shipping lane, average sea state can be estimated and Bufort scale with condence level results from the sea state analysis. This sea state analysis can determine the requirements of new vessel performance. In this case, a new vessel should be designed to operate in Bufort scale 3.9 to satisfy 90% confidence level as in Figure 12.3.

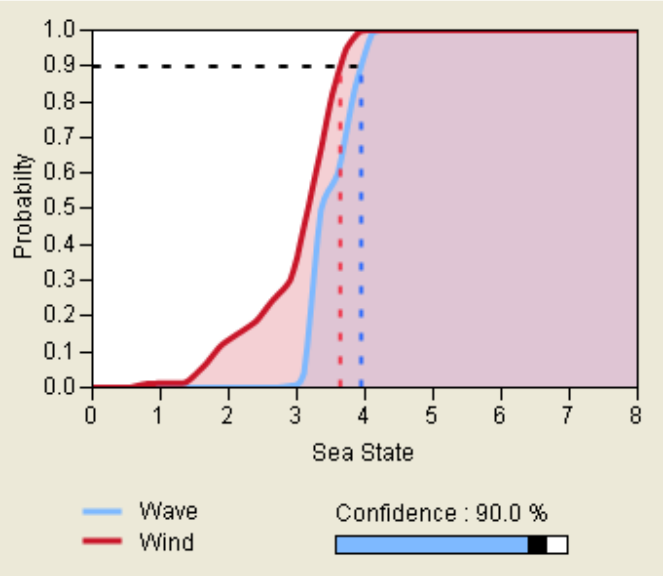

Figure 12.3 Sea State Analysis Results

The selected region shows pretty unstable condition mainly due to natural disaster, oil production and economic freedom in Figure 12.4. Among natural disasters, only a drought risk is predicted as the highest risk and this results can indicate what kind of cargo will need to operate the mission. For this mission, water supply can be one of important challenge. Therefore, cargo might include enough desalination equipments and water purifiers.

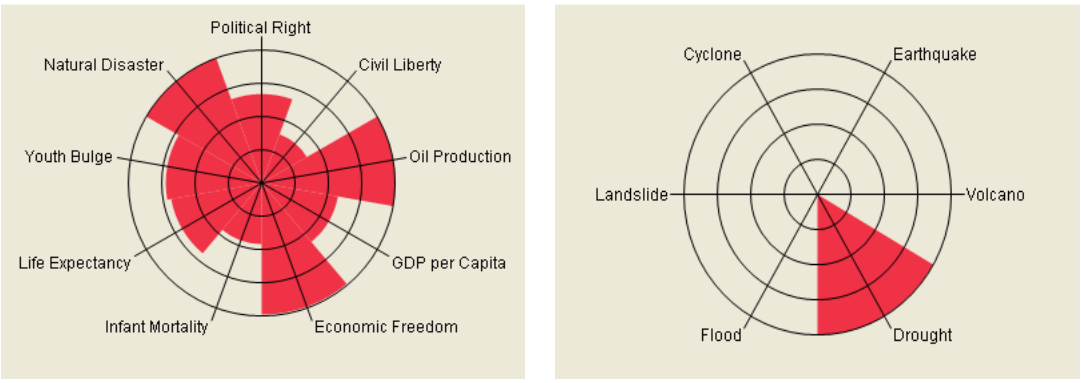

Figure 12.4 Instability Analysis Results

This decision support process can provide the information of the nearest available U.S. Navy base as in Figure 12.5. If the supply ability of the base is not enough to operate a mission, the shipping option should be changed into multiple source routing. In this scenario, NAS Rota is assumed to provide sufficient personnel and equipments.

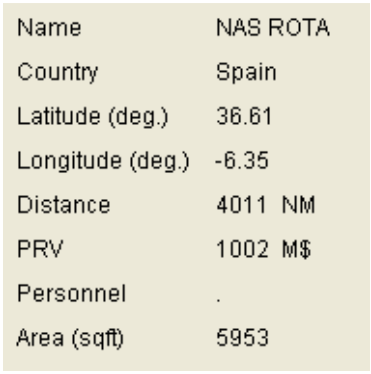

Figure 12.5 Information of the Nearest Navy Base

Next step is the preliminary design of new vessel from the limited information. Required performance from the sea state analysis and decision maker's preferences are main design variables in this stage as in Figure 12.6. Or, the specification of candidates can be input directly.

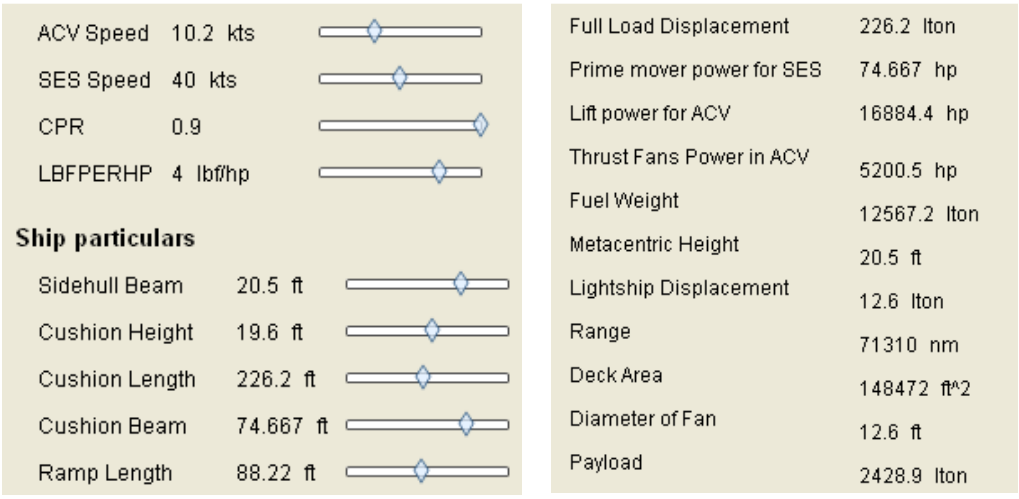

Figure 12.6 Specifications and Preliminary Design Results of MEC

Then, the operational analysis can be performed based on the data from above analyses. Figure 12.7 depicts the GUI for specification of MEC. Likewise, other vessel's specifications also can be changed by users.

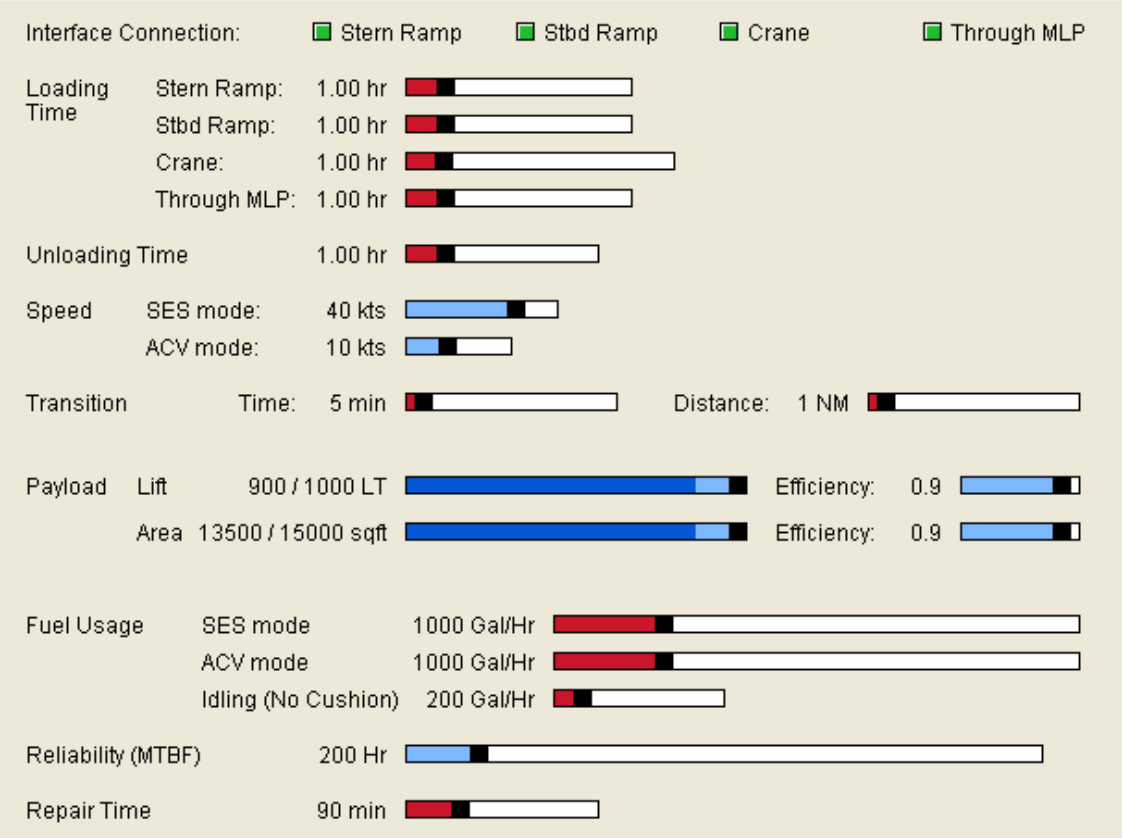

Figure 12.7 Input GUI for Specifications of MEC

One of most significant factor is the range. The Sea Base concept required two type of distances: distance from the U.S. Navy base to Sea Base, and distance from the Sea Base to beach spot. The former distance is automatically calculated by the dynamic map. The second distance should be decided by users. To support this decision, this method provide bathymetry information as well. In this scenario, the first distance is estimated as 4011 NM as shown in Figure 12.8, and the second disctance is decided as 70 NM from the shoure.

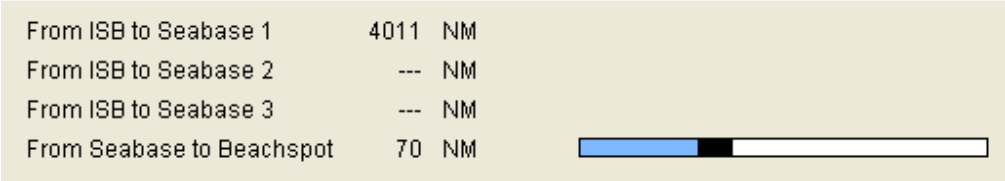

Figure 12.8 Input GUI for Distances

Due to bottleneck, the accessible beach spot has critical effect on the operating time. This can be determined based on the available coastline length estimated by coastline analysis. Input GUI is depict in the Figure 12.9.

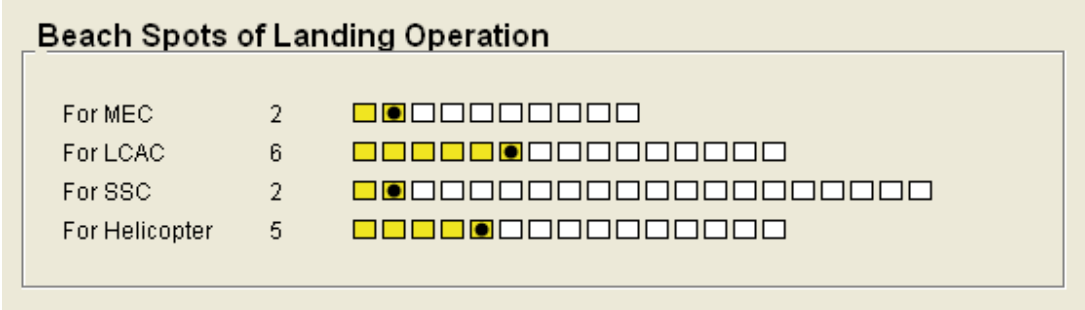

Figure 12.9 Input GUI for Landing Condition

Another important factor for operational analysis is the quantity of available equipments. The numbers of all available vessels can be changed by the GUI in Figure 12.10.

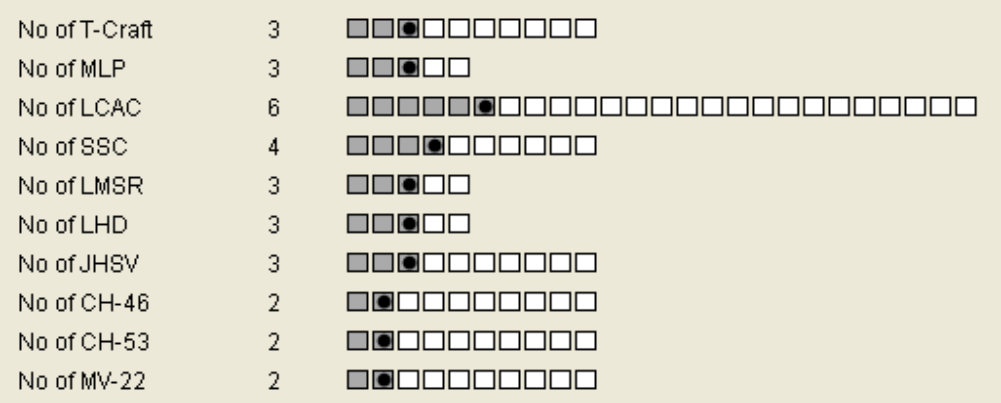

Figure 12.10 Input GUI for Available Vessels

Finally, the results of operational analysis can be acquired. Figure 12.11 and 12.12 describe the unloaded cargo by MEC and other vessels. Two MEC's can deliver more cargo than all the other vessels. Moreover, the time for the first unloaded cargo by MEC is 104 hours while the other vessels take 203 hours. MEC can start the operation 49% faster and it means that MEC can be a game changer by reducing response time and increasing the magnitude of first strike.

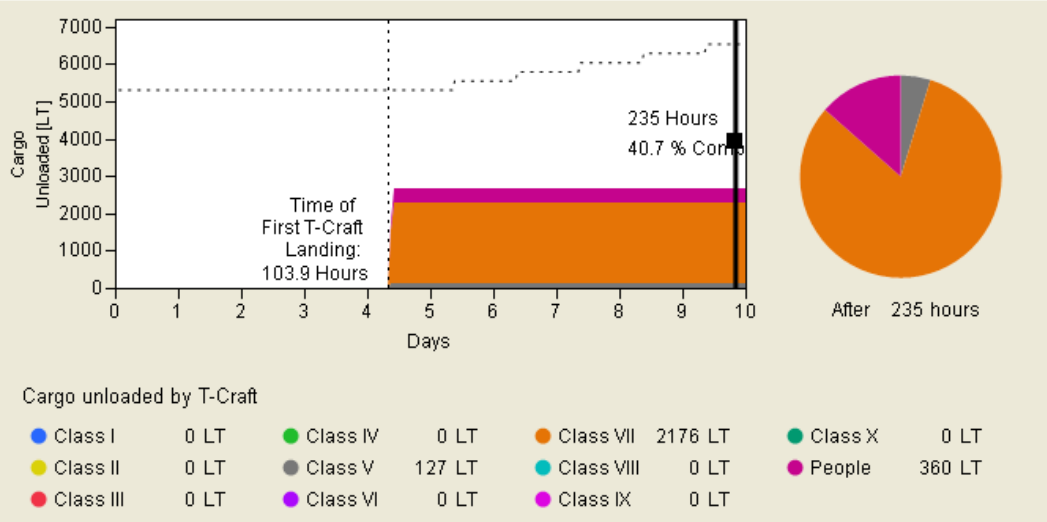

Figure 12.11 Operational research result: Cargo Unloaded by MEC

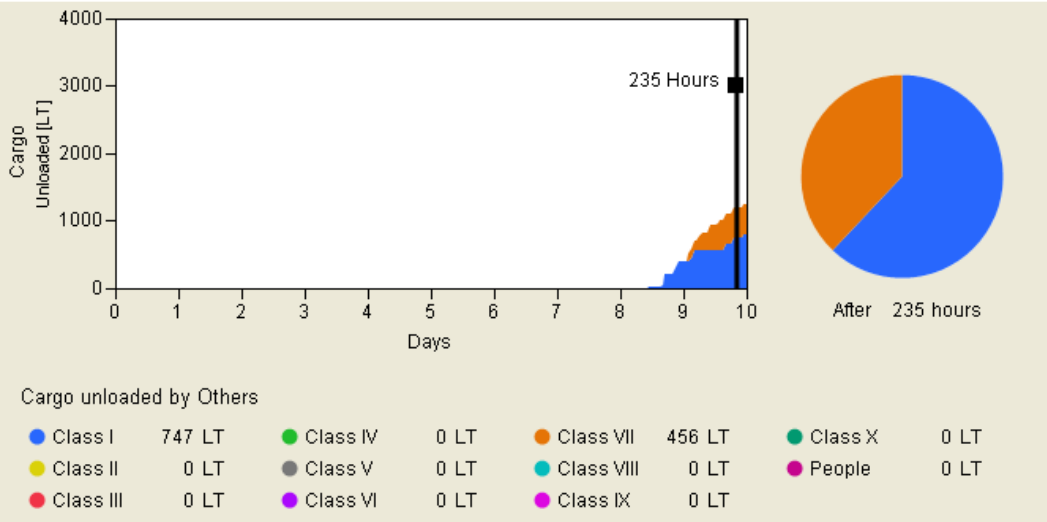

Figure 12.12 Operational research result: Cargo Unloaded by Other Vessels

Figure 12.13 shows the supplied combat power index. Likewise, MEC provides 92.4% of combat power in 44.1% of total required time. In addition, the instant supply of combat power has strategically significant meaning, compating to the steady supply of combat power by the other vessels.

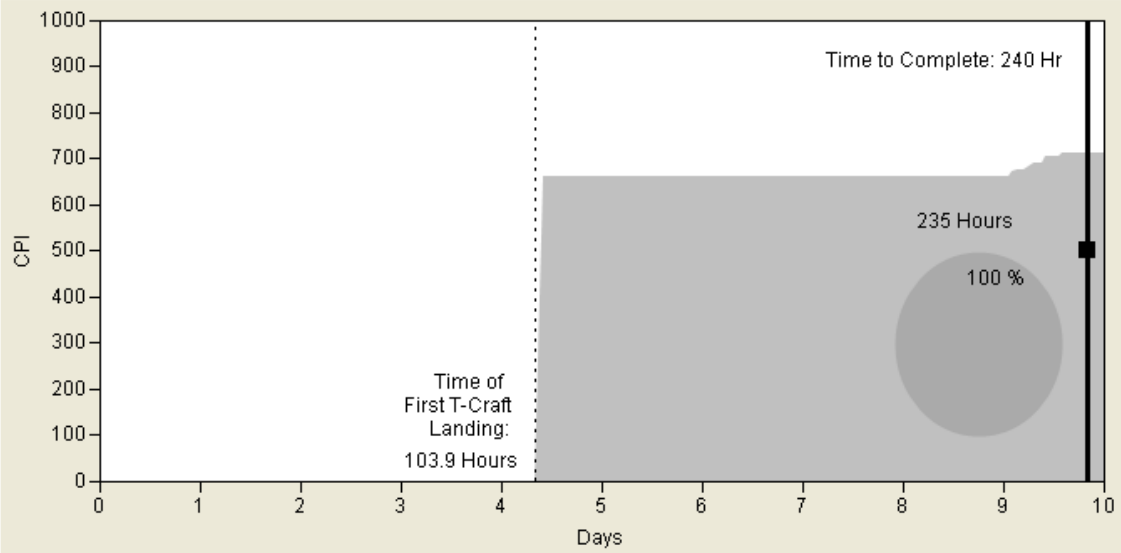

Figure 12.13 Operational research result: CPI

So far, the effectiveness of MEC is proved quantitatively. MEC can reduce the time to deliver the first cargo as 49% and take 66.7% of total cargo in this scenario. In addition, MEC can provide the strategic advantage by unloading all personnel and equipment with the ratio of 1096 ton per hour while the other vessels deliver the cargo 30.9 ton per hour. This highly upgraded ability of transportation is able to make MEC a game changer.

Furthermore, the usability of MEC can be estimated by the stochastic analysis. Figure 12.14 shows the average cumulative duration of the conflicts of the countries that have $5,000 to $10,000 GDP per capita. In the case of MEC with 40 years service life, it

might be used for 3.2 years of the mission. However, the MEC with 20 years service life might be employed for 1.4 years of the mission. This characteristics can make the cost-effective design of new vessel when the additional cost to enlongate the service life is analyzed.

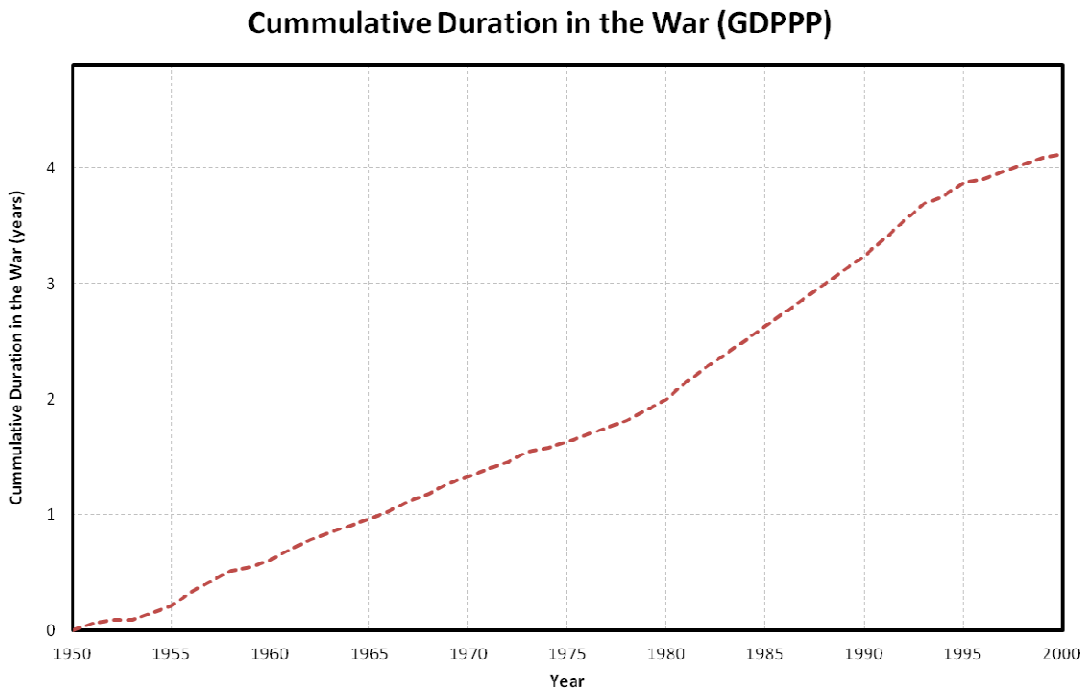

Figure 12.14 Cumulative Duration of the War (GDPPP)

CHAPTER XIII

DECISION SUPPORTING TOOL: DESTINA

13.1 Instability Analysis

In this research, JMP is used to develop an interactive decision supporting tool which allows necessary simulations required in the current research. JMP is a statistical analysis tool which supports the use of a scripting language. Therefore, this software provides benefits in terms of an efficient analysis of the enormous amount of database required in this research. Instability factor, causation with instability and weights for each factor mentioned in Chapter 5 is the inputs used in DESTINA as shown in Figure 13.1.

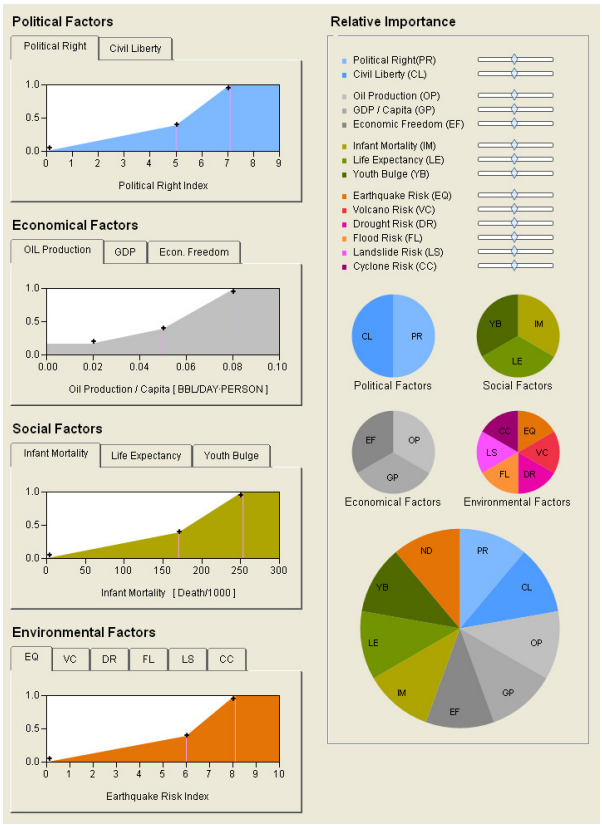

Figure 13.1 Input GUI of Instability Analysis in DESTINA

Each instability function can be adjust by dragging the marks in the graph in Figure 13.2(a) and Weight factor can be adjust by dragging the slider bars in the graph in Figure 13.2(b). The pie charts below the slider bars in Figure 13.2(c) provide the weight of each instability field at a glance.

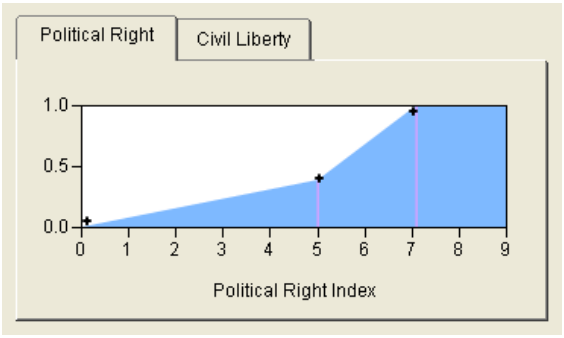

(a) Instability function

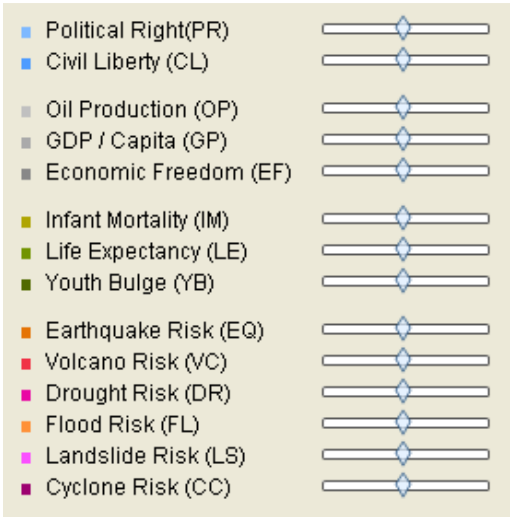

(b) Slider bars for weights

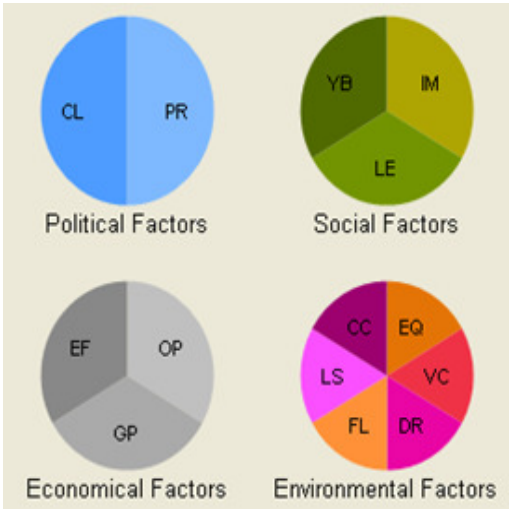

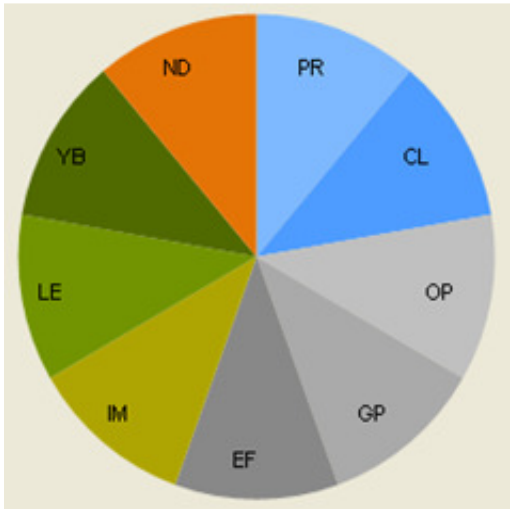

(c) Display of Each Weight

Figure 13.2 Input GUI of Instability Analysis in DESTINA

When a target region is selected, DESTINA provides instability analysis result as shown in Figure 13.3. On the left hand side, general information about the target region is displayed. The radar chart shown in the center demonstrates how instability index is calculated based on each factor considered in the analysis and on the right hand side at the bottom, information about the nearest U.S. base is provided.

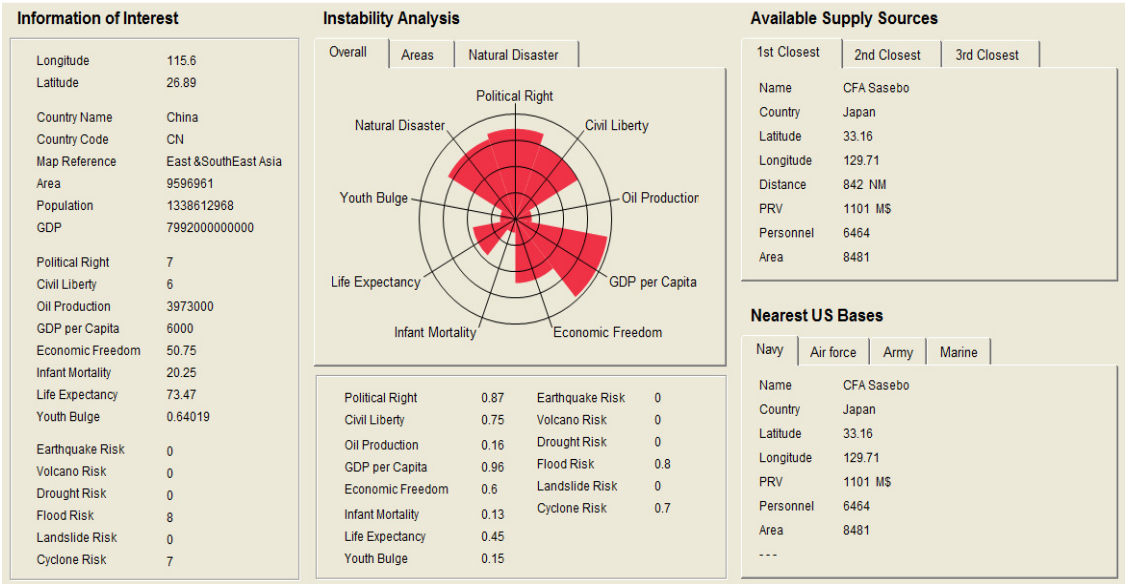

Figure 13.3 Output Display of Instability Analysis in DESTINA

Furthermore DESTINA provides a dynamic map as shown in Figure 13.4. This dynamic map can display instability indices re-calculated in real time as the given instability causation and weights are changed. The dynamic map of DESTINA consists of six layers as shown in Figure 13.5 and each of these layers can be turned on or off.

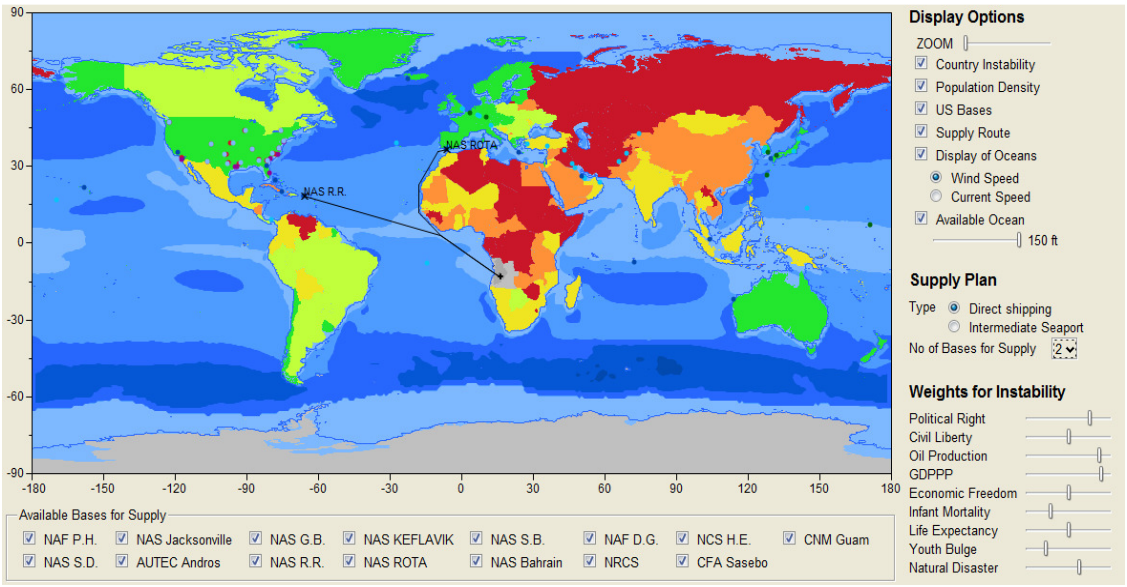

Figure 13.4 Dynamic Map of Instability Analysis in DESTINA

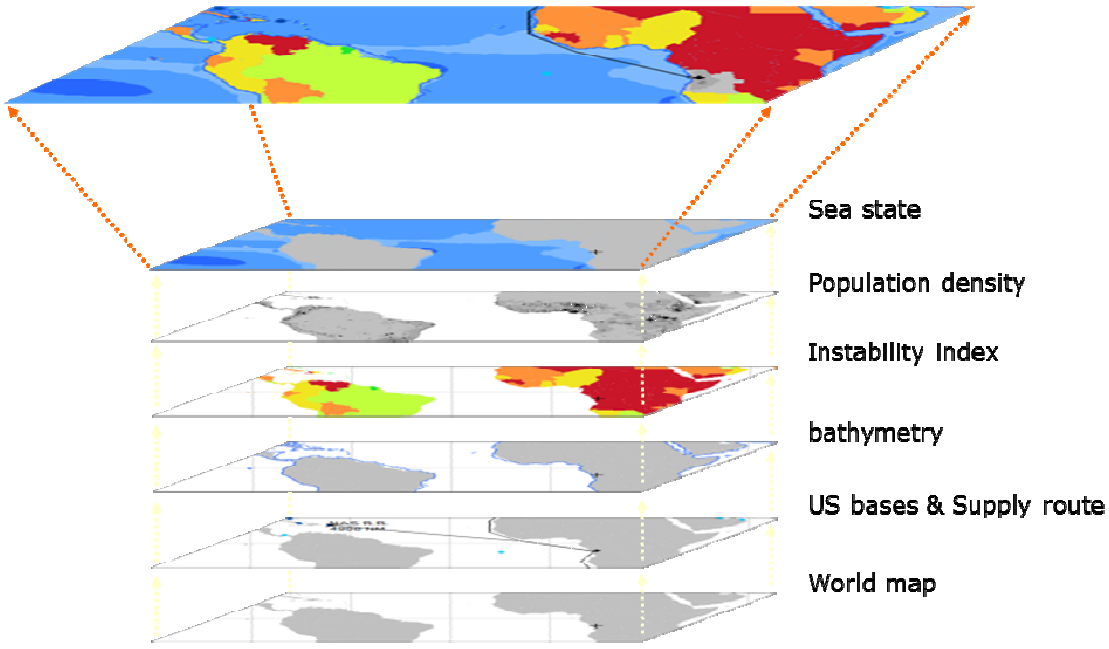

Figure 13.5 Layers of Dynamic Map in DESTINA

13.2 Shipping Lane Estimation and Sea State Analysis

DESTINA provides a dynamic interface to display the shipping lane and estimate shipping distance. When a user selects target position, the route and distance are displayed as shown in Figure 13.6.

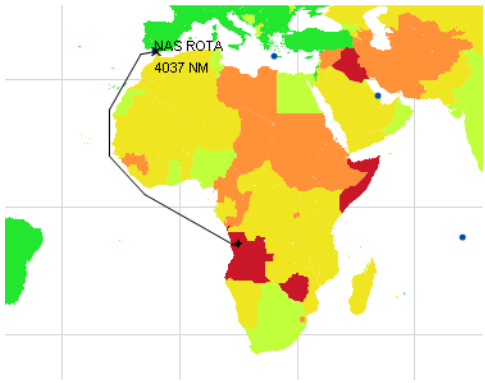

Figure 13.6 Shipping Lane and Distance Displayed in DESTINA

To consider the availability of the closest Navy Base, the user can decide at any point during the analysis which ISBs are available. Figure 13.7 depicts this using an example. In this example, the user select the target position to be within the borders of the country Angola. The route is heading for the closest ISB, Naval Station (NAVSTA) Rota in Spain. If NAVSTA Rota is set up as an unavailable base, DESTINA automatically reroute to the next closest base, in this case NAVSTA Roosevelt Roads in Puerto Rico.

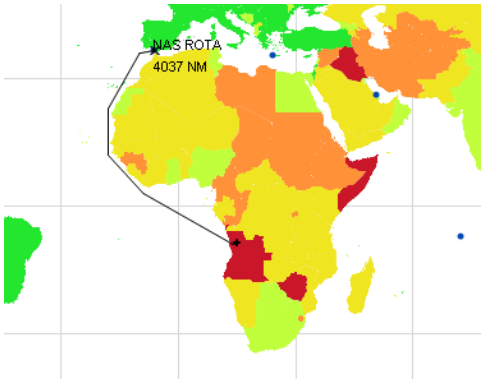

(a) Route to the Closest Navy Base

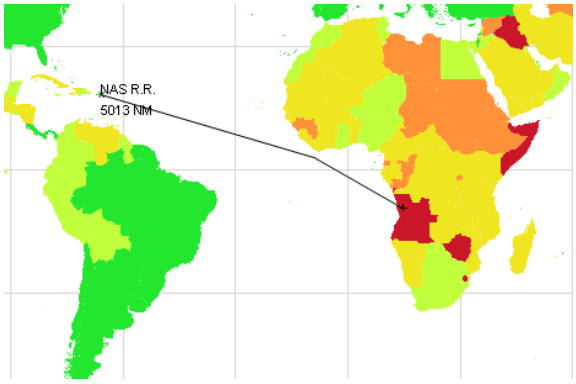

(b) Reroute when NASROTA is not available

Figure 13.7 Automatic Rerouting by Considering Available Bases

Another available options are the supply from multiple sources and intermediate seaport. This options providing more practical analysis environment to decision makers. Because each base has a ability to supply cargo and troops, several supply sources needs to selected to meet the needs of mission area. DESTINA provides the supply from multiple sources up to three Navy bases. For now, these options should be selected manually because of insufficient data about Navy bases. However, they can upgraded with the information of each base's supply ability. In the Figure 13.8, three supply routes by using intermediate seaport are described.

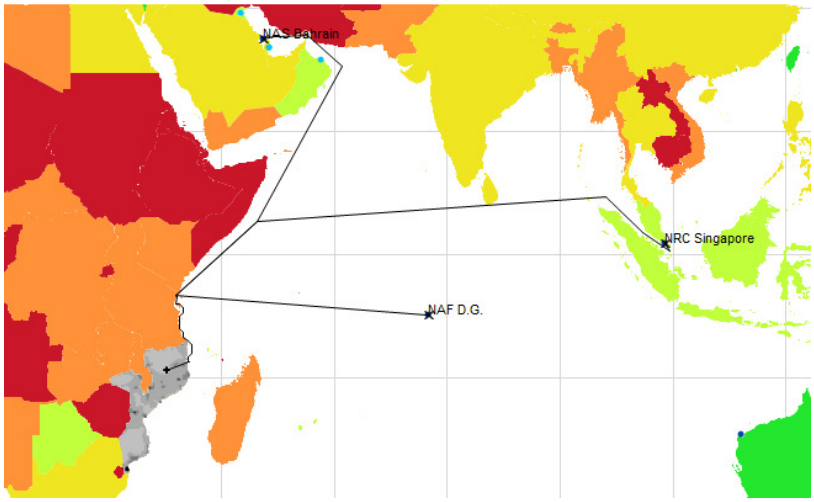

Figure 13.8 Shipping lane by using intermediate seaport from multiple sources

DESTINA provides the information of average sea state along shipping lane. The sea state data includes three categories: wind speed, current speed, and wave height. Sea state analysis is indispensible to design the ship, because the wave height is critical to decide maximum draft and all three data effect on the mission range and cruise speed. The examples of three distributions are shown in Figure 13.9. In addition, DESTINA

estimate the Beaufort scale with the confidence level based on the sea state distribution. Figure 13.10 shows the example of Beaufort scale with 90% confidence level.

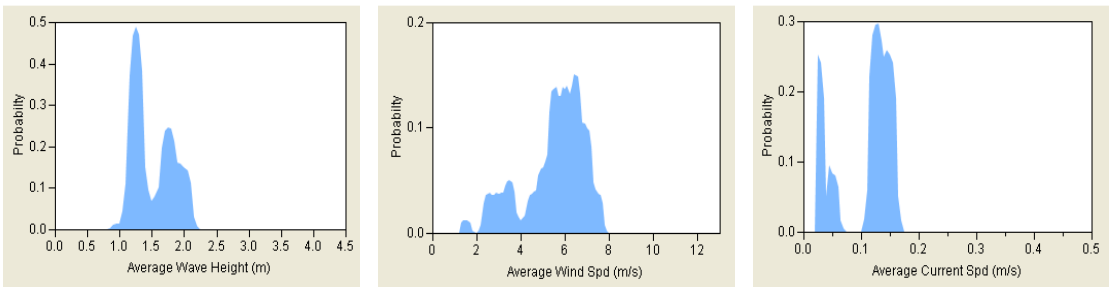

(a) Wave Height (b) Wind Speed (c) Current Speed

Figure 13.9 Three Factors of Sea State Analysis

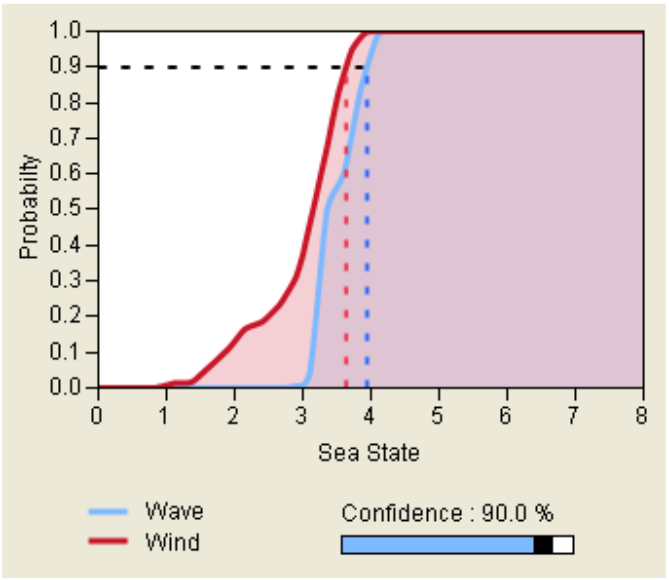

Figure 13.10 Beaufort Scale with Confidence Level

13.3 Disembarkation Analysis

DESTINA provides the coastline analysis as mentioned in Chapter 7. Figure 13.11 shows the results from disembarkation analysis from SRTM database with regard to the restriction by the given climing ability of vessels.

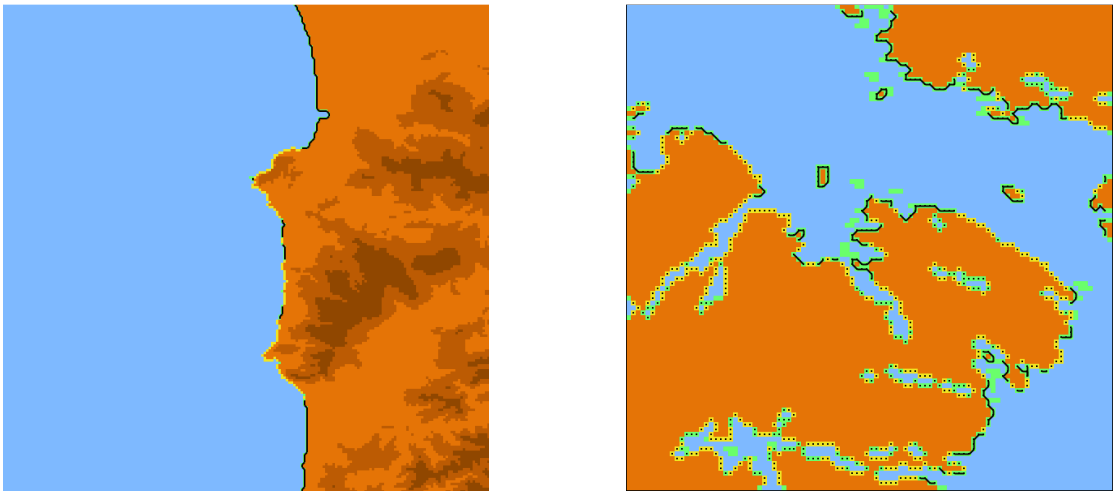

(a) Coastline in Oregon State (b) Southwest coastline in Chile

Figure 13.11 Coastline Analysis Results

13.4 Operational Analysis

DESTINA provides the interface to the operational analysis module developed by Elise Beisker. Inputs include the type of operation, operational environment, available assets and the specification of vessels. Over all input interface is shown in Figure 13.12.

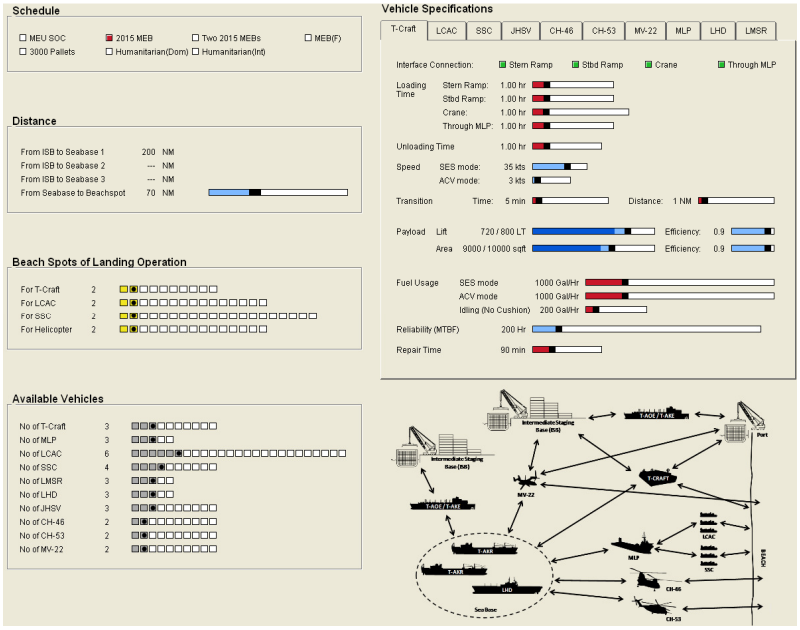

Figure 13.12 Input GUI of Operational Analysis in DESTINA

In the first input interface, the type of operation can be selected. User can decide one of seven types of operation: MEU SOC, 2015 MEB, two 2015 MEBs, MEB(F), 3000 pallets, domestic humaniterain mission and international humanitarian mission. This option is shown in Figure 13.13.

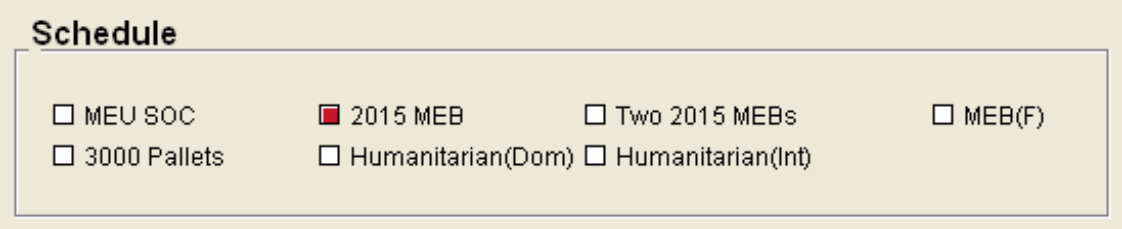

Figure 13.13 Input GUI of Type of Operation

In the next two input interface, operational environment is selected. Distances from Navy bases are automatically calculated by DESTINA. This option is shown in Figure 13.14.

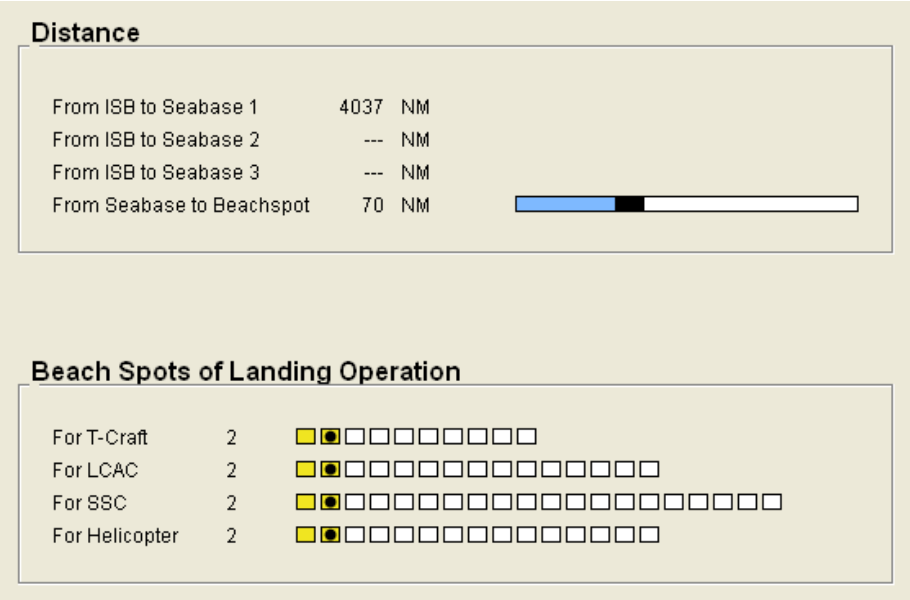

Figure 13.14 Input GUI of Operational Environment

The input interface at the left bottom is the available assets. The number of available assets are decided in this menu. This option is shown in Figure 13.15.

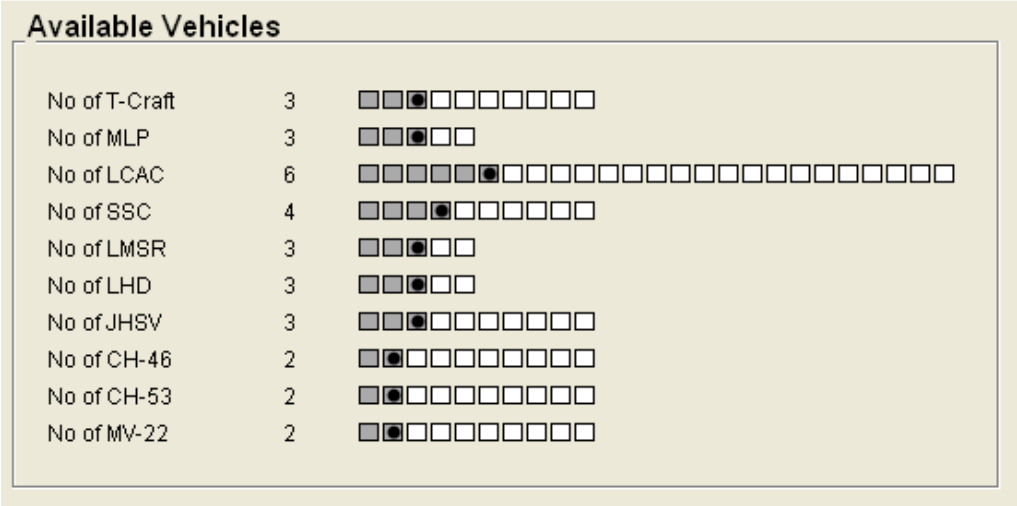

Figure 13.15 Input GUI of Available Assets

In the input interface at the right top, the specification of each vessel can be adjusted. The options for MEC and LCAC are shown in Figure 13.16.

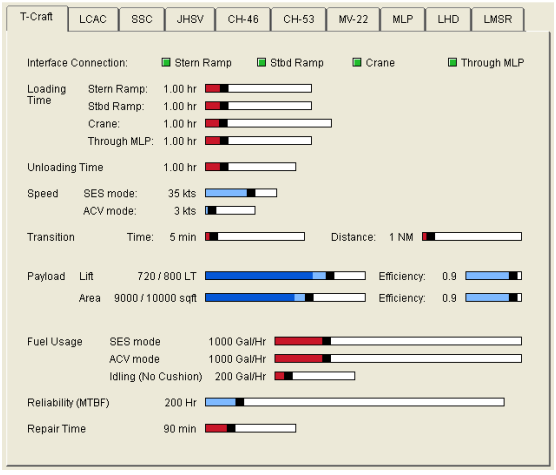

(a) MEC

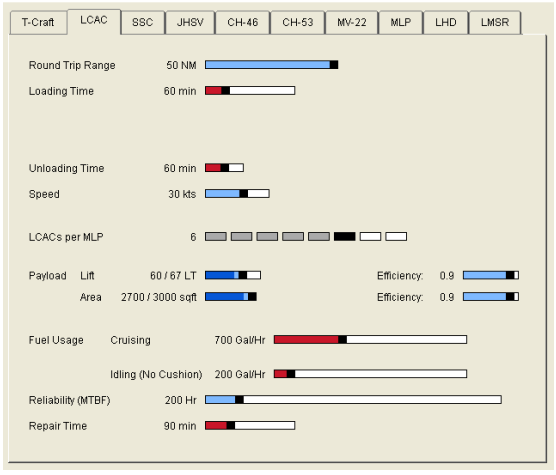

(b) LCAC

Figure 13.16 Input GUI of Specification of Vessel

Figure 13.17 shows an example of operational analysis results in DESTINA based on the given input. The operational analysis results of combat power index and cargo unloading progress are shown with regard to time measured from the day of an incident.

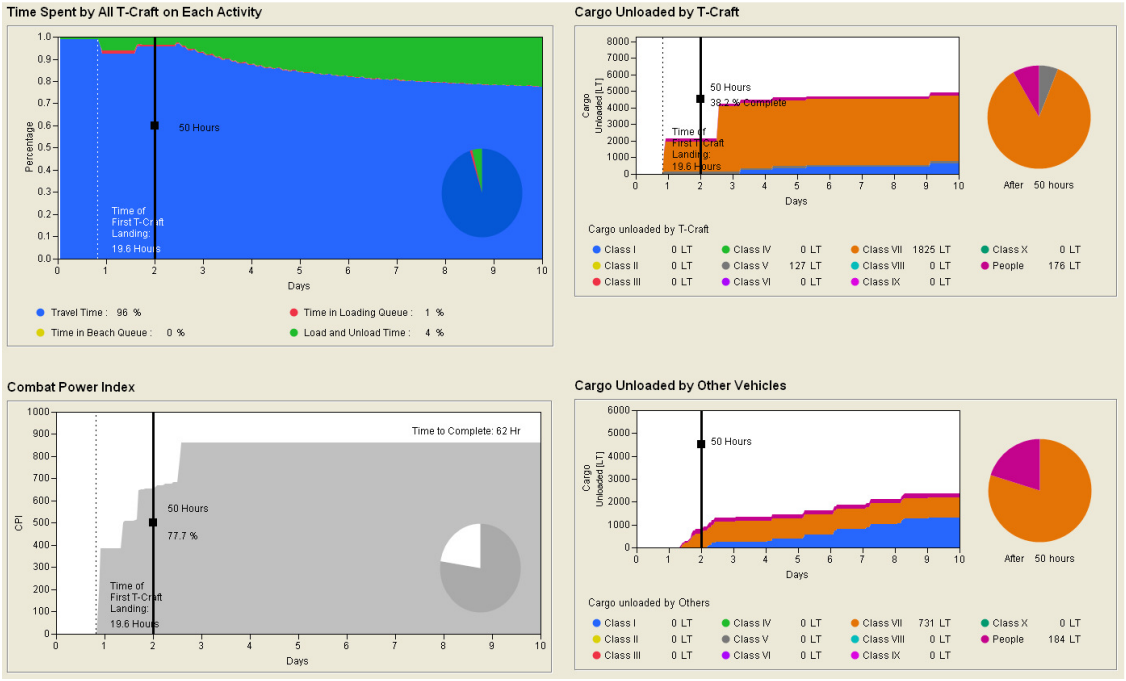

Figure 13.17 Output Display of Operational Analysis in DESTINA

12.5 Global Effectiveness Estimation

DESTINA uses Monte-Carlo simulation to estimate global effectiveness of the given vessel under development. The user can select the option about the number of experiments as shown in Figure 13.18. As a result of Monte-Carlo simulation, DESTINA displays the distribution of instability index and distance weighed by instability index. The distance is displayed as two formats of statistical distribution as shown in Figure 13.19: Cumulative distribution function and probability density function. Based on the distribution, the probability of direct shipping can be calculated as the graph in Figure 13.20.

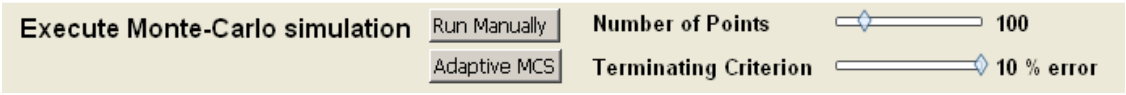

Figure 13.18 Options for Monte-Carlo Simulation in DESTINA

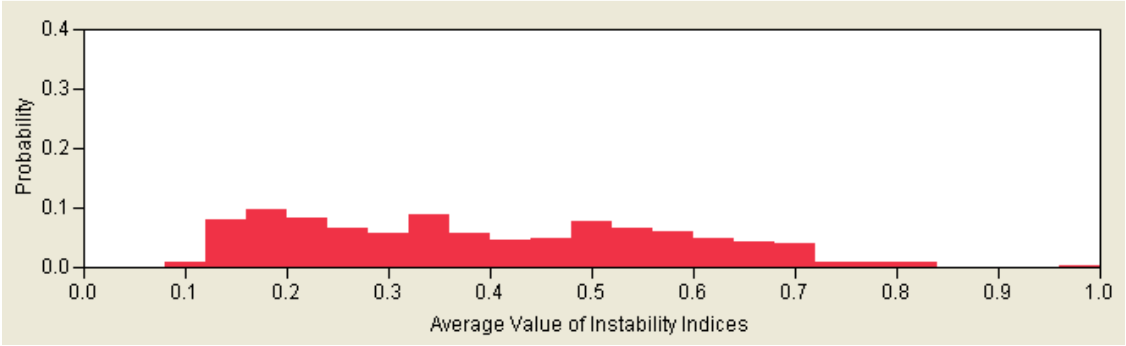

(a) Distribution of Instability Indices

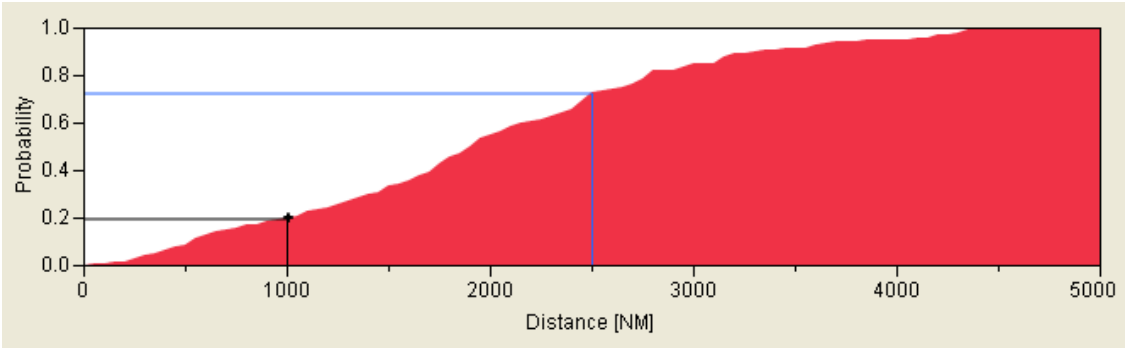

(b) Cumulative distribution function

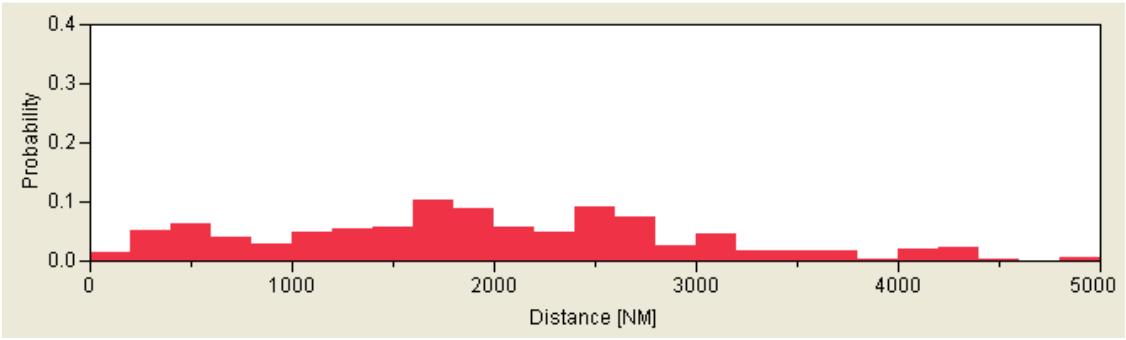

(c) probability density function

Figure 13.19 Graphs of Distribution from Monte-Carlo Simulation in DESTINA

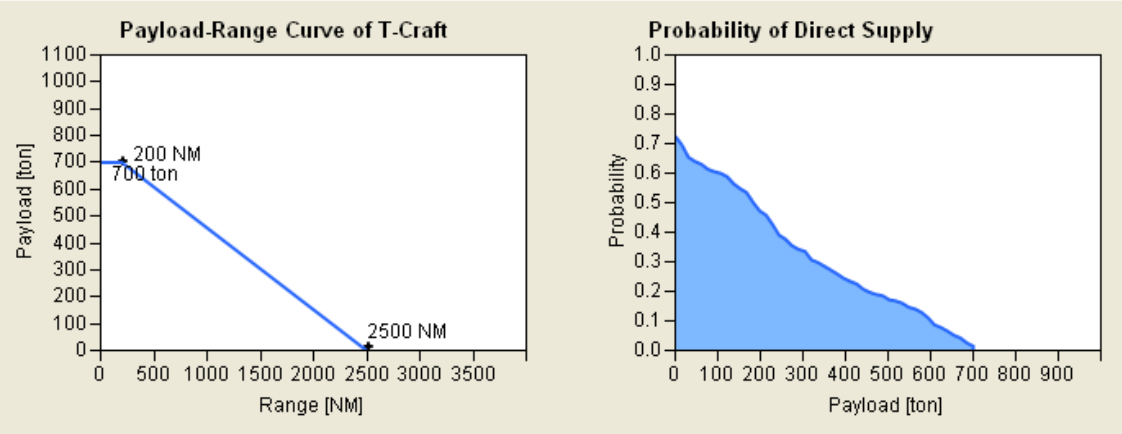

Figure 13.20 Graphs of Probability of Direct Supply Simulation in DESTINA

13.6 Preliminary Design of Medium Exploratory Connector

Preliminary design module in DESTINA needs the minimum information to estimate the range, payload and other ship specification. These information is decided in the input menu as showin in Figure 13.21. Also, possible type of MEC should be decided by the user in the menu in Figure 13.22.

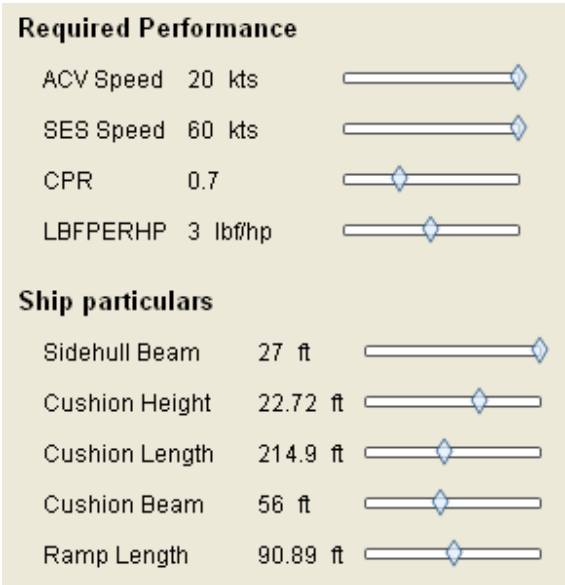

Figure 13.21 Graphs of Probability of Direct Supply Simulation in DESTINA

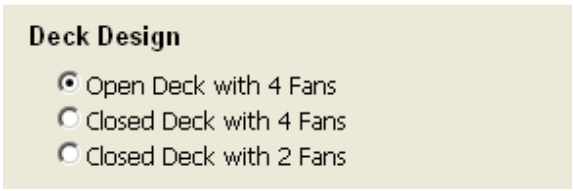

Figure 13.22 Types of MEC in DESTINA

These types of MEC are corresponding to MECs which have been developed so far. Those candidates are shown in Figure 13.23. From the left, MEC with open deck and 4 fans, MEC with closed deck and 4 fans and MEC with closed deck and 2 fans are displayed. Because the detailed specification is not published, the advantage and disadvantage of each candidate cannot be concluded yet.

Figure 13.23 Current candidates of MEC [133] [134] [135]

In order to understand the MEC, DESTINA provide 3D modeling similar to the actual models under development. The options for display is described in Figure 13.24. The modes of MEC are catamaran, SES and ACV modes. Figure 13.25 shows available combination of types and modes of MECs.

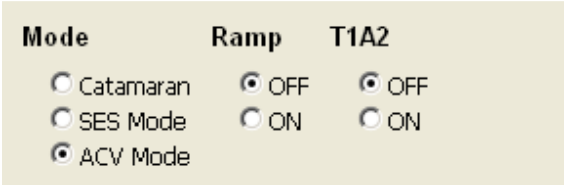

Figure 13.24 Display option of MEC in DESTINA

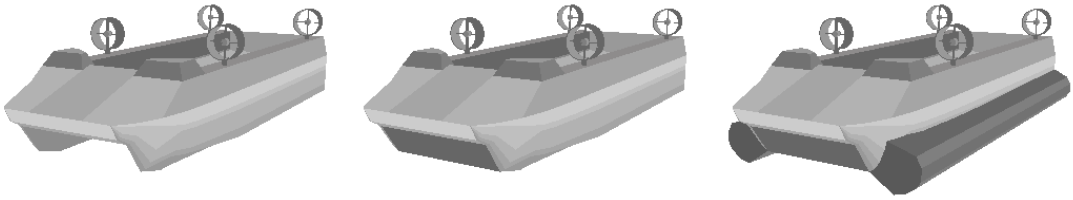

(a) 3D model of MEC with open deck and 4 fans

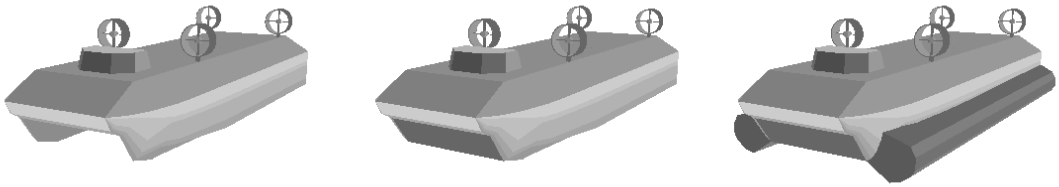

(b) 3D model of MEC with closed deck and 4 fans

(c) 3D model of MEC with closed deck and 2 fans

Figure 13.25 3D model of MEC with different deck shape and number of fans

Ramp in the MEC is extended during landing operations. This equipment is shown in Figure 13.26. In addition, DESTINA provide 3D modeling of T1A1 tank on the deck of MEC so that the decision maker intuitively understand the size of MEC by comparing the size of T1A1 tank and one of MEC. This comparison is depict in Figure 13.27.

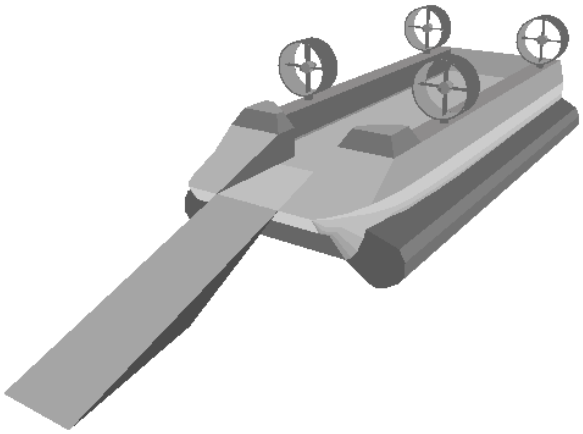

Figure 13.26 Landing Ramp of MEC

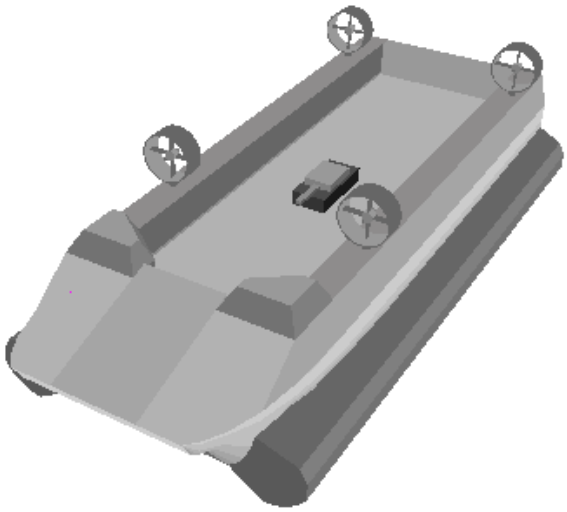

Figure 13.27 MEC with T1A1 Tank

13.7 Evaluation and Selection of Candidates

To support decision makers, Multi-Criteria Decision Making method is loaded in DESTINA. Among many of Multi-Criteria Decision Making method, DESTINA uses TOPSIS to evaluate and select the best candidate. The specification of candidates can be input by dragging the slider bars as shown in Figure 12.28. Then, DESTINA displays payload-range graphs at the bottom and the comparison of given information as shown in Figure 13.29.

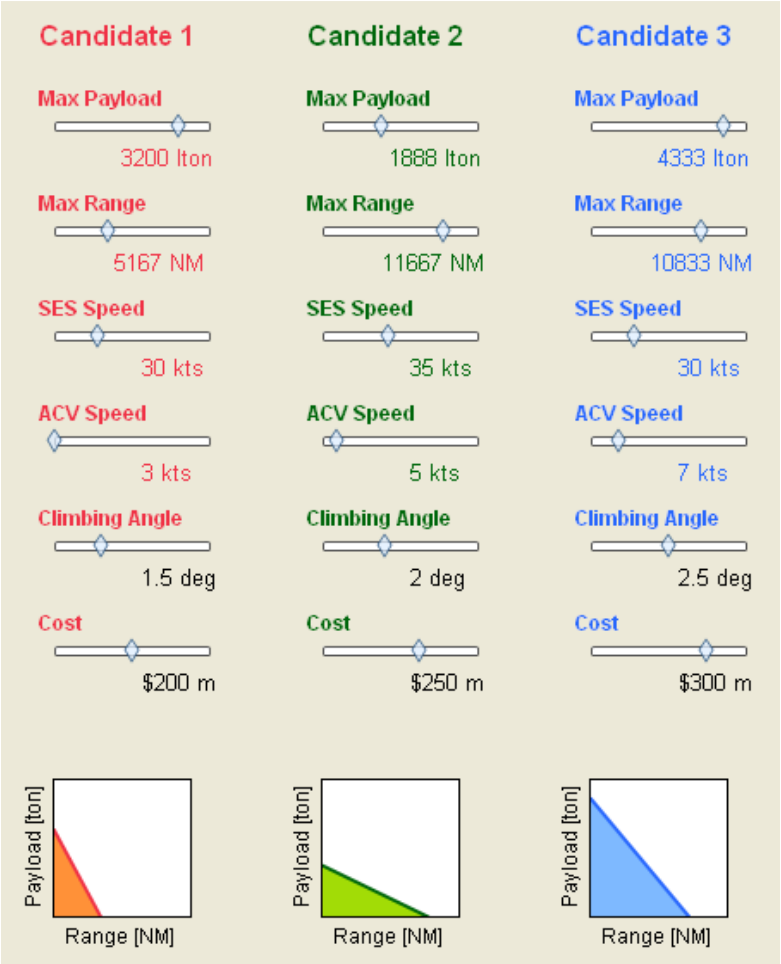

Figure 13.28 Input Interface for Multi-Criteria Decision Making

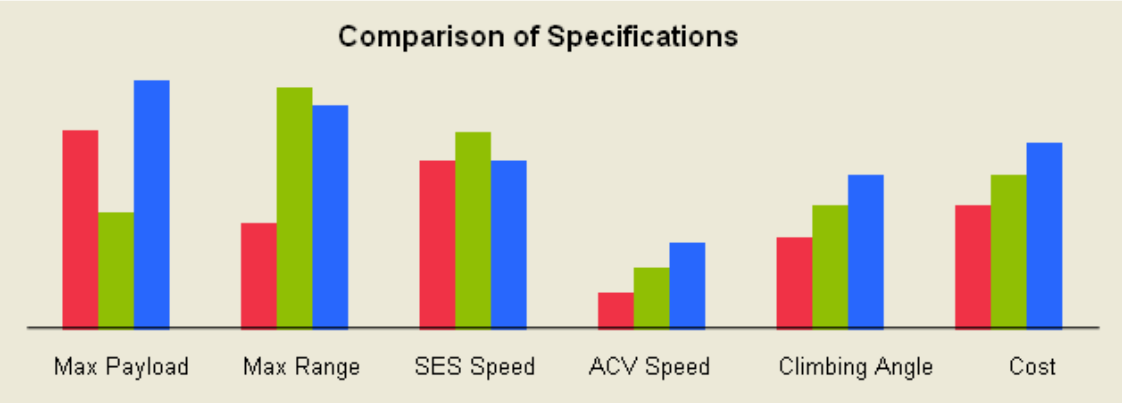

Figure 13.29 Comparison of Specifications

Based on the information from global effectiveness estimation, the probability of each candidate is calculated and displayed as shown in Figure 13.30.

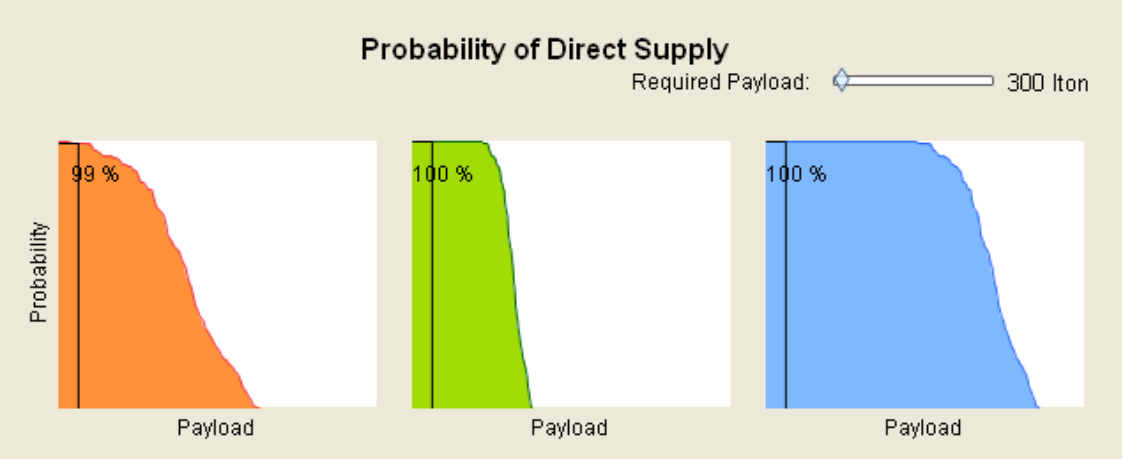

Figure 13.30 Probability of Direct Supply

Finally, Multi-Criteria Decision Making method is applied with the weights given by the user. In the left part of Figure 13.31, the slider bars can adjust each weight of criterion for decision making. In the right part of Figure 13.31, the scores from TOPSIS method are displayed with bar chart and the best candidate is selected.

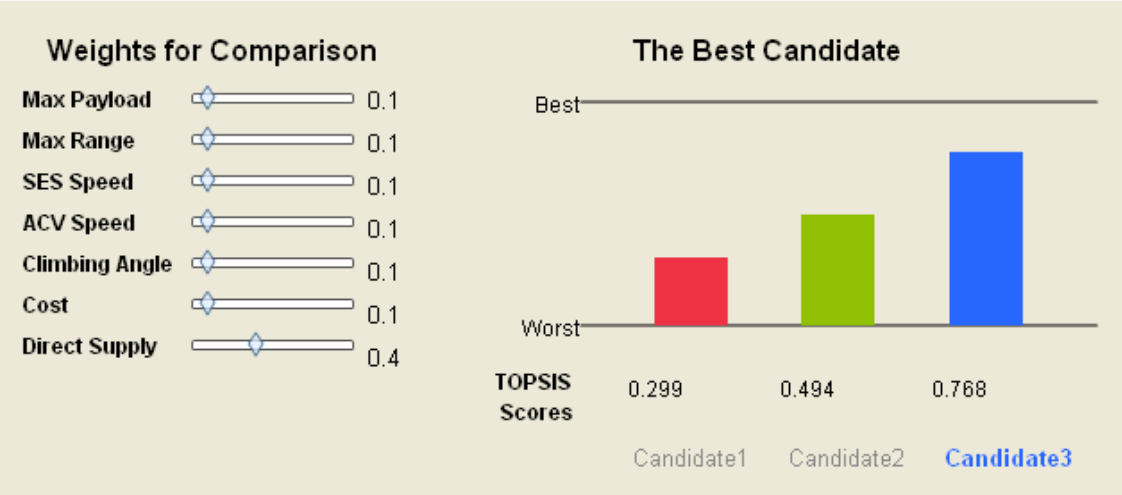

Figure 13.31 Input Interface for Multi-Criteria Decision Making

CHAPTER XIV

CONCLUSION AND FUTURE WORK

14.1 Summary of the Research and Contribution

So far, in order to meet the need to develop a new naval logistic asset that can respond to global missions effectively, this research develops the method to support decision making based on the requirement which must be satisfice-able within the budgetary constraints and address pressing real world needs. To produce feasible and viable requirements for naval logistic assets in complex military systems, this study conducts four major analyses: worldwide instability analysis by social, political, economic factors and natural disasters; operational analysis of various missions based on the discrete event simulation; sea state analysis along the shipping lane and disembarkation analysis for amphibious landing scenarios. The adaptive Monte-Carlo simulation with maximum entropy enables effective integration of these four analyses and consideration of uncertainties in operational and strategic environment. These statistical results are the keys to the preliminary design of new type of vessel and multi-criteria decision making of given candidates. To provide a fair and quatified comparison of candidates, the concept of probabilistic logistic utility is proposed. The probabilistic logistic utility index is calculated by linear mapping of the strategically weighted shipping distance distribution and the payload-range relation of a new vessel.

At first, the suggested method to measure the instability of a region including natural disasters complements the conventional instability analysis estimated by the

socio-economic, and political factors. Furthermore, this method calculates the instability of region by region - not country - so that the results show the solution of the problem which all area have the same instability even in large countries, in spite of the fact that natural risk factors are the values of the regions not countires. The results of suggested instability analysis method is verified by comparing the areas where U.S. military has dispatched.

Second, to provide an efficiently automated computational envirionment, the adaptive Monte-Carlo simulation with maximum entropy concept is developed and applied to the estimaton of the global effectiveness of a new vessel. The adaptive sampling technique enables the ability to terminate Monte-Carlo simulation at the appropriate timing, and maximum entropy concept provides the best set of additional sampling points based on the analogy between heat conduction and reliability of information.

Third, the computational burden reduces significantly by using the pre-calculated table of shipping lanes. This pre-calculated table consists of bottle neck points which are found in the superposition of international shipping lanes. This research topic is one of the keys that allow the Monte-Carlo simulation can be performed in reasonable time.

Fourth, to overcome imperfection of SRTM database and reduce computational cost more, The principle of coastal self-similarity is applied to the estimation of available coastline length. The principle of coastal self-similarity, the basis of fractal theory, can predict the coastline length from the low resolution geographical information without the use of high resolution database.

Finally, the decision supporting software DESTINA is developed to facilitate the above analyses results and global effectiveness estimation. DESTINA is coded in JMP, a statistics software due to its ability to handle large amounts of data, using the JMP scripting language. This real-time interactive software provides the visualization of information by text, numbers, graphs, and three dimensional visual models of the MEC to help decision makers instantly, efficiently and intuitively to understand what they are designing and what impacts the vessel can bring. Furthermore, the multi-crtieria decision making method launched in this software can directly assist the fair comparison of candidates so that decision makers select the most appropriate candidate based on the requirements to meet the needs in the future.

13.2 Future Work

In this research, the method to support decision making is developed and the application for the Medium Exploratory Connector is explained. This research will be improved if the following future works are included.

First, integration with the assets of U.S. Army and Air Force can make this research cover all military logistics. For example, the research by John Salmon is depicted in Figure 14.1. This research can provide the logistic information by the cargo airplanes of U.S. Air Force. In addition, the U.S. Army watercraft is an important factor for global logistic supply plan and the logistic system inland by the U.S. Army is an indispensable part of logistics chain as well. By including those available assets of Navy, Air Force and Army, decision makers can understand the impact of new vessel at the highest level of system-of-systems.

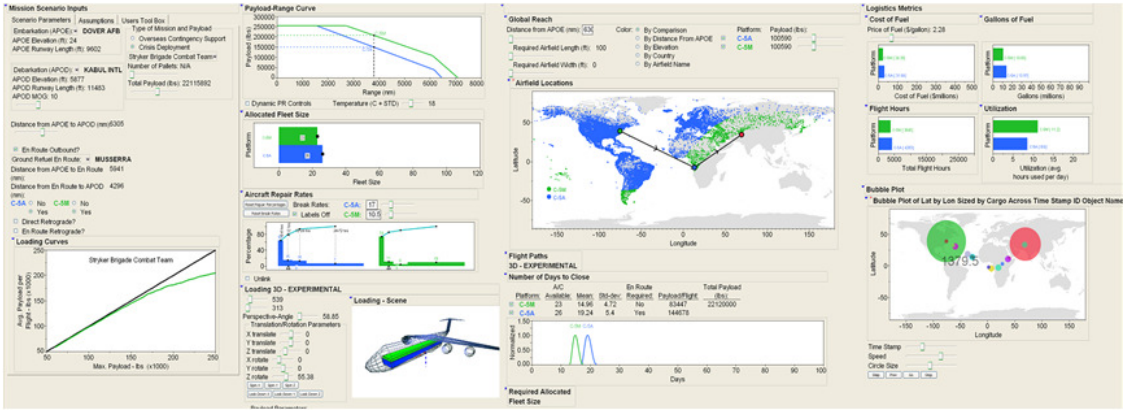

Figure 14.1 Software for the logistics of U.S. Air Force by John Salmon

Second, DESTINA candetermine the requirements for all type of assets. Therefore, if the preliminary design module of the vessel under designing is provided, the usability of DESTINA can be expanded into all designs of new vessel in the next generation. This capability is not limited to Navy ships. Practically, the watercraft of Army or cargo aircraft of Air Force can be a good application of this requirement analysis.

Third, the combination of fleets which significantly effects the operational efficiency. This research is currently being conducted in ASDL and this analysis could be collaborated and DESTINA to allow for additional analysis. For these capabilities, the appropriate optimization algorithm needs to be developed in order to cover requirement. Currently, the researches on the second and third topics are being conducted in Aerospace Systems Design Laboratory at Georgia Institute of Technology.

Lastly, the climate is largely dependent of seasonal condition. Accordingly, in order to acquire more accurate statistic information, the sea state needs to be analyzed

based on the different database of four seasons. Then, This would allow decision makers higher accuracy by selecting the season when the operation possibly is performed.

This research of the requirement analysis in the system engineering can be applicable to various fields of design processes including aerospace, mechanical, and all manufacturing areas. Diverse studies of factors corresponding products would increase the usability of the requirement analysis. Moreover, the research about uncertainties of forecasting hided in the stochastic process would enable to predict better.

APPENDIX A

Fuzzy Analysis of Statistical Evidence (FASE) modeling [11]

Let C be the class variable and A1,…, An be the attributes variables; and let Pos be the possibility measures. Based on the statistical inference developed in [12] we have

$$\text{Pos}(C \mid A1,\ldots, An) = \Pr(A1,\ldots, An \mid C) / \sup_C \Pr(A1,\ldots, An \mid C) \qquad \text{Eq. (A.1)}$$

if the prior belief is uninformative.

Pos (C | A1,…, An) can be interpreted as the fuzzy membership that an instance belong to class C, and Bel (C | A1,…, An) = 1- Pos (C | A1,…, An) is the belief measure or certainty factor (CF) that an instance belong to class C. The difference of Eq. (A.1) and the Bayes formula is simply the difference of normalization constant. In possibility measure the sup norm is 1, while in probability measure the additive norm (integration) is 1.

In machine learning, the number of attributes are usually very large, with limited number of training sample, the joint probability Pr (A1,…, An | C) can not be estimated directly from the data. This problem is similar to the curse of dimensionality. If estimate the conditional probability Pr (Ai | C) from each attribute separately, then we need a suitable operation to combine them together.

Next we give a definition of t-norm, which is often used for the conjunction of fuzzy sets. Definition A fuzzy intersection/t-norm is a binary operation T: $[0,1] \times [0,1] \rightarrow [0,1]$, which is communicative, associative and satisfies the following conditions [56].

(i) T (a, 1) = a, for all a.

(ii) T (a, b) ≤ T (c, d) whenever a ≤ c, b ≤ d. Eq. (A.2)

The following are examples of some t-norms that are frequently use in the literatures.

Minimum: M (a, b) = min (a, b)

Product: Π (a, b) = ab.

Bounded difference: W (a, b) = max (0, a + b -1).

And we have W ≤ Π ≤ M.

Based on different relationship of the attributes, we have different belief update rules. If A1, A2 are independent then we have (cf. Chen [10])

$$Pos(C|A1,A2) = Pos(C|A1)\ Pos\ (C|A2) / supC\ Pos\ (C|A1)\ Pos\ (C|\ A2) \quad \text{Eq. (A.3)}$$

and if A1, A2 are completely dependent, i.e. Pr (A1 |A2) = 1 and Pr (A2 |A2) = 1, then we have

$$Pos(C|A1,A2)=Pos(C|A1)\wedge Pos(C|A2)/supCPos(C|A1)\wedge Pos(C|A2) \quad \text{Eq. (A.4)}$$

where ∧ is a minim operation. This holds since Pos (C | A1, A2) = Pos (C |A1) = Pos (C | A2). Note that if A1, A2 are functions of each other, they are completely dependent; so the evidences are redundant.

In general the relations among the attributes are unknown, but, it seemed reasonable to employ a t-norm in between Π and M for belief update. For simplicity we restricted to the model that aggregate all attributes with a common t-norm ⊗ as follows

$$Pos(C|A1,\ldots,An) = \otimes\ i=1,\ldots,n\ Pos\ (C|Ai)\ /supC \otimes\ i=1,\ldots,n\ Pos\ (C|\ Ai)$$

Eq. (A.5)

If we choose $\otimes$ equal to the product Π, then Eq. (A.5) is equivalent to the naïve Bayesian classifier with uninformative prior. As shown in [12] product rule implies adding the weights of evidence. If attributes are completely dependent by employing the product rule we are basically counting the same evidence twice. The following are some characteristic properties of FASE.

(1) For any t-norm if attribute Ai is noninformative, i.e. Pos (C = cj | Ai) = 1, $\forall$j, then

$$Pos\ (C \mid A1,\ldots,\ An\ ) = Pos\ (C \mid A1,\ldots,Ai\text{-}1,\ Ai\text{+}1\ An\ ).$$ Eq. (A.6)

This holds since T (a, 1) = a.

Equation (A.6) indicates that a noninformative attribute did not contribute any evidence for overall classification, and it happens when an instance ai is missing or Ai is a constant. Similarly if Ai is a white noise then it provide little information for classification, since Pos (C = cj | Ai) $\approx$1, $\forall$j. Thus FASE is noise tolerant.

(2) For any t-norm if Pos (C | Ai) = 0 for some i, then

$$Pos\ (C \mid A1,\ldots,\ An\ ) = 0$$ Eq. (A.7)

This holds since T (a, 0) = 0.

Equation (A.7) indicates that the process of belief update is by eliminating the less plausible classes/hypothesis, i.e. Pos (C | Ai) $\approx$ 0, based on evidences. The ones that survive the process become truth.

(3) For any t-norm if Bel (C = cj | A1) = a, Bel (C = ck | A2) = b, j$\neq$k and b $\leq$ a, then

$$Bel\ (C = cj \mid A1, A2) = (a - b) / (1 - b) \qquad \text{Eq. (A.8)}$$

Since $(a - b) / (1 - b) \leq a$, Eq. (A.8) implies that if the evidences conflict, it will lower our confidence which class it belongs; however, the computation is the same no matter which t-norm is used.

The only situation where t-norm makes a difference is when we have $Bel\ (C = ci \mid A1) = a$, and $Bel\ (C = ci \mid A2) = b$, $0 < a, b \leq 1$. The t-norm will determine how much our confidence should increase. Thus, if we employ different t-norms to combine attributes the computations are quite similar with each other. This also explains, even though the independence assumption of the naïve Bayesian classifier is very often violated, it still can perform well.

In the case of computation of FASE, for continuous attributes we employ the kernel estimator for density estimation

$$p(x) = 1/nh\ \Sigma i\ K\ ((x - xi\ )/h) \qquad \text{Eq. (A.9)}$$

maximum likelihood estimates. The estimated probabilities from each attribute are normalized into possibilities and then combined by a t-norm as in (5). We examine the following two families of t-norms, since these t-norms contain wide range of fuzzy operators. One is proposed by Frank [31] as follows

$$Ts\ (a, b) = logs\ (1+ (sa - 1)\ (sb - 1) / (s - 1)), \text{ for } 0 < s < \infty. \qquad \text{Eq. (A.10)}$$

We have $Ts = M$, as $s \rightarrow 0$, $Ts = \Pi$, as $s \rightarrow 1$ and $Ts = W$, as $s \rightarrow \infty$.

The other is proposed by Schweizer & Sklar [91] as follows

$$T_p(a, b) = (\max(0, ap + bp - 1))^{1/p}, \text{ for } -\infty < p < \infty. \quad \text{Eq. (A.11)}$$

We have $T_p = M$, as $p \to -\infty$, $T_p = \Pi$, as $p \to 0$ and $T_p = W$, as $p \to 1$.

For binary classification FASE is equivalent to the likelihood ratio statistics. If we are interested in the disciminant power of each attribute, then Kullback's [60] information of divergence can be applied, which is given by

$$I(p1, p2) = \Sigma x\, (p1(x) - p2(x)) \log (p1(x)/p2(x)). \quad \text{Eq. (A.12)}$$

FASE does not require consideration of the prior. However, if we multiply the prior, in term of possibility measure, to the likelihood, then it discounts the evidence of certain classes. So in a loose sense prior can also be considered as a kind of evidence.

APPENDIX B

Kosimo Database (intensity level 4 only) [121]

Table B.1 Kosimo Database (intensity level 4 only)

name	start	duration (years)	political system 1	political system 2	economic-political type of state
Afghanistan II (Soviet intervention)	1979	9	6 USR	7 AFG	SH/EL
Afghanistan III (civil war II)	1988	3	2 PAK	7 AFG	EL
Afghanistan IV (civil war III)	1992	1	7 AFG	AND	EL
Afghanistan V (civil war IV)	1993	6	7 AFG	AND	EL
Algeria (independence II)	1954	8	5 MOR	1 FRA	EL/IS
Angola (civil war I)	1975	1	3 SAF	7 ANG	EL
Angola (civil war II)	1976	15	AND	7 ANG	SHE/EL
Angola (civil war)	1997	2	6 ANG	(UNITA)	EL
Angola (independence)	1961	13	6 USR	5 POR	EL/IS
Argentina (Montoneros)	1969	8	AND	2 ARG	SL
Argentina-United Kingdom (Falkland II)	1982	0	5 ARG	1 UKI	SL / IS
Armenia-Azerbaijan (Nagorno-Karabakh II)	1991	3	AND	4 AZI	EL/EL
Bosnia-Herzegovina (Moslems-Croats)	1992	2	3 KRO	7 BOS	OS
Bosnia-Herzegovina (re-conquest Krajina/Westslavonia)	1995	0	7 BOS	AND	OS
Bosnia-Herzegovina (Serbs-Croats)	1992	2	7 BOS	AND	OS
Burma/Myanmar (minorities)	1948	51	AND	2 MYA	EL
Burundi I (genocide)	1972	1	5 BUI	6 TAZ	EL/EL
Burundi II (Hutu)	1988	0	AND	5 BUI	EL
Burundi III (civil war)	1993	6	6 BUI	AND	EL
Cambodia II	1970	5	7 DRV	7 KHM	EL
Chad I	1966	9	5 LIB	7 CHA	EL
Chad II	1975	4	6 LIB	7 CHA	EL
Chad III	1980	0	AND	7 CHA	EL
Chad V	1983	7	AND	7 CHA	EL
China (civil war)	1945	4	AND	AND	EL
China (Tibet II)	1954	5	AND	6 CHN	SHE
China-India (war)	1962	1	6 CHN	2 IND	SHE/EL
China-Vietnam (war)	1979	0	6 CHN	6 DRV	SHE/SHE
Columbia (Violencia I)	1948	5	AND	7 COL	EL
Congo (Brazzaville, regime crisis)	1997	0	AND	6 CON	EL
Croatia (occupation East Slavonia)	1991	4	3 YUG	3 KRO	OS/OS
Croatia (Reconquest of Kraijan/Westslavonia)	1995	0	3 CRO	AND	OS
Cuba (revolution)	1956	3	AND	7 CUB	EL
Cyprus IV (Turkey invasion)	1974	0	5 GRC	7 CYP	ISE/EL
Ecuador-Peru (Amazons 5)	1995	0	2 ECU	3 PER	EL / EL
Ecuador-Peru (Amazons II)	1981	0	3 PER	2 ECU	SL/EL
Ecuador-Peru (Amazons III)	1981	0	3 PER	2 ECU	SL/EL

Table B.1 Kosimo Database (intensity level 4 only, continued)

name	start	duration (years)	political system 1	political system 2	economic-political type of state
Egypt (Suez-war)	1956	1	1 UKI	4 EGY	IS/EL
Egypt-Israel (6-days-war)	1967	0	4 EGY	1 ISR	ISE/EL
El Salvador (civil war)	1981	11	7 NIC	3 SAL	EL
Eritrea III (civil war)	1967	26	AND	5 ETH	EL
Eritrea-Ethiopia	1998	1	4 ERI	4 ETH	EL/EL
Ethiopia (Tigray)	1974	17	AND	6 ETH	EL
Greece (civil war II)	1946	3	AND	7 GRC	EL
Guatemala II	1960	12	4 CUB	3 GUA	EL
Guatemala III	1980	19	AND	3 GUA	EL
Guinea-Bissau (civil war)	1998	1	6 GNB	AND	EL
Honduras-El Salvador (soccer-war I)	1969	1	3 HON	3 SAL	EL/EL
India II (partition)	1942	6	AND	1 UKI	EL
India IV (Kashmir I)	1947	2	2 PAK	2 IND	EL
India XVI (Kashmir IV)	1965	5	6 PAK	2 IND	EL/EL
India XVII (Bangladesh III)	1971	0	2 IND	7 PAK	EL/EL
Indochina Ia	1945	9	1 FRA	7 DRV	IS/EL
Indochina Ib	1955	18	7 DRV	7 RVN	IS/EL
Indochina II (cease-fire)	1973	3	7 DRV	7 RVN	EL/EL
Indochina II (Vietnam-war)	1964	9	7 DRV	7 RVN	IS/EL
Indochina IIIa	1977	1	6 DRV	7 KHM	SHE/EL
Indochina IIIb	1978	13	6 DRV	AND	SHE/EL
Indonesia (East-Timor (civil war I))	1974	1	AND	5 INS	EL
Indonesia (East-Timor III)	1976	23	5 INS	AND	EL
Indonesia (independence)	1945	4	AND	1 UKI	IS/EL
Indonesia (South-Moluccas)	1950	15	AND	4 INS	EL
Iran-Iraq I (Gulf-war)	1980	8	5 IRQ	6 IRN	EL/EL
Iraq (Curds I)	1961	9	5 IRN	5 IRQ	EL
Iraq-Kuwait VI (USA-intervention)	1990	1	6 IRQ	1 USA	EL/IS
Israel II (Palestine-war)	1948	1	5 EGY	1 ISR	EL/EL
Israel IV (Yom-Kippur-war)	1973	0	2 EGY	1 ISR	ISE/EL
Kenya (independence,MauMau)	1952	4	AND	1 UKI	IS/EL
Korea II (Korean War)	1950	3	6 PRK	5 ROK	EL/EL
Laos II (civil war)	1963	12	7 DRV	7 LAO	EL
Lebanon (Shiit militia)	1988	2	5 SYR	7 LEB	EL
Lebanon II	1975	1	1 ISR	7 LEB	SL
Lebanon VI	1982	2	7 LEB	1 ISR	SL
Lebanon VII	1984	5	AND	7 LEB	SL
Lebanon VIII	1989	1	6 IRQ	7 LEB	EL/EL
Liberia (civil war)	1989	6	AND	7 LBR	EL
Madagasy Republic (independence)	1947	13	AND	1 FRA	IS/EL
Malaya (independence)	1948	12	7 CHN	1 UKI	EL/IS
Malaya-Indonesia (Sarawak/Sabah)	1963	3	2 MAL	3 INS	IS/EL
Morocco (independence)	1944	12	AND	1 FRA	EL/IS
Mozambique (civil war; RENAMO)	1978	16	6 SAF	7 MZM	ISE/EL

Table B.1 Kosimo Database (intensity level 4 only, continued)

name	start	duration (years)	political system 1	political system 2	economic-political type of state
Mozambique (independence)	1964	11	AND	5 POR	EL/IS
Nicaragua I (revolution)	1977	2	6 CUB	7 NIC	EL
Nicaragua II (Contras)	1981	9	1 USA	7 NIC	EL
Nigeria (Biafra-secession)	1967	3	1 FRA	7 NIG	EL
Paraguay (coup d'état)	1947	0	AND	7 PAR	EL
Peru (Illuminated path II)	1980	16	AND	3 PER	EL
Rhodesia (civil war)	1972	7	6 ZAM	7 ZIM	EL
Russia (Czechnia)	1991	8	AND	2 RUS	OS
Rwanda (civil war)	1990	4	AND	5 RWA	EL
Sierra Leone (civil war)	1991	8	AND	7 SIE	EL
Somalia (civil war I)	1988	3	AND	7 SOM	EL
Somalia (civil war II)	1991	8	AND	AND	EL
Somalia-Ethiopia (Ogaden II)	1976	2	5 SOM	7 ETH	EL/EL
Sri Lanka (Tamils II)	1983	4	AND	2 SRI	EL
Sri Lanka (Tamils III)	1987	8	AND	3 SRI	EL
Sri Lanka (Tamils IV)	1995	4	AND	3 SRI	EL
Sudan (autonomy for Southern region)	1955	8	1 ISR	2 SUD	EL
Sudan (civil war I)	1963	9	AND	7 SUD	EL
Sudan (civil war II)	1983	5	AND	7 SUD	EL
Sudan (civil war III)	1989	10	AND	7 SUD	EL
Tajikistan (civil war II)	1992	0	7 TAJ	2 RUS	OS
Turkey (Curds II)	1989	10	2 TUR	AND	IS
Uganda-Tanzania (border-war)	1978	1	5 UGA	6 TAZ	EL/EL
Vietnam (civil war)	1960	1	7 DRV	7 RVN	EL/EL
Yemen (70-days-war)	1994	0	7 JEM	AND	EL
Yemen AR (civil war I)	1948	0	AND	7 YAR	EL
Yemen AR (civil war II)	1962	6	4 EGY	7 YAR	EL
Yemen PR (Aden-civil war)	1986	0	AND	5 JEM	EL
Zaire (Kabila)-RCD (Rassemblement Congolese pour la democratie)	1998	1	AND	6 CON	EL
Zaire (Katanga-secession (Shaba))	1960	3	1 BEL	7 ZAI	EL
Zaire- AFDL(Kabila)	1996	2	AND	6 CON	EL
Zaire-Belgium (Belgian intervention)	1960	0	7 ZAI	1 BEL	IS/EL

APPENDIX C

Weibull distribution

The probability density function of a Weibull random variable x is:[84]

$$f(x;\lambda,k) = \frac{\kappa}{\lambda}\left(\frac{x}{\lambda}\right)^{\kappa-1} e^{-\left(\frac{x}{\lambda}\right)^{\kappa}}, \text{if } x \geq 0$$

$$= 0, \text{if } x < 0 \qquad \text{Eq. (C.1)}$$

where $k > 0$ is the shape parameter and $\lambda > 0$ is the scale parameter of the distribution. Its complementary cumulative distribution function is a stretched exponential function. The Weibull distribution is related to a number of other probability distributions; in particular, it interpolates between the exponential distribution (k = 1) and the Rayleigh distribution (k = 2).

If the quantity x is a "time-to-failure", the Weibull distribution gives a distribution for which the failure rate is proportional to a power of time. The shape parameter, k, is that power plus one, and so this parameter can be interpreted directly as follows:

(1) A value of k<1 indicates that the failure rate decreases over time. This happens if there is significant "infant mortality", or defective items failing early and the failure rate decreasing over time as the defective items are weeded out of the population.

(2) A value of k=1 indicates that the failure rate is constant over time. This might suggest random external events are causing mortality, or failure.

(3) A value of k>1 indicates that the failure rate increases with time. This happens if there is an "aging" process, or parts that are more likely to fail as time goes on.

In the field of materials science, the shape parameter k of a distribution of strengths is known as the Weibull modulus.

The form of the density function of the Weibull distribution changes drastically with the value of k. For $0 < k < 1$, the density function tends to ∞ as x approaches zero from above and is strictly decreasing. For $k = 1$, the density function tends to $1/\lambda$ as x approaches zero from above and is strictly decreasing. For $k > 1$, the density function tends to zero as x approaches zero from above, increases until its mode and decreases after it. It is interesting to note that the density function has infinite negative slope at x=0 if $0 < k < 1$, infinite positive slope at x= 0 if $1 < k < 2$ and null slope at x= 0 if $k > 2$. For k= 2 the density has a finite positive slope at x=0. As k goes to infinity, the Weibull distribution converges to a Dirac delta distribution centred at $x = \lambda$. Moreover, the skewness and coefficient of variation depend only on the shape parameter.

The cumulative distribution function for the Weibull distribution is

$$f(x;\lambda,k) = 1 - e^{-\left(\frac{x}{\lambda}\right)^{\kappa}}, \text{if } x \geq 0$$
$$= 0, \text{if } x < 0 \qquad \text{Eq. (C.2)}$$

The failure rate h (or hazard rate) is given by

$$f(x;\lambda,k) = \frac{\kappa}{\lambda}\left(\frac{x}{\lambda}\right)^{\kappa-1} \qquad \text{Eq. (C.3)}$$

The moment generating function of the logarithm of a Weibull distributed random variable is given by [52]

$$E\left[e^{t\log X}\right] = \lambda^t \Gamma\left(\frac{t}{k} + 1\right) \qquad \text{Eq. (C.4)}$$

where Γ is the gamma function. Similarly, the characteristic function of log X is given by

$$E\left[e^{it\log X}\right] = \lambda^{it}\Gamma\left(\frac{it}{k}+1\right) \quad \text{Eq. (C.5)}$$

In particular, the nth raw moment of X is given by

$$m_n = \lambda^n\Gamma\left(1+\frac{n}{k}\right) \quad \text{Eq. (C.6)}$$

The mean and variance of a Weibull random variable can be expressed as

$$\mathrm{E}(X) = \lambda\Gamma\left(1+\frac{1}{k}\right) \quad \text{Eq. (C.7)}$$

and

$$\mathrm{var}(X) = \lambda^2\left[\Gamma\left(1+\frac{2}{k}\right) - \left(\Gamma\left(1+\frac{1}{k}\right)\right)^2\right] \quad \text{Eq. (C.8)}$$

The skewness is given by

$$\gamma_1 = \frac{\Gamma\left(1+\frac{3}{k}\right)\lambda^3 - 3\mu\sigma^2 - \mu^3}{\sigma^3} \quad \text{Eq. (C.9)}$$

where the mean is denoted by μ and the standard deviation is denoted by σ.

The excess kurtosis is given by

$$\gamma_2 = \frac{-6\Gamma_1^4 + 12\Gamma_1^2\Gamma_2 - 3\Gamma_2^2 - 4\Gamma_1\Gamma_3 + \Gamma_4}{\left[\Gamma_2 - \Gamma_1^2\right]^2} \quad \text{Eq. (C.10)}$$

where $\Gamma_i = \Gamma(1+i/k)$. The kurtosis excess may also be written as:

$$\gamma_2 = \frac{\lambda^4\Gamma\left(1+\frac{4}{k}\right) - 4\gamma_1\sigma^3\mu - 6\mu^2\sigma^2 - \mu^4}{\sigma^4} - 3 \quad \text{Eq. (C.11)}$$

A variety of expressions are available for the moment generating function of X itself. As a power series, since the raw moments are already known, one has

$$\mathrm{E}[e^{tX}] = \sum_{n=0}^{\infty}\frac{t^n\lambda^n}{n!}\Gamma\left(1+\frac{n}{k}\right) \quad \text{Eq. (C.12)}$$

Alternatively, one can attempt to deal directly with the integral

$$\mathrm{E}[e^{tX}] = \int_0^\infty e^{tx}\,\frac{k}{\lambda}\left(\frac{x}{\lambda}\right)^{k-1} e^{-(x/\lambda)^k}dx \qquad \text{Eq. (C.13)}$$

If the parameter k is assumed to be a rational number, expressed as k = p/q where p and q are integers, then this integral can be evaluated analytically.[13]

With t replaced by −t, one finds

$$\mathrm{E}[e^{-tX}] = \frac{1}{\lambda^k t^k}\frac{p^k\sqrt{q/p}}{(\sqrt{2\pi})^{q+p-2}}\,G^{\,p\ \ q}_{\,p\ \ q}\left(\left.\begin{matrix}\frac{1-k}{p} & \cdots & \frac{p-k}{p}\\ \frac{0}{q} & \cdots & \frac{q-1}{q}\end{matrix}\right|\frac{p^p}{(q\lambda^k t^k)^q}\right) \qquad \text{Eq. (C.14)}$$

where G is the Meijer G-function.

The characteristic function has also been obtained by Muraleedharan et al.[136].

The information entropy is given by

$$\mathrm{H} = \gamma\left(1-\frac{1}{k}\right) + \ln\left(\frac{\lambda}{k}\right) + 1 \qquad \text{Eq. (C.15)}$$

where γ is the Euler–Mascheroni constant.

The fit of data to a Weibull distribution can be visually assessed using a Weibull Plot. The Weibull Plot is a plot of the empirical cumulative distribution function of data on special axes in a type of Q-Q plot. The axes are $\ln\left(-\ln\left(1-F(x)\right)\right)$ versus $\ln x$. The reason for this change of variables is the cumulative distribution function can be linearized:

$$F(x) = 1 - e^{-\left(\frac{x}{\lambda}\right)^k} \qquad \text{Eq. (C.16)}$$

$$-\ln\big(1 - F(x)\big) = (x/\lambda)^k \qquad \text{Eq. (C.17)}$$

$$\ln\big(-\ln\big(1 - F(x)\big)\big) = k \ln x - k \ln y \qquad \text{Eq. (C.18)}$$

which can be seen to be in the standard form of a straight line. Therefore if the data came from a Weibull distribution then a straight line is expected on a Weibull plot.

There are various approaches to obtaining the empirical distribution function from data: one method is to obtain the vertical coordinate for each point using where is the rank of the data point and is the number of data points.[71]

Linear regression can also be used to numerically assess goodness of fit and estimate the parameters of the Weibull distribution. The gradient informs one directly about the shape parameter and the scale parameter can also be inferred.

The Weibull distribution is used in the following areas:

- In survival analysis
- In reliability engineering and failure analysis
- In industrial engineering to represent manufacturing and delivery times
- In extreme value theory
- In weather forecasting: To describe wind speed distributions, as the natural distribution often matches the Weibull shape
- In communications systems engineering: In radar systems to model the dispersion of the received signals level produced by some types of clutters, To model fading channels in wireless communications, as the Weibull fading model seems to exhibit good fit to experimental fading channel measurements

- In General insurance to model the size of Reinsurance claims, and the cumulative development of Asbestosis losses
- In forecasting technological change (also known as the Sharif-Islam model)[93]
- In hydrology the Weibull distribution is applied to extreme events such as annual maximum one-day rainfalls and river discharges. The blue picture illustrates an example of fitting the Weibull distribution to ranked annually maximum one-day rainfalls showing also the 90% confidence belt based on the binomial distribution. The rainfall data are represented by plotting positions as part of the cumulative frequency analysis.
- In describing the size of particles generated by grinding, milling and crushing operations, the 2-Parameter Weibull distribution is used, and in these applications it is sometimes known as the Rosin-Rammler distribution. In this context it predicts fewer fine particles than the Log-normal distribution and it is generally most accurate for narrow particle size distributions. The interpretation of the cumulative distribution function is that F(x; k; λ) is the mass fraction of particles with diameter smaller than x, where λ is the mean particle size and k is a measure of the spread of particle sizes.

The translated Weibull distribution contains an additional parameter. It has the probability density function

$$f(x; k, \lambda, \theta) = \frac{\kappa}{\lambda}\left(\frac{x-\theta}{\lambda}\right)^{\kappa-1} e^{-\left(\frac{x-\theta}{\lambda}\right)^{\kappa}} \qquad \text{Eq. (C.19)}$$

for $x \geq \theta$ and $f(x; k, \lambda, \theta) = 0$ for $x < \theta$, where $k > 0$ is the shape parameter, $\lambda > 0$ is the scale parameter and θ is the location parameter of the distribution. When $\theta = 0$, this reduces to the 2-parameter distribution.

The Weibull distribution can be characterized as the distribution of a random variable X such that the random variable

$$Y = \left(\frac{X}{\lambda}\right)^k \qquad \text{Eq. (C.20)}$$

is the standard exponential distribution with intensity 1.

The Weibull distribution interpolates between the exponential distribution with intensity $1/\lambda$ when $k = 1$ and a Rayleigh distribution of mode when $k = 2$.

The Weibull distribution can also be characterized in terms of a uniform distribution: if X is uniformly distributed on (0,1), then the random variable is Weibull distributed with parameters k and λ. This leads to an easily implemented numerical scheme for simulating a Weibull distribution.

The Weibull distribution (usually sufficient in reliability engineering) is a special case of the three parameter Exponentiated Weibull distribution where the additional exponent equals 1. The Exponentiated Weibull distribution accommodates unimodal, bathtub shaped and monotone failure rates.

The Weibull distribution is a special case of the generalized extreme value distribution. It was in this connection that the distribution was first identified by Maurice Fréchet in 1927.[137] The closely related Fréchet distribution, named for this work, has the probability density function

$$f_{Frechet}(\mathrm{x};\mathrm{k},\lambda) = \frac{\kappa}{\lambda}\left(\frac{\mathrm{x}}{\lambda}\right)^{-1-\kappa} \mathrm{e}^{-\left(\frac{\mathrm{x}}{\lambda}\right)^{-\kappa}} =* f_{Weibull}(x;-k,\lambda) \qquad \text{Eq. (C.21)}$$

The distribution of a random variable that is defined as the minimum of several random variables, each having a different Weibull distribution, is a poly-Weibull distribution.

The Weibull distribution was first applied by Rosin & Rammler to describe particle size distributions. It is widely used in mineral processing to describe particle size distributions in comminution processes. In this context the cumulative distribution is given by

$$\mathrm{f}(\mathrm{x};\mathrm{P}_{80},\mathrm{m}) = 1 - e^{\ln 0.2\left(\frac{x}{P_{80}}\right)^{m}}, \text{if } \mathrm{x} \geq 0$$

$$= 0, \text{if } \mathrm{x} < 0 \qquad \text{Eq. (C.22)}$$

Where, x: Particle size

P_{80}: 80th percentile of the particle size distribution

m: Parameter describing the spread of the distribution

APPENDIX D

Treaties with the United States

Table D.1 Number of Treaties: Military [104]

Country	Defense	Mutual Security	Peace Corps	Terrorism
Norfolk Island	48			
China	0		1	
Macau	0			
Saint Barthelemy	34			
France	34	1		
Guadeloupe	34	1		
Martinique	34	1		
French Guiana	34	1		
New Caledonia	34	1		
French Polynesia	34	1		
Saint Pierre and Miquelon	34	1		
Reunion	34	1		
French Southern and Antarctic Lands	34	1		
Wallis and Futuna	34	1		
Mayotte	34	1		
Denmark	15			
Faroe Islands	15			
Greenland	15			
Netherlands Antilles	27			
Aruba	27			
Netherlands	27	1		
Anguilla	117	1	1	
Falkland Islands (Islas Malvinas)	117	1		
United Kingdom	117	1		
Guernsey	117	1		
South Georgia and South Sandwich Islands	117	1		
Isle of Man	117	1		
British Indian Ocean Territory	117	1		
Jersey	117	1		
Cayman Islands	117	1		
Saint Helena	117	1		
Turks and Caicos Islands	117	1	1	

Table D.1 Number of Treaties: Military [104] (continued)

Country	Defense	Mutual Security	Peace Corps	Terrorism
British Virgin Islands	117	1		
Virgin Islands	117	1		
Andorra	0			
United Arab Emirates	3			
Afghanistan	4		1	
Antigua and Barbuda	3		1	
Albania	6		1	
Armenia	1		1	
Angola	1			
Antarctica	0			
Argentina	11		1	
Austria	2	1		
Australia	48			1
Azerbaijan	2		1	
Bosnia and Herzegovina	3			
Barbados	1		1	
Bangladesh	4		1	
Belgium	14	1		
Burkina Faso	2		1	
Bulgaria	7		1	
Bahrain	5		1	
Burundi	2		1	
Benin	6		1	
Brunei	0			
Bolivia	8			
Brazil	11		1	
Bahamas, The	16			
Bhutan	0			
Botswana	4		1	
Belarus	1			
Belize	5		1	
Canada	74			
Congo, Democratic Republic of the	6		1	
Central African Republic	2		1	
Congo, Republic of the	0		1	
Switzerland	6			
Cote d'Ivoire	1		1	
Chile	18			

Table D.1 Number of Treaties: Military [104] (continued)

Country	Defense	Mutual Security	Peace Corps	Terrorism
Cameroon	1		1	
Colombia	16		1	
Costa Rica	5		1	
Cuba	6			
Cape Verde	3			
Cyprus	1	1	1	
Czech Republic	1	1	1	
Germany	64	1		
Djibouti	4			
Dominica	1		1	
Dominican Republic	10		1	
Algeria	1			
Ecuador	8		1	
Estonia	3		1	
Egypt	7			
Western Sahara	0			
Eritrea	2		1	
Spain	21			
Ethiopia	9		1	
Finland	5			
Fiji	2		1	
Micronesia, Federated States of	1		1	
Gabon	3			
Grenada	3		1	
Georgia	4		1	
Ghana	10		1	
Gambia, The	2	1	1	
Guinea	4		1	
Equatorial Guinea	1		1	
Greece	19	1		
Guatemala	9		1	
Guinea-Bissau	1		1	
Guyana	3		1	
Honduras	15		1	
Croatia	4			
Haiti	5		1	
Hungary	6		1	1
Indonesia	9		1	

Table D.1 Number of Treaties: Military [104] (continued)

Country	Defense	Mutual Security	Peace Corps	Terrorism
Ireland	2			
Israel	16	1		1
India	8		1	
Iraq	4			
Iran	8		1	
Iceland	10	1		
Italy	29	1		
Jamaica	3		1	
Jordan	7		1	
Japan	76			
Kenya	3		1	
Kyrgyzstan	5		1	
Cambodia	4		1	
Kiribati	0		1	
Comoros	1		1	
Saint Kitts and Nevis	3		1	
Korea, North	0			
Korea, South	47	1		
Kosovo	1			
Kuwait	2			
Kazakhstan	6		1	
Laos	2			
Lebanon	5			
Saint Lucia	2		1	
Liechtenstein	0			
Sri Lanka	4		1	
Liberia	12		1	
Lesotho	0		1	
Lithuania	5			
Luxembourg	9	1	1	
Latvia	4	1	1	
Libya	4			
Morocco	2		1	
Monaco	0			
Moldova	2			
Montenegro	3			
Madagascar	2		1	
Marshall Islands	1		1	

Table D.1 Number of Treaties: Military [104] (continued)

Country	Defense	Mutual Security	Peace Corps	Terrorism
Macedonia	2			
Mali	7		1	
Burma	1			
Mongolia	3		1	
Mauritania	3			
Mauritius	1		1	
Maldives	2			
Malawi	3		1	
Mexico	9		1	
Malaysia	6		1	
Mozambique	4		1	
Namibia	1			
Niger	4		1	
Nigeria	6	1	1	
Nicaragua	8		1	
Norway	25	1		
Nepal	2		1	
Niue	0		1	
New Zealand	6			
Oman	3		1	
Panama	7		1	
Peru	12		1	
Papua New Guinea	3		1	
Philippines	33	1	1	
Pakistan	12		1	
Poland	10		1	
Palestain	0			
Portugal	14	1		
Palau	0		1	
Paraguay	6		1	
Qatar	0			
Malta	1		1	
Romania	6		1	
Serbia	3			
Russia	4			
Rwanda	3		1	
Saudi Arabia	7			
Solomon Islands	2	1	1	

Table D.1 Number of Treaties: Military [104] (continued)

Country	Defense	Mutual Security	Peace Corps	Terrorism
Seychelles	2	1	1	
Sudan	4			
Sweden	3			
Singapore	9			
Slovenia	4			1
Slovakia	2			
Sierra Leone	2		1	
San Marino	0			
Senegal	6		1	
Somalia	2		1	
Suriname	3	1	1	
Sao Tome and Principe	2			
El Salvador	6		1	
Syria	0			
Swaziland	1		1	
Chad	5		1	
Togo	2		1	
Thailand	10	1	1	
Tajikistan	3			
Timor-Leste	2		1	
Turkmenistan	2		1	
Tunisia	8		1	
Tonga	4		1	
Turkey	20	1	1	
Trinidad and Tobago	2	1		
Tuvalu	0		1	
Taiwan	3			
Tanzania	1		1	
Ukraine	9		1	
Uganda	3		1	
United States	9999			
Uruguay	7		1	
Uzbekistan	5		1	
Holy See (Vatican City)				
Saint Vincent and the Grenadines	1		1	
Venezuela	4		1	
Vietnam	1			
Vanuatu	0		1	

Table D.1 Number of Treaties: Military [104] (continued)

Country	Defense	Mutual Security	Peace Corps	Terrorism
Samoa	1		1	
Yemen	2		1	
South Africa	7			
Zambia	2	1		
Zimbabwe	1		1	

Table D.2 Number of Treaties: Natural Disasters [104]

Country	Disaster Assistance	Peace Corps	Humanitarian Assistance
Afghanistan		1	
Albania		1	
Algeria			
Andorra			
Angola			
Anguilla		1	
Antarctica			
Antigua and Barbuda		1	
Argentina		1	
Armenia		1	
Aruba			
Australia			
Austria			
Azerbaijan		1	
Bahamas, The			
Bahrain		1	
Bangladesh		1	
Barbados		1	
Belarus			
Belgium			
Belize		1	
Benin		1	
Bhutan			
Bolivia			
Bosnia and Herzegovina			
Botswana		1	
Brazil		1	
British Indian Ocean Territory			
British Virgin Islands			
Brunei			
Bulgaria		1	
Burkina Faso		1	
Burma			
Burundi		1	
Cambodia		1	
Cameroon		1	
Canada			

Table D.2 Number of Treaties: Natural Disasters [104] (continued)

Country	Disaster Assistance	Peace Corps	Humanitarian Assistance
Cape Verde			
Cayman Islands			
Central African Republic		1	
Chad		1	
Chile			
China		1	
Colombia		1	
Comoros		1	
Congo, Democratic Republic of the		1	
Congo, Republic of the		1	
Costa Rica		1	
Cote d'Ivoire		1	
Croatia			
Cuba			
Cyprus		1	
Czech Republic		1	
Denmark			
Djibouti			
Dominica		1	
Dominican Republic		1	
Ecuador		1	
Egypt			
El Salvador		1	
Equatorial Guinea		1	
Eritrea		1	
Estonia		1	
Ethiopia		1	
Falkland Islands (Islas Malvinas)			
Faroe Islands			
Fiji		1	
Finland			
France			
French Guiana			
French Polynesia			
French Southern and Antarctic Lands			
Gabon			
Gambia, The		1	
Georgia		1	

Table D.2 Number of Treaties: Natural Disasters [104] (continued)

Country	Disaster Assistance	Peace Corps	Humanitarian Assistance
Germany			
Ghana		1	
Greece			
Greenland			
Grenada		1	
Guadeloupe			
Guatemala		1	
Guernsey			
Guinea		1	
Guinea-Bissau		1	
Guyana		1	
Haiti		1	
Holy See (Vatican City)			
Honduras		1	
Hungary		1	
Iceland			
India		1	
Indonesia		1	
Iran	1	1	
Iraq			
Ireland			
Isle of Man			
Israel			
Italy	1		
Jamaica		1	
Japan			
Jersey			
Jordan		1	
Kazakhstan		1	
Kenya		1	
Kiribati		1	
Korea, North			
Korea, South			
Kosovo			
Kuwait			
Kyrgyzstan		1	
Laos			
Latvia		1	

Table D.2 Number of Treaties: Natural Disasters [104] (continued)

Country	Disaster Assistance	Peace Corps	Humanitarian Assistance
Lebanon			
Lesotho		1	
Liberia		1	
Libya			
Liechtenstein			
Lithuania			
Luxembourg		1	
Macau			
Macedonia			
Madagascar		1	
Malawi		1	
Malaysia		1	
Maldives			
Mali		1	
Malta		1	
Marshall Islands		1	
Martinique			
Mauritania			
Mauritius		1	
Mayotte			
Mexico	1	1	
Micronesia, Federated States of		1	
Moldova			
Monaco			
Mongolia		1	
Montenegro			
Morocco		1	
Mozambique		1	
Namibia			
Nepal		1	
Netherlands			
Netherlands Antilles			
New Caledonia			
New Zealand			
Nicaragua		1	
Niger		1	
Nigeria		1	
Niue		1	

Table D.2 Number of Treaties: Natural Disasters [104] (continued)

Country	Disaster Assistance	Peace Corps	Humanitarian Assistance
Norfolk Island			
Norway			
Oman		1	
Pakistan		1	
Palau		1	
Palestain			
Panama		1	
Papua New Guinea		1	
Paraguay		1	
Peru		1	
Philippines		1	
Poland		1	
Portugal			
Qatar			
Reunion			
Romania		1	
Russia			
Rwanda		1	
Saint Barthelemy			
Saint Helena			
Saint Kitts and Nevis		1	
Saint Lucia		1	
Saint Pierre and Miquelon			
Saint Vincent and the Grenadines		1	
Samoa		1	
San Marino			
Sao Tome and Principe			
Saudi Arabia			
Senegal		1	
Serbia			
Seychelles		1	
Sierra Leone		1	
Singapore			
Slovakia			
Slovenia			
Solomon Islands		1	
Somalia		1	
South Africa			

Table D.2 Number of Treaties: Natural Disasters [104] (continued)

Country	Disaster Assistance	Peace Corps	Humanitarian Assistance
South Georgia and South Sandwich Islands			
Spain			
Sri Lanka		1	
Sudan			1
Suriname		1	
Swaziland		1	
Sweden			
Switzerland			
Syria			
Taiwan			
Tajikistan			
Tanzania		1	
Thailand		1	
Timor-Leste		1	
Togo		1	
Tonga		1	
Trinidad and Tobago			
Tunisia		1	
Turkey		1	
Turkmenistan		1	
Turks and Caicos Islands		1	
Tuvalu		1	
Uganda		1	
Ukraine		1	
United Arab Emirates			
United Kingdom			
Uruguay		1	
Uzbekistan		1	
Vanuatu		1	
Venezuela		1	
Vietnam			
Virgin Islands			
Wallis and Futuna			
Western Sahara			
Yemen		1	
Zambia			
Zimbabwe		1	

REFERENCES

[1] Alves, N. A., Berg, B. A., and Villanova, R., Ising model Monte Carlo simulation: Density of states and mass gap, Physics Review Letter B41, 383, 1990.

[2] Balestrini-Robinson, S. Quantitative Technology Assessment for Large Scale Complex System-of-Systems, ONR project report, 2010

[3] Beisecker, E. Framework for robust design: A forecast environment using intelligent discrete event simulation, Ph.D. thesis, 2012

[4] Bennett, C. H. Efficient estimation of free energy differences from Monte Carlo data, Journal of Computational Physics Vol. 22, 1976

[5] Bhanot, B. et al, A new method for the partition function of discrete systems with application to the 3D Ising model, Physics Letter B, 183-331, 1987

[6] Bhanot, B. et al, Accurate estimate of ν for the three-dimensional Ising model from a numerical measurement of its partition function, Physical Review Letters Vol. 59, 1987

[7] Bond, Jenkins, and Schock, Mapping mass political conflict and civil society: Issues and prospects for the automated development of event data, Journal of Conflict Resolution, 1997

[8] Brooks, N. and Adger W. N. Country level risk measures of climate-related natural disasters and implications for adaptation to climate change. Working Paper 26, 2003

[9] Button, R. W. et al, A Preliminary Investigation of Ship Acquisition Options for Joint Forcible Entry Operations. RAND Corporation, 2005

[10] Button, R. W. et al, War fighting and logistic support of joint forces from the joint sea base, RAND Corporation, 2007

[11] Chen, R. S. The human dimension of vulnerability. In Industrial Ecology and Global Change, Cambridge, UK: ambridge University Press. pp. 85–105, 1994

[12] Chen, Y.Y. Bernoulli trials: froma a fuzzy measure point of view, J. Math. Anal. Appl. 175, pp. 392-404

[13] Chen, Y.Y. Fuzzy analysis of statistical evidence, IEEE Transactions on Fuzzy Systems, I, pp. 796-799

[14] Chen, Y.Y. Statistical Inference based on the Possibility and Belief Measures, Trans. Amer. Math. Soc. 347, pp. 1855-1863

[15] Cheng J, Tellambura, C. and Beaulieu, N.C. Performance of Digital Linear Modulations on Weibull Fading Channels, IEEE Transactions on Communications, vol. 52, pp. 1265-1268, 2004

[16] CIA World Factbook, https://www.cia.gov/library/publications/the-world-factbook/

[17] CIESIN, Gridded Population of the World (GPW) project, http://sedac.ciesin.columbia.edu/, 2000

[18] Clark, A. V. Seapower 21: Projecting decisive joint capabilities, in Proceedings of the U.S. Naval Institute, October 2002

[19] Committee on Sea Basing: Ensuring Joint Force Access from the Sea,NRC Sea basing: Ensuring joint force access from the sea, 2005

[20] Cover, T.M. and Thomas, M. Elements of information theory, New York: Wiley, 1991

[21] Crevecoeur, G. U. Reliability assessment of ageing operating systems, Eur. J. Mech. & Env. Eng., 39(4), 1994, pp. 219-228

[22] Crevecoeur, G.U. A Model for the Integrity Assessment of Ageing Repairable Systems, IEEE Trans. Reliability, 42(1), 1993, pp. 148-155

[23] Dalton, J. H. et al Forward … from the sea, U.S. Naval Institute Proceedings,1994

[24] Dilley, M. et al Natural disaster hotspots: A global risk analysis, Synthesis report, International Bank for Reconstruction and Development, The World Bank and Columbia University, 2005

[25] DoD Joint Publication 1-02, DOD Dictionary of Military and Associated Terms, November 08 2010

[26] DoD Sea basing joint integrating concept, version 1.0. Department of Defense, August 2005

[27] DoD, System engineering fundamentals, System engineering college, Department of Defense, Defense acquisition university press, 2011

[28] DoD, Defense acquisition guidebook, 2010

[29] DoD, DoD Directive 5000.01 The Defense Acquisition System, 2003

[30] DoD, DoD Modeling and Simulation Glossary, http://www.msco.mil/MSGlossary.html

[31] Eckhardt, R. Stan Ulam, John von Neumann, and the Monte Carlo method. Los Alamos Science, Special Issue (15): 131–137, 1987

[32] Federation of American Scientists, https://www.fas.org

[33] Ferrenberg, A. M. and Swendsen, R. H., New Monte Carlo technique for studying phase transitions, Physics Review Letter.61. 2635, 1988

[34] Ferrenberg, A. M. and Swendsen, R. H., Optimized Monte Carlo data analysis, Physics Review Letter.63. 1195, 1989

[35] Financial Tracking Service, http://www.reliefweb.int/fts/

[36] Fosdick, L. D., Monte Carlo computations on the Ising Model, Methods in Computational Physics, Academic Press, 1963

[37] Frank, M.J. On the simultaneous associativity of F (x, y) and x + y – F (x, y). Aequationes Math., 19, pp. 194-226, 1979

[38] Fratarangelo, P. et al, Sea basing, 2005

[39] Fréchet, Maurice, "Sur la loi de probabilité de l'écart maximum", Annales de la Société Polonaise de Mathematique, Cracovie 6: 93–116, 1927

[40] Freedomhouse organization, http://www.freedomhouse.org

[41] Gale P. A. Ship design, McGraw-Hill's Encyclopedia of Science & Technology

[42] Global Security Organization, http://www.globalsecurity.org/military/intro/supclass.htm

[43] Google Earth, http://www.google.com/earth/index.html

[44] Greene, R., et al, GIS-based multi-criteria analysis. Geography Compass 5/6: 412–432

[45] Gurr, T. R. and Moore, H. Ethno-political rebellion: A cross-sectional analysis of the 1980s with risk assessments for the 1990s, American Journal of Political Science, 1997

[46] Heritage foundation, http://www.heritage.org

[47] http://news.cnet.com/8301-13639_3-9854633-42.html

[48] http://newwars.wordpress.com/2010/05/11/marines-from-procurement-tragedy-to-triumph/

[49] http://srtm.csi.cgiar.org/SELECTION/inputCoord.asp

[50] http://srtm.csi.cgiar.org/SELECTION/listImages.asp

[51] http://www.boatdesign.net/forums/boat-design/t-craft-16917-2.html

[52] http://www.boatdesign.net/forums/boat-design/t-craft-16917-6.html

[53] http://www.defenseimagery.mil/imageRetrieve.action?guid=3eb5385de2ded3944ac1a4e08c148ce0a2be2cc2&t=2

[54] http://www.flickr.com/photos/tailspin_tommy/1439676091

[55] http://www.nvr.navy.mil/nvrships/details/agf11.htm

[56] http://www.nvr.navy.mil/nvrships/details/cg47.htm

[57] http://www.nvr.navy.mil/nvrships/details/FFG7.htm

[58] http://www.quantico.usmc.mil/seabasing/docs/Joint_Seabasing_Components.pdf

[59] https://sites.google.com/site/sanbales2/seabasingconcept.jpg

[60] Hubbard, D. The Failure of Risk Management: Why It's Broken and How to Fix It. John Wiley & Sons, 2009

[61] International Society on Multiple Criteria Decision Making, http://www.mcdmsociety.org

[62] Jenkins, J. C. and Bond, D. Conflict-carrying capacity, political crisis, and reconstruction: A framework for the early warning of political system vulnerability. Journal of Conflict Resolution 45 (1): 3-31, 2001

[63] Johnson, N.L., Kotz, S., and Balakrishnan, N. Continuous Univariate Distributions. Vol. 1, Wiley Series in Probability and Mathematical Staticstics: Applied Probability and Statistics (2nd Ed.), John Wiley and Sons, New York.

[64] Kalos, M. H. and Whitlock, P. A. Monte Carlo Methods. Wiley-VCH, ISBN 978-3-527-40760-6., 2008

[65] Kareiva et al., Domesticated Nature: Shaping Landscapes and Ecosystems for Human Welfare. Science 316, 2007

[66] King, G. and Zeng, L. Improving forecasts of state failure, World Politics 53:623-58, 2001

[67] Klir, G.H. and Yuan, B. Fuzzy set and Fuzzy Logic: Theory and Application. Prentice Hall, 1995

[68] Kossiakoff, A. and Sweet, W. N. Systems engineering principle and practice, Wiley-Interscience, 2003

[69] Koullias, S. Surface effect ship sizing & synthesis, 2010

[70] Kullback S. Information Theory and Statistics, Dover, New York, 1997

[71] Lee, J., New Monte Carlo Algorithm: Entropic Sampling, Physical Review letters Vol.71, 1993

[72] Lee, K. C., A new efficient Monte Carlo technique, Journal of Physics. A 23, 2087, 1990

[73] Maiden, Terence. T-Scale: Origins and Scientific Basis. TORRO, 2012

[74] Mandelbrot, B., How Long Is the Coast of Britain? Statistical Self-Similarity and Fractional Dimension, Science, 1967

[75] Manual on Marine Meteorological Services Volume I (Annex VI to WMO Technical Regulations) Global Aspects WMO-No. 558 2012 edition

[76] Marinari, E., Complex zeroes of the d = 3 Ising model: Finite-size scaling and critical amplitudes, Nuclear Physics B, 1984

[77] Met Office, http://www.metoffice.gov.uk/weather/marine/guide/beaufortscale.html

[78] Met Office, National Meteorological Library and Archive Fact sheet 6 — The Beaufort Scale, 2011

[79] Metropolis, N. The beginning of the Monte Carlo method, Los Alamos Science, 1987

[80] Modeling and Simulation Coordination Office, DoD Modeling and Simulation Glossary, http://www.msco.mil/MSGlossary.html

[81] Muraleedharan, G.; Rao, A.G.; Kurup, P.G.; Nair, N. Unnikrishnan; Sinha, Mourani, Coastal Engineering, Coastal Engineering 54 (8): 630–638, 2007

[82] National Institute of Standards and Technology, Engineering statistics handbook, 2008.

[83] Nelson W. Applied Life Data Analysis, Wiley-Blackwell, 2003

[84] New York Post, http://www.nypost.com/f/print/news/international/earthquake_ rocks_haiti_h66t3XFZda88Hf6ukrnhmL

[85] NIST Engineering Statistics Handbook, National Institute of Standards and Technology, updated in April 2012

[86] O'Brien, S. Analyzing complex threats for operations and readiness (ACTOR), Center for army analysis report CAA-R-01-59, 2001.

[87] O'Brien, S. Anticipating the good, the bad, and the ugly: An early warning approach to conflict and instability analysis, Journal of conflict resolution, 2002.

[88] O'Loughlin, K. F., and Lander, J. F. Caribbean Tsunamis: A 500-Year History from 1498-1998. Doredrecht, The Netherlands: Kluwer Academic Publishers. 263 pp

[89] Office of the Deputy Under Secretary of Defense for Acquisition and Technology, Systems and Software Engineering, Systems Engineering Guide for Systems of Systems Version 1.0, 2008

[90] Office of the Under Secretary of Defense for Acquisition, Technology, and Logistics, Defense science board task force on seabasing, 2003

[91] O'Keefe, S et al ...From the Sea, U.S. Naval Institute Proceedings, 1992

[92] ONR ONR baa announcement 05-020, sea base connector transformable-craft prototype demonstrator Office of Naval Research, 2005

[93] ONR Fact Sheet: Innovative Naval Prototype (INP) Transformable Craft (T-Craft) - Office of Naval Research, http://www.onr.navy.mil/en/Media-Center/Fact-Sheets/INP-Transformable-Craft.aspx

[94] Papoulis A. and Pillai, S. U. Probability, Random Variables and Stochastic Processes, McGraw-Hill Eutope, 1991

[95] Peter A. Gale, Ship design, McGraw-Hill's Encyclopedia of Science & Technology

[96] Portworld, http://www.portworld.com/

[97] RADM, Ship Acquisition, NDIA 10th Annual Expeditionary Warfare Conference , 2005

[98] RAND Corporation, Warfighting and Logistic Support of Joint Forces from the Joint Sea Base, 2007

[99] REUK, Wind Speed Distribution Weibull, WEB: www.reuk.co.uk/Wind-Speed-Distributin-Weibull.htm

[100] Rupesinghe, K. and Kuroda, M. Early warning and conflict resolution, New York: St. Martin’s, 1992

[101] Sacks, J. et al Design and analysis of computer experiments, Statistics Science, 1989

[102] Sagias, N.C. and Karagiannidis, G.K. Gaussian class multivariate Weibull distributions: theory and applications in fading channels, Institute of Electrical and Electronics Engineers. Transactions on Information Theory 51 (10), 3608 – 3619

[103] Saucier, W. J. Principles of Meteorological Analysis,1955

[104] Schroeder, Daniel V. An Introduction toThermal Physics. Addison Wesley Longman, 1999

[105] Schweizer, B. and Sklar, A. Associative functions and abstract semi-groups, Publ. Math. Debrecen, 10, pp. 69-81, 1963

[106] Sebastini, P. Maximum Entropy Sampling and Optimal Bayesian Experimental Design, Journal of the Royal Statistical Society, 2000

[107] Sharif M.N. and Islam M.N. The Weibull distributaion as a general model for forecasting technological change, Technological Forecasting and Social Change, Vol. 18 Issue 3, November, pp. 247-256, 1980

[108] Sharpe, R. Jane's Fighting Ships 1998–99, 1998

[109] Shewry, M.C. and Wynn. H.P. Maximum Entropy Sampling, Journal of Applied Statistics, 1987

[110] StatSoft, Inc. Electronic Statistics Textbook. Tulsa, OK: StatSoft. WEB: http://www.statsoft.com/textbook/

[111] The Centre for Research on the Epidemiology of Disasters, http:// www.cred.be

[112] The Heidelberg Institute for International Conflict Research, http://www.hiik.de/en/kosimo/

[113] Thomas, G. Terry, Systems engineering : the product, the process, and the performance

[114] Till, G. Naval transformation, ground forces, and the expeditionary impulse: The sea-basing debate. Strategic Studies Institute, U.S. Army War College, December 2006

[115] Ting, C. Y. Life cycle cost estimation for MEC, MEC CONOPS Workshop, 2011

[116] Tison, D. C. Army equipment modernization plan, 2012

[117] Treaty Affairs Staff, Office of the Legal Adviser, U.S. Department of State, Treaties in Force: A List of Treaties and Other International Agreements of the United States in Force on January 1, 2012

[118] Truver, S. 'sea power 21' ... for the common good, NATO's Nations and Partners for Peace, no. 1, pp. 118-124, 2004

[119] Tupper, E. C., Introduction to naval architecture, Oxford, 2000

[120] Tyndall Center for Climate Change Research. Norwich, UK: University of East Anglia. 25 pp, 2003

[121] U.S. Bureau of the Census, International Database, www.census/gov/ipc/www

[122] U.S. Geological Survey, Shuttle Radar Topography Mission http://srtm.usgs.gov/index.php

[123] United Nations Data Retrieval System, http://data.un.org/Data.aspx?d=PopDiv&f=variableID%3A77

[124] USD/DAU Defense acquisition guidebook, WEB: dag.dau.mil, February 19 2010

[125] Walter J. S., Principles of Meteorological Analysis, University of Chicago Press, 1955

[126] Watkins , J. D. The Maritime Strategy, U.S. Naval Institute Proceedings, 1986

[127] WBG http://www.worldbank.org/hazards

[128] World water organization, http://www.theworldwater.org

[129] Yoon, K. Systems Selection by Multiple Attribute Decision Making, Ph.D. dissertation, Kansas State University, 1980.

[130] Yoon, K.P. and Hwang, C. Multiple Attribute Decision Making: An Introduction, SAGE publications, 1995

[131] Zavadskas, E.K. et al Evaluation of Ranking Accuracy in Multi-Criteria Decisions, Informatica 17 (4): 601–618, 2006